Investigating the role of Junctional Adhesion Molecule-C (JAM-C) in endothelial cell biology *in vitro* and *in vivo* using human and mouse models

Robert William John Beal

A thesis submitted for the degree of

Doctor of Philosophy

Barts & The London School of Medicine and Dentistry

Queen Mary, University of London

Centre for Microvascular Research
William Harvey Research Institute
John Vane Science Centre
Charterhouse Square
London, EC1M 6BQ

Acknowledgements

I would like to thank Professor Sussan Nourshargh for giving me the opportunity to carry out this PhD and supervising and for her fantastic support and guidance in this project for the past four years. I must also thank Dr Egle Solito for acting as my second supervisor and the Wellcome Trust for the funding support of this project.

A big thanks goes to all the members of Centre for Microvascular Research, both past and present, for all their support and advice during my PhD. In particular to Dr's Natalia Reglero, James Whiteford, Matthew Golding and Tom Nightingale, who have provided invaluable advice, suggestions and laughs along the way. Particular thanks also goes to Sam Arokiasamy, Giulia De Rossi and Chris Schultz, who I have shared the PhD journey with and have become great friends.

A special thank you to my parents Nigel and Helen and brother Chris for their constant love, support and guidance. You have always encouraged me to strive for the best and without you, I certainly wouldn't be where I am today.

Finally, and most importantly, to Dee, who has been my unwavering rock throughout the whole PhD journey and who has put up with a lot for the last five years. I finally did it! To you and to my parents, I dedicate this thesis.

Abstract

Junctional adhesion molecule C (JAM-C) is a component of endothelial cell (EC) tight junctions that has been implicated in a number of endothelial functions, such as angiogenesis and trafficking of leukocytes through the endothelium during inflammation. Work within our lab has identified that loss of JAM-C at EC junctions results in increased reverse transendothelial migration (rTEM) of neutrophils back into the circulation, a response that has been associated with the dissemination of inflammation to distant organs. Whilst the mechanism by which JAM-C is lost or redistributed away from EC junctions has begun to be elucidated, little is known about how loss of endothelial JAM-C impacts the functions of ECs. As such, this thesis aimed to investigate the effect of JAM-C deficiency on EC functions to unravel possible molecular and cellular mechanisms of mediating neutrophil rTEM.

To address the effect of JAM-C deficiency on EC functions, an *in vitro* RNA interference (RNAi) approach was used to efficiently knock-down (KD) JAM-C in human umbilical vein ECs (HUVECs). Importantly, KD of JAM-C did not affect expression of other key EC junctional markers such as JAM-A and VE-Cadherin and cell proliferation and apoptosis were similarly unaffected. Gene expression profiling using microarrays revealed that JAM-C depleted HUVECs exhibited a pro-inflammatory phenotype under basal conditions that was characterised by increased expression of pro-inflammatory genes such as *ICAM1* and *IL8.*

Following IL-1β-induced inflammation, no difference in expression of pro-inflammatory genes was detected between control and JAM-C KD HUVECs. However, protein levels of secreted chemokines such as IL-8 were reduced in JAM-C KD HUVECs following stimulation with IL-1β. This was corroborated by *in vivo* studies demonstrating reduced levels of secreted chemokines in the plasma of mice where JAM-C was conditionally deleted from ECs.

A novel finding of this work is the demonstration that JAM-C KD HUVECs exhibit increased autophagy under basal conditions. This might provide a potential mechanism for the reduced chemokine secretion that is observed in this system,

whereby chemokines are preferentially trafficked for autophagosome-mediated degradation.

Taken together, these findings indicate a multi-functional role for JAM-C in regulating EC homeostasis under basal conditions. JAM-C KD ECs respond aberrantly to inflammatory stimuli by secreting reduced chemokine levels, a consequence that could provide novel insights into the mechanisms of neutrophil rTEM under conditions of endothelial JAM-C loss.

Table of Contents

Acknowledgements **2**

Abstract **3**

Table of Contents **5**

List of Figures **10**

List of Tables **12**

Abbreviations **13**

Statement of originality **17**

1 General Introduction **18**

1.1 Inflammation 18

1.1.1 Leukocyte adhesion cascade 18

1.2 Endothelial Cells 21

1.2.1 Characteristics, development and role in homeostasis 21

1.2.2 Control of EC gene expression 23

1.3 Endothelial cells in inflammation 24

1.3.1 Generation of chemokines by endothelial cells 24

1.3.2 Endothelial cell adhesion molecules 25

1.4 Endothelial cell junctions 28

1.4.1 Adherens junctions 28

1.4.2 Tight junctions 30

1.4.3 Formation of EC junctions 31

1.5 Junctional adhesion molecules (JAMs) 32

1.5.1 Expression 32

1.5.2 Structure and interactions 34

1.5.3 Functions of the JAM family in the endothelium and beyond 36

1.6 JAM-C 38

1.6.1 Expression 38

1.6.2 JAM-C ligands 39

1.6.3 Role of JAM-C in vascular processes 40

1.6.4 JAM-C and leukocyte migration 41

1.6.5 Additional roles for JAM-C in inflammation and cancer 42

1.7 Autophagy 45

1.7.1 Autophagy in infection and inflammation 46
1.7.2 Autophagy in endothelial cells 47
1.8 Aims 49
2 Materials and Methods 51
2.1 Animals 51
2.1.1 Mouse Strains 51
2.1.2 Anaesthetics 52
2.2 Reagents 52
2.2.1 Antibodies 52
2.2.2 Fluorescent Dyes 54
2.2.3 Inflammatory Stimuli 54
2.2.4 Kits 55
2.2.5 Cell/tissue lysis buffers 55
2.2.6 Other Reagents 56
2.3 Cell culture 56
2.3.1 HUVECs 56
2.3.2 siRNA transfection 57
2.3.3 Cell stimulation 58
2.3.4 Proliferation Assay 58
2.3.5 Cell viability and apoptosis assays 58
2.4 In vivo inflammation models 59
2.4.1 Neutrophil depletion 59
2.4.2 Cremaster inflammation model 59
2.5 Characterisation of neutrophil depletion 60
2.5.1 Immunofluorescence labelling of leukocytes 60
2.5.2 Flow cytometry 60
2.6 Gene expression analysis 60
2.6.1 RNA extraction from cell culture 60
2.6.2 Analysis of RNA quality 60
2.6.3 Gene expression microarray 61
2.6.4 Gene expression data analysis 61
2.6.5 Quantitative real-time polymerase chain reaction (qPCR) 62
2.7 Inflammatory Mediator analysis 64
2.7.1 Preparation of cremaster lysate samples 64
2.7.2 Preparation of plasma samples 64

2.7.3 Proteome Profiler™ and cytokine arrays 64
2.7.4 Enzyme-linked Immunosorbent Assay (ELISA) 66
2.8 Immunofluorescence Confocal Microscopy 66
2.8.1 Immunofluorescent labelling of cells 66
2.8.2 Immunofluorescent labelling of tissue 68
2.8.3 Confocal Microscopy 68
2.9 Western Blotting 68
2.10 Statistics 69
3 Investigating the impact of JAM-C deficiency on endothelial cell junctions, survival and proliferation *in vitro* 70
3.1. Introduction 70
3.2. Aims 71
3.3. Results 73
3.3.1. Cellular localisation of JAM-C in endothelial cells *in vitro* 73
3.3.2. siRNA mediated KD of JAM-C expression in HUVECs 75
3.3.3. JAM-C KD does not affect expression of key EC junctional molecules 80
3.3.4. JAM-C KD does not affect EC morphology or proliferation 82
3.3.5. JAM-C KD does not impact EC viability 84
3.4. Discussion 87
4 Loss of endothelial cell JAM-C triggers autophagy *in vitro* 91
4.1 Introduction 91
4.1.1 Autophagy and cellular homeostasis 91
4.1.2 Methods for analysing autophagy 92
4.2 Aims 93
4.3 Results 95
4.3.1 Starvation induces autophagy in HUVECs 95
4.3.2 Pharmacological inhibition of starvation induced autophagy by 3-MA 98
4.3.3 JAM-C KD induces autophagy in HUVECs 99
4.3.4 JAM-C KD induced autophagy in HUVECs is inhibited by 3-MA 104
4.3.5 IL-1β-mediated increase in LC3-II is not inhibited by 3-MA. 104
4.4 Discussion 105
5 Investigating the effects of JAM-C KD on EC gene expression 110
5.1 Introduction 110
5.1.1 Control of EC gene expression 110
5.1.2 Junctional molecules and gene expression 110

5.2 Aims 111
5.3 Results 113
5.3.1 Quality control assessment of EC RNA and gene expression PCA 113
5.3.2 JAM-C KD in HUVECs triggers gene expression changes under basal conditions 115
5.3.3 Pathway analysis of JAM-C KD EC gene expression 118
5.3.4 Validation of differentially expressed genes by qPCR 121
5.3.5 JAM-C KD increases the basal activation of the NFκB pathway in HUVECs 124
5.3.6 JAM-C KD HUVECs show increased protein expression of IL-8 and ICAM-1 128
5.3.7 Differential gene expression analysis of IL-1β stimulated HUVECs 130
5.3.8 Impact of IL-1β on differential gene expression in JAM-C KD HUVECs 133
5.3.9 Differential expression of semaphorins by JAM-C KD HUVECs 139
5.4 Discussion 142
5.4.1 JAM-C regulates EC gene expression under basal conditions 142
5.4.2 JAM-C KD ECs respond aberrantly to cytokine stimulation 145
5.4.3 JAM-C regulates Semaphorin expression during inflammation 146
5.4.4 Mechanism of JAM-C regulated gene expression in ECs 148
5.4.5 Summary of key findings 149
6 Investigating the role of EC JAM-C in inflammatory mediator generation 151
6.1 Introduction 151
6.2 Aims 152
6.3 Results 153
6.3.1 Effect of JAM-C KD on IL-1β-stimulated HUVEC chemokine generation 153
6.3.2 Mouse model of EC JAM-C deficiency 157
6.3.3 Establishment of a mouse neutrophil depletion protocol 159
6.3.4 Impact of EC JAM-C deficiency on tissue mediator generation 161
6.3.5 Local administration of IL-1β increased circulating chemokine levels 165
6.4 Discussion 167
6.4.1 Loss of JAM-C reduces IL-8 secretion from cultured ECs 167
6.4.2 EC JAM-C regulates tissue chemokine production and secretion *in vivo* 168
6.4.3 Key findings 170
7 General Discussion 172
7.1 Project overview 172
7.2 *In vitro* KD of JAM-C enabled the functional study of JAM-C in EC biology 172
7.3 JAM-C KD ECs exhibit increased autophagy *in vitro* 173

7.4 JAM-C controls pro-inflammatory gene expression under basal conditions..... 174
7.5 JAM-C regulates semaphorin gene expression in ECs..... 175
7.6 JAM-C regulates chemokine secretion *in vivo*..... 176
7.7 Future perspectives..... 178
7.7.1 Targeted KD of additional EC junctional molecules and comparison with EC JAM-C KD phenotype..... 178
7.7.2 Investigation into the impact of increased pro-inflammatory gene expression under basal conditions..... 179
7.7.3 Physiological impact of increased EC autophagy in JAM-C deficient ECs..... 179
7.7.4 Mechanism of reduced chemokine secretion and impact on neutrophil TEM 180
7.8 Wider implications of this work..... 181
7.9 Conclusions..... 183
Appendices..... 184
References..... 187

List of Figures

Figure 1.1. The leukocyte adhesion cascade. 21
Figure 1.2. Organisation of endothelial cell junctions. 29
Figure 1.3. Schematic structure of JAM-C and its type II PDZ binding domain. 35
Figure 1.4. Expression of JAM-C in mouse tissue 39
Figure 2.1. Human Cytokine Array Panel 65
Figure 2.2. Immunofluorescence staining of confluent HUVECs. 67
Figure 3.1. JAM-C is largely expressed at cell-cell junctions in unstimulated HUVECs. 74
Figure 3.2. JAM-C is present at the junctions of HDMECs under resting conditions. 75
Figure 3.3. Comparison of different methods used for siRNA KD of JAM-C in HUVECs. 77
Figure 3.4. Immunofluorescence confocal microscopy validation of KD of JAM-C using the nucleofection method. 78
Figure 3.5 JAM-C KD in HUVECs does not impact VE-Cadherin expression. 79
Figure 3.6. JAM-C KD does not impact JAM-A expression. 81
Figure 3.7. JAM-C KD does not impact EC morphology. 83
Figure 3.8. JAM-C KD does not affect proliferative potential of HUVECs. 84
Figure 3.9. JAM-C KD does not impact EC viability. 86
Figure 4.1. Overview of the molecules involved in autophagosome formation and the various sites of pharmacological inhibition. 93
Figure 4.2. Starvation induces autophagy in HUVECs. 96
Figure 4.3. Starvation induces LC3 puncta formation in HUVECs 97
Figure 4.4. The PI3K inhibitor 3-MA inhibits starvation induced autophagy in HUVECs. 99
Figure 4.5. Autophagy is increased in JAM-C KD HUVECs under basal conditions. 100
Figure 4.6. JAM-C KD HUVECs exhibit increased LC3 punctae formation. 102
Figure 4.7. JAM-C mediated autophagy in HUVECs is dependent on PI3K activity. 103
Figure 4.8. IL-1β stimulation of HUVECs increases LC3-II protein levels in HUVECs. 105
Figure 5.1. Dual purification of HUVEC protein and RNA for microarray analysis 114
Figure 5.2. Principle component analysis of replicate samples in gene expression microarray. 115
Figure 5.3. Top 100 differentially expressed genes between control and JAM-C KD HUVECs under basal conditions. 118
Figure 5.4. Network pathway analysis of differentially expressed genes following JAM-C KD in HUVECs. 120
Figure 5.5. qPCR validation of candidate genes selected from the microarray and pathway analysis. 123

Figure 5.6. NFκB pathway is upregulated in JAM-C KD HUVECs. 126
Figure 5.7. Immunofluorescence staining of total and phospho-p65 in JAM-C KD HUVECs. ... 127
Figure 5.8. IL-8 and ICAM-1 proteins are elevated in JAM-C KD HUVECs. 129
Figure 5.9. The top 100 differentially expressed genes between control and JAM-C KD HUVECs following IL-1β stimulation. 135
Figure 5.10. Normalised differential expression heatmap of IL-1β stimulated HUVECs. 137
Figure 5.11. Several members of the Semaphorin family of molecules are differentially expressed in JAM-C KD HUVECs following IL-1β stimulation. 140
Figure 5.12. qPCR validation of Semaphorin gene expression in JAM-C KD HUVECs..... 141
Figure 6.1. ELISA analysis of IL-1β induced chemokine generation by JAM-C KD HUVECs. 154
Figure 6.2. Cytokine array analysis of secreted mediators from JAM-C KD HUVECs. 156
Figure 6.3. Immunofluorescence staining of EC JAM-C in cremaster muscle venules. 158
Figure 6.4. GR-1 mediated depletion of circulating mouse neutrophils 160
Figure 6.5. Cytokine array analysis of IL-1β-induced cremaster muscle chemokine generation. 162
Figure 6.6. Analysis of chemokine levels in IL-1β-stimulated cremaster muscles as quantified by ELISA. 164
Figure 6.7. Analysis of plasma chemokine levels post-IL-1β stimulation of cremaster muscles. 166

List of Tables

Table 1.1. Expression and functions of the members of the JAM family. 33
Table 2.1. List of human siRNA oligonucleotide primers 58
Table 2.2. List of qPCR human oligonucleotide primers 63
Table 5.1. List of biological processes upregulated in JAM-C KD HUVECs. 119
Table 5.2. List of selected candidate genes to be validated by qPCR that are significantly differentially expressed following JAM-C KD. 121
Table 5.3. Top 25 significantly upregulated differentially expressed genes induced by IL-1β in HUVECs. 131
Table 5.4. Top 25 significantly downregulated differentially expressed genes following IL-1β stimulation of HUVECs 132
Table 5.5. Candidate genes from unstimulated comparison subjected to differential expression analysis following IL-1β stimulation. 135
Table 5.6. Gene ontology enrichment analysis (GO) of dysregulated genes in IL-1β stimulated JAM-C KD HUVECs. 138
Table 5.7. Candidate genes isolated from GSEA analysis. 138

Abbreviations

3-MA	3-Methyladenine
ACK	Ammonium-chloride-potassium
Akt	Protein kinase B
AP-1	Activator protein 1
ATG16L	Autophagy-related protein 16
ATG5	Autophagy-related protein 5
ATG7	Autophagy-related protein 7
bFGF	Basic fibroblast growth factor
BSA	Bovine serum albumin
CAR	Coxsackievirus and adenovirus receptor
CCL	Chemokine (CC motif) ligand
cDNA	Complementary DNA
CLMP	CAR-like membrane protein
cRNA	Complementary RNA
CTX	Cortical thymocyte marker for Xenopus
Cx43	Connexin 43
CXCL	Chemokine (CXC motif) ligand
DAMP	Danger associated molecular pattern
DAPI	4',6-Diamidino-2-phenylindole
EBM	Endothelial cell basal medium
EC	Endothelial cell
ECGS	Endothelial cell growth supplement
ECM	Extracellular matric
ECPCR	Endothelial cell protein C receptor
ELISA	Enzyme-linked immunosorbent assay
eNOS	Endothelial nitric oxide synthase
ER	Endoplasmic reticulum
Erg	Ets-related gene
ERK1	Extracellular signal-regulated kinase 1
ERK2	Extracellular signal-regulated kinase 2

ESAM	Endothelial cell-selective adhesion molecules
ETS	E26 transformation specific
FCS	Fetal calf serum
FDR	False detection rate
FoxO1	Forkhead box protein O1
G-CSF	Granulocyte-colony-stimulating factor
GR1	Granulocyte-differentiation antigen 1
GRASP55	Golgi reassembly-stacking protein 55
GSEA	Gene set enrichment analysis
HDMECs	Human dermal microvascular endothelial cells
HGM	HUVEC growth medium
HIF1α	Hypoxia-inducible factor-1 alpha
HMGB1	High mobility group box 1
HUVECs	Human umbilical vein endothelial cells
i.m.	Intramuscular
i.p.	Intraperitoneal
i.v.	Intravenous
I/R	Ischemia-reperfusion
ICAM1	Intercellular adhesion molecule 1
ICAM-2	Intercellular adhesion molecule 2
IF	Immunofluorescence
IFNγ	Interferon gamma
IκB	Inhibitor of kappa B
IKK	IκB kinase
IL-15	Interleukin 15
IL-18	Interleukin 18
IL-1α	Interleukin 1-α
IL-1β	Interleukin 1-β
IL-6	Interleukin 6
IRF6	Interferon regulatory factor 6
IRF7	Interferon regulatory factor 7
JAM	Junctional adhesion molecule

JAM4	Junctional adhesion molecule 4
JAM-A	Junctional adhesion molecule A
JAM-B	Junctional adhesion molecule B
JAM-C	Junctional adhesion molecule C
JAM-L	Junctional adhesion molecule-like
JNK	c-Jun N-terminal kinase
KD	Knockdown
KO	Knockout
LC3	Microtubule-associated protein 1A/1B-light chain 3
LDH	Lactate dehydrogenase
LFA-1	Lymphocyte function-associated antigen 1
LPS	Lipopolysaccharide
Ly6G	Lymphocyte antigen 6 complex, locus G
Mac-1	Macrophage antigen-1
MAPK	Mitogen activated kinase
miRNA	Micro RNA
mRNA	Messenger RNA
mTOR	Mammalian target of rapamycin
MyD88	Myeloid differentiation primary response gene 88
NE	Neutrophil elastase
NFκB	Nuclear factor kappa-light-chain-enhancer of activated B cells
NGS	Normal goat serum
NO	Nitric oxide
oxLDL	Oxidised low-density lipoprotein
PAMP	Pathogen associated molecular pattern
PAR-3	Partitioning defective 3 homolog
PBS	Phosphate buffered saline
PE	Phosphatidylethanolamine
PECAM-1	Platelet endothelial cell adhesion molecule 1
PFA	Paraformaldehyde
PI3K	Phosphatidylinositol-4,5-bisphosphate 3-kinase
PRR	Pattern recognition receptor

PS	Phosphatidylserine
PSGL1	P-selectin glycoprotein ligand-1
qPCR	Quantitative polymerase chain reaction
Rab8a	Ras-related protein Rab-8A
Rap1	Ras-related protein 1
RNAi	RNA interference
ROS	Reactive oxygen species
rTEM	Reverse transendothelial migration
SDS	Sodium dodecyl sulphate
SEM	Standard error of mean
SEMA3A	Semaphorin 3A
SEMA3E	Semaphorin 3E
SEMA4F	Semaphorin 4F
SEMA7A	Semaphorin 7A
shRNA	Short hairpin RNA
sICAM1	Soluble ICAM-1
siRNA	Small interfering RNA
SIRT1	Sirtuin-1
sJAM-C	Soluble JAM-C
sVCAM1	Soluble VCAM-1
T1D	Type-1 Diabetes
TEM	Transendothelial migration
TNFα	Tumour necrosis factor α
VCAM1	Vascular cell adhesion molecule 1
VE-Cadherin	Vascular endothelial cadherin
VEGF	Vascular endothelial growth factor
VEGFR2	Vascular endothelial growth factor receptor 2
VLA-4	Very late antigen 4
vWF	von Willebrand factor
ZO-1	Zona occludens 1
ZO-2	Zona occludens 2
ZO-3	Zona occludens 3

Statement of originality

The approach and experiments presented here are novel. The author has personally undertaken all the work described here, unless stated otherwise.

1 General Introduction

1.1 Inflammation

Inflammation is the first line response of the body to injury or pathogens. Inflammation is commonly acute, where the end result is tissue healing and removal of the inflammatory trigger. By contrast, chronic inflammation is a prolonged and excessive response that goes beyond healing and can become detrimental to the host (Murakami and Hirano, 2012). This involves tissue destruction combined with unresolved active inflammation. As such, chronic inflammation is associated with many human diseases, including atherosclerosis, arthritis and cancer among others (Maskrey et al., 2011). Inflammation itself is characterised by the classical symptoms of redness, swelling, heat and pain. These are caused by an increase in blood flow to the affected area (redness), leakage of plasma and proteins into tissues causing oedema (swelling), and release of inflammatory mediators by tissue resident cells and infiltrating leukocytes. This process is tightly regulated, and dysregulation results in chronic inflammation and complications thereof (Medzhitov, 2008).

1.1.1 Leukocyte adhesion cascade

Leukocytes circulating in the blood are the defence armoury of the host and hence need to find a way to migrate from the blood into sites of tissue inflammation. Pathogen associated molecular patterns (PAMPs) and damage associated molecular patterns (DAMPs) stimulate sentinel cells such as tissue macrophages and dendritic cells (e.g. Kupffer cells, Langerhans cells) in the damaged tissue to release a range of pro-inflammatory mediators that initiates the process of attracting circulating leukocytes (e.g. neutrophils and monocytes) (Davies et al., 2013, Chen et al., 2016). These mediators include vasoactive amines, cytokines, chemokines, lipid mediators and enzymes, all of which promote rapid leukocyte recruitment and migration.

The leukocyte adhesion cascade is a multistep process by which circulating cells adhere to blood vessel walls and eventually migrate into inflamed tissues. This cascade can be split into four principal steps: rolling, adhesion, crawling and extravasation (See Figure 1.1; (Ley et al., 2007)).

Initial leukocyte capture and rolling is mediated by selectin molecules expressed on both leukocytes (L-selectin) and the endothelium (P- and E-selectin). For example, neutrophil rolling on endothelial E-selectin is mediated through the P-selectin glycoprotein ligand-1 (PSGL1), which is also the dominant ligand for both E-selectin and L-selectin also. These selectin-ligand interactions enable leukocytes to adhere to the endothelium under conditions of flow. Selectins actually require shear to support leukocyte attachment due to their catch bond character, where the strength of each bond increases as shear is applied. Selectin-ligand engagement and initial leukocyte rolling leads to downstream signalling events in the leukocyte such as through p38 MAPK in neutrophils that are bound to E-selectin on the endothelium, which in turn induces integrin activation. Indeed, integrins also participate in leukocyte rolling. Very Late Antigen-4 (VLA-4) has been shown to be important for monocyte and T cell rolling on VCAM-1 expressed by endothelial cells. In addition, the rolling of leukocytes on E-selectin induces a conformational change in the leukocyte integrin lymphocyte function-associated antigen-1 (LFA-1), which allows it to form transient interactions with the endothelial adhesion molecule intercellular adhesion molecule 1 (ICAM-1). The process of rolling enables the leukocyte to be brought into close contact with the endothelium, allowing for activation of the leukocyte and subsequent adhesion to the surface of the endothelium.

The slowing of rolling and subsequent arrest of leukocytes on the endothelium is triggered by chemokines and other chemoattractants, as well as binding to EC adhesion molecules such as ICAM-1 and also vascular cell adhesion molecule 1 (VCAM-1). Chemokines can be generated and displayed on the luminal surface of the endothelium, transported from their abluminal surface, deposited by activated platelets or mast cells, or delivered to ECs by microparticles. Chemokine binding to high affinity G-protein coupled receptors (GPCRs) on the leukocytes increases integrin avidity by increases both affinity and valency. The engagement of the chemokine receptors triggers intracellular signalling within seconds, in a process referred to as inside-out signalling. This signalling induces a conformational change in the integrin from a bent conformation to an extended high-affinity conformation that opens the ligand binding pocket. Different leukocyte subsets require activation of at least one of the major leukocyte integrins, such as LFA-1, macrophage antigen-1 (Mac-1) and

VLA-4. Integrin clustering and conformational changes upon arrest contribute to outside-in signalling events. The cytosolic tail of LFA-1 changes conformation upon binding to ICAM-1 which contributes to rapid leukocyte adhesion and arrest under flow conditions.

In addition to chemokines, other pro-inflammatory mediators such as prostanoids and leukotrienes are also important during leukocyte rolling and adhesion. For example, leukotriene B_4 (LTB_4) is known to induce adhesion of neutrophils to endothelial cells and this is dependent on the activity of β2 integrins, which is significantly increased by LTB_4 binding to the BLT-1 receptor on neutrophils (Subramanian et al., 2017). Prostaglandins such as PGE1, PGE2 and PGF have long been known to induce leukocyte migration (Shibuya et al., 1976). PGE2 significantly increases the chemotactic response of monocytes towards the chemokines CCL2 and CCL5 (Panzer and Uguccioni, 2004), while PGD2 has been shown to mediate the chemotaxis of leukocytes both *in vitro* and *in vivo* (Ricciotti and FitzGerald, 2011).

The final step of leukocyte extravasation is migration through the venular wall, known as transendothelial migration (TEM). Before they traverse the endothelium though, leukocytes often crawl on the luminal side of the blood vessel seeking preferred sites to cross. This is mediated by leukocyte expressed integrin αMβ2 (Macrophage antigen-1, Mac-1) interaction with ICAM-1 expressed on ECs (Phillipson et al., 2006, Schenkel et al., 2004b). Most TEM occurs via the paracellular route, which involves penetrating the endothelial barrier through junctions between adjacent ECs. A number of molecules present in these junctions actively participate in TEM, such as platelet endothelial cell adhesion molecule (PECAM-1) and the junctional adhesion molecule (JAM) family of molecules (described later). Clustering of EC integrin ligands at junctions provides the platform for leukocytes to engage with the junction (Carman and Springer, 2004). Breaching of the endothelium is then regulated by adhesion molecules expressed in the junctions between ECs. Transcellular TEM, where leukocytes breach the endothelium through the body of ECs, represents only a minority of events in most systems. This is not the case in the brain, where paracellular TEM events are highly restricted to ensure the maintenance of high endothelial barrier integrity (Muller, 2011). Emerging evidence regarding TEM suggest that many of the same molecules implicated in paracellular migration also control transcellular TEM

(Muller, 2013). Leukocyte migration through the endothelial barrier often occurs in a rapid manner, taking anywhere between 2-5 minutes. Following this, leukocytes must then migrate through the endothelial basement membrane and pericyte sheath in order to reach the affected tissue, a process which takes significantly longer (up to 15 minutes).

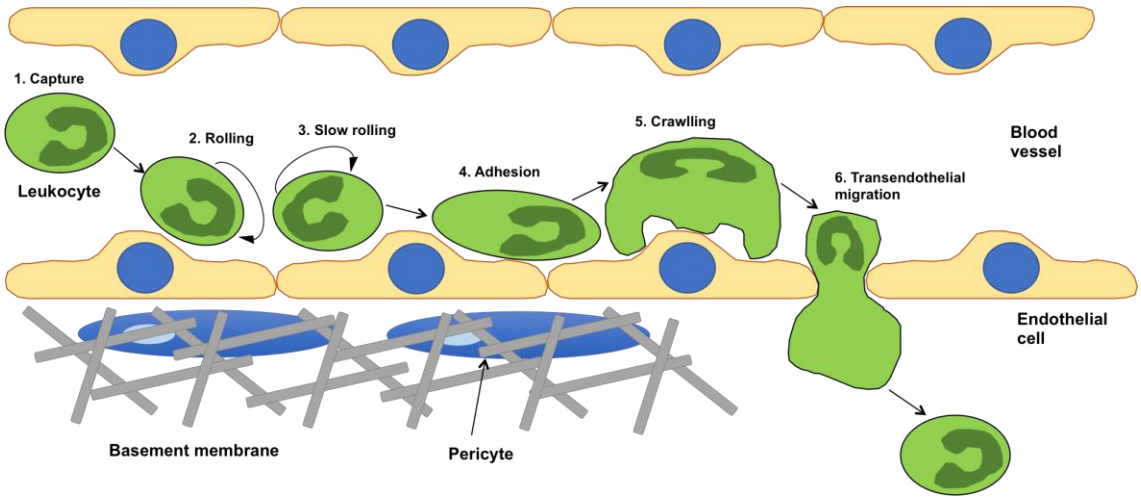

Figure 1.1. The leukocyte adhesion cascade. In response to injury or infection, circulating leukocytes are attracted to damaged tissues by pro-inflammatory cytokines and chemokines. The initial capture of leukocytes onto the endothelial wall begins with leukocyte rolling, which is mediated through interactions of selectins expressed on both the endothelium and leukocyte with their cognate ligands. Chemokines expressed and displayed by the endothelium activate the leukocytes, slowing the rolling and leading to increased binding of leukocyte integrins to endothelial adhesion molecules such as ICAM-1. As these interactions are strengthened, the rolling arrests and the leukocytes firmly adhere to the endothelium. Leukocytes then crawl along the endothelium until the find a suitable site to transmigrate, which they do through either the transcellular or paracellular route.

1.2 Endothelial Cells

1.2.1 Characteristics, development and role in homeostasis

ECs line the entire vascular and lymphatic system and exhibit many important properties, including regulation of thrombosis and of vascular tone, maintenance of blood flow, angiogenesis, platelet adherence, and regulation of immune responses (Landmesser et al., 2004). The endothelium is an important physical barrier that separates the blood (and lymph) from the surrounding tissue and plays an active role in relaying signals from the tissue to the blood to help meet the requirements of the perfused organs.

ECs are characterised by a number of features: (1) In vessels, ECs form very elongated and thin shapes, often hexagonal in shape (Adamson, 1993); (2) Formation of cell-cell junctions crucial to their wide ranging functions (discussed in section 1.4 onwards); (3) Presence of Weibel-Palade bodies, rod shaped organelles specific for ECs that contains von Willebrand Factor (vWF) protein, but also other proteins such as P-selectin and IL-8. These organelles secrete their vWF stores by exocytosis (Nightingale, 2013); (4) Expression of a number of cell surface adhesion molecules, such as PECAM-1, Vascular Cell Adhesion Molecule 1 (VCAM-1), E-selectin, and additional cell-cell adhesion molecules such as vascular endothelial cadherin (VE-Cadherin) that are enriched at junctions between ECs (Nourshargh and Alon, 2014); (5) The overall phenotype of ECs can vary greatly, depending on their vascular bed, tissue localisation and vessel type, e.g. arterial vs venous and vascular vs lymphatic (Bouis et al., 2001);

During embryonic development, ECs arise in concert with the hematopoietic lineage. In fact, both endothelial and hematopoietic cells are derived from the same progenitor cell, the hemangioblast (Choi et al., 1998). The cardiovascular system is the first organ to develop in the gastrulating embryo. The organisation of ECs into vessels in the absence of any vascular system in known as vasculogenesis. Angiogenesis is the continued expansion of the vascular tree in the embryo and continues into maturity, where it is important for wound healing and tumour metastasis (Cines et al., 1998)

ECs are important in inhibiting coagulation through a number of mechanisms, including expressing tissue factor inhibitors (Lupu et al., 1997), expression of heparin sulphate proteoglycans that inactive thrombin (Mertens et al., 1992), and production of endothelial cell protein C receptor (ECPCR) to inhibit the clotting cascade (Thiyagarajan et al., 2007). ECs also produce nitric oxide (NO) and prostacyclin to inhibit platelet aggregation (Moncada et al., 1976). Resting ECs very rarely interact with circulating leukocytes, as they sequester ligands and chemokines intracellularly and suppress the transcription of other inflammatory molecules (Deanfield et al., 2007). For example, P-selectin is found stored within Weibel-Palade bodies and has been shown to be recruited to this organelle during its formation at the trans-golgi network (Metcalf et al., 2008). This has been shown to be functionally important, where mice lacking vWF and therefore Weibel-Palade bodies, cannot store P-selectin properly and subsequently show decreased leukocyte adhesion (Denis et al., 2001).

1.2.2 Control of EC gene expression

The E26 transformation specific (ETS) family of transcription factors are essential for controlling EC gene expression under basal conditions. Indeed, ETS binding motifs have been found in a number of key EC expressed genes, such as *VEGFR2, TIE2, ENOS* and *CDH5* (Shah et al., 2016). In particular, the ETS related gene, or Erg, is a crucial regulator of EC homeostasis and gene expression. It is key in regulating the transcription of a number of EC junctional genes such as VE-Cadherin and Claudin-5, as well as in maintaining vessel development and vessel stability (Birdsey et al., 2008, Yuan et al., 2012). Particularly important is the anti-inflammatory actions of Erg, where it represses the expression of pro-inflammatory genes such as *ICAM1, VCAM1* and *IL8.* This repression is brought about through inhibition of nuclear factor kappa-light-chain-enhancer of activated B cells (NFκB) subunit p65 binding to its target gene promoters (Dryden et al., 2012, Sperone et al., 2011).

A range of other molecules are also key for regulating EC gene expression *in vitro* and in the mature vasculature *in vivo*. Sirtuin-1 (SIRT1) controls the angiogenic activity of ECs through regulation of chromatin remodelling and therefore gene expression (Potente et al., 2007). *In vivo*, where ECs in blood vessels are constantly exposed the laminar shear stress, an anti-oxidant and anti-apoptotic gene expression phenotype is induced, which is cytoprotective and helps ensure EC homeostasis is maintained (Wasserman et al., 2002).

Angiopoietin-1 controls vascular development through the transcription factor Forkhead Box protein O1 (FoxO1), leading to a pro-survival phenotype and maturation of blood vessels (Daly et al., 2004). Angiopoietin-1 has also been shown to induce Erg phosphorylation through PI3K/Akt signalling, increasing the transcription of Erg-responsive genes such as Delta-like ligand 4 (Dll4) and so regulating vascular tone and stability (Shah et al., 2017). In addition, angiopoietin-1 controls EC proliferation and migration through increased expression of IL-8, resulting from elevated MAPK and PI3K signalling, inducing increased DNA binding of the transcription factor AP-1 to the IL-8 promoter (Abdel-Malak et al., 2008).

1.3 Endothelial cells in inflammation

ECs can be activated by a number of stimuli, and this activation can be classed as either type I or type II. Type I activation is independent of further gene expression, while type II activation is dependent on additional transcription (Pober and Sessa, 2007). Type I activation involves binding of ligands to G-protein coupled receptors on the cell surface, triggering intracellular G-protein signalling and a subsequent increase in release of Ca^{2+} from the endoplasmic reticulum (ER). This increases blood flow, blood pressure (Harris et al., 2008) and vascular leakiness, as well as playing a major role in leukocyte recruitment. This type of activation is very short lived, only lasting for about 10-20 minutes. Longer activation and prolonged inflammatory responses require type II activation, mediators of which include tumour necrosis factor α (TNFα) and interleukin 1 β (IL-1β). Stimulants such as these lead to activation of transcription factors (e.g. nuclear factor kappa-light-chain-enhancer of activated B cells (NFκB) and activator protein 1 (AP-1)) that initiate the transcription of pro-inflammatory genes. TNFα and IL-1β also cause vascular leakiness through the reorganisation of EC actin and tubulin cytoskeletons. Leukocyte recruitment is much more efficient following type II activation due to the synthesis and release of chemokines (e.g. CXCL1, IL-8, CCL2) and upregulation of adhesion molecule expression (e.g. E-selectin, ICAM-1 and VCAM-1) that facilitate efficient emigration of leukocytes into inflamed tissues (Ley and Reutershan, 2006).

1.3.1 Generation of chemokines by endothelial cells

The production of chemokines by ECs is crucial for the efficient recruitment of leukocytes to sites of injury or infection. Primarily, chemokines act to induce integrin expression, clustering and activation on target leukocytes, such as LFA-1, resulting in the arrest of rolling leukocytes and the promotion of TEM (Turner et al., 2014). Perhaps the most studied chemokine is IL-8 (CXCL8), and its mouse homologs Cxcl1, Cxcl2 and Cxcl5, which are highly chemotactic and crucial for neutrophil recruitment. It is also chemotactic for monocytes and some lymphocytes. These chemokines all bind with various affinities to the receptor CXCR2 on target leukocytes, activating downstream signalling pathways induce the subsequent firm adhesion of leukocytes.

Binding of IL-8 to its receptor stimulates the formation of β2 integrin complexes in neutrophils (Detmers et al., 1990) and has been shown to induce β2 integrin mediated arrest of neutrophils *in vivo* (Bargatze and Butcher, 1993). Downstream signalling events of IL-8 receptor engagement include MAPK and PKC activation, which are both needed for IL-8 stimulated adhesion of neutrophils through Mac-1 *in vitro* (Takami et al., 2002) Binding of IL-8 to its receptor CXCR2 on target leukocytes has also been shown to induce signalling through the phosphatidylinositol 3-kinase/protein kinase B (PI3K/Akt) pathway, resulting in the mobilisation of molecules key for leukocyte TEM such as the integrin Mac-1 (Smith et al., 2006).

The synthesis of chemokines by ECs is well established and this process can be upregulated by inflammatory stimuli (Oynebraten et al., 2004). Human lung microvascular ECs have been shown to constitutively express CCL2 and IL-8, and their increased expression can be induced by interleukin 1-alpha (IL-1α), interferon-gamma (IFNγ) and TNFα (Brown et al., 1994). Some chemokines, such as IL-8, are preformed and are contained in Weibel-Palade bodies alongside vWF and as a result IL-8 is rapidly released within minutes of stimulation by histamine and thrombin (Utgaard et al., 1998). Furthermore, additional chemokines such as Gro-α (CXCL1) and CCL2 have been demonstrated to reside pre-stored in small vesicles, and CCL26 (Eotaxin 3) has been shown to be present in Weibel-Palade bodies (Oynebraten et al., 2004). These chemokines are stimulated to be secreted rapidly from ECs by secretagogues such as histamine, whereas others such as CXCL10 (IP-10) and CCL5 (RANTES) are not.

1.3.2 Endothelial cell adhesion molecules

As explained in section 1.1.1, EC adhesion molecules are critical for leukocyte TEM. The selectins are a family of lectin-like transmembrane glycoproteins that function to mediate leukocyte rolling (as described in section 1.1.1). Only P- and E-selectin are expressed by ECs. The expression of E-selectin is upregulated in inflammation, while P-selectin is constitutively expressed by some vascular beds and is stored in Weibel-Palade bodies enabling it to be rapidly mobilised upon stimulation (Granger and Senchenkova, 2010). Ligands for E- and P-selectin on circulating leukocytes, such as

PSGL1, enable the efficient capture and rolling of leukocytes on vessel walls, further enabling their activation by chemokines displayed by those ECs.

Another important family of EC adhesion molecules are the Immunoglobulin-like adhesion molecules, namely ICAM-1, ICAM-2 and VCAM-1 and PECAM-1. These molecules bind cognate integrins expressed by rolling leukocytes to ensure slow leukocyte rolling is translated into arrest and firm adhesion. ICAM-1 and VCAM-1 expression is kept low under basal conditions but its expression can be rapidly induced by a number of inflammatory stimuli. By contrast, ICAM-2 expression remains significant in most vascular beds under basal conditions (Granger and Senchenkova, 2010). VCAM-1 is important for monocyte and lymphocyte adherence to ECs, through its interaction with the $\alpha_4\beta_1$ integrin VLA-4. β_2 integrins, such as Mac-1 and LFA-1, bind to ICAM-1 expressed on ECs and mediate adhesion of a number of leukocyte subtypes, especially neutrophils, monocytes and lymphocytes. Importantly, ICAM-1 and VCAM-1, are known to cluster on the EC at contact sites with the leukocyte, helping to firmly adhere the leukocyte to the surface of the endothelium prior to TEM (Tilghman and Hoover, 2002, van Buul et al., 2010, Wojciak-Stothard et al., 1999).

PECAM-1 was the first EC membrane protein shown to mediate neutrophil TEM *in vivo* and *in vitro*. PECAM-1 expressed on the endothelium interacts homophilically with PECAM-1 expressed on leukocytes, an interaction which has been shown to be required for leukocyte TEM (Muller et al., 1993). Blockade of PECAM-1 on either ECs or leukocytes with blocking antibodies abrogates leukocyte TEM, but has no effect on leukocyte adhesion to the endothelium (Muller, 1995).

In the majority of mouse strains, PECAM knockout blocks leukocyte TEM and arrests leukocytes on the apical side of the endothelium. This however, is not the case for all strains of mice. The commonly used C57BL/6 mice are unresponsive to either PECAM blockade or genetic deletion in terms of leukocyte TEM. Instead, leukocytes in this strain are arrest post TEM in the basement membrane. This highlights the complexity in the functional role of PECAM depending on the mouse strain used (Schenkel et al., 2004a, Sullivan and Muller, 2014).

Further studies into this phenomenon have shown that PECAM also regulates leukocyte TEM in a tissue and stimulus specific manner (Woodfin et al., 2007). Here

the authors show that PECAM-1 mediates leukocyte TEM responses to stimuli such as IL-1β in the mouse cremaster muscle and lungs but not in response to stimuli such as TNFα or adenovirus. In addition, cultured ECs only exhibit PECAM-1 dependent neutrophil TEM responses after stimulation with IL-1β, but not IL-8 or LTB_4. Clearly, PECAM-1 is not as essential for leukocyte TEM as originally described and its role in TEM is mouse strain, tissue and stimulus specific.

VE-Cadherin is a major EC surface adhesion molecule usually localised to junctional regions, which negatively regulates leukocyte TEM. It has been shown that blocking VE-Cadherin *in vivo* enhances neutrophil TEM (Gotsch et al., 1997) and that it is transiently removed from EC junctions during TEM (Allport et al., 2000). Under resting conditions, receptor-type tyrosine-protein phosphatase (VE-PTP) associates with VE-Cadherin and thus maintains it in a state of dephosphorylation. This stabilises VE-Cadherin at adherens junctions and therefore maintains the barrier function (Muller, 2014).

The adhesion of leukocytes to ECs has been shown to trigger the dissociation of this VE-Cadherin/VE-PTP complex, enabling VE-Cadherin to be phosphorylated. This occurs through a VCAM-1-Rac1-Pyk2 kinase signalling pathway (Nottebaum et al., 2008). The phosphorylation of VE-Cadherin inhibits binding of partners B-catenin and p120, facilitating its removal from adherens junctions. This process is essential for leukocyte TEM to occur, as mutation of either C-terminal tyrosine in the cytoplasmic tail of VE-Cadherin drastically reduces leukocyte TEM (Allingham et al., 2007).

These adhesion molecules are also important for other EC functions, such as angiogenesis. Endothelial expressed E- and P-selectin has been shown to be important in regulating skin wound healing, where deficiency of one or both delays healing (Yukami et al., 2007). The same is also true of ICAM-1. E-selectin has also been shown to be expressed in proliferating ECs in models of non-inflammatory angiogenesis (Kraling et al., 1996). Soluble forms of these adhesion molecules have also been shown to regulate angiogenesis. Soluble ICAM-1 (sICAM-1) has been shown to induce EC migration, tube formation and tumour growth *in vivo* (Gho et al., 2001, Gho et al., 1999), while E-selectin and soluble VCAM-1 (sVCAM-1) were shown to be chemotactic for ECs *in vitro* and angiogenic stimuli *in vivo* (Bodolay et al., 2002).

Numerous other adhesion molecules are expressed by ECs, with their pattern of expression and localisation, such as at junctional regions, playing a key role in inflammation and leukocyte TEM, as discussed below.

1.4 Endothelial cell junctions

Key to the function of ECs is their ability to form cell-cell junctions and therefore act as gatekeepers for access of blood borne proteins and circulating immune cells to the interstitial tissue. ECs adhere to each other through these junctions, the interactions in which are mediated by a number of transmembrane proteins. These proteins are linked to intracellular partners that help stabilise the junctions through anchoring the actin cytoskeleton (Bazzoni, 2004). During the process of leukocyte transmigration, the interaction of leukocytes with EC junctional molecules ensures that the barrier between the blood and the tissue remains intact. EC junctions, established at the contact point between two adjacent ECs (see Figure 1.2), form two principal modes of cell-cell adhesion; adherens junctions and tight junctions, each of which is described in detail below:

1.4.1 Adherens junctions

Adherens junctions are found across the mature vasculature, in both blood and lymphatic vessels. In ECs, they are characterised by the expression of an EC specific cadherin, namely VE-Cadherin. This molecule is expressed during development once cells become committed to the EC lineage (Breier et al., 1996). ECs have also been shown to express other cadherins such as N-Cadherin and T-Cadherin, albeit at much lower levels (Ivanov et al., 2001, Navarro et al., 1998). In stable adherens junctions, VE-Cadherin is found bound to its partner molecules, the catenins, which anchor the junctions into the actin cytoskeleton of the cell. Most well studied of these are β-catenin and plakoglobin. Binding of these catenins to VE-Cadherin at cell-cell contacts stabilises them and sequesters them at the membrane, inhibiting their activity to shuttle to the nucleus and regulate gene transcription (Yamada et al., 2005). Thus, reduced expression of VE-Cadherin may increase the free cytosolic pool of catenins and therefore increase transcriptional activity resulting from their signalling.

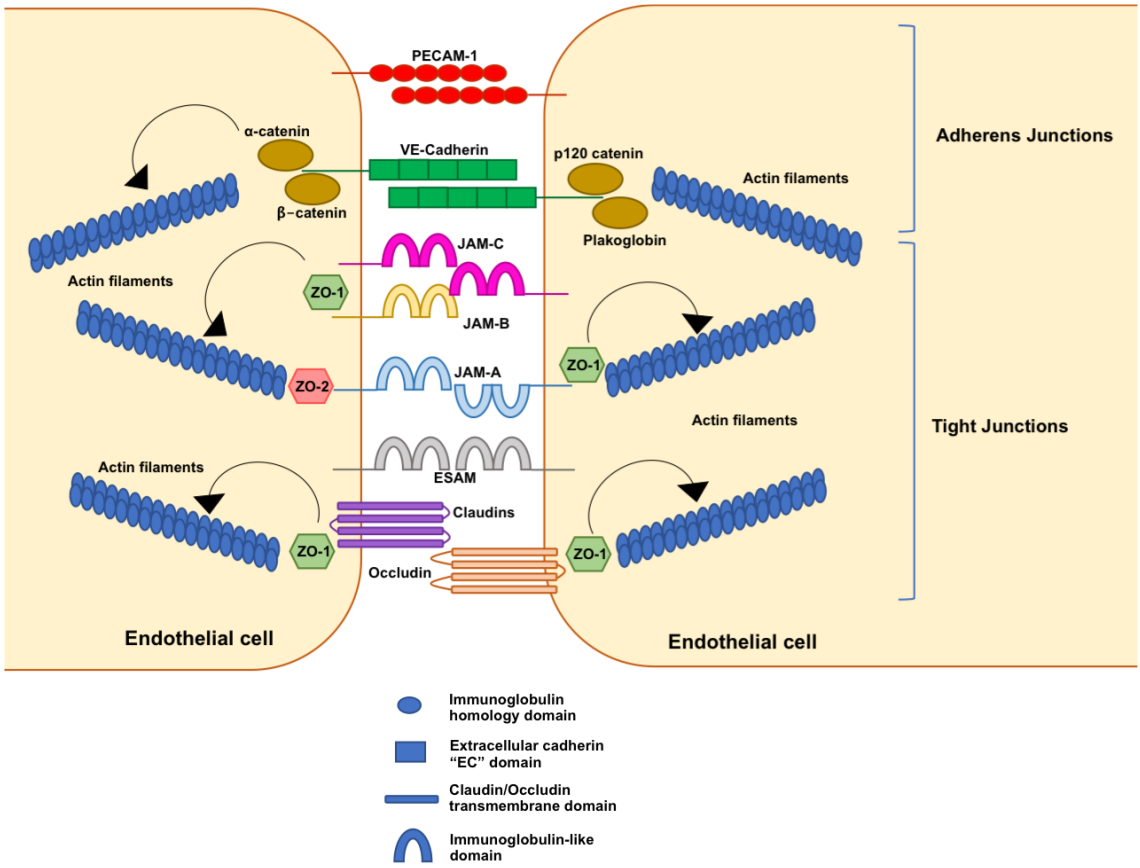

Figure 1.2. Organisation of endothelial cell junctions.
Endothelial junctions are split into two distinct types; adherens and tight junctions. Adherens junctions, shown here at the top, classically contain transmembrane proteins such as VE-Cadherin and PECAM-1. These are the first junctions to form during EC junction biogenesis and are heavily cross-linked to the actin cytoskeleton through the activity of VE-Cadherin binding proteins such as α- and β-catenin. Tight junction proteins were originally characterised by the expression of zona occludens proteins, ZO-1 and ZO-2 being the most prominent. These intracellular proteins have been shown to bind a number of transmembrane proteins at tight junctions, such as the claudins, occludin and members of the JAM family. Hetero- and homophilic interactions between members of the JAM family are often found at the edges of tight junctions, immediately adjacent to areas of adherens junctions. While adherens junctions are primarily important for structural organisation, tight junctions, as the name might suggest, form an impervious barrier to blood and tissue fluid.

PECAM-1 is another transmembrane protein that is often found at the edge of adherens junctions is ECs but is not restricted to this compartment. It can also be found on non-junctional apical membranes, as well as being expressed on both leukocytes and platelets. It is important for regulating leukocyte transmigration and has been shown in a number of models to regulate vascular permeability. Both PECAM-1 knockdown (KD) ECs and PECAM-1 knockout (KO) mice exhibit increased

permeability and vascular leakage (Muller, 1995, Privratsky and Newman, 2014). It has also been shown to associate with β-catenin, suggesting it uses a similar mechanism to signal from EC adherens junctions.

Adherens junctions are crucial in forming stable cell-cell contacts and supporting the formation of a confluent EC monolayer. These molecules also have complex interactions with the intracellular cytoskeletal network. As such, adherens junctions are crucial for EC functionalities. For example, VE-Cadherin deficient ECs are unable to respond to vascular endothelial growth factor (VEGF) stimulation (Carmeliet et al., 1999). It was also discovered in the same study that VE-Cadherin associates with vascular endothelial growth factor receptor 2 (VEGFR2) at adherens junctions to induce PI3K activation upon VEGF binding to VEGFR2, thus promoting EC survival.

1.4.2 Tight junctions

In epithelial cells, tight junctions are mostly found at the apical side of the junction and the adherens junctions located below in a more basolateral manner. In ECs, the distribution of the two types is much less defined and they are more intermingled throughout the whole junction/cleft, forming a zipper-like structure (Dejana, 2004). The tight junctions, originally defined as the zona occludens, as the name would suggest form tight contacts between adjacent ECs to act primarily as a diffusion barrier (Bazzoni, 2004). Tight junctions vary considerably according to their localisation within the wider vascular tree. Areas exposed to high laminar flow, such as aortic ECs, have very well organised tight junction structures more located to the apical side. By contrast post-capillary venules, which are the primary sites of leukocyte transmigration, have much less complex tight junction structures.

A number of molecules classically define the tight junctions of ECs. Occludin was the first transmembrane protein of tight junctions to be identified, where it is present at high concentrations in brain ECs especially. As such, it is a crucial determinant of brain EC permeability, an important function in this tissue bed (Hirase et al., 1997). Of the claudin molecules, Claudin-5 is the most prominent in ECs, where it acts to limit paracellular permeability across EC monolayers (Kluger et al., 2013). Intriguingly, VE-Cadherin in adherens junctions has been shown to regulated Claudin-5 expression by

preventing the nuclear translocation of β-catenin which represses Claudin-5 expression. This indicates cross-talk can occur between these two junctional structures in ECs (Gavard and Gutkind, 2008).

Zona occludens-1 (ZO-1) is perhaps the most well studied tight junction protein. Along with its closely related family members zona occludens-2 (ZO-2) and zona occludens-3 (ZO-3), these are cytosolic proteins that associate peripherally with tight junction structures to organise and assemble molecular complexes. ZO-1 can bind to a number of tight and adherens junctions molecules such as occludin, claudins, JAMs and VE-Cadherin, and also links into the actin cytoskeleton through proteins such as cortactin and cingulin-like 1 (Bazzoni et al., 2000, Tornavaca et al., 2015, Odenwald et al., 2017). Recently, it has been identified that ZO-1 is an important regulator of cell-cell tension and adherens junctions in ECs, angiogenesis and barrier formation (Tornavaca et al., 2015).

1.4.3 Formation of EC junctions

The mechanisms by which EC junctions are established are poorly understood. Its widely accepted that significant actin cytoskeleton rearrangements are likely to be involved during initial contacts between two adjacent ECs. One recent study has used subconfluent human umbilical vein endothelial cells (HUVECs) to determine the initial events in formation of EC adherens junctions (Hoelzle and Svitkina, 2012). Here, protruding lamellipodia convert into filopodia-like bridge structures in initial cell-cell contacts. These bridges are highly enriched with VE-Cadherin and filopodia markers such as fascin. The actin network within these filopodia collapses into tight actin bundles as the bridges are formed. Non-muscle myosin II invades and incorporates into the maturing bridges to ensure stabilisation of these nascent structures. The activity of myosin II in these bridges is essential for continued bridge maturation and VE-Cadherin accumulation.

It is not known how formation and stabilisation of adherens junctions in ECs then leads to tight junction formation. In epithelial cells, E-Cadherin contacts in adherens junctions are important for the organisation of tight junctions (Contreras et al., 2002).

Presumably a similar mechanism occurs in ECs, where the establishment of stable VE-Cadherin contacts would enable the organisation of tight junctions.

1.5 Junctional adhesion molecules (JAMs)

One important family of molecules involved in the formation of EC tight junctions are the JAMs. These molecules are members of the CTX (Cortical Thymocyte marker for Xenopus) family and belong to the wider immunoglobulin superfamily of molecules. The family consists of three closely related molecules, Junctional adhesion molecule-A, -B and -C (JAM-A, JAM-B and JAM-C), also known as the classical members. The family also includes the related proteins junctional adhesion molecule-4 (JAM4), JAM-like (JAM-L), Coxsackie and adenovirus receptor (CAR), CAR-like membrane protein (CLMP) and endothelial cell-selective adhesion molecule (ESAM). Much of the functions of the classical JAMs have been identified through their roles in tight junctions of epithelial and ECs (Ebnet et al., 2004).

1.5.1 Expression

JAM-A has been shown to be expressed on the surface of both epithelial and ECs (Liu et al., 2000), together with various blood cells (including platelets, monocytes, and lymphocytes) and tissue resident immune cells (macrophages and dendritic cells) (Gupta et al., 2000, Malergue et al., 1998, Williams et al., 1999). JAM-B expression by contrast is restricted to the endothelium, both vascular and lymphatic (Palmeri et al., 2000), and no expression has been reported on any circulating cells. Similar to JAM-A, JAM-C is expressed on both epithelial and ECs, as well as a number of other cell types discussed in section 1.3.4. No expression has yet been found on circulating mouse blood cells, however it is expressed on various human leukocyte subsets.

All of the JAMs localise to the tight junction regions of polarised epithelial and ECs, however they differ in their sub-compartmental localisation. JAM-C co-localises with ZO-1 at tight junctions, whereas JAM-A only partially co-localises with ZO-1 (Aurrand-Lions et al., 2001b) and JAM-B is found more diffusely at the lateral membrane. The difference in expression is also apparent in different tissue. For example, high endothelial venules (HEVs) and lymphatic ECs have high levels of JAM-B and JAM-C, but lower levels of JAM-A (Aurrand-Lions et al., 2001b).

Table 1.1. Expression and functions of the members of the JAM family.

Molecule	Expression	Functions
JAM-A	Epithelial cells, endothelial cells, platelets, monocytes, lymphocytes, macrophages, dendritic cells	Angiogenesis - Blockade of JAM-A reduces bFGF driven angiogenesis. bFGF stimulates dissociation of JAM-A from $\alpha_V\beta_3$ to stimulate angiogenic signalling; Inhibits VEGF-R2 driven angiogenesis. Leukocyte trafficking – Binds LFA-1 expressed on leukocytes; Acts in sequence with PECAM-1 and ICAM-2 to guide neutrophil TEM; Relocalised away from EC junctions to help guide leukocyte TEM.
JAM-B	Endothelial cells	Leukocyte trafficking – Regulates T cell migration; Interacts with $\alpha_4\beta_1$ integrin on T cells to increase adhesion to ECs. Stem cell homeostasis – Maintains hematopoietic stem cells in the bone marrow through interaction with JAM-C
JAM-C	Epithelial cells, endothelial cells, platelets (humans), fibroblasts, Schwann cells, lymphocytes	Angiogenesis – Blockade of JAM-C reduces tumour growth and angiogenesis; sJAM-C is a potent inducer of angiogenesis. Permeability – JAM-C is pro-permeability; Loss of or blockade of JAM-C reduces permeability in a VE-Cadherin dependent manner. Platelets – mediates binding of platelets to DCs to induce lymphocyte proliferation and platelet phagocytosis by DCs. Binds $CD34^+$ hematopoietic stem cells to regulate homing to bone marrow niches. Leukocyte trafficking – Binds Mac-1 integrin to direct neutrophil TEM and TEpM; Blockade results in reduced monocyte TEM; Mediates leukocyte infiltration in response to I/R injury; I/R injury causes redistribution and loss of junctional JAM-C, resulting in increased neutrophil rTEM; Regulates chemokine secretion in lymph node fibroblasts important for controlling T cell homing. Inflammatory diseases: Increased expression in arthritic synovium resulting in increased neutrophil infiltration; oxLDL induces JAM-C redistribution in atherogenic lesions and increases leukocyte infiltration into plaques.
JAM-L	Neutrophils, monocytes	Leukocyte trafficking – Important for TEpM of neutrophiils. Binds to CD49d/CD29 integrin on monocytes to increase adhesion to ECs.
CAR	Endothelial cells (lymphatic only), epithelial cells, cardiomyocytes	Spermatogenesis: Regulates spermatid polarity and male fertility through its interaction with JAM-C
ESAM	Platelets, endothelial cells	Leukocyte trafficking – Regulates leukocyte migration; ESAM KO mice exhibit reduced leukocyte TEM but with no effect on adhesion or rolling.
JAM4	Epithelial cell	Permeability: Regulates epithelial cell permeability

1.5.2 Structure and interactions

The classical JAM family members have very similar structures, sharing about 35% sequence identity in mice (Aurrand-Lions, 2000), and have less identity (about 15%) to the more distant family members (e.g. JAM-L). The JAMs are type I transmembrane glycoproteins, with a structure composed of two Immunoglobulin (Ig)-like extracellular domains, a transmembrane domain and a short cytoplasmic tail containing a type II PDZ binding motif and ZO-1 binding domain. The two Ig domains are made up of one V-type domain containing a J-like sequence at the N-terminal end and a C2-type domain which is proximal to the transmembrane domain. For JAM-C, both the V-type and C2-type domain contain one disulphide. In JAM-B and JAM-C, the V-type domain has one disulphide bridge as for JAM-A, whereas the C2-type domain contains two disulphide bridges (see Figure 1.3). The type II PDZ binding motifs in the classical JAMs can interact with a number of intracellular scaffolding proteins which helps form polarity complexes (Ebnet, 2003). The non-classical JAMs differ mainly in their C-terminal sequences, which are longer and contain and type I PDZ binding motifs instead of type II motifs.

JAMs can form homophilic interactions in *trans* via their extracellular domains, and they can also form heterophilic, interactions with other JAM family members or integrins, in either cis or *trans* configurations. For example, JAM-B and JAM-C form a heterophilic interaction between adjacent ECs (Lamagna et al., 2005b), while JAM-A is able to interact with LFA-1 on leukocytes and $\alpha_V\beta_3$ integrin on the endothelium (Fraemohs et al., 2004, Naik and Naik, 2006). JAM-B can also interact with $\alpha_4\beta_1$ integrin on leukocytes (Ludwig et al., 2009).

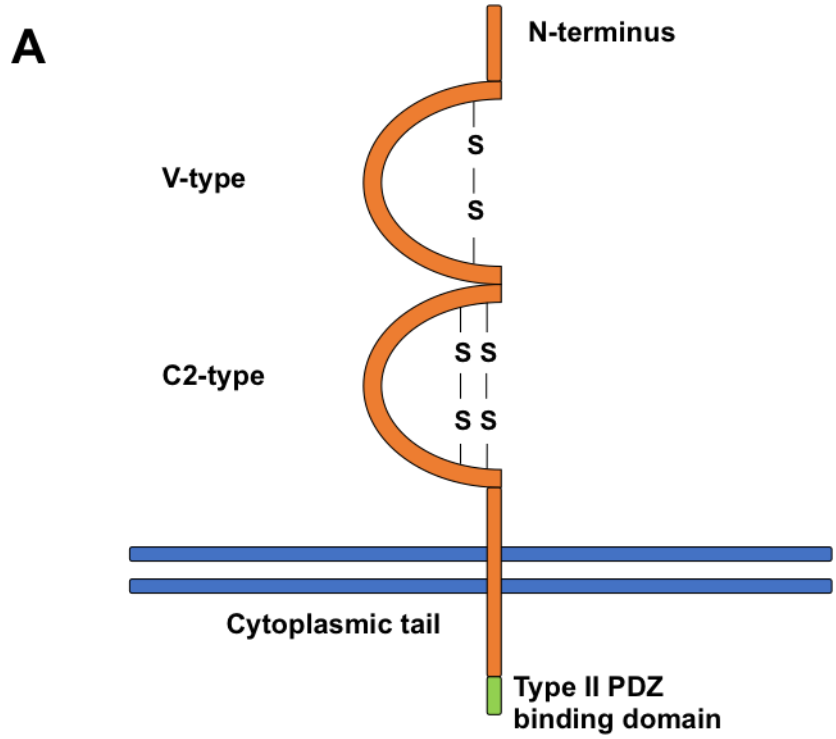

B

	Amino acid				
Molecule	C^{-4}	C^{-3}	C^{-2}	C^{-1}	C-term
JAM-A	S	S	F	L	V
JAM-B	K	S	F	I	I
JAM-C	S	S	F	V	I

Figure 1.3. Schematic structure of JAM-C and its type II PDZ binding domain. (A) Structure of JAM-C. From the N-terminal end, the JAM-C extracellular domain contains two Ig-like domains, one V-like and one C2-like, held in conformation by disulphide bridges. This is followed by a short single pass transmembrane domain and a short cytoplasmic tail, which contains a type II PDZ binding domain at the C-terminus. This domain enables binding of JAM-C to PDZ domain containing proteins such as ZO-1.
(B) Amino acid sequence of the type II PDZ binding domains of JAM-A, -B and –C. Al three of the classical JAMs share high sequence similarity in their PDZ-binding domains, reflecting both their overall sequence and structural homology and also their ability to similarly bind proteins such as ZO-1. The five amino acid sequence of the PDZ binding domain begins at the C-terminus in the JAMs, here shown as C-term, with each corresponding amino acid referred to as C^{-1}, C^{-2} and so on.

1.5.3 Functions of the JAM family in the endothelium and beyond

The functional roles of EC JAMs have been intensely studied, indicating their important roles in inflammation and leukocyte trafficking, vascular permeability and angiogenesis.

JAM-A was the first family member identified to play a role in leukocyte transmigration (Martin-Padura et al., 1998). This study showed that blockade of JAM-A inhibited monocyte transmigration across endothelial monolayers *in vitro* and into sites of inflammation in a mouse subcutaneous air pouch model(79)(78). Use of JAM-A deficient mice subsequently highlighted the importance of JAM-A in leukocyte transmigration (Cera et al., 2004). Further analysis of this phenomenon revealed that JAM-A controls leukocyte TEM by interacting with LFA-1 on leukocytes (Ostermann et al., 2002). Some *in vitro* studies have indicated that the relocalisation of JAM-A away from EC junctions following inflammatory stimulation could be responsible for guiding leukocyte TEM (Stamatovic et al., 2012). There are inconsistencies in the literature though for the importance of JAM-A in regulating this process. Some have reported that inflammatory stimulation of ECs with TNFα and IFNγ under flow conditions, where JAM-A is redistributed away from lateral junctions, has no effect on leukocyte TEM (Shaw et al., 2001). *In vivo* studies conducted by our lab identified that sequential action of intercellular adhesion molecule 2 (ICAM-2), JAM-A and PECAM-1 modulated IL-1β-induced migration of neutrophils through venular walls (Woodfin et al., 2009).

JAM-A and JAM-B also have a role in angiogenesis, with the majority of work being conducted in relation to JAM-A. It was shown that basic fibroblast growth factor (bFGF) activation of ECs caused a dissociation of JAM-A:$\alpha_V\beta_3$ integrin interaction that allowed angiogenic signalling to proceed (Naik et al., 2003). Blockade of JAM-A signalling reduces bFGF induced angiogenesis, and JAM-A deficient mice have impaired bFGF-induced angiogenesis (Cooke et al., 2006). Recent evidence has highlighted a role for JAM-A in regulating wound induced inflammation and angiogenesis. Chatterjee et al., showed that JAM-A deficient mice have spontaneous corneal wounding associated with angiogenesis. This is correlated with increased Vascular endothelial growth factor A (VEGF-A) and VEGF receptor 2 (VEGF-R2) signalling, suggesting that JAM-A also regulates VEGF-R2 driven angiogenesis (Chatterjee et al., 2013).

JAM-B has been less well studied in leukocyte TEM. It is known to interact with $\alpha_4\beta_1$ integrin, which in turn mediates T-lymphocyte adhesion to ECs via VCAM-1 (Berlin et al., 1993). JAM-B has been implicated in leukocyte extravasation into mouse skin (Ludwig et al., 2005) and there is evidence for its involvement in supporting T cell rolling and adhesion via interactions with $\alpha_4\beta_1$ integrin expressed on the T cells (Ludwig et al., 2009). JAM-B has also been shown to maintain hematopoietic stem cells in the bone marrow through a JAM-C dependent interaction (Arcangeli et al., 2011), and in regulating VEGF/VEGFR2 signalling during angiogenesis (Meguenani et al., 2015). However most of the interest in JAM-B has been in relation to its interaction with JAM-C in the endothelium (see section 0).

JAML has been shown to be expressed on both neutrophils and monocytes. In neutrophils, it regulates transepithelial migration (TEpM) (Zen et al., 2005), while in monocytes it binds to CD49d/CD29 integrin expressed on ECs and ensures increased adhesion to ECs (Luissint et al., 2008). ESAM expression is restricted to platelets and EC tight junctions, where it plays a role in neutrophil TEM. ESAM KO mice display much reduced leukocyte transmigration, while adhesion and rolling where unaffected. In addition, these mice exhibited reduced vascular permeability as stimulated by VEGF, due to reduced Rho activation at EC junctions (Wegmann et al., 2006). CAR has been shown to be crucial for spermatogenesis in mice through its interactions with JAM-C in spermatozoa, postulating a role for both molecules in spermatogenesis and male fertility (Mirza et al., 2006). JAM4 was originally identified as an adhesion molecule that regulates epithelial permeability. No roles have yet been found for this molecule in leukocyte migration. Studies on JAM4 KO mice have revealed no clear phenotype and so the physiological role of this molecule is unclear (Nagamatsu et al., 2006).

1.6 JAM-C

1.6.1 Expression

JAM-C was originally identified in 2000 as a novel immunoglobulin superfamily member similar in sequence to JAM-A and expressed in both vascular and lymphatic ECs (Aurrand-Lions et al., 2001a). Following this, it was demonstrated that this expression of JAM-C localised to the tight junctions of ECs (Aurrand-Lions et al., 2001b). The literature suggests that JAM-C exhibits different expression patterns between various types of ECs. Orlova et al., 2006 showed that in human dermal microvascular ECs (HDMECs), JAM-C is redistributed to the junctions of ECs from an intracellular pool upon stimulation with vasoactive factors such as VEGF or histamine (Orlova et al., 2006). In HUVECs JAM-C is constitutively expressed at EC junctions and this is reportedly increased following cell stimulation by VEGF or histamine (Orlova et al., 2006). However this contrasts with other reports which showed that surface JAM-C expression is low In HUVECs, but that there is a significant intracellular pool of JAM-C (Sircar et al., 2007). Application of inflammatory stimuli such as lipopolysaccharide (LPS) and IL-1β did not increase the junctional expression of JAM-C in this model. Data acquired as part of the present work in our lab has shown that JAM-C is expressed at the cell surface of HUVECs where it is most abundant at the cell-cell junctions.

Unsurprisingly, JAM-C is also expressed in epithelial cells, where like JAM-A, it localises to tight junctions, see Figure 1.4 (Ebnet, 2003, Zen et al., 2004). In particular, it has been shown to be important in the formation of tight junctions in the human retinal pigment epithelium (Economopoulou et al., 2009). Expression of JAM-C has also been found in a number of other tissues, including nerves, fibroblasts, platelets and leukocytes. Our laboratory discovered JAM-C expression in peripheral nerves, where the expression was found to be localised to Schwann cells at junctions (see Figure 1.4) between myelin end loops (Scheiermann, 2007). Further investigations revealed that Schwann cell JAM-C KO mice exhibited several neural and behavioural defects (Colom et al., 2012), postulating a role for JAM-C in modulating neuronal responses. Fibroblasts from a number of tissue sources, such as cornea, lung and skin, express JAM-C in adherens-like junctions and colocalise with ZO-1 expression. More recently JAM-C expression has also been shown in lymph node fibroblast reticular cells where it is important for regulating T cell emigration from lymph nodes (Frontera et al., 2011).

Platelets also express JAM-C, where it was identified as a receptor for Mac-1 integrin expressed on leukocytes (Santoso et al., 2002). In atherosclerotic lesions, JAM-C is highly expressed in both endothelial and smooth muscle cells (Keiper et al., 2005). Human leukocytes but not mouse leukocytes express JAM-C, therefore highlighting a potential species difference in roles of JAM-C. JAM-C expression has been found on both naïve and activated T cells (Immenschuh et al., 2009) as well as B lymphocytes where it is postulated it might present a marker for distinguishing germinal center B cells (Ody et al., 2007).

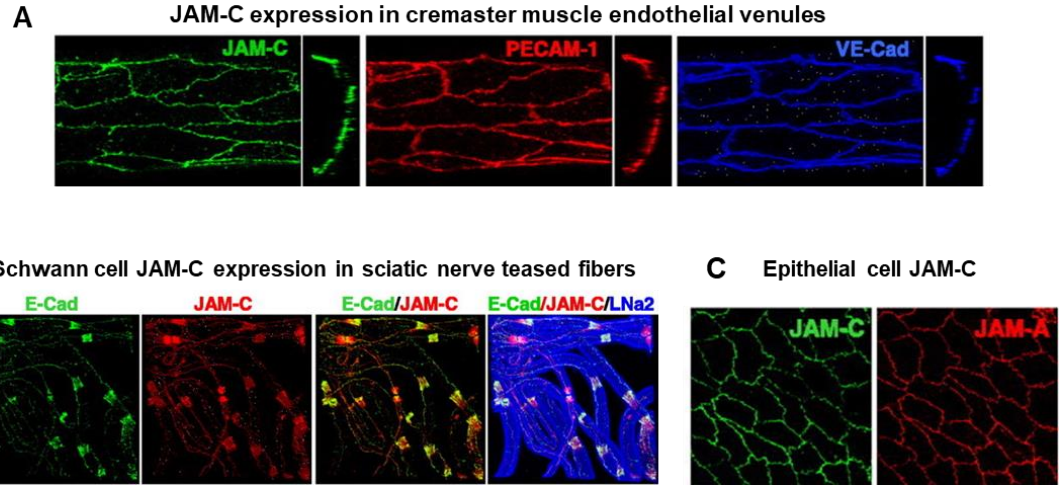

Figure 1.4. Expression of JAM-C in mouse tissue.
(A) ECs from cremaster venules co-stained for EC markers VE-Cadherin and PECAM-1; (B) epithelial cell layer of cremaster muscle; (C) Sciatic nerves stained for adherens junction marker E-Cadherin, Schwann cell basement membrane marker laminin α2, and JAM-C. Figure adapted from Colom et al., 2012

1.6.2 JAM-C ligands

A number of ligands for JAM-C have been identified. At EC tight junctions, JAM-C forms homodimers *in trans* with JAM-C, as well as heterodimers with JAM-B on adjacent ECs (Arrate et al., 2001, Lamagna et al., 2005b). It has also been shown to interact with the β2-integrin Mac-1 that is present on a number of leukocytes and therefore a Mac-1-JAM-C interaction is likely involved in supporting leukocyte adhesion and transmigration (Chavakis et al., 2004, Santoso et al., 2002). The PDZ binding motif of JAM-C has been shown to interact with the cell polarity protein protease activated

receptor 3 (PAR-3), thereby proposing a role for JAM-C in regulating cellular polarity (Ebnet, 2003, Ebnet et al., 2017). Through the type II PDZ binding domain, JAM-C is able to bind to the tight junction protein ZO-1 in epithelial cells (Ebnet, 2003). Co-localisation of ZO-1 and JAM-C has been demonstrated in ECs (Orlova et al., 2006), but a direct interaction has not yet been identified. JAM-C has also been shown to colocalise with the JAM family member CAR in mouse testis, where JAM-C is crucial for the differentiation of spermatids into spermatozoa (Gliki et al., 2004).

1.6.3 Role of JAM-C in vascular processes

Important endothelial functions such as angiogenesis and vascular permeability are regulated by JAM-C. Soluble JAM-C (sJAM-C) is a potent mediator of angiogenesis, where it stimulates EC migration *in vitro* and also *in vivo* across Matrigel membranes (Rabquer et al., 2010). Antibody-mediated blockade of JAM-C significantly reduces tumour growth and angiogenesis in mice injected with carcinoma cells (Lamagna et al., 2005a). Vascular permeability is increased by the presence of JAM-C at EC junctions. Silencing of JAM-C in cultured ECs increases VE-Cadherin cell-cell contacts in a Ras related protein 1 (Rap1) dependent manner, resulting in decreased permeability (Orlova et al., 2006). Overexpression of JAM-C increases permeability, as do permeability inducing stimuli such as thrombin, which increases junctional JAM-C expression in ECs (Li et al., 2009).

JAM-C expressed on human platelets mediates the adhesion of dendritic cells (DCs) to those platelets through interaction with Mac-1. It has been shown that under conditions of flow, the initial interaction between DCs and platelets is mediated through a Mac-1/JAM-C interaction. This interaction induces differentiation of the DCs and subsequently enables them to induce lymphocyte proliferation. Prolonged DC-platelet interactions through Mac1/JAM-C result in platelet phagocytosis and also in DC apoptosis, which is dependent on that JAM-C/Mac-1 interaction. Indeed, the pre-treatment of DCs with sJAM-C decreases DC apoptosis (Langer et al., 2007). DCs are implicated in the progression of atherosclerosis, where they are found in the intima of atherosclerosis-prove vessels. As such, it is speculated by the authors here that high platelet concentrations in atherosclerosis lesions may recruit DCs through JAM-C/Mac-1 and so perpetuate the inflammation. However, it is important to note here that

platelet expressed JAM-C has only been demonstrated in humans and not mice and as such, demonstrating this mechanism in mice *in vivo* would be rather difficult.

Platelet expressed JAM-C is also important for facilitating the binding of CD34+ hematopoietic progenitor cells, presenting a potential role for JAM-C in directing homing of these cells to bone marrow niches (Stellos et al., 2012). Indeed, in this study it was shown that platelets activated with thrombin *in vitro* had increased JAM-C expression and also correlated with increased P-selectin expression on platelets from coronary artery patients. Adherence of CD34+ progenitor cells to platelets was block in this *in vitro* model by the addition of antibodies against JAM-C or its counter-receptor MAC-1 reduced this adhesion and this occurred under conditions of flow.

1.6.4 JAM-C and leukocyte migration

Two studies in 2004 dictated a role for JAM-C in regulating neutrophil TEM and also trans-epithelial migration. In both studies it was found this migration occurs in a Mac-1 dependent manner, relying on the previously established interaction of EC JAM-C with Mac-1 integrin expressed on leukocytes (Zen et al., 2004). In ECs, JAM-C does not participate in adhesion of leukocytes, but rather diapedesis through the endothelial barrier (Chavakis et al., 2004). Further studies identified that the accumulation of leukocytes to inflammatory sites is reduced when treated with JAM-C functional blocking antibodies. Conversely, transgenic mice overexpressing JAM-C recruited significantly more leukocytes to the lungs of mice challenged with LPS (Aurrand-Lions et al., 2005).

JAM-C has also been shown to regulate monocyte TEM, using both *in vitro* and *in vivo* models. Treatment with anti-JAM-C blocking antibodies suppresses TNF-stimulated monocyte recruitment in mouse cremaster muscles (Bradfield et al., 2007). Monocyte TEM across HUVEC monolayers was reduced by blocking the JAM-C/JAM-B interaction in the same study, which also resulted in an increase in monocyte reverse TEM (rTEM) from the abluminal compartment.

Work conducted by our laboratory has determined that JAM-C is key in mediating leukocyte infiltration in response to inflammatory stimuli such as ischemia/reperfusion

(I/R) injury. Treatment of mice with soluble JAM-C reduced leukocyte infiltration in both kidney and cremaster muscle I/R models (Scheiermann et al., 2009). JAM-C KO mice exhibited markedly reduced leukocyte adhesion and TEM across venules in the same cremaster I/R model. This is in contrast to the findings of Chavakis et al., discussed previously, which postulated no role for JAM-C in leukocyte adhesion to HUVECs stimulated with Phorbol 12-myristate 13-acetate (PMA) (Chavakis et al., 2004), where JAM-C localises mainly to the cell-cell junctions. This can be consolidated by further findings from Scheiermann et al., which showed that the expression pattern of EC JAM-C was changed by I/R injury, with reduced expression at EC junctions and increased expression at non-junctional membranes that can support adhesion (Scheiermann et al., 2009). Further confirming this role of JAM-C in directing leukocyte TEM in I/R injury, transgenic mice overexpressing JAM-C had increased leukocyte adhesion and TEM in this model.

While JAM-C is important for directing leukocyte TEM in inflammation, disrupted expression of JAM-C has been shown to support aberrant modes of neutrophil TEM. Indeed, where I/R induces reduced expression of junctional JAM-C, increased frequency of hesitant and neutrophil rTEM is observed. This frequency is further increased in conditional EC JAM-C KO mice and by using JAM-C blocking antibodies. Furthermore, EC JAM-C KO mice exhibit neutrophil rTEM following inflammatory stimuli that don't normally support such modes of migration, such as IL-1β (Woodfin et al., 2011). Further investigations into the mechanisms behind this have revealed that I/R injury drives release of LTB4 by the injured tissue, which acts to recruit neutrophils and induce release of neutrophil elastase (NE), which in turn is a potent protease that cleaves EC JAM-C as neutrophils transmigrate the endothelium (Colom et al., 2015).

1.6.5 Additional roles for JAM-C in inflammation and cancer

Aside from its crucial role in leukocyte trafficking, JAM-C also has a number of additional roles in inflammation, inflammatory diseases and cancer. For example, JAM-C expressed on fibroblast reticular cells in lymph nodes is crucial for regulating chemokine secretion. Indeed, it was found that blocking JAM-C *in vivo* significantly reduced the amount of secreted CCL21 and CXCL12 from these cells, resulting in

reduced T cell egress and increased retention within lymph nodes (Frontera et al., 2011).

In human synovial tissue from rheumatoid arthritis, JAM-C expression was elevated and similarly this was the case in antigen-induced arthritic mice. In the latter, treatment with anti-JAM-C antibodies reduced the disease severity, with reduced levels of circulating arthritis markers such as amyloid A. This also correlated with reduced neutrophil infiltration (Palmer et al., 2007). In a separate study, myeloid cell adhesion to arthritic synovial tissue was also dependent on JAM-C expression (Rabquer et al., 2008).

JAM-C has also been studied within a variety of atherosclerosis models. Typically, atherosclerosis is seen as a primarily monocyte driven process, where monocyte interactions with the inflamed and activated endothelium induces monocyte extravasation and subsequent differentiation into macrophages that produce reactive oxygen species, pro-inflammatory cytokines and that ingest vast quantities of oxidised low-density lipoprotein (oxLDL) (Prame Kumar et al., 2018). Monocytes are recruited to the subendothelial intima through the tightly regulated leukocyte adhesion cascade, where activation of endothelial cells upregulates adhesion molecules (E-selectin, ICAM-1, VCAM-1) and chemokines (CCL2, CCL5, CXCL1) that are necessary for monocyte migration (Pamukcu et al., 2010). Early on in the progression of the disease, the atherosclerotic monocytes differentiate into foam cells due to their large quantities of ingested oxLDL to form the early plaque, or fatty streaks, within the intima of inflamed vessels. Over time, these fatty streaks develop into mature atherosclerotic plaques due to the accumulation of inflammatory leukocytes and lipid, which is surrounded by a cap of smooth muscle cells and extra cellular matrix. Thinning and subsequent rupture of the plaque releases plaque debris and causes thrombosis, coagulation and eventually artery stenosis (Woollard and Geissmann, 2010).

More evidence is emerging for the role of neutrophils within the pathogenesis of atherosclerosis, where they have been identified in both human and murine atherosclerotic lesions (Drechsler et al., 2010, van Leeuwen et al., 2008). Indeed, mouse neutrophils have been detected in both early lesions in the subendothelial intima, and also within rupture prone lesions (Rotzius et al., 2009). Data from human

studies have identified that neutrophils are present in the culprit lesions of myocardial infarction patients. Further study of human plaque samples has revealed that intra-plaque haemorrhage may release further neutrophils into the lesion, thus enriching neutrophils released proteases and increasing plaque fragility. Recent data from mouse atherosclerosis studies suggests neutrophils accumulate in large arteries very soon after high-fat diet feeding starts, where the lesion size is directly correlated with neutrophil size (van Leeuwen et al., 2008). The importance of neutrophils recruitment in the onset of atherosclerosis is highlighted by mouse studies using LTB_4 deficient mice. Here, where neutrophil recruitment is significantly impaired due to deficiency in LTB_4, the lesion size is significantly reduced and the levels of lesion leukocytes (macrophages and T cells) are also lower.

The study of JAM-C expression in atherosclerosis models has revealed that oxLDL induces a redistribution of JAM-C away from EC junctions, mediating leukocyte adhesion and TEM into atherosclerotic plaques and as such contributing to increased disease pathogenesis (Keiper et al., 2005). Efforts to interfere with JAM-C in atherosclerosis lead to increased monocyte rTEM out of inflamed lesions *in vivo*, thus decreasing the size of the atherosclerotic plaques. This makes targeting JAM-C an attractive target in this disease (Bradfield et al., 2016). However, one must consider the impact on neutrophil migration when targeting JAM-C in this model, where there would presumably also be an increase in neutrophil rTEM from these inflammatory sites, thus increasing the circulating population of activated neutrophils that may be detrimental to secondary organs such as the lungs and kidneys.

In type 1 diabetes (T1D), JAM-C was expression is upregulated around pancreatic islets of Langerhans in a virus induced T1D model. Treatment with JAM-C blocking antibodies in these mice reduced T1D incidence. Overexpression of JAM-C in ECs did not accelerate T1D disease progression. This highlights a likely role for JAM-C in regulating the trafficking of autoreactive T cells to β-cells in the pancreas (Christen et al., 2013).

Due to its significant role in regulating leukocyte TEM, much interest has also focussed on how JAM-C might be involved in regulating tumour cell migration and therefore metastasis. Indeed, it was found that adhesion of the cancer cell line NHI-H522 to ECs

was blocked by sJAM-C, postulating a role for JAM-C in tumour cell-EC interactions (Santoso et al., 2005). Recent work has found JAM-C to be expressed in tumours with a high metastatic potential (Fuse et al., 2007). In a model of metastatic melanoma, JAM-C KO mice showed reduced B16 melanoma cell metastasis to the lungs of challenged mice (Langer et al., 2011). Studies in ovarian cancer models established that EC JAM-C KO mice have increased survival, whereas JAM-C overexpressing transgenic mice have conversely reduced survival. Tumour growth was reduced in EC JAM-C KO mice, where vessels had reduced pericyte coverage and increased vascular leakage, indicating a role for JAM-C in organising functional tumour vessels (Leinster et al., 2013).

1.7 Autophagy

It is clear that JAM-C is key for regulating a number of EC functions, both under homeostatic and inflammatory conditions. This is highlighted by the disruption of processes such as leukocyte trafficking and angiogenesis when JAM-C expression is disrupted, targeted or re-distributed. It could be said that disruption of EC JAM-C, and perhaps more widely junctional integrity, impacts upon the homeostatic state of ECs and so resulting in the various phenotypes detailed above. A key process in the maintaining cellular homeostasis is autophagy, which is triggered by numerous cellular stressors and insults, as discussed in more detail below. As part of the work in this thesis, it was hypothesised that disruption of EC JAM-C expression would represent such a cellular insult and could therefore impact on EC autophagy.

Autophagy itself is an evolutionary conserved cellular process important in protein degradation. It is classically determined as a process of self-eating, where it functions to degrade long-lived proteins and dysfunctional organelles such as mitochondria and ribosomes. This enables the recycling of cellular nutrients to enable cell survival during times of cellular hardship, such as during starvation. Increasingly, autophagy is becoming recognised as a selective process, where proteins are deliberately targeted for degradation (Kaur and Debnath, 2015).

The molecular pathway of autophagy is a complex one, with a number of dedicated autophagy proteins (ATG proteins) and non-ATG signalling proteins involved. Initial stages of autophagy begin with formation of an isolation membrane, or phagophore,

which most likely derives from the endoplasmic reticulum or the trans-golgi, though this is yet to be fully defined. This membrane expands to engulf the target cargo/proteins/organelle, thus sequestering them in a double membrane autophagosome. These autophagosomes are matured by fusion with lysosomes, forming autophagolysosomes which promotes the degradation of the autophagosome content. Amino acids and other nutrients are then transported back into the cytosol (Glick et al., 2010).

More connections are being made between the autophagy pathway and protein secretion through unconventional routes. The ATG proteins have been implicated in secretion of Acb1 protein in yeast (Duran et al., 2010). They have also been found to be important for autophagy-mediated secretion of pro-inflammatory mediators such as IL-1β and high mobility group box 1 (HMGB1) (Dupont et al., 2011), which is discussed in more detail below.

1.7.1 Autophagy in infection and inflammation

Multiple studies have highlighted the important role of autophagy in conferring resistance to various pathogens that infect mammalian organisms. It functions to control infection with such microbes by helping in their degradation, as well as helping to coordinate an effective immune response. This importance is highlighted by the fact that loss of the key autophagy related protein 5 (ATG5) in neutrophils and macrophages leads to increased susceptibility to infections with *L. monocytogenes* and *T. gondii* (Zhao et al., 2008). Typically, cells of the innate immune system are the first line of defence to such pathogens, where engagement of pattern recognition receptors (PRRs) leads to their activation. Activation of PRRs by pathogens has also been shown to result in upregulation of autophagy in immune cells (Oh and Lee, 2014). In a related manner, autophagy also plays an important role in the cross-presentation of intracellular antigens to MHC class II antigens (Crotzer and Blum, 2009). This helps in the activation of CD4+ T helper cells, and as such leads to the coordination of an effective immune response.

The relationship between inflammation and autophagy during sterile conditions and non-pathogen induced inflammation is complex. Essentially autophagy is

characteristically an anti-inflammatory process, acting to suppress inflammasome activation under basal conditions (Deretic et al., 2013). This is highlighted by the fact the mice deficient in the autophagy related protein 16 (ATG16L) have increased production of IL-1β and IL-18 (Saitoh et al., 2008). Under sterile conditions, autophagy acts to rid cells of any cellular debris and defunct organelles that could act as endogenous inflammatory stimuli. Confirming this, blockade of autophagy by pharmacological or genetic means results in an accumulation of defective mitochondria and therefore and increase in endogenous inflammasome agonists. Autophagy also acts to suppress inflammatory signalling pathways, such as the NFκB pathway, so as to prevent aberrant inflammation under basal conditions. Here, IκB kinase (IKK) proteins are targeted for degradation by autophagy, through a pathway involving the chaperone protein Hsp90 (Trocoli and Djavaheri-Mergny, 2011).

As mentioned briefly earlier, a number of ATG proteins are known to function in unconventional secretion of pro-inflammatory mediators such as IL-1β and HMGB1. Indeed, it is thought that this autophagy-dependent secretion of IL-1β is important in the early acute phase of inflammasome activation. Investigations into the mechanisms behind this unconventional secretion have found that it is dependent on ATG5, as IL-1β secretion is completely ablated in ATG5-/- macrophages (Dupont et al., 2011). In addition, it seems the autophagy machinery cooperates with the golgi reassembly-stacking protein 55 (GRASP55) and the exocytosis regulator protein Ras related protein Rab8a (Rab8a) to achieve this unconventional secretion. In the same study, it was found that HMGB1 is a substrate for the same secretion model, raising the possibility that a number of other inflammatory mediators such as chemokines could be regulated in a similar manner. The latter is an issue addressed as part of the present work.

1.7.2 Autophagy in endothelial cells

The role of autophagy in EC physiology is becoming increasingly recognised. In normal quiescent cultures of ECs, there is a low level of basal autophagic flux, highlighted by the accumulation of autophagosomes in the presence of the late stage autophagy inhibitor chloroquine (Jiang, 2016). Stimuli such as oxLDL and LPS can trigger

autophagy in cultured ECs. *In vivo*, shear stress also induces autophagy, which acts in a cytoprotective manner to reduce oxidative stress, oxidative insults and inflammation. In the same manner, an increase in EC autophagy is associated with an increase in endothelial nitric oxide synthase (eNOS) expression under shear flow conditions (Guo et al., 2014).

More recent work has highlighted emerging roles for EC autophagy in regulating the haemostatic and angiogenic functions of ECs. Autophagy has been shown to be important for the secretion of vWF from Weibel-Palade Bodies *in vitro* and mice deficient in Autophagy related protein 7 (ATG7) show defective vWF release *in vivo* (Torisu et al., 2013). Another cytoprotective role of autophagy in ECs is highlighted by its role in regulating angiogenesis. Angiogenesis is crucial in recovery from ischemic events where hypoxic environments place extreme stress on the cells of the affected tissue. Pharmacological or genetic inhibition of autophagy results in decreased angiogenesis in ischemia models. Autophagy isn't necessary for production of angiogenic factors such as VEGF, but rather is important for reactive oxygen species (ROS) production and Akt signalling that direct effective angiogenesis (Du et al., 2012).

1.8 Aims

Studying JAM-C function *in vivo* has been somewhat limited by the severe phenotype that full JAM-C KO mice exhibit, with developmental, hematopoietic, neural and cardiovascular defects and male sterility (Imhof et al., 2007). As such, researchers have moved to using cell lineage-specific JAM-C knockouts, such as the Schwann cell specific JAM-C KO used to study the neural role of JAM-C (Colom et al., 2012). Our lab has acquired an endothelial specific JAM-C KO mouse line, where *JAM3* is selectively deleted in ECs by a Cre-recombinase expressed under the control of an endothelial expressed Tie2 promoter (Langer et al., 2011, Pellegrini et al., 2011, Woodfin et al., 2011). Using this tool as well as RNA interference (RNAi) approaches for knocking down JAM-C in ECs *in vitro*, the present project aims to further investigate the role of JAM-C in EC biology. The principal aims addressed in this project are as follows:

1) **To investigate the impact of JAM-C deficiency on EC junctions and EC morphology, proliferation and survival *in vitro***

   Cultured HUVECs were used to assess the role of JAM-C in EC biology *in vitro*. For this purpose, small interfering (siRNA) was employed to target JAM-C expression in cultured ECs, upon which they were assessed for junctional molecule expression and basic cellular characteristics such as proliferation and apoptosis.

2) **To investigate the impact of EC JAM-C deficiency on EC autophagy**

   The role of EC junctional molecules in regulating autophagy is poorly understood. We hypothesised that loss of EC JAM-C impacts the homeostatic status of ECs, such that autophagy is upregulated. The *in* vitro model of JAM-C KD HUVECs was thus used to assess this hypothesis, while classical pharmacological inhibition of autophagy was used to confirm a role for autophagy in this model.

3) **To investigate the impact of loss of JAM-C on global EC gene expression profiles.**

   Due to its critical role in ECs, we hypothesised that loss of EC JAM-C could impact gene expression profile of cultured ECs. To address this, a gene expression microarray study was be performed on cultured JAM-C deficient ECs, both under basal and IL-1β stimulated conditions. Differential gene expression analysis and

pathway analysis was used to investigate gene expression changes in JAM-C KD HUVECs, analysis that provided insight into potential pathways through which JAM-C regulates EC functions *in vitro.*

4) **To investigate the impact of JAM-C deficiency on chemokine generation and secretion by ECs.**

   The generation of chemokines by ECs is essential for directing effective leukocyte recruitment to sites of inflammation. Furthermore, disrupted EC JAM-C expression leads to aberrant modes of neutrophil TEM in *in vivo* models of inflammation. As such, we hypothesised that JAM-C deficient ECs could have disrupted generation of chemokines that may provide mechanistic insight into the phenomenon of neutrophil rTEM. This possibility was primarily investigated in an *in vivo* setting, using local inflammatory stimulation of EC JAM-C KO mice.

2 Materials and Methods

2.1 Animals

All mice were housed in individually ventilated cages under conditions of controlled 12-hour light/dark cycles in a constant temperature (21 ± 2^{o}C). Male and female mice were used for experiments between the ages of 4 and 15 weeks. All animal procedures were subject to Queen Mary, University of London ethical approval and carried out in accordance with the United Kingdom Home Office Animals Scientific Procedures Act 1986. Mice were humanely culled by cervical dislocation in agreement with Home Office regulations.

2.1.1 Mouse Strains

C57BL/6 Wild Type (WT) mice

Male WT C57BL/6 mice were purchased from Charles River Laboratories (Margate, Kent, UK).

Endothelial JAM-C KO mice (Tie2Cre;JAM-C$^{flox/flox}$)

An *in vivo* model of endothelial specific JAM-C deficiency was obtained by Cre-recombinase directed removal of a portion of exon 1 of the *Jam3 gene* containing a region of the promoter sequence and the start of the protein coding sequence. This region of exon 1 is flanked by loxP sites (JAM-C$^{flox/flox}$) which enabled deletion of the region using Cre-Lox recombination. JAM-C$^{flox/flox}$ mutants were crossed with mice transgenic for Cre recombinase under the endothelial specific Tie2-promoter/enhancer (Tie2Cre;JAM-C$^{flox/flox}$). Due to variable expression of Tie2 in ECs, with this strategy a full endothelial JAM-C KO mouse was not generated, but there was significant JAM-C KO (EC JAM-C KO). The extent of this KD has previously been reported to be in the region of 40-60%, depending on mouse variability (Woodfin et al., 2011). For simplification of nomenclature, Tie2Cre;JAM-C$^{flox/flox}$ mice and JAM-C$^{flox/flox}$ mice will be henceforth referred to as EC JAM-C KO and littermate control mice respectively. The mice were generated as described previously (Langer et al., 2011, Pellegrini et al., 2011, Woodfin et al., 2011). All genotyping was performed by Matthew Golding.

2.1.2 Anaesthetics

Ketamine	Narketan®-10 solution, 100 mg/ml (Vetoquinol UK, Buckingham, UK)
Xylazine	Rompun® 2% w/v, 20 mg/ml (Bayer HealthCare, Berkshire, UK)

2.2 Reagents

2.2.1 Antibodies

Primary antibodies

Target	***Antibody***
β-actin	Mouse anti-mouse β-actin, clone AC-15 (Sigma, St Louis, MO, USA)
β-tubulin	Mouse anti-rat β-tubulin, clone TUB 2.1 (Sigma)
B220	PE/Cyanine7 rat anti-mouse/human CD45R/B220, clone RA3-6B2 (eBioscience, Santa Clara, CA, USA)
CD3	PerCP/Cy5.5 hamster anti-mouse CD3, clone 17A2 (eBioscience)
CD16/CD32	Rat anti-mouse CD16/CD32, clone 2.4G2 (BD Biosciences, Franklin Lakes, NJ, USA)
CD31 (PECAM-1)	1. Goat anti-human CD31, clone M-20 (Santa Cruz, Dallas, TX, USA) 2. Mouse anti-human CD31, clone WM-59 (eBioscience) 3. Rat anti-mouse CD31, clone MEC13.3 (BD Biosciences) 4. Rat anti-mouse CD31, clone C390 (eBioscience)
CD45	Pacific Blue™ rat anti-mouse CD45, clone 30-F11 (Biolegend, London, UK)
CD115	Anti-mouse CD115 (c-fms) Alexa Fluor®488, clone AF598 (eBioscience)
ICAM-1	1. Rabbit anti-human ICAM-1, clone H-108 (Santa Cruz)

	2. Mouse anti-human ICAM-1, clone BBIG-I1 (R&D systems, Minneapolis, MN, USA)
ICAM-2	Rat anti-mouse CD102, clone mIC2/4 (AbD Serotec, Oxford, Oxfordshire, UK)
JAM-A	1) Mouse anti-human JAM-A, clone J10.4 (Gift, C.A. Parkos, Atlanta, USA) 2) Mouse anti-human JAM-A, clone 1H2A9 (Gift, C.A. Parkos)
JAM-C	1. Rabbit anti-human JAM-C, clone J85 (Gift, B.A. Imhof, Geneva, Switzerland) 2. Rabbit anti-mouse JAM-C clone J74 (Gift, B.A. Imhof)
LC3	1. Rabbit anti-human LC3B, (Cell Signalling, Hitchin, Hertfordshire, UK) 2. Mouse anti-human LC3, clone 5F10 (Nanotools, Teningen, Germany)
NF-κB p65	1. Mouse anti-NF-κB p65, clone L8F6, (Cell Signalling) 2. Rabbit anti-phospho-NF-κB p65, clone 93H1, (Cell Signalling)
VE-Cadherin	1. Goat anti-human VE-Cadherin, clone C-19 (Santa Cruz) 2. Mouse anti-human Cadherin-5, clone 75/Cadherin-5 (BD Biosciences) 3. Rat anti-mouse VE-Cadherin, clone BV14 (eBioscience)

Secondary antibodies

Antibody	***Conjugate***	***Source***
Goat anti-rabbit IgG	Horseradish Peroxidase	Dako (Glostrup, Denmark)
Goat anti-mouse IgG	Horseradish Peroxidase	Dako (Glostrup, Denmark)
Rabbit anti-mouse IgG	Horseradish Peroxidase	Dako (Glostrup, Denmark)

Mouse anti-rabbit IgG	Horseradish Peroxidase	Dako (Glostrup, Denmark)
Rabbit anti-goat IgG	Horseradish Peroxidase	Dako (Glostrup, Denmark)
Donkey anti-rabbit IgG	Alexa Fluor 488	Invitrogen (Carlsbad, CA, USA)
Donkey anti-rabbit IgG	Alexa Fluor 555	Invitrogen (Carlsbad, CA, USA)
Goat anti-rabbit IgG	Alexa Fluor 488	Invitrogen (Carlsbad, CA, USA)
Chicken anti-mouse IgG	Alexa Fluor 488	Invitrogen (Carlsbad, CA, USA)
Chicken anti-goat IgG	Alexa Fluor 647	Invitrogen (Carlsbad, CA, USA)
Donkey anti-mouse IgG	Alexa Fluor 647	Invitrogen (Carlsbad, CA, USA)
Donkey anti-goat IgG	Alexa Fluor 488	Invitrogen (Carlsbad, CA, USA)

2.2.2 Fluorescent Dyes

Mouse IgG1	
Rabbit IgG	Purified normal rabbit IgG isotype control (Peprotech, Rocky Hill, NJ, USA)
Rat IgG2a	Purified rat IgG2a κ isotype control, clone RTK2758 (Biolegend)

2.2.3 Inflammatory Stimuli

Mouse interleukin-1β	Recombinant mouse IL-1β/IL-1F2, Cat # 401-ML/CF (R&D systems)
Human interleukin-1β	Recombinant human IL-1β/IL-1F2, Cat # 201-LB (R&D systems)

Lipopolysaccharide (LPS)	LPS from *Escherichia coli* 0111:B4, Cat # L4391 (Sigma)

2.2.4 Kits

Human CXCL1/Gro-α DuoSet ELISA	Cat # DY275 (R&D systems)
Human IL-8 ELISA Ready-SET-Go!®	Cat # 88-8086 (eBioscience)
Human TNFα ELISA Ready-SET-Go!®	Cat # 88-7346 (eBioscience)
Mouse CCL2/JE/MCP-1 DuoSet ELISA	Cat # DY479 (R&D systems)
Mouse/Rat CCL5/RANTES Quantikine ELISA	Cat # MMR00 (R&D systems)
Mouse CXCL1/KC DuoSet ELISA	Cat # DY453 (R&D systems)
Mouse LIX/CXCL5 DuoSet ELISA	Cat # DY443 (R&D systems)
Mouse LIX/CXCL5 Quantikine ELISA	Cat # MMX00 (R&D systems)
Mouse TNFα ELISA Ready-SET-Go!®	Cat # 88-7490 (eBioscience)
Proteome Profiler™ Human XL Cytokine Array Kit	Cat # ARY022B (R&D systems)
Human Cytokine Array Kit	Cat # ARY005 (R&D systems)
Proteome Profiler™ Mouse XL Cytokine Array	Cat # ARY028 (R&D systems)

2.2.5 Cell/tissue lysis buffers

ACK lysis buffer	150 mM NH_4Cl, 10 mM $KHCO_3$, 0.1 mM EDTA, pH 7.3 in H_2O
Cremaster lysis buffer	PBS with 1% Triton X-100 and 1% protease and phosphatase inhibitor cocktail
RIPA buffer	150 mM NaCl, 1% IGEPAL®CA-630, 0.5% sodium deoxycholate, 0.1% SDS, 50 mM Tris, pH 8.0 (Sigma)

2.2.6 Other Reagents

Bovine Serum Albumin (BSA)	Standard Grade Powder, Fraction V, Cat # BP9701 (Fisher Scientific, Loughborough, UK)
Magnetic Dynabeads	Dynabeads® Sheep Anti-Rat IgG, Cat # 11035 (ThermoFisher)
EDTA	Ethylenediaminetetraacetic acid disodium salt dehydrate, Cat # E5134 (Sigma)
Fetal Bovine Serum (FBS)	FBS, qualified, heat inactivated, Cat # 10500064 (ThermoFisher) FBS, non-heat inactivated, Cat # FB-1001 (LabTech, Uckfield, UK)
Protease inhibitor cocktail	Halt™ Protease and Phosphatase Inhibitor Cocktail (100X), Cat # 78440 (ThermoFisher)
Normal Goat Serum (NGS)	Goat serum donor herd, Cat # G6767 (Sigma)
Triton™ X-100	Laboratory grade, Cat # T8787 (Sigma)

2.3 Cell culture

2.3.1 HUVECs

Human umbilical vein ECs (HUVECs), isolated and pooled from 2-3 different umbilical cords, were obtained from PromoCell (Heidelberg, Germany). HUVECs were maintained in HUVEC Growth Medium (HGM, M199 + Glutamax; Gibco, Paisley, UK) supplemented with 20% fetal bovine serum (FBS, LabTech, Uckfield, UK), 10 U/ml Heparin (Sigma) and 100 µg/ml endothelial growth supplement (ECGS) (Sigma)). Cells were kept in 5% CO_2 humidified atmosphere at 37°C. Once they had reached 70-80% confluency HUVECs were split and used for experiments between passages 3-6. For

passaging, cells were washed once with phosphate buffered saline (PBS) containing calcium and magnesium salts (Gibco) and detached using 0.025% Trypsin/0.01% EDTA (Gibco) or 1X TrypLE^{TM} Express reagent (Life Technologies, Paisley, UK), and then subcultured.

HUVECs were sourced from Promocell at passage 0 and were expanded to passage 2 in EC basal medium (EBM, Promocell) at which point aliquots were frozen down for storage. Aliquots of ≈ 1 x 10^6 cells were suspended in 1 ml FBS supplemented with 10% dimethyl sulphoxide (DMSO, Sigma) and frozen at -80^{o}C overnight, then transferred to a liquid nitrogen tank. For usage, aliquots were thawed at 37^{o}C, resuspended in 1 volume of M199 media and plated between three 145 cm^2 tissue culture plates (Nunc, ThermoFisher, Waltham, MA, USA), previously coated with 1% w/v pig skin

2.3.2 siRNA transfection

siRNA oligonucleotides are listed in Table 1. HUVECs were transiently transfected with siRNA using the Amaxa Nucleofector^{TM} system (Lonza, Basel, Switzerland). Passage three HUVECs were dissociated with TrypLETM Express, centrifuged at 288xg for 5 min, and resuspended at 2 x 10^6 cells per 100 µl nucleofection buffer containing 140 pmoles of siRNA. The suspension was then transferred to a 0.1 cm cuvette (GeneFlow, Lichfield, Staffs, UK), placed in the nucleofector and pulsed using the HUVEC-old programme (U-001). Cells were rescued immediately in 0.5 ml of HGM and seeded at 300,000 or 500,000 cells per well of a six well plate for protein/RNA extraction or immunofluorescence (IF) staining, respectively. Plates were coated in gelatin (1% w/v), and coverslips coated in gelatin (1% w/v), fibronectin (10 µg/ml) and rat collagen-I (0.03 µg/ml), as described above. Transfected HUVECs were used for experiments 48-72 hours post transfection, allowing cells to reach confluency and for the siRNA KD to reach optimal efficiency. Level of protein KD was assessed by Western Blot, qPCR and by IF staining.

siRNA oligo	*Sequence*
Human JAM-C siRNA 1	5'-AUGUAGUUAACUCCAUCUGGUUUCC-3'
Human JAM-C siRNA 2	5'-AUUGCUGGAUUUGAGAUUUACAGCC-3'
Control siRNA (Luciferase)	5'-CGUACGCGGAAUACUUCGA-3'

Table 2.1. List of human siRNA oligonucleotide primers

2.3.3 Cell stimulation

48-72h after siRNA transfection the response of ECs to different stimuli were investigated. Unless otherwise indicated, confluent HUVECs were cultured for 2 hours in M199 supplemented with FBS (5%) and then stimulated with Interleukin-1 beta (IL-1β 1 ng/ml, R&D systems) or lipopolysaccharide (LPS 100 ng/ml, R&D systems) for 4 hours. Following 4h stimulation, conditioned medium was collected, aliquoted and frozen at -80^{o}C for subsequent analysis of secreted proteins. Cells were then lysed appropriately depending on the experimental needs (see below). For stimulating autophagy, cells were cultured in a specific EC starvation medium (Tebu-Bio, Rambouillet, France) for 2 hours. In addition, Bafilomycin A1 (100 nM) and 3-Methyladenine (5 mM) (both from Sigma) were used to inhibit different stages of the autophagic pathway.

2.3.4 Proliferation Assay

Differences in cell proliferation were measured using an MTT cell proliferation assay purchased from ATCC (Manassas, VA, USA), according to manufacturer's instructions.

2.3.5 Cell viability and apoptosis assays

Cell viability of HUVECs was measured using a lactate dehydrogenase (LDH) cytotoxicity assay kit (ThermoFisher). Briefly, cells were analysed for LDH release by colourimetric absorbance at 490nm and compared to a positive control of lysed cells.

Apoptosis of HUVECs was measured using a mitochondrial membrane potential apoptosis kit (Life Technologies). Cells were stained for Alexa Fluor 488 annexin V and MitoTracker® Red and analysed by Flow Cytometry. Percentage of apoptotic cells in HUVEC samples were compared to a positive control of HUVECs given heat shock treatment (95^{o}C for 10 minutes) to induce high levels of apoptosis.

2.4 In vivo inflammation models

2.4.1 Neutrophil depletion

In some experiments, mice were depleted of their circulating neutrophils by intraperitoneal (i.p.) injection of anti-granulocyte-differentiation antigen 1 (GR1) antibody at 25 µg/day for three consecutive days (Voisin et al., 2009). Blood samples were then taken from the tail vein the day after antibody treatment and the levels of neutrophils and monocytes determined by flow cytometry.

2.4.2 Cremaster inflammation model

Male mice were anaesthetised by intramuscular (i.m.) injection of 1 ml/kg ketamine (40 mg) and xylazine (2 mg) and then administered an intrascrotal (i.s.) injection of inflammatory stimulus or pharmacological agent prepared in a 400 µl sterile PBS bolas. Control mice were injected with PBS only. In some experiments mice were pre-treated with the JAM-C blocking antibody H33 or isotype control (10 mg/kg), which was administered by intravenous (i.v.) injection. After a 4-hour *in vivo* test period, mice were culled by cervical dislocation and cremaster muscles collected for subsequent analysis.

2.5 Characterisation of neutrophil depletion

2.5.1 Immunofluorescence labelling of leukocytes

Blood from tail vein samples was collected into 50 µl 5 mM EDTA and erythrocytes were removed by incubation with ACK lysis buffer (see section 1.2.5) at room temperature for 5 mins. Samples were then washed twice by centrifugation in PBS (300g, 5 mins, 4^{o}C). Cells were then incubated with fluorescently labelled primary antibody cocktail containing Ly6G, CD115 and CD45 to label neutrophils, monocytes and the whole leukocyte population. Samples were incubated for 1-2 hours at 4^{o}C in the dark.

2.5.2 Flow cytometry

Labelled cells were washed with PBS by centrifugation at 300g for 5 mins at 4^{o}C, before resuspension in 200 µl cold PBS to achieve a single cell suspension. Samples were run on a LSRFortessa flow cytometer (BD Biosciences) using FACSDiva software, with at least 5,000 events per sample acquired. Data was then analysed using FlowJo version 7.6 software (Treestar).

2.6 Gene expression analysis

2.6.1 RNA extraction from cell culture

RNA was extracted from cultured ECs using the AllPrep RNA/Protein kit (Qiagen), according to manufacturer's instructions. Briefly, cells were washed in PBS and lysed with Buffer APL before being bound to and spun through an AllPrep spin column. RNA bound to the column while protein washed through, and protein was extracted using protein cleanup spin columns. RNA was eluted from the AllPrep spin columns in Buffer RLT, mixed 1:1 with 70% ethanol and purified using RNeasy spin columns.

2.6.2 Analysis of RNA quality

The quality of extracted RNA from both tissue and cell culture samples was analysed using the Agilent 2100 Bioanalyser system (Agilent, Santa Clara, CA, USA). This

analysed RNA integrity and displayed the quality as a RIN score, ranging from 1.0 (fully degraded RNA) to 10.0 (fully intact RNA), as well as giving the ratio of 28S to 18S rRNA in the sample. A RIN score of 7.0 and above was considered to be of appropriate quality for subsequent use in microarray analysis, as advised by Dr Charles Mein (Barts and the London Genome Centre).

2.6.3 Gene expression microarray

HUVECs were transfected with control or JAM-C specific siRNA as previously specified and left unstimulated or subjected to IL-1β treatment for 4 hours. Three independent experiments were performed to give biological triplicates to be used for the gene expression microarray analysis. RNA was isolated and analysed for quality as previously described in section 2.6.2.

RNA was subjected to gene expression microarray analysis using HumanHT-12 v4 Expression BeadChip technology (Illumina, San Diego, CA, USA)). Briefly, the protocol involved a two-step reverse transcription process to create cDNA, followed by a single *in vitro* transcription amplification step that creates biotin labelled cRNA. Gene specific probes are attached to beads and assembled into array chips. The cRNA is hybridised to the probes and then stained with streptavidin-Cy3 for fluorescence emission detection of the probes.

2.6.4 Gene expression data analysis

Data was extracted using Genome Studio software (Illumina) and then analysed using Bioconductor and Limma. Pathway analysis was performed using Ingenuity Pathway Analysis software (Qiagen). Heatmaps were generated using Cluster 3.0 and Java TreeView software. Genes were clustered using Kendall's tau rank correlation coefficient, in collaboration with Dr Michael Barnes and Dr Claudia Cabrera of the Department of Bioinformatics, WHRI.

2.6.5 Quantitative real-time polymerase chain reaction (qPCR)

Isolated RNA (500 ng) was reverse transcribed to complementary (cDNA) in 20 µl reaction volume using iScript™ cDNA synthesis kit (Bio-Rad) according to the manufacturer's protocol. The cDNA was then diluted to 2.5 µg/ml prior to use in qPCR reactions. Primers were designed and obtained from Integrated DNA Technologies (IDT, Coralville, IA, USA). qPCR reactions were conducted using the 7900HT Fast Real-Time PCR system (Applied Biosystems, Forster City, CA, USA) in 384-well microplates. For each reaction, cDNA was added at 125 ng/ml and primer mix at 100 nM, with the reaction mix completed by the addition of iQ SYBR® Green Supermix (Bio-Rad). Reaction conditions were as follows: One step of 50°C for 2 mins, one at 95°C for 10 mins, then 40 cycles of 95°C for 15 seconds (denaturation step) and 60°C for 1 minute (annealing and elongation step). Data was analysed using the ΔΔCt method (Livak and Schmittgen, 2001). A list of primers is detailed in Tables 2a and 2b.

Gene	***Sense/Antisense***	***Sequence***	***Product size***
ACTB	Sense	5'-GCGAGAAGATGACCCAGAT-3'	261 bp
	Antisense	5'-TGGTGGTGAAGCTGTAGCC	
CXCL1	Sense	5'-AACCGAAGTCATAGCCACAC-3'	124 bp
	Antisense	5'-CCTCCCTTCTGGTCAGTTG-3'	
CCL2	Sense	5'-CAGAAGTGGGTTCAGGATTCC-3'	87 bp
	Antisense	5'-ATTCTTGGGTTGTGGAGTGAG-3'	
HIF1A	Sense	5'- AGTGTACCCTAACTAGCCGAG-3'	181 bp
	Antisense	5'- TTTGATGGGTGAGGAATGGG-3'	
HMGB1	Sense	5'- GGAGAGTAATGTTACAGAGCGG-3'	145 bp
	Antisense	5'- GATCTCCTTTGCCCATGTTTAG-3'	
ICAM1	Sense	5'-CGGAAGGTGTATGAACTGAGC-3'	179 bp

	Antisense	5’-CAGCGTAGGGTAAGGTTCTTG-3’	
CXCL8	Sense	5’-ACTGAGAGTGATTGAGAGTGGAC-3’	112 bp
	Antisense	5’-AACCCTCTGCACCCAGTTTTC-3’	
JAM-C	Sense	5’-CAAGGACGACTCTGGGCAGT-3’	112 bp
	Antisense	5’-CCCAATAATTCCGCCAATGTTC-3’	
PPIA	Sense	5’-CCCACCGTGTTCTTCGACATT-3’	275 bp
	Antisense	5’-GGACCCGTATGCTTTAGGATC-3’	
SEMA3E	Sense	5’- ACCCCACGATCTTTACAAGCG-3’	148 bp
	Antisense	5’- AGGTCCCAGCATCTGATTTGT-3’	
SEMA3G	Sense	5’- CTCAAAGTCATCGCTCTCCAG-3’	142 bp
	Antisense	5’- GAGAGCCCACGTATAGCATTTG-3’	
SEMA4C	Sense	5’- TCAACTTCATCCGCTTCCTGC-3’	139 bp
	Antisense	5’- CCCTTCCCATCTTCAAACTCTC-3’	
SEMA4F	Sense	5’- GAAATGTCCTTTTGAGCCAGC-3’	148 bp
	Antisense	5’- GGTATCTGTCCGAATCCAGTC-3’	
SEMA6B	Sense	5’- GTGTCGGATGAAGGGCAAAC-3’	136 bp
	Antisense	5’- GGGTGTCTATGCTGTAGTTGG-3’	
VCAM1	Sense	5’-CAGTAAGGCAGGCTGTAAAGA-3’	137 bp
	Antisense	5’-TGGAGCTGGTAGACCCTCG-3’	

Table 2.2. List of qPCR human oligonucleotide primers

2.7 Inflammatory Mediator analysis

2.7.1 Preparation of cremaster lysate samples

Stimulation of the cremaster was carried out as previously described in section 1.4.2. Cremaster muscles were isolated following cervical dislocation culling of the mice. Both cremaster muscles were isolated, snap frozen in liquid nitrogen and kept at -80^{o}C prior to homogenisation. To prepare the lysates, cremasters were mixed with cremaster lysis buffer (see section 1.2.5) in 2ml homogenisation tubes containing 2.8 mm ceramic beads (Stretton Scientific, Stretton, Derbyshire, UK). Homogenisation used a Precellys®24 homogeniser (Stretton Scientific) at 6500 rpm for 3x20s, which was then repeated to ensure full homogenisation. Samples were then frozen for 1 hour at -80^{o}C, then thawed and centrifuged at 10,000g for 5 mins. Supernatants were collected and stored at -80^{o}C until further analysis.

2.7.2 Preparation of plasma samples

Blood was obtained by either cardiac puncture using a 27-gauge needle, or from the descending vena cava using a 21-gauge needle, and a 1 ml syringe filled with 50 µl 5 mM EDTA. 0.5-1 ml blood was collected per mouse. Plasma was obtained by centrifugation of the blood at 10,000g for 10 mins, upon which the supernatant containing the plasma was collected, snap frozen in liquid nitrogen and stored at -80^{o}C.

2.7.3 Proteome Profiler^{TM} and cytokine arrays

Mouse cremaster tissue samples were analysed using the Proteome Profiler^{TM} Mouse XL Cytokine Array. Cremaster samples were pooled from three individual mice per group, before addition to the array panel. The procedure was followed according to the manufacturer's instructions. However, instead of using streptavidin-HRP conjugate, streptavidin conjugated to IRDye® 800CW (LI-COR, Lincoln, NE, USA) was used to detect the presence of mediators. Array panels were imaged using the Odyssey® Classic Infrared Imaging System (LI-COR). Images were analysed using

ImageStudio Lite software (LI-COR) to determine the pixel intensity of each cytokine spot.

To analyse release of inflammatory mediators *in vitro*, conditioned media from HUVECs stimulated for 4 hours were added to a Proteome Profiler™ Human XL Cytokine Array or to a standard Human Cytokine Array kit. The procedure was followed as described previously for the mouse array. An example image of the array membranes can be seen in Figure 2.1.

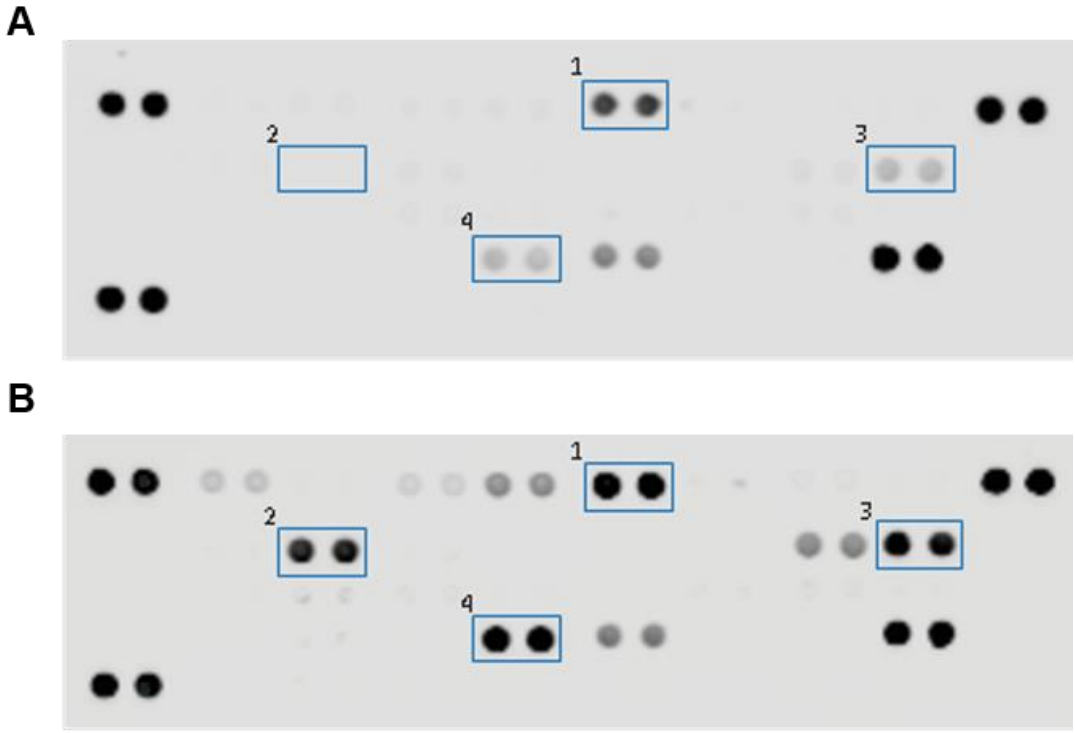

Figure 2.1. Human Cytokine Array Panel
Conditioned cell culture medium from untreated (A) and IL-1β stimulated (B) HUVECs were incubated with the cytokine array panel membranes overnight at 4°C. Bound cytokines were detected by IRDye® 800CW Streptavidin and read using an Odyssey® CLx imaging system. Increases in highlighted cytokines were visible following IL-1β stimulation. [1]CXCL1/GRO α, [2]IL-1β, [3]IL-8, [4]CCL2/MCP-1.

2.7.4 Enzyme-linked Immunosorbent Assay (ELISA)

Mouse tissue and plasma samples were assayed for CXCL1, CCL2, CCL5, CXCL5 and Granulocyte colony-stimulating factor (G-CSF) using the kits detailed in section 1.2.4, according to manufacturer's instructions.

Levels of human TNFα, CXCL1 and IL-8 in cell culture supernatants and cell lysates of HUVECs were measured by ELISA kits purchased from eBioscience, according to manufacturer's protocols.

2.8 Immunofluorescence Confocal Microscopy

2.8.1 Immunofluorescent labelling of cells

HUVECs were cultured on 10 mm diameter glass coverslips for immunofluorescence staining, as previously described (Section 2.2.3). Following stimulation, cells were fixed in either 4% paraformaldehyde (PFA, Sigma) for 15 minutes at room temperature, or in 100% ice-cold methanol for 5 minutes at -20^{o}C. Following fixation in 4% PFA, cells were then permeabilised with 0.1% Triton X-100 for 10 minutes at room temperature. Any auto-fluorescence was quenched by the use of 0.1 M ammonium chloride in PBS for 5 minutes at room temperature. Coverslips were blocked in 2% bovine serum albumin (BSA, ThermoFisher) in PBS for 30 minutes at room temperature to minimise any non-specific binding of antibodies. Primary antibodies or cellular dyes were then incubated with the samples for 1 hour at room temperature or overnight at 4^{o}C. Cells were then washed 3 times in PBS before incubation with fluorescently labelled secondary antibodies for 1 hour at room temperature. After further washing, samples were mounted on slides (VWR, Lutterworth, Leicestershire, UK) using ProLong Gold Antifade Mountant media with 4',6-Diamidino-2-phenylindole (DAPI) (ThermoFisher). Figure 2.2 shows a representative image of confluent HUVECs immuno-stained in this way to show that the handling of the cells enabled formation of confluent monolayers with intact junctions (VE-Cadherin, green) and caused minimal stress to the cells as shown by the absence of any stress fibres (F-actin, stained with phalloidin, red).

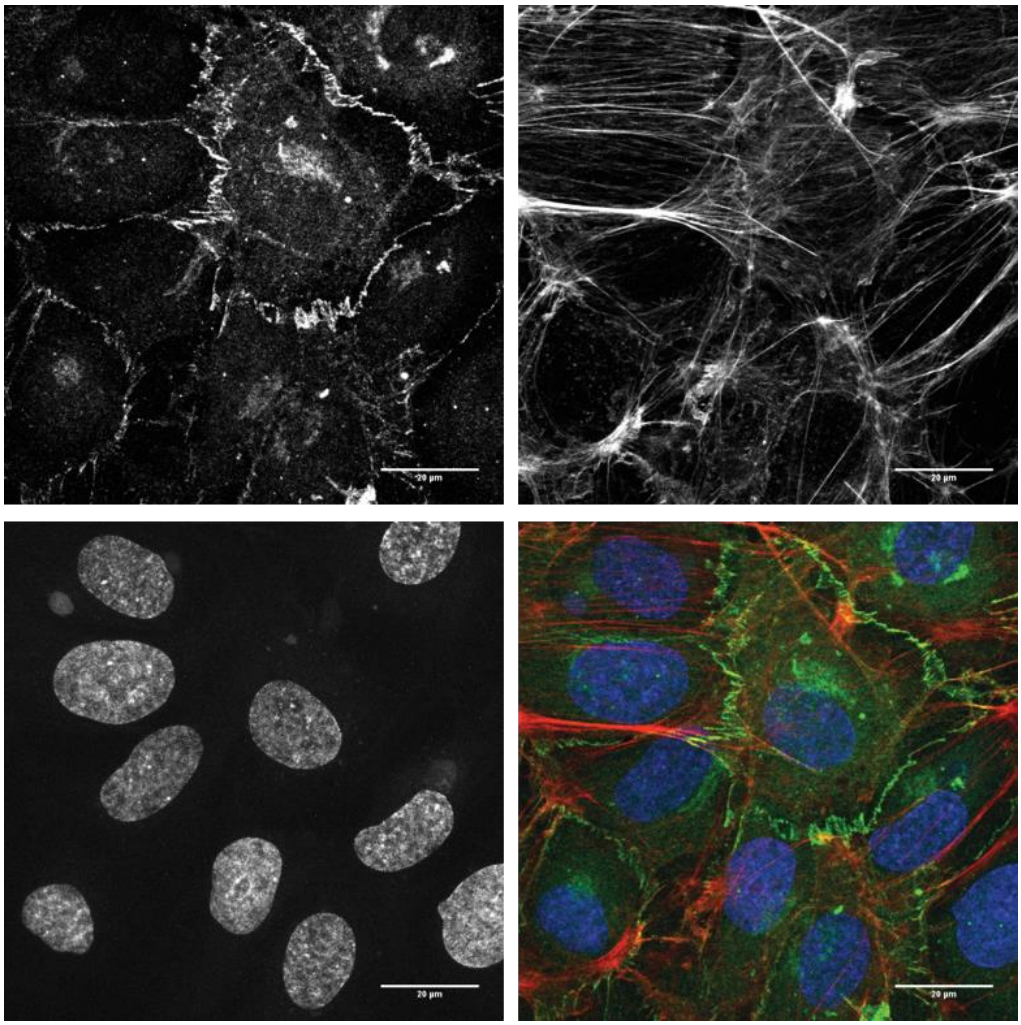

Figure 2.2. Immunofluorescence staining of confluent HUVECs. Human Umbilical Endothelial Cells (HUVECs) were fixed and immunofluorescently stained for VE-Cadherin (Top left panel, green), F-actin (Top right panel, red) and DAPI (Bottom left panel, blue). Scale bars represent 20 µm.

2.8.2 Immunofluorescent labelling of tissue

Mice were culled by cervical dislocation and cremaster muscles were exteriorised and surgically removed. A midline incision was made in the scrotum and the testicles drawn out, the cremaster separated from the connective tissue and then fully dissected from the testis. The cremasters were then pinned out on dental wax and fixed in 4% PFA for 10-20 minutes at 4^{o}C. Blocking and permeabilisation was carried out in PBS containing 12.5% fetal calf serum (FCS), 12.5% normal goat serum (NGS) and 0.5% Triton X-100 for 2 hours at room temperature. Primary antibodies (JAM-C, CD31, VE-Cadherin) were incubated in PBS containing 5% FCS and 5% NGS at 4^{o}C overnight (Colom et al., 2015, Woodfin et al., 2011). After washing for 30 minutes in PBS three times, tissues were incubated with secondary antibodies in PBS again containing 5% FCS and 5% NGS for 3 hours at 4^{o}C. Finally, tissues were washed extensively in PBS before proceeding to analysis by confocal microscopy.

2.8.3 Confocal Microscopy

Both immunofluorescently labelled HUVECs and cremaster muscles were analysed using a Zeiss LSM-5 Pascal or Zeiss LSM 800 laser-scanning confocal microscope (Carl Zeiss AG Ltd, Jena, Germany). Z-stack images were taken using a 63X oil-dipping objective (1.4 numerical aperture) and single-track scanning mode. Images were then analysed using ImageJ and Imaris (Bitplane, Zurich, Switzerland) software.

2.9 Western Blotting

HUVECs or MLECs were lysed using RIPA buffer (Sigma) containing protease inhibitor cocktail (Life Technologies). If necessary, protein concentrations of cell lysates were then determined by BCA assay (Life Technologies). 2X SDS-PAGE loading buffer (100 mM Tris-HCl (pH 6.8), 4% (w/v) SDS, 0.2% bromophenol blue, 20% glycerol, 10% β-mercaptoethanol) was added to cell lysates in a 1:1 ratio and samples were then boiled at 95^{o}C for 5 minutes to denature proteins. Samples were electrophoresed and separated on precast 16% RunBlue gels (Expedeon) using Tris-Glycine Buffer (Expedeon) for 45 minutes to 1 hour at 150V. Separated protein was then transferred onto PVDF membrane using the wet transfer method. Gel and membrane were

sandwiched together and submerged in transfer buffer (20% methanol, 25mM Tris 190mM Glycine) for 1 hour at 100V.

Next, membranes were stained with Ponceau Red solution (Sigma) for 5 mins at room temperature to check for efficiency of transfer and protein integrity. Membranes were then destained with deionised water and blocked for 1 hour in PBS containing 5% BSA/0.05% Tween 20. Primary antibodies against proteins of interest were diluted in 5% BSA PBS/0.05% Tween and incubated with the membrane overnight at 4^{o}C. Primary antibody was washed off with PBS/0.05% Tween for 10 minutes three times, and membranes were incubated with HRP-conjugated secondary antibodies diluted in PBS containing 5% milk/0.05% Tween for 1 hour at room temperature. Finally, membranes were washed extensively with PBS/0.05% Tween and bands visualised using SuperSignal^{TM} West Pico Chemiluminescent Substrate (ThermoFisher) and developed on an SRX-101A Medical Film Processor (Konica-Minolta, Ramsey, NJ, USA).

2.10 Statistics

All data were expressed as mean ± standard error of the mean (SEM). Data analysis was carried out using GraphPad Prism software (GraphPad, San Diego, CA, USA), with data being classed as significant when p values were below 0.05. Statistical significance was evaluated by unpaired two-tailed Student's t-test or by one-way ANOVA.

3 Investigating the impact of JAM-C deficiency on endothelial cell junctions, survival and proliferation *in vitro*

3.1. Introduction

As described in detail in Chapter 1, JAM-C is a tight junction protein expressed by a number of cell types including ECs and epithelial cells. Investigating the functional role of JAM-C, numerous studies have identified roles for this adhesion molecule within processes such as angiogenesis, permeability, neural functions and leukocyte migration (Bradfield et al., 2007, Li et al., 2009, Orlova et al., 2006, Rabquer et al., 2010, Scheiermann et al., 2009, Woodfin et al., 2011, Leinster et al., 2013). Despite such studies, the role of EC JAM-C in ECs under basal conditions remains unclear. The aim of this project was to address this issue and gain better insights into how EC JAM-C regulates EC functions. As highlighted in Chapter 1, the full JAM-C KO mouse is severely sick that limits its use experimentally, notably severe hydrocephaly, cardiovascular problems and male sterility among others (Pellegrini et al., 2011, Wyss et al., 2012). In addition to this, JAM-C is deleted in every cell type and tissue in this model. Whilst the use of an endothelial specific JAM-C KO mouse was employed in Chapter 6, initial studies were aimed at establishing an *in vitro* model of JAM-C deficiency in cultured ECs. It was considered that such a model would provide a simple system for biochemical assays and would also be amenable to high resolution imaging.

There are a number of methods that can be used to KD expression of a desired molecule in cells in culture *in vitro*, and the most widely employed method is to utilise the RNAi system (Wilson and Doudna, 2013). Endogenously within the cell, small non-coding RNAs, known as microRNAs (miRNA), regulate gene expression by driving messenger RNA (mRNA) degradation or by repressing transcription. These are transcribed in the nucleus and then exported into the cytoplasm, upon which they are cleaved to short double stranded RNAs by the endonuclease enzyme Dicer. These short RNAs are loaded into the RNA-induced silencing complex (RISC), where the dsRNA is unwound to form single stranded RNA, which guides the RISC to mRNA that has a complementary sequence. Subsequently, the target mRNA is cleaved by the RISC complex and then degraded, resulting in no translation of the gene of interest (Martin

and Caplen, 2007). Biomedical research has taken advantage of this in-built system through the design of small RNA sequences to target specific genes for silencing. Two of the most widely used methods in this respect are transient transfection with siRNA or short hairpin RNA (shRNA). These custom synthesised siRNAs can be used to target genes of interest, where upon transfection into cells it engages the RNA-induced silencing complex (RISC) and silences gene expression in the same manner as for endogenous miRNAs. shRNA works in a similar manner to siRNA, where a custom siRNA is designed incorporating a short loop between the two strands. The shRNA requires a transfection vector for delivery into cells, such as a plasmid or viral vector. Once transfected into the cell and transcribed by host polymerases, the shRNA is exported and then cleaved by Dicer to form siRNA and the process proceeds as previously described.

There are some caveats to using either method. Transfection with siRNA is only transient leading to a short lived KD of the gene of interest. shRNA transfection on the other hand provides a long lasting KD that can be passed on to subsequent generations of cells, especially when a viral vector that integrates into the host genome is used. However, use of shRNA does have inherent disadvantages. For example, the shRNA could be incorporated into a region of the genome which is silenced or has low transcriptional activity and as such the shRNA would be ineffective. In addition, the use of viral vectors (especially retroviruses) may impact on the transfected cell itself and cause immune or inflammatory responses that would be associated with viral infection. As such, the aims of each individual project must be carefully considered before deciding on a chosen KD system (Moore et al., 2010, Rao et al., 2009).

3.2. Aims

To enable studies into the effect of JAM-C deficiency on EC biology and functions, a robust protocol was established for creating JAM-C KD ECs *in vitro*. Following this, the basic properties of JAM-C KD ECs was assessed, before investigating the JAM-C KD ECs in more complex functional studies. Collectively the following objectives were addressed in this chapter.

- To establish a reliable experimental protocol for KD of JAM-C in human ECs *in vitro*.
- To analyse the expression of other EC junctional molecules in conditions of JAM-C KD.
- To verify that JAM-C KD had no adverse effect on basic EC functions, such as morphology, proliferation and viability.

3.3. Results

3.3.1. Cellular localisation of JAM-C in endothelial cells *in vitro*

Before attempting to knock-down JAM-C in ECs *in vitro*, the cellular localisation of JAM-C in cultured ECs was first investigated. In quiescent macrovascular ECs (HUVECs, Figure 3.1) JAM-C localised to the inter-endothelial cell junctions and was also present intracellularly, although the precise location of the latter was not investigated here. Interestingly, JAM-C also showed expression in the nucleus of quiescent HUVECs, as shown by co-localisation with DAPI staining. Staining of HUVECs with isotype control antibody can be found in Appendix 1, where isotype control shows no junctional or intracellular JAM-C staining as compared to that observed when using the JAM-C specific antibody.

In resting microvascular ECs (HDMECs, Figure 3.2) JAM-C showed a similar pattern of immuno-staining to that observed in HUVECs. Here, JAM-C was localised to both the junctional and intracellular compartment, with expression also being detected in the nucleus in a similar manner to that seen in HUVECs. In HDMECs, the morphology of the junctions was however different to that noted in HUVECs, with the profile being less serrated and more continuous. VE-Cadherin and JAM-C largely localised to the same regions in the junctional compartment under basal conditions.

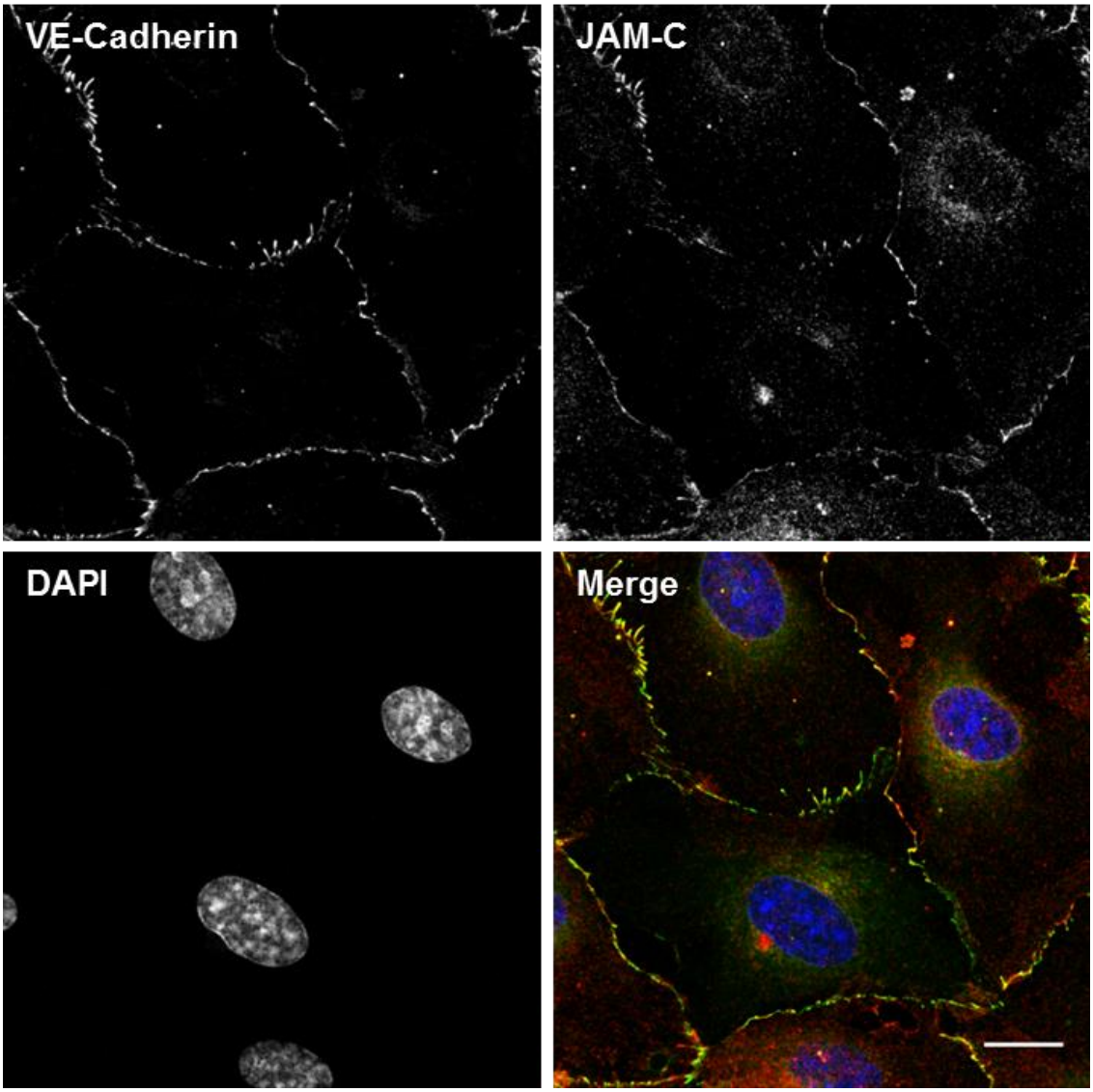

Figure 3.1. JAM-C is largely expressed at cell-cell junctions in unstimulated HUVECs. Untransfected HUVECs were cultured for 48-72 h to reach confluence and then fixed for 15 mins in 4% PFA at room temperature. Cells were then immuno-stained for VE-Cadherin (top-left), JAM-C (top-right) and DAPI (bottom-left). Images were taken using a Zeiss LSM800 confocal microscope; scale bars represent 15 µm.

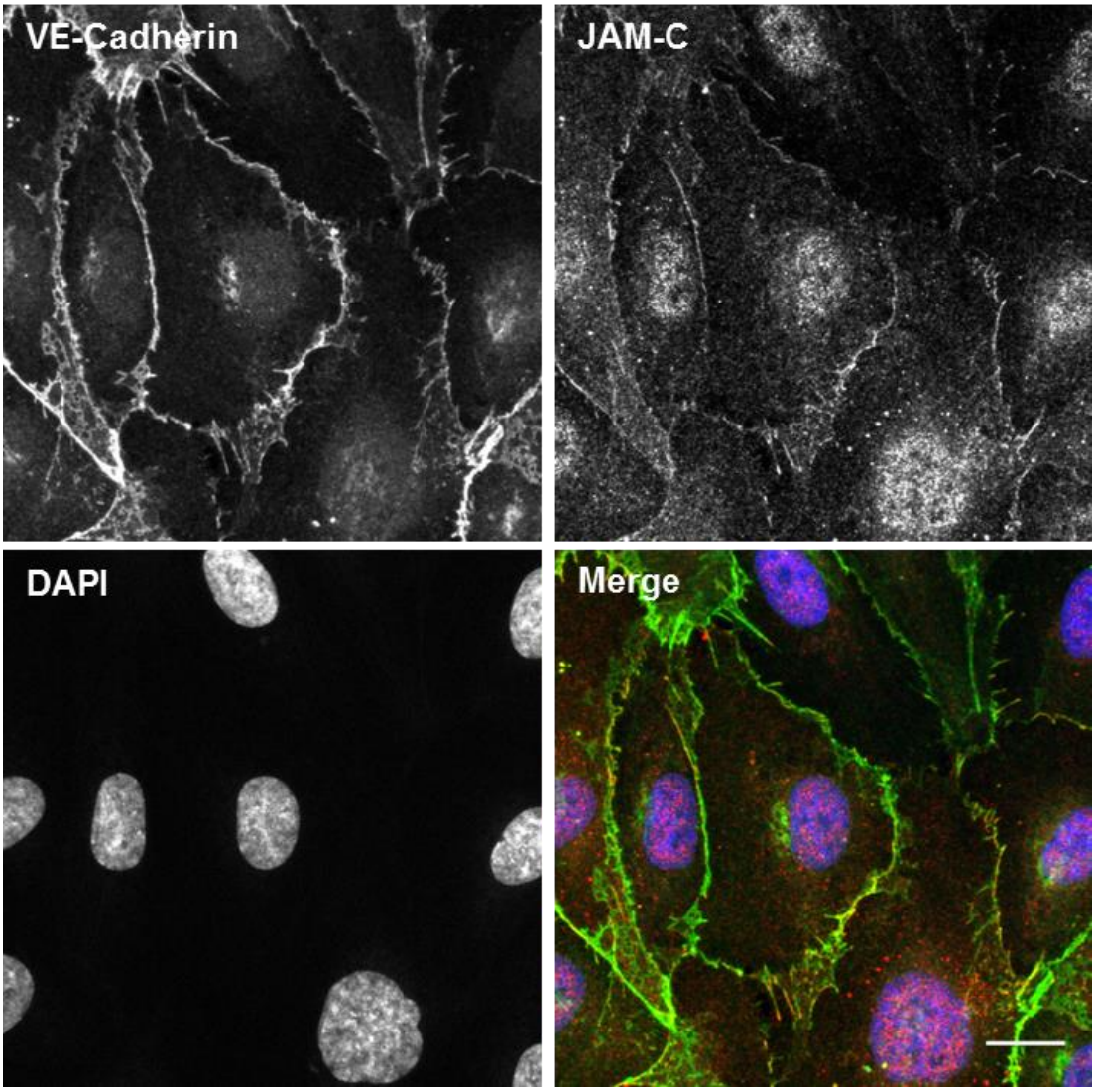

Figure 3.2. JAM-C is present at the junctions of HDMECs under resting conditions.
Untransfected HDMECs were cultured for 48-72 h to reach confluence and then fixed for 15 mins in 4% PFA at room temperature. Cells were then immuno-stained for VE-Cadherin (top-left), JAM-C (top-right) and DAPI (bottom-left). Images were taken using a Zeiss LSM800 confocal microscope; scale bars represent 15 µm.

3.3.2. siRNA mediated KD of JAM-C expression in HUVECs

To KD JAM-C in ECs, transfection of primary HUVECs with siRNA targeted to JAM-C was chosen as the preferred method. Two different approaches were used to achieve this knock-down. Initially, transfection using JetPEI® reagent was employed, which is a polyethylenimine based low-toxicity transfection reagent. This method packages the siRNA into positively charged vesicles that are taken up by endocytosis. Using this

approach, HUVECs were transfected with either JAM-C siRNA or control siRNA. The siRNA sequences targeting JAM-C was taken from a publication where the authors used the sequences to effectively KD JAM-C in cultured HUVECs (Li et al., 2009). The siRNA consisted of two pooled sequences. Using this tool, a visible KD of JAM-C was observed in JAM-C siRNA transfected cells compared to control siRNA transfected cells, as assessed by Western Blot (Figure 3.3A, lanes 1&2). However, the level of KD was variable in repeat experiments (Figure 3.3A, lanes 3&4) and on average only achieved a modest 46% KD compared to control cells when analysed 48-72h post-transfection (Figure 3.3C).

Following these results, a different method of transfection was utilised, namely electroporation using the Amaxa^{TM} Nucleofector^{TM} system (Liu et al., 2011). In this method, electrical pulses are used to create pores in the cell membrane, allowing the siRNA to be transferred directly into the cytoplasm and nucleus of the cell. Using this approach, a much more robust and reproducible KD of JAM-C protein was achieved in JAM-C siRNA transfected HUVECs (Figure 3.3B). Specifically, the KD of JAM-C achieved was on average greater than 90% and remained highly significant 48-72 post-transfection (Figure 3.3D).

To further verify this KD, HUVECs transfected with either control or JAM-C siRNA and then grown on 10 mm glass coverslips were fixed and immuno-stained for JAM-C. The confocal microscopy images shown in Figure 3.4 highlight the near complete loss of JAM-C expression in HUVECs transfected with JAM-C siRNA (right panel) compared to control siRNA transfected HUVECs (left panel). The images demonstrate the loss of both junctional JAM-C and the intracellular pool of JAM-C that was observed in Figure 3.1. Interestingly, unlike previous works (Figure 3.1 and Figure 3.2), a nuclear pool of JAM-C was not detected in control HUVECs in this instance. This perhaps suggests a methodological anomaly of the JAM-C immuno-staining rather than real expression.

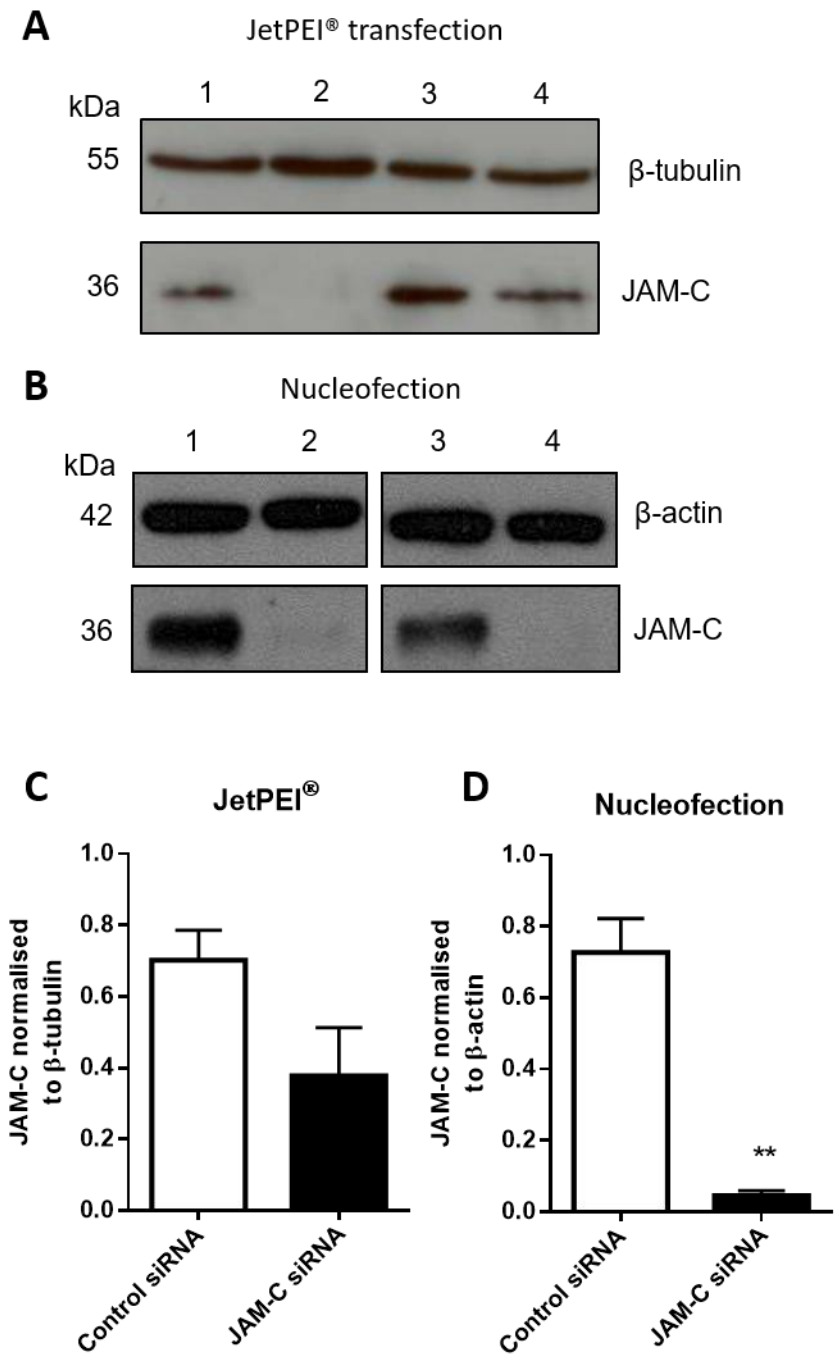

Figure 3.3. Comparison of different methods used for siRNA mediated KD of JAM-C in HUVECs.

(A) After 24 h of growth, HUVECs were transfected with control or JAM-C siRNA using JetPEI® transfection reagent and cultured for a further 48 h. Cells were lysed and analysed for level of JAM-C protein by Western Blot.

(B) HUVECs were transfected with control or JAM-C siRNA using the Amaxa™ Nucleofection system. Cells were cultured for 48-72 h then lysed and analysed for JAM-C protein by Western Blot.

(C&D) Quantification of JAM-C protein in (A) and (B) respectively, where JAM-C protein levels were normalised to loading control (β-tubulin or β-actin). Error bars represent SEM from n=4 (C) and n=5 (D) experiments. Statistical significance determined by Mann-Whitney test, **=$p<0.01$.

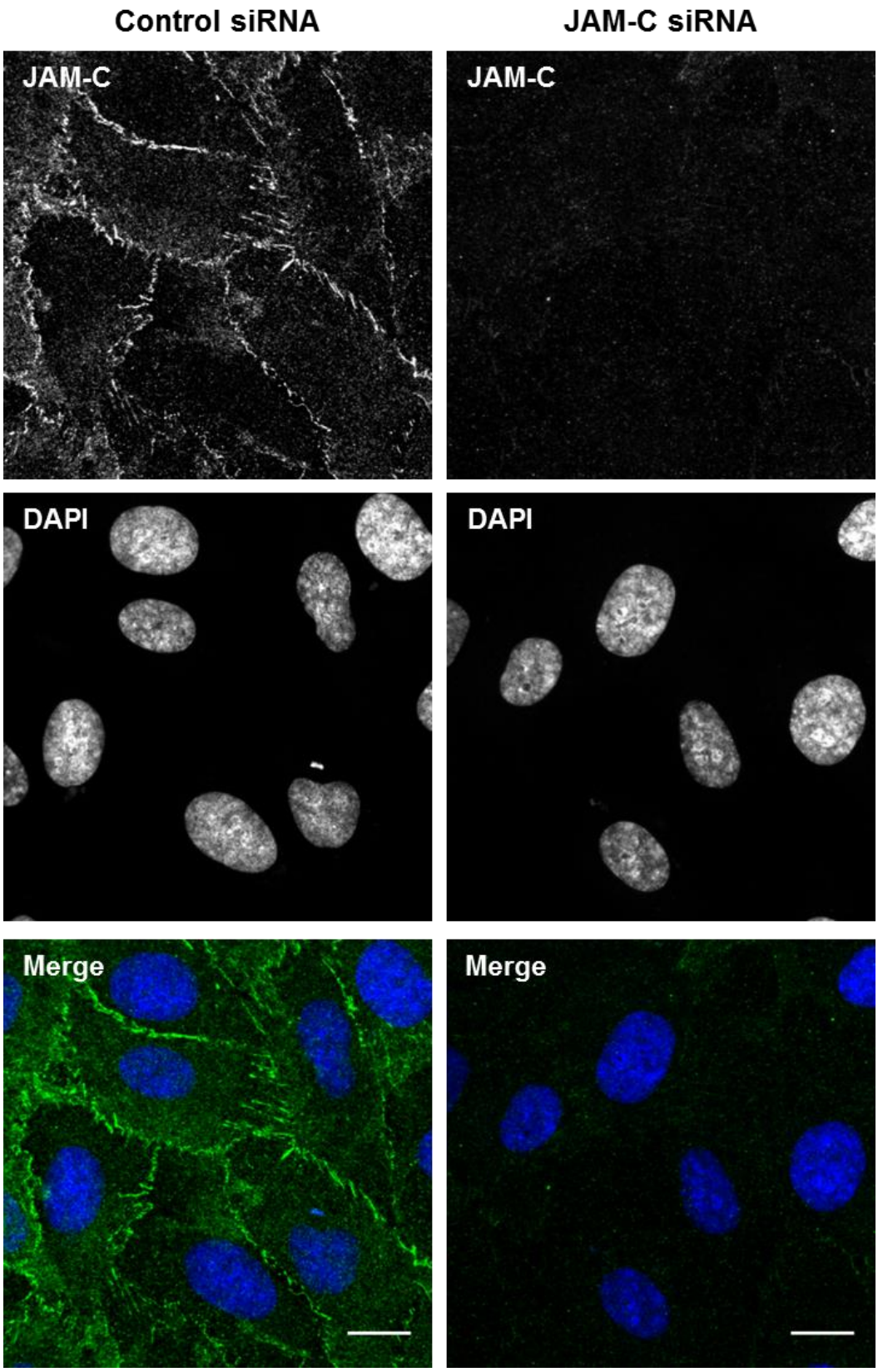

Figure 3.4. Immunofluorescence confocal microscopy validation of KD of JAM-C using the nucleofection method.

HUVECs were transfected with either control siRNA (left panel) or JAM-C siRNA (right panel) and then cultured for 72 h to reach confluence and then fixed for 15 mins in 4% PFA at room temperature. Cells were then immuno-stained for JAM-C and DAPI. Images were taken using a Zeiss LSM800 confocal microscope; scale bars represent 15 µm.

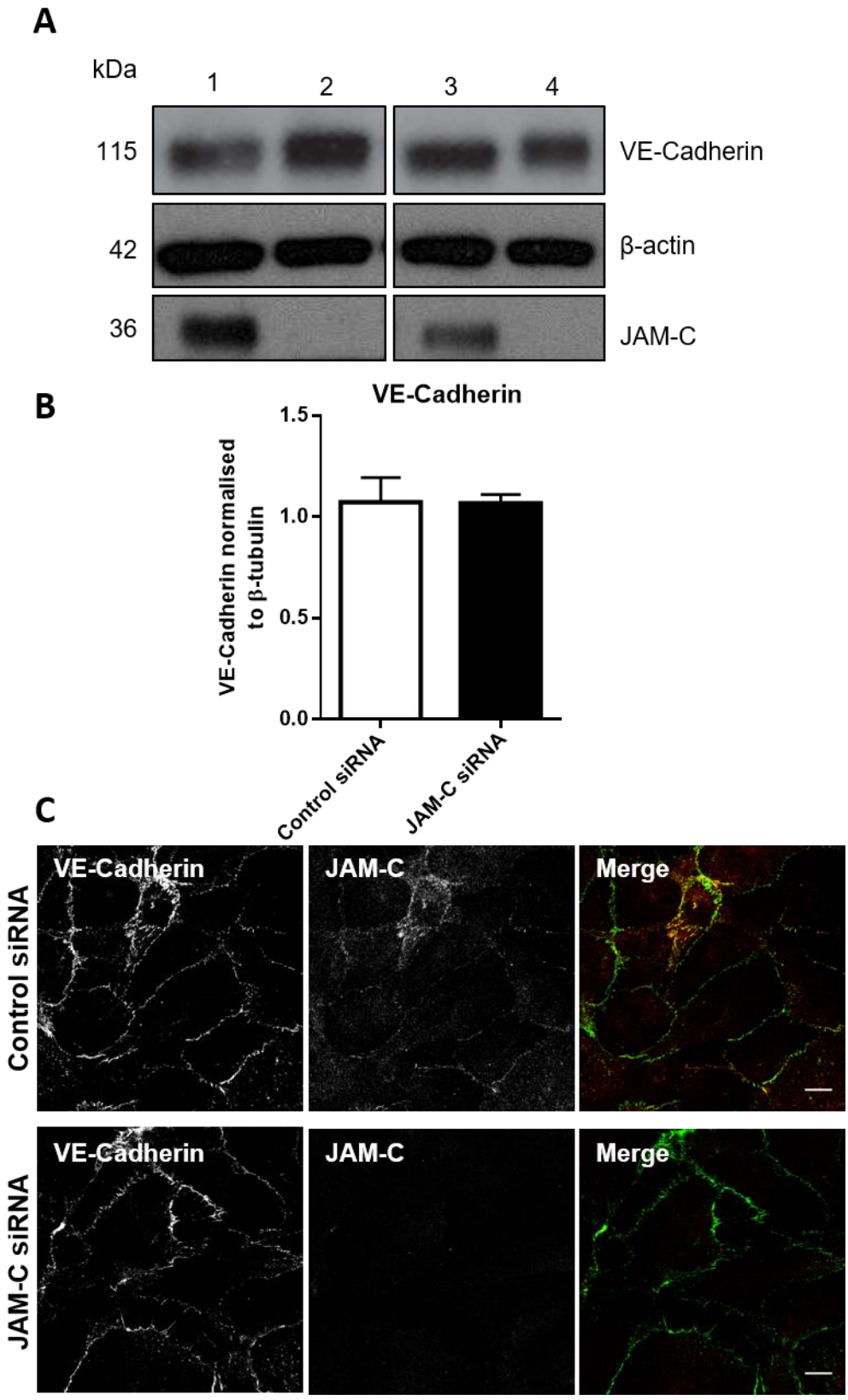

Figure 3.5 JAM-C KD in HUVECs does not impact VE-Cadherin expression.
(A) HUVECs were transfected with either control siRNA (lanes 1 & 3) or JAM-C siRNA (lanes 2 & 4) and then cultured for 48-72 h to reach confluence. Cells were then lysed and analysed for JAM-C and VE-Cadherin protein by Western Blot.
(B) Quantification of (A), where VE-Cadherin protein levels were normalised to β-actin loading control. Error bars represent SEM from and n=5 experiments.

(C) Immunofluorescence confocal microscopy of control and JAM-C KD HUVECs, cultured for 72h post-transfection then fixed for 15 mins in 4% PFA at room temperature. Fixed cells were then immuno-stained for VE-Cadherin (left-panels) and JAM-C (middle-panels). Images were taken using a Zeiss LSM-5 Pascal confocal microscope; scale bars represent 15 µm.

3.3.3. JAM-C KD does not affect expression of key EC junctional molecules

Prior to investigating the functional effects of JAM-C KD on ECs, it was first necessary to analyse the effect of the KD on general EC characteristics to ensure no adverse effects existed that could compromise further studies. Firstly, the expression level of additional EC junctional molecules was investigated under conditions of JAM-C KD.

The expression of the adherens junctional protein VE-Cadherin was analysed in JAM-C siRNA transfected HUVECs (hereafter referred to as JAM-C KD HUVECs). Western Blot analysis of these KD HUVECs under basal conditions indicated no change in VE-Cadherin protein expression between control and JAM-C KD HUVECs (Figure 3.5A&B). Additionally, immunofluorescence confocal microscopy of JAM-C KD HUVECs (Figure 3.5C, bottom panel) also showed no discernible change in VE-Cadherin expression when compared to control HUVECs (Figure 3.5C, top panel). Indeed, the localisation of VE-Cadherin was also unaffected, where it seemed to remain highly localised to the junctional compartment in the same manner to that observed under control conditions. However, without quantification of the micrographs in this figure these observations remain solely qualitative without such measurements.

The expression of the junctional protein JAM-A was also assessed in this model, as it is a close family member of JAM-C and an important component of EC tight junctions. Figure 3.6 shows immunofluorescence confocal microscopy images of control and JAM-C KD HUVECs immuno-stained for VE-Cadherin, JAM-C and JAM-A. As was observed with VE-Cadherin, no discernible change in JAM-A expression or localisation was observed under conditions of JAM-C KD. Quantification of total JAM-A levels by Western Blot and junctional JAM-A from the micrographs are needed confirm these observations

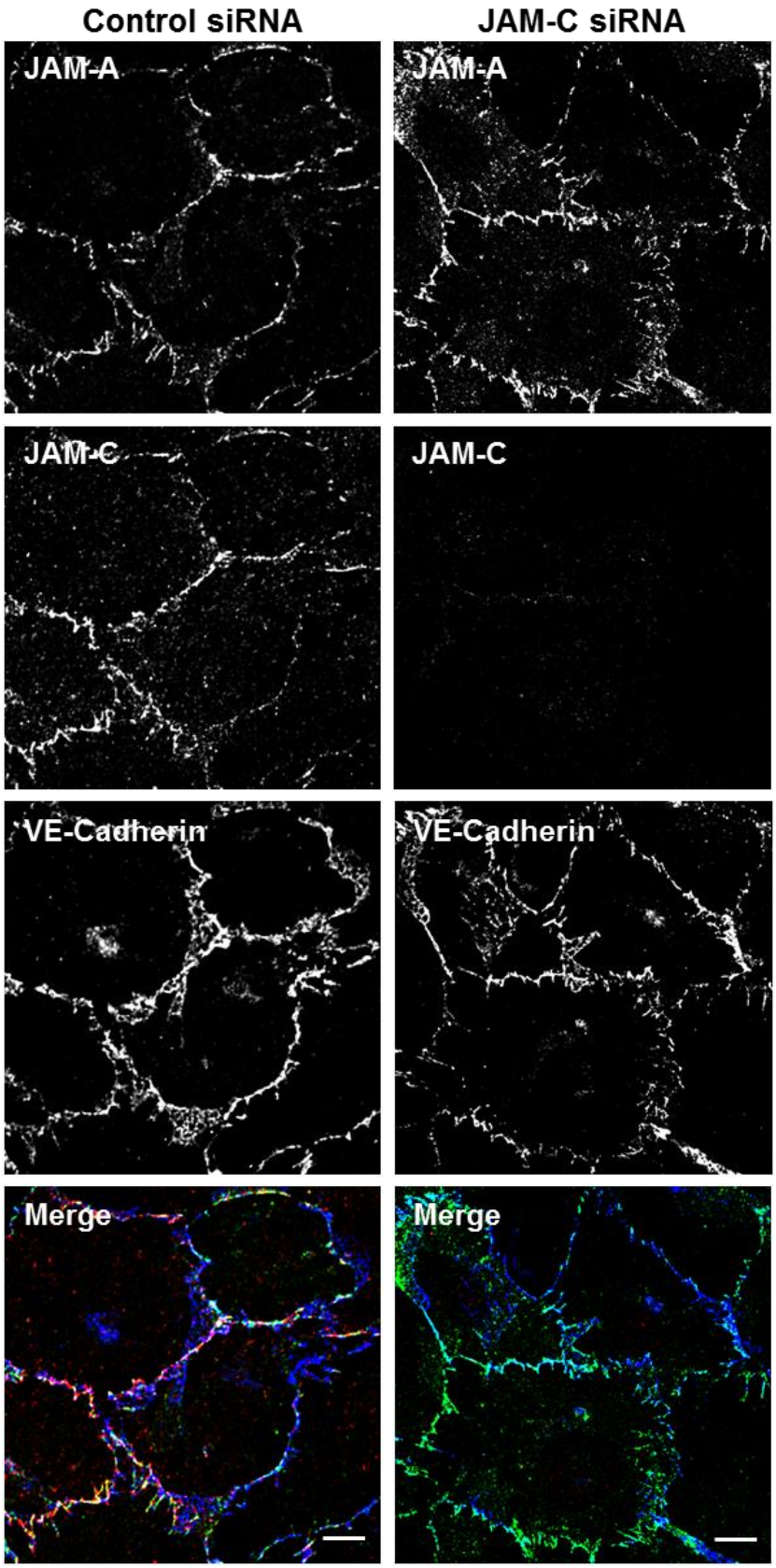

Figure 3.6. JAM-C KD does not impact JAM-A expression.
HUVECs were transfected with either control siRNA (left panel) or JAM-C siRNA (right panel), then cultured for 72 h to reach confluence and fixed for 15 mins in 4% PFA at room temperature. Cells were then immuno-stained for JAM-A (top-panels), JAM-C (middle-panels) and VE-Cadherin (bottom-panels). Images were taken using a Zeiss LSM-5 Pascal confocal microscope; scale bars represent 20 µm.

3.3.4. JAM-C KD does not affect EC morphology or proliferation

It was also necessary to assess the cellular morphology of the ECs that had been transfected with JAM-C siRNA. To achieve this, HUVECs were immuno-stained with VE-Cadherin to mark cell borders and assess cell shape, phalloidin to identify the F-actin cytoskeleton and DAPI to identify nuclear morphology. VE-Cadherin staining revealed no distinct changes in cellular size and shape

Figure 3.7 top panel) in JAM-C KD HUVECs compared to control HUVECs, although these parameters were not quantified from the micrographs. Finally, nuclear morphology also remained unaffected by JAM-C KD as assessed by DAPI staining.

F-actin stress fibers are necessary for ECs to maintain cell-cell contact and also for their interaction with the extracellular matrix (ECM) (Tojkander et al., 2012). HUVECs often display more actin stress fibers than microvascular ECs such as HDMECs, due to reduced stability of their adherens junctions and in particular discontinuous expression of VE-Cadherin (Millan et al., 2010). F-actin immuno-staining revealed stress fiber formation in both control and JAM-C KD HUVECs, with no discernible differences between them. In order to confirm and quantify these observations, protein extracts from control and JAM-C siRNA transfected cells would be analysed by Western Blot for the G- and F-actin pools and the F/G actin ratio calculated.

Another key feature of ECs is their proliferative capacity, which is crucial for their functionality in angiogenesis (Adair and Montani, 2010). As such, the proliferative capacity of JAM-C KD ECs was assessed using an MTS-based proliferation assay, where the MTS substrate is hydrolysed to a formazan product by dehydrogenase enzymes in metabolically active cells. The amount of formazan product measured at 490 nm is directly proportional to the number of living cells in culture. Using this method, control and JAM-C KD HUVECs were compared alongside untransfected HUVECs over 24-72 h of culture. After 72 h of culture, untransfected HUVECs showed significant proliferation when compared to the 24 h time-point (Figure 3.8B). The transfection procedure itself slightly reduced the proliferative capacity of HUVECs, though this was not significant. No differences were observed between control and JAM-C KD HUVECs over 72 h of culture, a period during which both cell types showed significant proliferation.

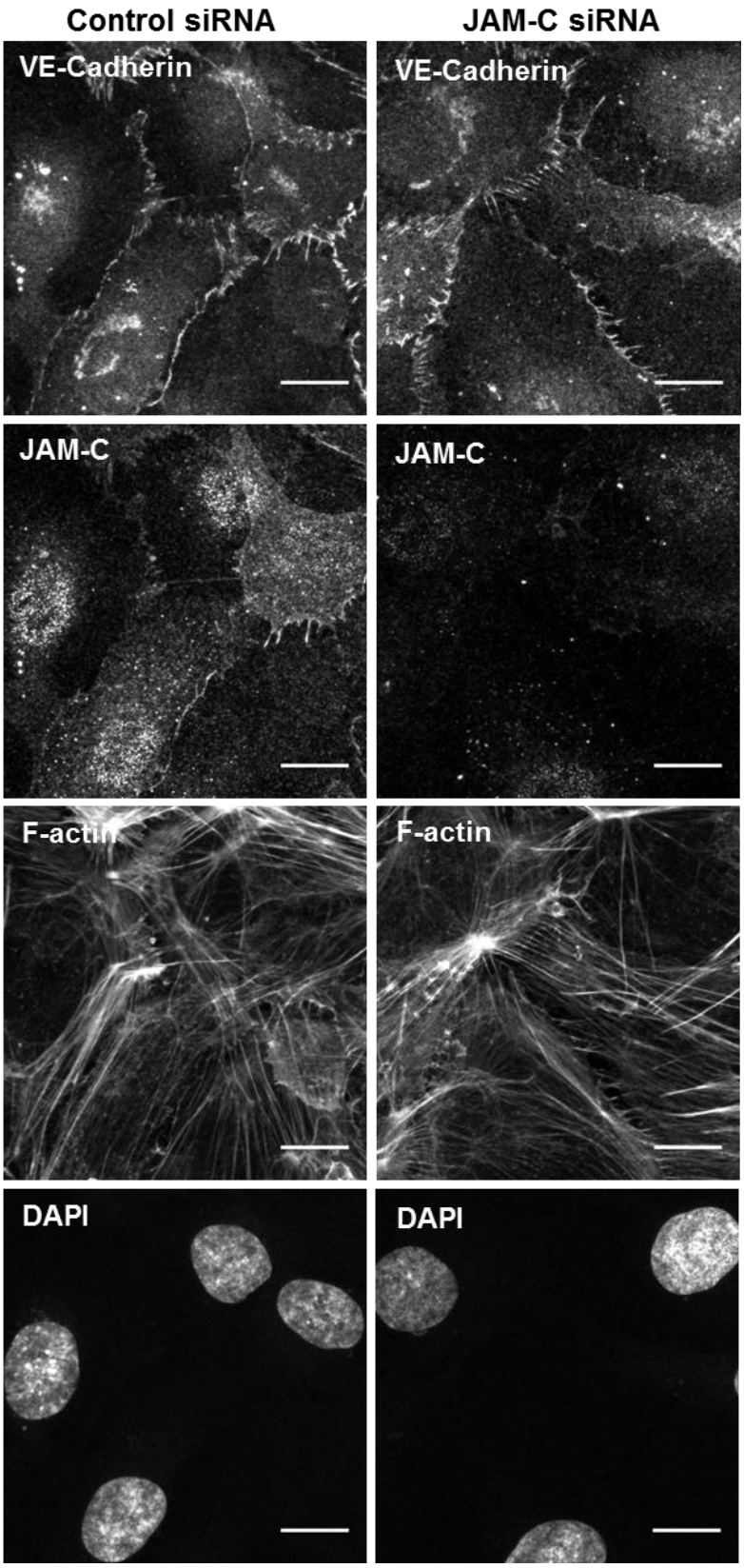

Figure 3.7. JAM-C KD does not impact EC morphology.
HUVECs were transfected with either control siRNA (left panel) or JAM-C siRNA (right panel), then cultured for 72 h to reach confluence and fixed for 15 mins in 4% PFA at room temperature. Cells were then immuno-stained for VE-Cadherin, JAM-C, F-actin and DAPI. Images were taken using a Zeiss LSM800 confocal microscope; scale bars represent 15 µm.

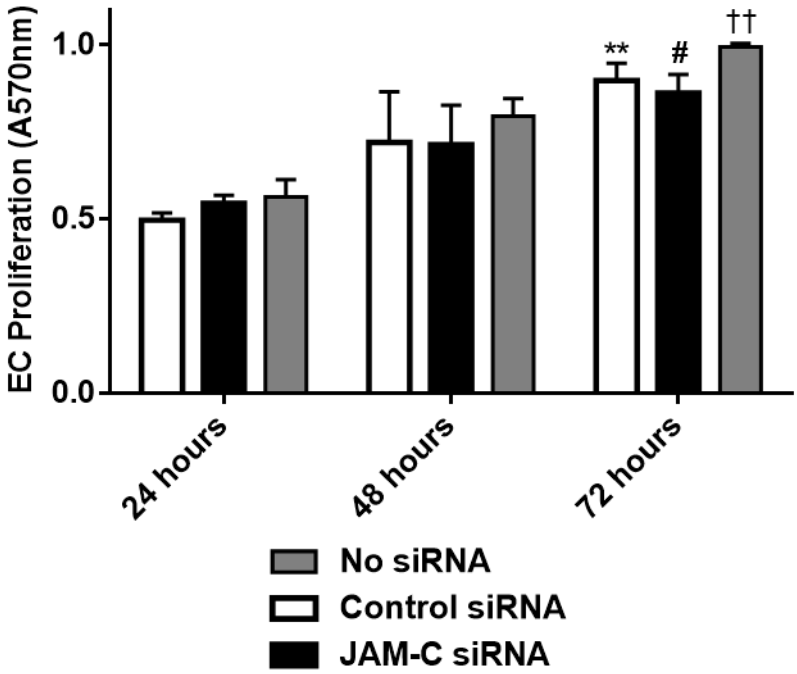

Figure 3.8. JAM-C KD does not affect proliferative potential of HUVECs.
(A) HUVECs were transfected with either control siRNA (top panels) or JAM-C siRNA (bottom panels) and then cultured for 48 h. Bright-field images of confluent cells were taken using an inverted Olympus IX81 microscope.
(B) HUVECs transfected with control or JAM-C siRNA were analysed for proliferation using an MTS based proliferation assay. Briefly, transfected cells were seeded at 5,000 cells per well in 96 well plates, then analysed for proliferation over 24-72 h. MTS compound was added to the cells to enable the detection of formazan product through absorbance at 570 nm. Transfected cells were compared alongside untransfected HUVECs. Error bars represent SEM from 3 independent experiments. Statistical significance determined by two-way ANOVA, **=$p<0.01$ compared to control siRNA 24 h, #=$p<0.05$ compared to JAM-C siRNA 24 h, ††=$p<0.01$ compared to no siRNA 24 h.

3.3.5. JAM-C KD does not impact EC viability

Finally, it was necessary to examine whether KD of JAM-C in HUVECs resulted in decreased cell viability due to increased levels of cell death. It was important to verify the viability state of the ECs before embarking on further studies, such as those into gene expression and responses to inflammation that are documented in Chapters 5 & 6. As such, two mechanisms of cell death were investigated in this model of *in vitro* EC JAM-C KD, those being apoptotic and necrotic cell death.

In normal, healthy cells, phosphatidylserine (PS) residues are found in the inner leaflet of the plasma membrane. Upon induction of apoptosis, these PS residues are

translocated to the outer leaflet and therefore externalised, providing a marker for apoptosis. The protein Annexin-V is a specific binding protein of PS and so can therefore be used to detect apoptosis (Bossy-Wetzel and Green, 2000). As such, control and JAM-C KD HUVECs were immuno-stained for Annexin-V and DAPI and then analysed by FACS. Double negative cells were determined as live viable cells, while Annexin-V positive cells were determined as apoptotic (Figure 3.9A). The majority of both control and JAM-C KD HUVECs were found to be viable and there was no difference in apoptotic cells found between the two conditions (Figure 3.9B).

Control and JAM-C KD HUVECs were also assessed for release of lactate dehydrogenase (LDH), a commonly used measure of necrotic cell death. LDH is released by cells when the cell membrane is compromised, as happens during necrosis. The level of LDH released into the supernatant of cultured cells can then be calculated by absorbance. As seen for apoptosis, no difference between control and JAM-C KD HUVECs was observed for LDH release (Figure 3.9C).

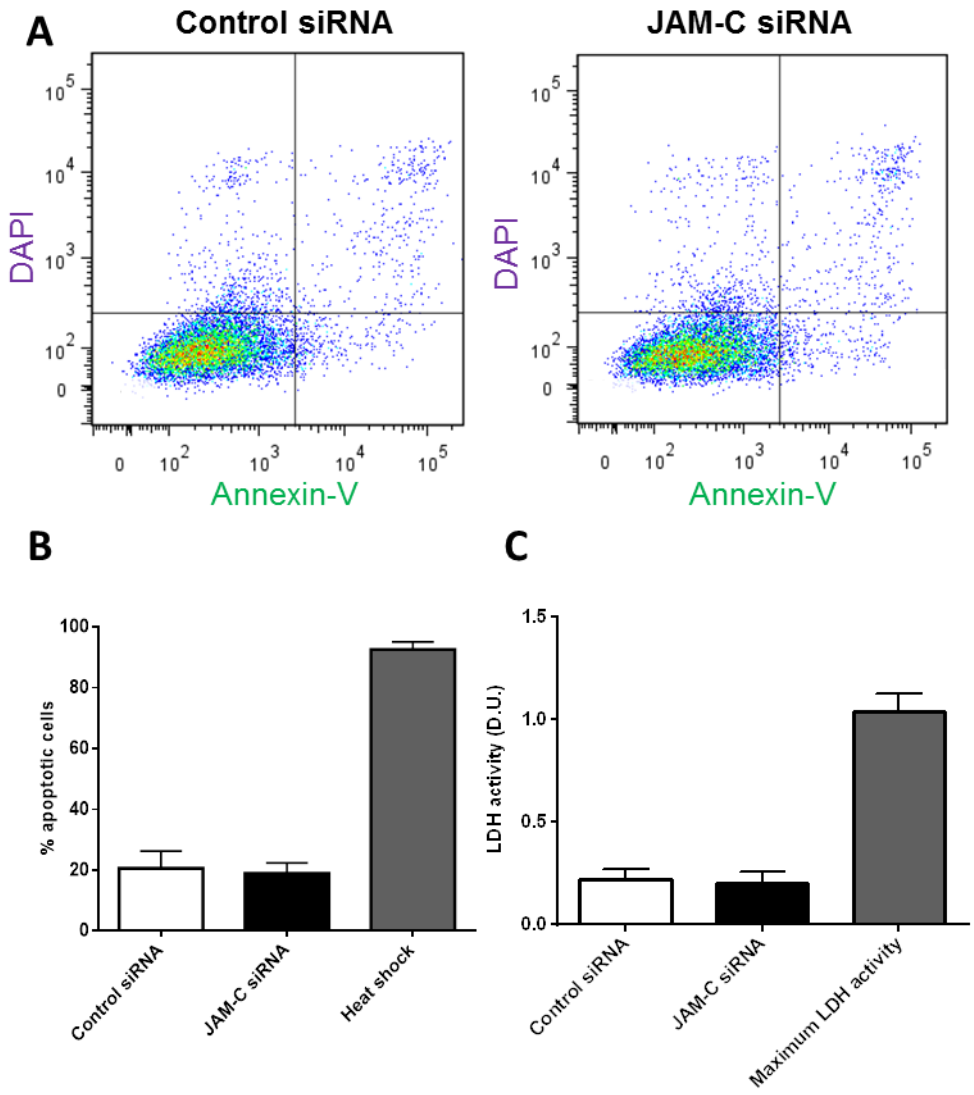

Figure 3.9. JAM-C KD does not impact EC viability.
(A) HUVECs were transfected with either control siRNA (top panels) or JAM-C siRNA (bottom panels) and then cultured for 48-72 h to reach confluence. Cells were then detached and stained with Annexin-V and DAPI. Samples were run on an LSRFortessa flow cytometer and analysed using FACSDiva software.
(B) Quantification of data in (A). Viable cells were determined as Annexin-V^-/$DAPI^-$. Apoptotic cells were determined as those Annexin-V^+/$DAPI^-$ or Annexin-V^+/$DAPI^-$. Transfected HUVECs were compared to cells treated with 95°C heat-shock for 10 mins as a positive control. Error bars represent SEM from three independent experiments.
(C) Control and JAM-C KD HUVECs were analysed for cellular cytotoxicity by LDH release assay. Sample medium from transfected HUVECs was tested for production of formazan product following addition of kit reagents. The absorbance of each sample was analysed and compared to a positive control sample. Error bars represent SEM from three independent experiments. This part of the work was done in collaboration with Dr Natalia Reglero.

3.4. Discussion

While a great deal is known about the role of JAM-C in biological processes such as angiogenesis, permeability and leukocyte migration, little is known about how JAM-C functions within the ECs themselves and more importantly, what the effect of JAM-C deficiency is on ECs. As such, this chapter sought to establish a robust protocol for *in vitro* KD of JAM-C in cultured ECs.

Initially, attempts were undertaken to investigate the localisation of JAM-C in cultured ECs *in vitro* by immunofluorescence confocal microscopy. Using both HUVECs and HDMECs, JAM-C localised to the inter-endothelial junctions and also to intracellular stores. Intriguingly JAM-C also showed expression in the nucleus on some occasions, perhaps suggesting a potential role for JAM-C in the nucleus that is yet to be identified. It must be stressed that this localisation was not observed in every case, highlighting either heterogeneity in JAM-C expression across batches of cultured HUVECs, or perhaps some non-specific binding of the antibody to the nucleus. This nuclear localisation is somewhat controversial, as JAM-C is a transmembrane junctional protein and so many argue against it having a role in the nucleus. However, a number of junctional and junctional associated molecules such as ZO-2 and ZONAB have been shown to localise to the nucleus (Balda et al., 2003, Islas et al., 2002, Traweger et al., 2003), so it is not inconceivable for JAM-C to localise there and have a nuclear function. This potential expression is interesting in the context of the results that will be discussed in Chapter 5 on gene expression and as such this expression requires further investigation.

To date, there have been a number of studies investigating the localisation of JAM-C in a similar manner. The majority of reports suggest that in HUVECs, JAM-C localises to EC junctions under resting conditions in agreement with the data presented in the first part of this chapter (Chavakis et al., 2004, Li et al., 2009, Orlova et al., 2006, Sircar et al., 2007). In addition, Orlova et al., showed that this expression at EC junctions is not affected by stimuli such as histamine and VEGF. In contrast, another study in HUVECs suggested that JAM-C was only present at EC junctions following VEGF stimulation (Lamagna et al., 2005b). While the data in this chapter indicate that JAM-C is present at junctions of HDMECs under resting conditions, conflicting data has previously been

reported in the same cell type where it was shown JAM-C is only expressed at the junctions following stimulation with VEGF or histamine.

In order to investigate the effects of loss of JAM-C on EC function, it was necessary to establish a protocol of targeted KD of JAM-C in ECs *in vitro*. For this purpose, transfection of HUVECs with siRNA targeted to JAM-C was chosen as the preferred method. siRNA was chosen over shRNA to attain the JAM-C KD for a number of reasons. Firstly, as HUVECs can only be passaged a limited number of times until they lose their endothelial characteristics (Liao et al., 2014, Prasad Chennazhy and Krishnan, 2005), the use of shRNA to produce a stably transfected cell line was not deemed necessary. Secondly, a number of studies have used siRNA to KD JAM-C in various cell types to good effect (Bradfield et al., 2007, Economopoulou et al., 2009, Li et al., 2009, Orlova et al., 2006), indicating that this was a good method to replicate. Indeed, the siRNA sequences from one such study (Li et al., 2009) were used in this study to KD JAM-C in HUVECs. Transfection of HUVECs with this siRNA targeted to JAM-C yielded a reproducible and highly significant KD of JAM-C, in excess of 90%. Thus, a reliable protocol was established for KD of JAM-C in ECs *in vitro* which would allow for investigations into the functions of EC JAM-C.

It must be stressed that the use of siRNA to KD expression of any molecule is not without limitations, the most notable of which is the off-target effects of the siRNA. It could be possible that any subsequent effects observed when analysing JAM-C KD HUVECs are due to siRNA impacting the expression of one or more additional genes in the cell rather than just JAM-C. Indeed, it has been established that siRNA can exert effects of mRNA silencing when there are as many as five mismatches in the siRNA sequence. As such, it is important to recognise this potential caveat during the experimental design and to design methods to reduce the off-target effects. Reducing the concentration of individual siRNA sequences is an effective way to reduce the possibility of off-target effects, or even combining a pool of two or more siRNAs targeted to the same molecule in much reduced concentrations (Jackson and Linsley, 2010). Given that the two siRNA sequences used to KD JAM-C in this model are taken from published research and were also used in combination at lower concentrations (70 nM per siRNA) to achieve effective KD than would be required for one siRNA alone, we were confident that any subsequent functional effects of JAM-C KD were in fact

due to an impact on JAM-C expression. To conclusively ensure the effects of the siRNA are target specific, a rescue experiment can be performed. This would involve the overexpression of a JAM-C construct on a JAM-C KD background and then analysing the subsequent functionality of those cells, specifically addressing whether the over-expression ameliorates the phenotype seen under conditions of JAM-C KD. While this was not performed in the current project, ongoing works are evaluating this as a possible validation of the EC JAM-C KD phenotypes that are discussed in the subsequent chapters.

Prior to embarking on functional studies into the effects of JAM-C KD in ECs, this chapter also assessed the expression level and localisation of additional junctional molecules following JAM-C KD. Using both total protein analysis by Western Blot and immunofluorescence confocal microscopy it was confirmed that JAM-C KD had no impact on VE-Cadherin expression or localisation in HUVECs, corroborating previous findings (Li et al., 2009, Orlova et al., 2006). While it was not investigated in this setting, Li et al also demonstrated that PECAM-1 expression is also unaffected. The present study also confirmed that both expression and localisation of the tight junction molecule JAM-A, a close family member of JAM-C, remained unperturbed by JAM-C KD. Studies on JAM-C KD in epithelial cells have repeated the same findings (Economopoulou et al., 2009), where the authors suggested that loss of JAM-C does not lead to a compensatory change in the expression of other JAM family members. As such, results suggest that much like epithelial cells, ECs do not compensate for loss of JAM-C by upregulating JAM-A expression. The findings from this section were crucial to the subsequent studies reported in this thesis. If JAM-C KD had caused disrupted expression of additional junctional molecules, it could be argued that any phenotype seen in JAM-C ECs would be attributed to the secondary disrupted expression rather than the loss of JAM-C expression itself. As this was not the case, any cellular phenotypes reported in JAM-C KD ECs could therefore be directly linked to JAM-C deficiency.

Finally, it was necessary to check the morphology and viability of JAM-C KD ECs to confirm they were suitable for functional analysis. Nuclear morphology was unaffected, as was the actin cytoskeleton as identified by no changes in F-actin structures between control and JAM-C KD HUVECs (Figure 3.7). HUVECs form loose

and discontinuous adherens junctions, resulting in the formation of actin stress fibers and therefore increased cell tension (Millan et al., 2010). VE-Cadherin binds to β-catenin at the adherens junctions and β-catenin can in turn bind to α-catenin. It is suggested that α-catenin can either bind to F-actin or β-catenin, but not both, so in stable adherens junctions α-catenin is recruited to the VE-Cadherin/β-catenin complex and stress fiber formation is reduced (Drees et al., 2005, Yamada et al., 2005). However, disruption of adherens junctions specifically would enable α-catenin to bind to F-actin and regulate stress fiber formation. Such a mechanism could account for the presence of some stress fibers in both control and JAM-C KD HUVECs in this model where some disruption of the adherens junctions is observed. This was interesting given the previous findings of Orlova et al., that reported a reduction in F-actin stress fibers in JAM-C KD HDMECs, a response that contributes to reduced EC contractility (Orlova et al., 2006). The differences between the findings of the present study and published works could be due to heterogeneity in EC type and source. There are no direct reports published on EC morphology, confluency or proliferation in JAM-C KD ECs and hence the data generated as part of this thesis provides a valuable resource. The present work also showed that JAM-C KD had no impact on cell viability in ECs due to apoptosis or necrosis. Increased cell death could impact greatly on EC functional studies, particularly into EC inflammatory responses. Taken together, these findings allowed for the current model of *in vitro* EC JAM-C KD to be extended to novel functional studies.

Summary of key findings

- Targeted siRNA to JAM-C effectively depletes expression in HUVECs as indicated by both immunoblot and immunofluorescence.
- Loss of JAM-C from HUVECs does not affect expression of junctional markers JAM-A or VE-Cadherin.
- Loss of JAM-C does not significantly impact basic cellular properties such as proliferation or apoptosis.

4 Loss of endothelial cell JAM-C triggers autophagy *in vitro*

4.1 Introduction

4.1.1 Autophagy and cellular homeostasis

The cellular process of autophagy is intrinsically linked to the homeostatic status of the cell itself. Many cellular insults or stressors that can affect the status of the cell and therefore impact upon homeostasis can also result in the upregulation of autophagy. Such stressors can include nutrient deprivation, hypoxia, damaged organelles, protein aggregates and infection by pathogens, among many others (Ryter et al., 2013). In essence, autophagy can be thought of as a process that is upregulated during times of cell stress that serves to maintain homeostasis and ultimately cell survival (Kroemer et al., 2010, Levine et al., 2011, Awan and Deng, 2014).

Recently, upregulation of autophagy has been associated with the disruption of tight junction integrity (Nighot et al., 2015). Here it was demonstrated that increased autophagy reduces intestinal epithelial permeability to small molecules and ions by targeting claudin-2 for endo-lysosomal degradation. However, to date there have been no publications reporting a direct role of EC junctional molecules as regulators of autophagy. In this context, unpublished works from our laboratory have indicated that mice with conditional KD of JAM-C in ECs exhibited increased autophagy. To build on these novel findings using a well-controlled and established *in vitro* model, the present works aimed to elucidate the potential impact of JAM-C deficiency on EC autophagy.

In a related manner, it has been shown that the main components of plasma membrane gap junctions in epithelial cells, the connexins, control autophagy through interactions with proteins involved in autophagosome formation (Bejarano et al., 2014). While a multitude of different cells types have gap junctions, ECs are known to only contain adherens and tight junctions (Bazzoni, 2004). Junction stability through regular junctional molecule expression is undoubtedly crucial for maintaining normal EC function, as highlighted by the embryonic lethality of junctional molecule KO mice, such as VE-Cadherin (Carmeliet et al., 1999) and ZO-1 (Katsuno et al., 2008). As such, disrupted expression of junctional molecules might represent a potential cellular insult

that could impact upon EC homeostasis and thus stimulate autophagy. This concept was investigated here in the context of JAM-C.

4.1.2 Methods for analysing autophagy

The level of the lipidated form of the protein Microtubule-associated protein 1A/1B-light chain 3 (LC3) is a commonly used method of measuring autophagy both *in vitro* and *in vivo*. LC3-I is the cytosolic form of LC3, which upon autophagic stimuli is cleaved and conjugated to phosphatidylethanolamine (PE) to form LC3-II and recruited to the autophagosome membrane (Tanida et al., 2008) (See Figure 4.1). Hence, increased levels of LC3-II protein can be used as a method to measure autophagy in cultured HUVECs. In addition to this, pharmacological inhibitors of autophagy, such as Bafilomycin A1 and 3-methyladenine (3-MA), are also useful tools for studying autophagy (Figure 4.1). Bafilomycin A1, a V-ATPase inhibitor, inhibits the acidification of lysosomes and as such is used to inhibit the fusion of autophagosomes and lysosomes, which would normally lead to autophagosome content degradation (Yang et al., 2013). Bafilomycin A1 treatment therefore creates an accumulation of LC3-II positive autophagosomes under any given condition and serves as a reliable readout for rates of autophagic flux (Barth et al., 2010). Class III PI3Ks have been shown to be crucial in the early steps of autophagosome biosynthesis in mammalian cells. These PI3Ks form a core initiation complex with Beclin-1 and the p150 PI3K adaptor protein to enable autophagosome isolation membrane nucleation, the critical first step in the formation of the autophagosome (Pyo et al., 2012, Miller et al., 2010). As such, inhibition of class III PI3Ks is a commonly used mechanism to prevent autophagosome formation, the most widely used of which is 3-MA. To stimulate autophagy, a number of different approaches may be taken. One of the most widely used methods is nutrient deprivation, or starvation, which induces autophagy to recycle cellular constituents for energy consumption and to maintain cell survival (Shang et al., 2011, Xiong et al., 2014). The other commonly used method is to treat with the mammalian target of rapamycin (mTOR) inhibitor rapamycin, which has been shown to be a potent inducer of autophagy in many cell lines (Sarkar et al., 2009, Wu et al., 2013). mTOR is a negative regulator of autophagy and so inhibition of its kinase activity releases the negative checkpoint, allowing autophagy to proceed (He and Klionsky, 2009).

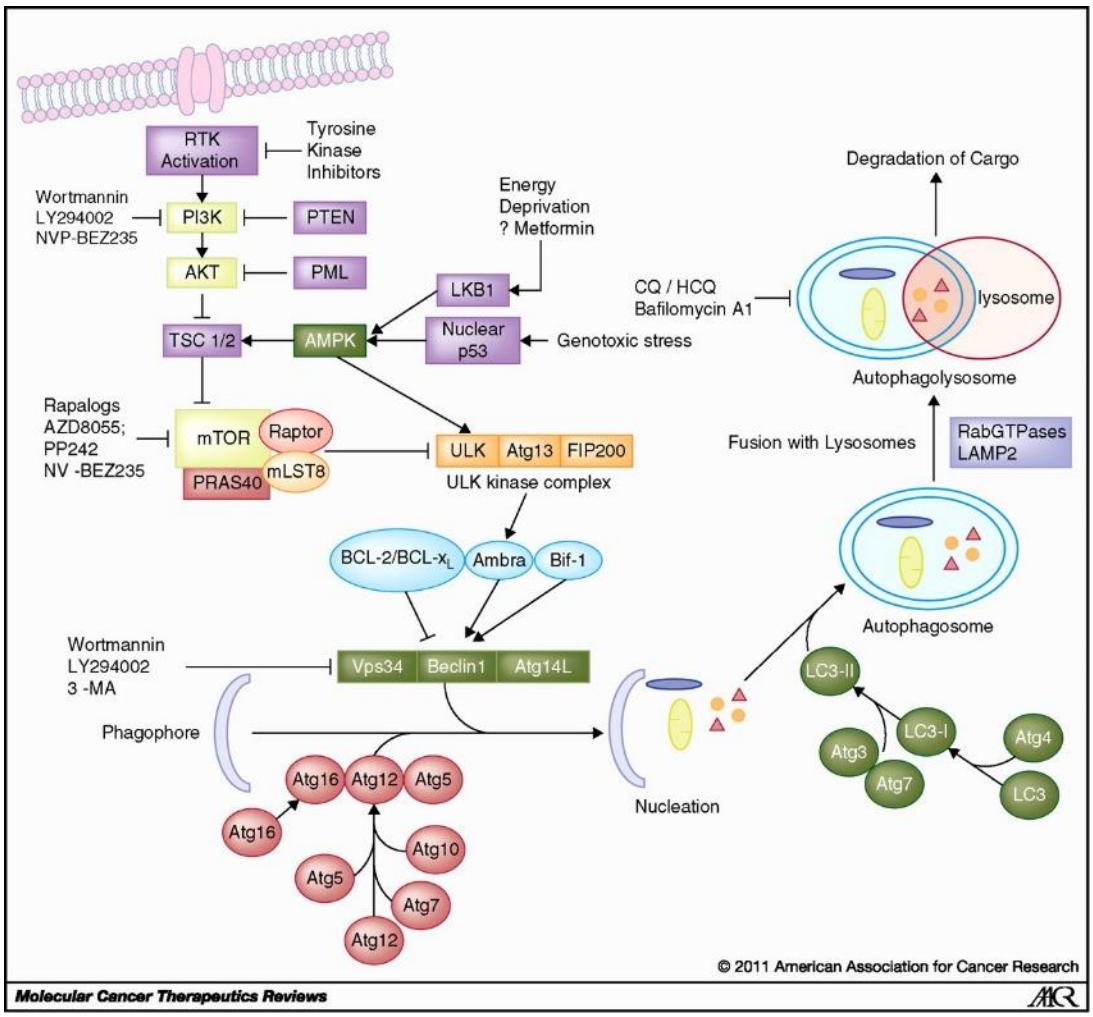

Figure 4.1. Overview of the molecules involved in autophagosome formation and the various sites of pharmacological inhibition. Taken from (Yang et al., 2011)**.**

4.2 Aims

The results in the previous chapter demonstrated that KD of JAM-C in HUVECs had no effect on cell viability nor did it result in increased EC apoptosis. With that in mind and given the previous findings that loss of JAM-C from EC tight junctions results in a number of phenomena (such as increased neutrophil rTEM and decreased EC permeability), we hypothesised that loss of JAM-C impacts upon the cellular status of the ECs, which could result in the upregulation of autophagy as a counteractive measure to maintain homeostasis. This hypothesis is supported by preliminary *in vivo* works stemming from our laboratory and to extend to an *in vitro* setting, objectives of the present work included:

- To establish reliable methods for the detection of autophagy in cultured ECs in our laboratory.
- To determine whether the loss of JAM-C from ECs triggers autophagy *in vitro*.

4.3 Results

4.3.1 Starvation induces autophagy in HUVECs

Prior to investigating the role of JAM-C in EC autophagy, the response of ECs to established autophagic stimuli and inhibitors was characterised. Thus, HUVECs were subjected to nutrient starvation for 2 h and compared to HUVECs cultured in complete growth media. Figure 4.2 shows the response of HUVECs to starvation, where a significant increase in LC3-II protein is seen by Western Blot following 2 h of starvation (lanes 1 & 2, $p<0.05$). Treatment of HUVECs with 100 nM Bafilomycin A1 to inhibit autophagosome and lysosome fusion resulted in a significant increase in LC3-II levels under both basal and starved conditions (Figure 4.2, lanes 3 & 4, $p<0.0001$). More significantly, HUVECs subjected to both starvation and Bafilomycin treatment showed a significantly greater level of LC3-II protein compared to cells treated with Bafilomycin alone ($p<0.01$). These results indicate that starvation induces a *bona fide* increase in autophagic flux in cultured ECs.

To corroborate these findings, HUVECs subjected to starvation were immuno-stained for detection of LC3 puncta representing autophagosomes. Immunofluorescence confocal microscopy of control and starved HUVECs (Figure 4.3) highlighted increased numbers of LC3 puncta in starved HUVECs compared to their non-starved control counterparts. Under basal conditions LC3 immunostaining was much more diffusely distributed in the perinuclear region, indicative of more cytosolic LC3-I protein in non-starved control cells. By contrast, starved HUVECs exhibited a more vesicular immunostaining for LC3, which was less diffusely distributed. Treatment of HUVECs with both starvation and Bafilomycin A1 induced a drastic increased in LC3 positive puncta, correlating well with the Western Blot data indicated in Figure 4.2. Starvation induces autophagy in HUVECs.

Immunostaining with isotype control to demonstrate specificity to LC3 can be found in Appendix 2. Here, in HUVECs treated with both starvation and Bafilomycin A1, isotype control staining identified no puncta that are observed compared to that seen when the LC3 specific antibody is used.

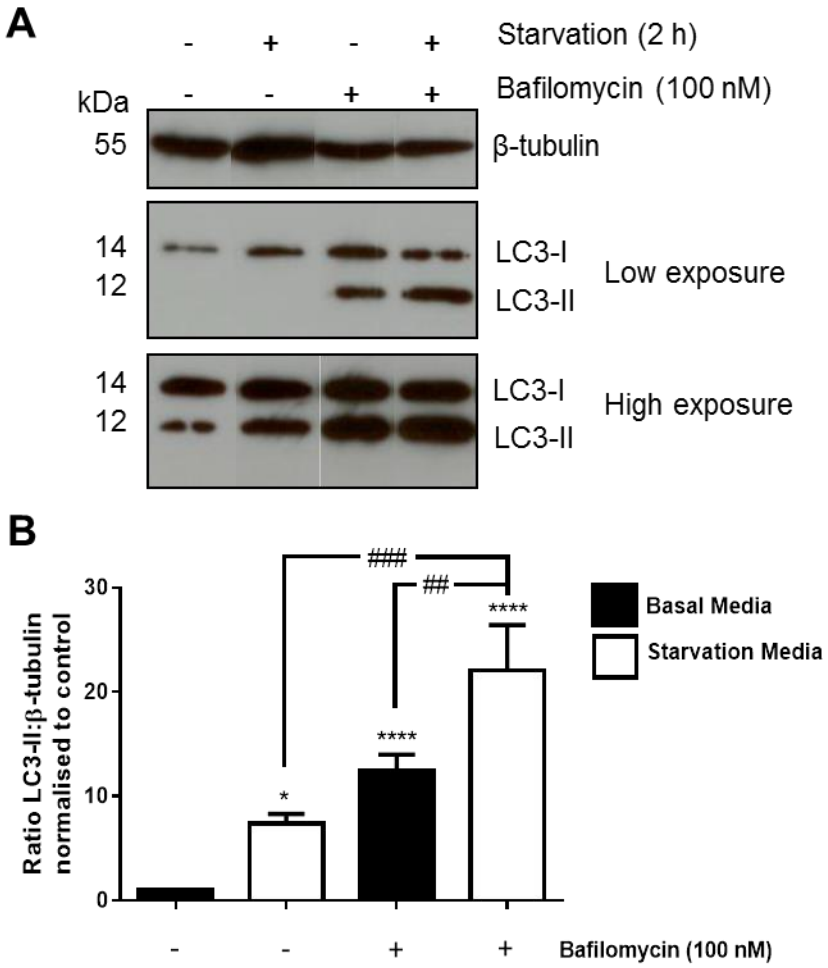

Figure 4.2. Starvation induces autophagy in HUVECs.
(A) Confluent HUVECs were treated with complete growth or starvation medium for 2 h, in the presence of Bafilomycin A1 (100 nM) or vehicle control. Cells were lysed and then analysed for changes in LC3-II protein levels by Western Blot.
(B) LC3-II protein levels were quantified and normalised to β-tubulin loading control using ImageJ software. Each experiment was expressed as fold increase in LC3-II protein levels compared to untreated control cells. Error bars represent SEM from n= 6-9 experiments. Statistical significance calculated by one-way ANOVA, * = $p<0.05$ ** = $p<0.01$ **** = $p<0.0001$ all compared to non-starved cells, ## = $p<0.01$ compared to Bafilomycin treated cells, ### = $p<0.001$ compared to starved cells.

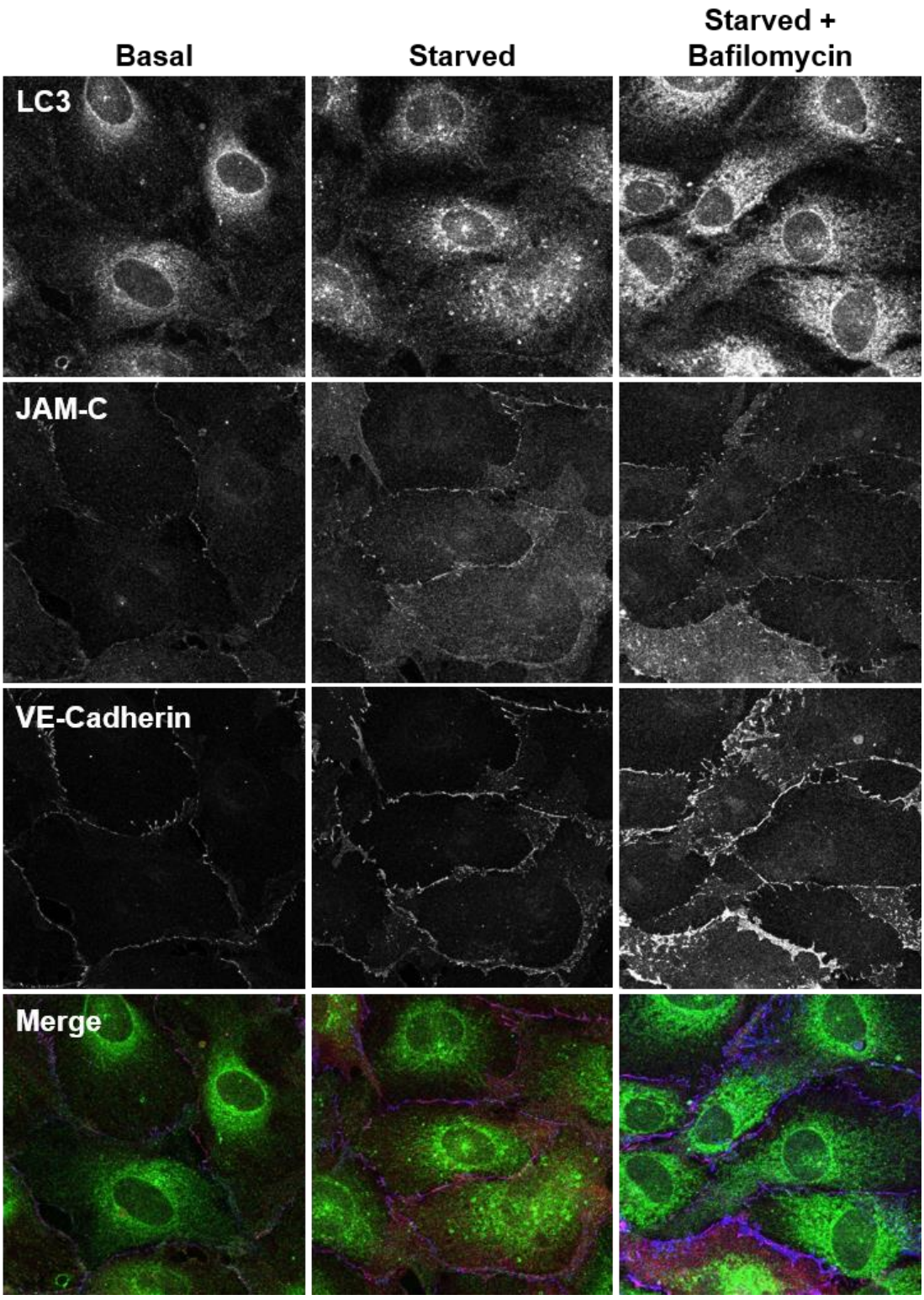

Figure 4.3. Starvation induces LC3 puncta formation in HUVECs. Untransfected HUVECs were cultured for 48-72 h to reach confluence, then cultured with either starvation medium or complete growth medium for 2h. Bafilomycin A1 inhibitor or vehicle control was added for the same time period as indicated. Cells were fixed in 100% methanol for 3-5 mins at -20^{o}C, then immuno-stained for and LC3 (green), JAM-C (red) and VE-Cadherin (blue). Images were taken using a Zeiss LSM800 confocal microscope, scale bars represent 15µm.

4.3.2 Pharmacological inhibition of starvation induced autophagy by 3-MA

The formation of autophagosomes through the canonical route is dependent on the activity of PI3Ks. This can be either through the regulation of mTOR activity by PI3Ks or by PI3K recruitment to the Beclin1 complex at the initiation of autophagosome formation. As such, inhibition of PI3Ks enables identification of canonical autophagic responses to stimuli. Thus, treatment of HUVECs with the PI3K inhibitor 3-MA for 2 h slightly reduced the LC3-II levels compared to vehicle control treated HUVECs (Figure 4.4, lanes 1 & 3), though this was not significant. Treatment of HUVECs with 3-MA when cultured under starved conditions for 2 h resulted in significantly reduced LC3-II protein ($p<0.05$) to levels similar to that observed under basal growth conditions (Figure 4.4, lanes 2 & 4). These results demonstrated that starvation-induced autophagy, and to a certain extent basal autophagy, in HUVECs is dependent on PI3K activity.

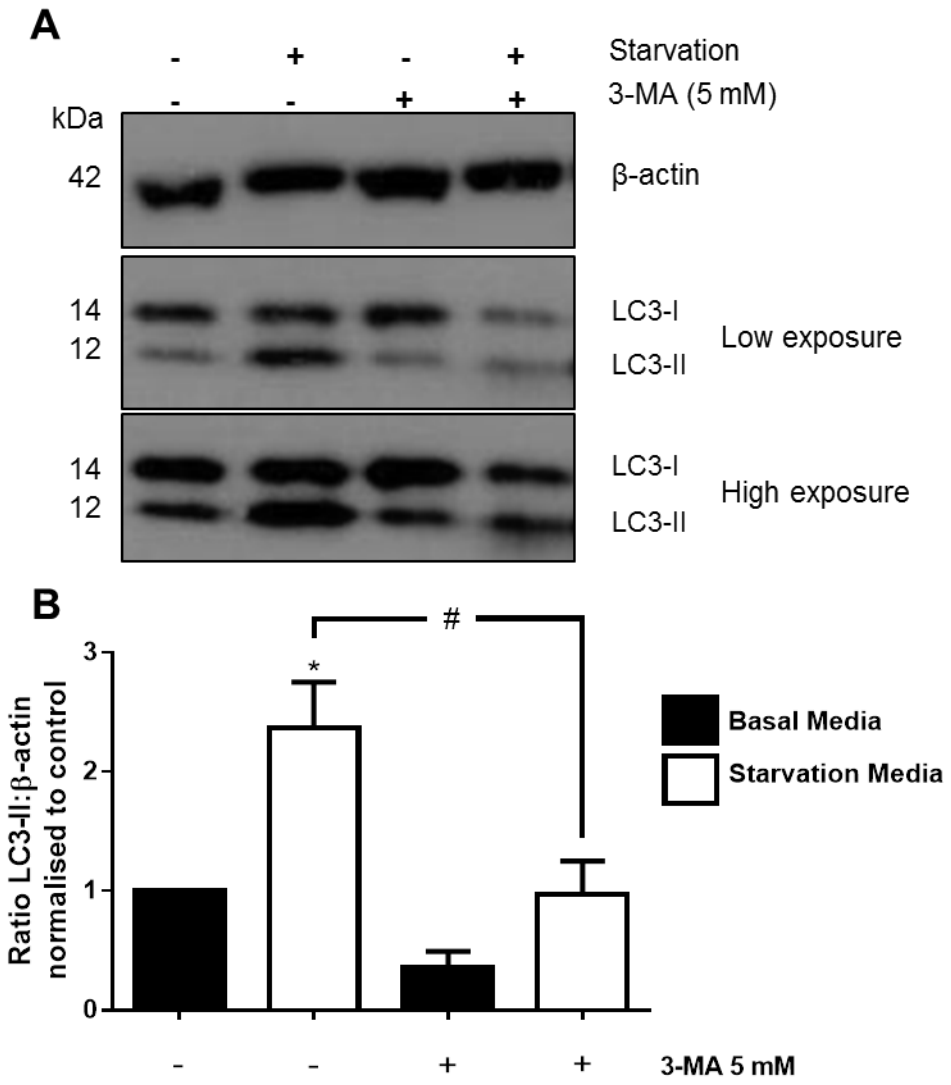

Figure 4.4. The PI3K inhibitor 3-MA inhibits starvation induced autophagy in HUVECs.
(A) Confluent HUVECs were cultured in complete growth or starvation medium for 2 h in the presence of 3-MA (5 mM) or vehicle control. Cells were lysed and then analysed by Western Blot for levels of LC3-II protein.
(B) LC3-II protein levels were quantified and normalised to β-actin loading control using ImageJ software. Each experiment was expressed as fold increase in LC3-II protein levels compared to untreated control cells Error bars represent SEM from n=3 experiments. Statistical significance calculated by unpaired t-test, *,# = $p<0.05$.

4.3.3 JAM-C KD induces autophagy in HUVECs

To investigate the potential role of JAM-C in regulating EC autophagy, the established method of siRNA mediated JAM-C KD in HUVECs was employed (See Chapter 3). KD of JAM-C in HUVECs resulted in a statistically significant increase in LC3-II protein levels ($p<0.01$) under basal growth conditions nearly three-fold over that in control HUVECs (Figure 4.5, lanes 1 & 2). When control and JAM-C KD HUVECs were treated with Bafilomycin A1 for 4 h, a significant increase ($p<0.05$) in LC3-II levels was still observed

in JAM-C KD HUVECs (Figure 4.5, lanes 3 & 4). These results demonstrated that loss of JAM-C resulted in an increase in autophagic flux, in a similar manner to that observed for starvation-induced autophagy (Section 4.3.1).

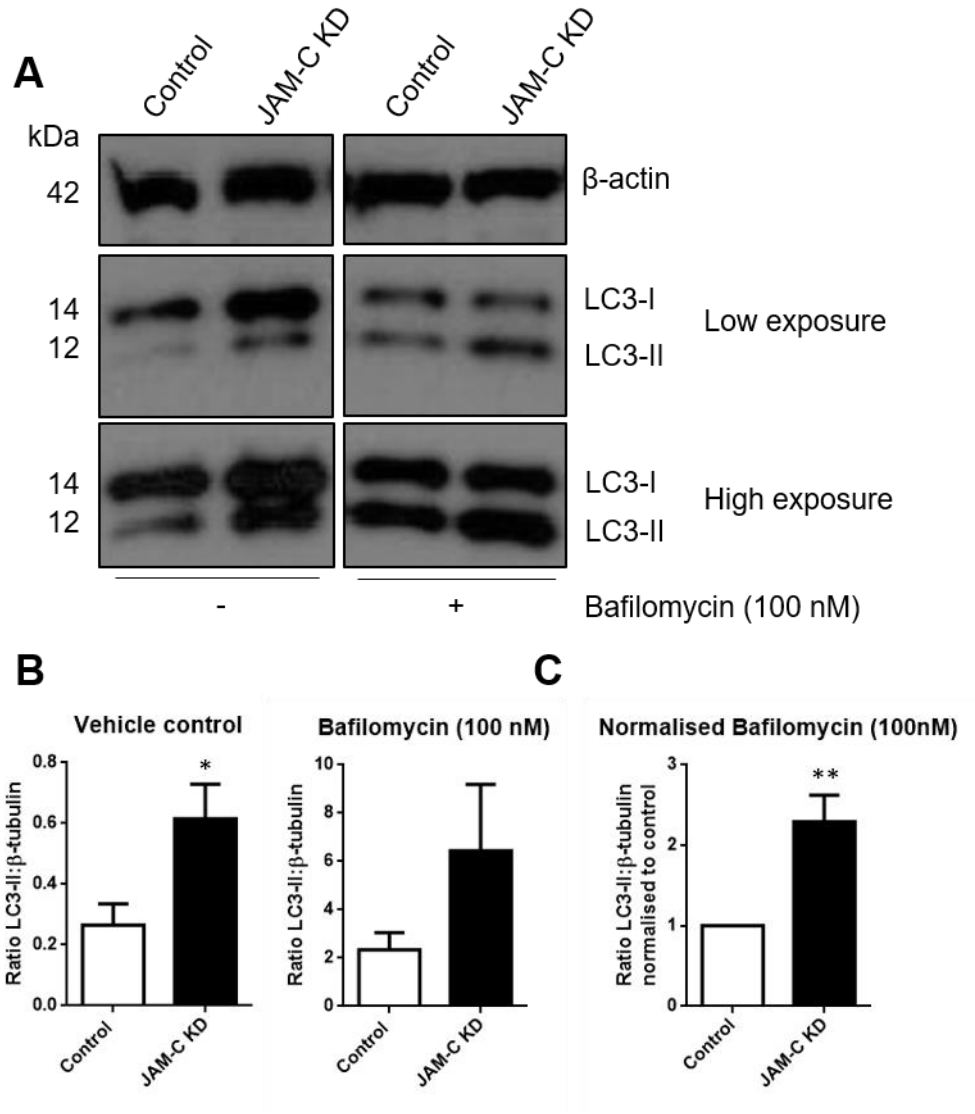

Figure 4.5. Autophagy is increased in JAM-C KD HUVECs under basal conditions.
(A) HUVECs were transfected with control or JAM-C siRNA, then cultured for 72 h for maximum efficiency of KD. Bafilomycin or vehicle control was added at 100 nM for 4 h and cells then lysed and assessed for LC3-II protein levels.
(B) LC3-II protein levels were quantified and normalised to β-actin using ImageJ and GraphPad Prism software. Error bars represent SEM from n=7-8 experiments. * = $p<0.05$ paired t-test. This work was conducted in collaboration with Dr Natalia Reglero.
(C) LC3-II protein levels from bafilomycin treated cells shown in (B) were normalised to control for each experiment and plotted. Error bars represent SEM from n=7 independent experiments. ** = $p<0.01$ paired t-test

These findings were confirmed by immuno-staining of control and JAM-C KD HUVECs for LC3 puncta. Thus, control and JAM-C KD HUVECs were cultured on 10 mm diameter

glass coverslips, fixed and immuno-stained for VE-Cadherin to identify confluent ECs, JAM-C to assess the level of JAM-C KD and LC3 to identify autophagosomes. LC3 positive puncta could be identified in about 50% of control HUVECs (Figure 4.6, left panel). By contrast JAM-C KD HUVECs (Figure 4.6, right panel) exhibited LC3 puncta in the majority of cells and which were increased in prevalence per cell. The LC3 immuno-staining was perinuclear in localisation, in a similar manner to that seen under starvation conditions (Section 4.3.1).

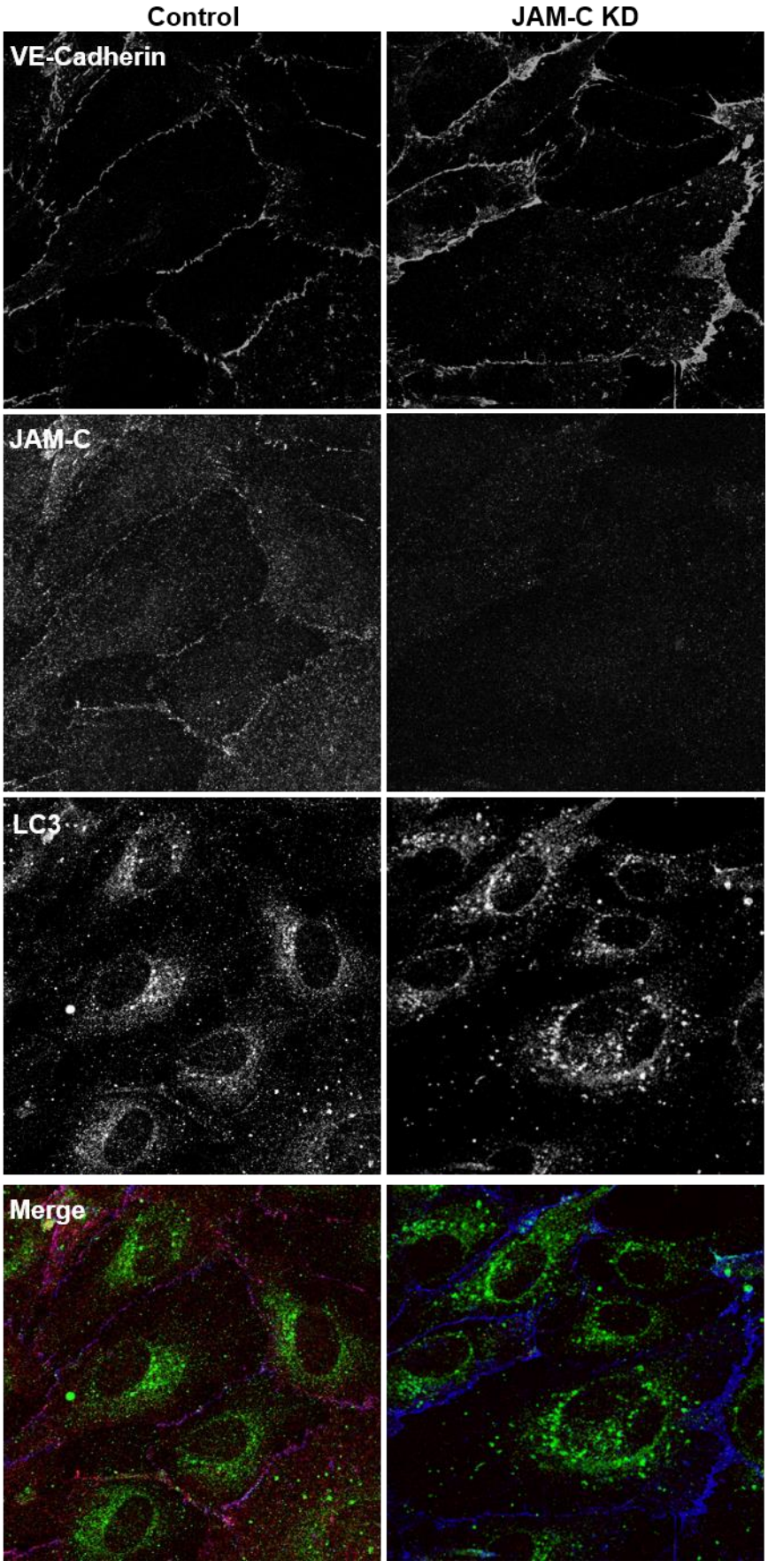

Figure 4.6. JAM-C KD HUVECs exhibit increased LC3 puncta formation.
HUVECs were transfected with control or JAM-C siRNA, then cultured for 72 h to achieve maximum efficiency of KD. Cells were then fixed in 100% methanol at -20°C for 3-5 min. Cells

were immuno-stained for VE-Cadherin (blue), JAM-C (red) and LC3 (green) and imaged using a Zeiss LSM 800 confocal microscope. Scale bars represent 20 µm.

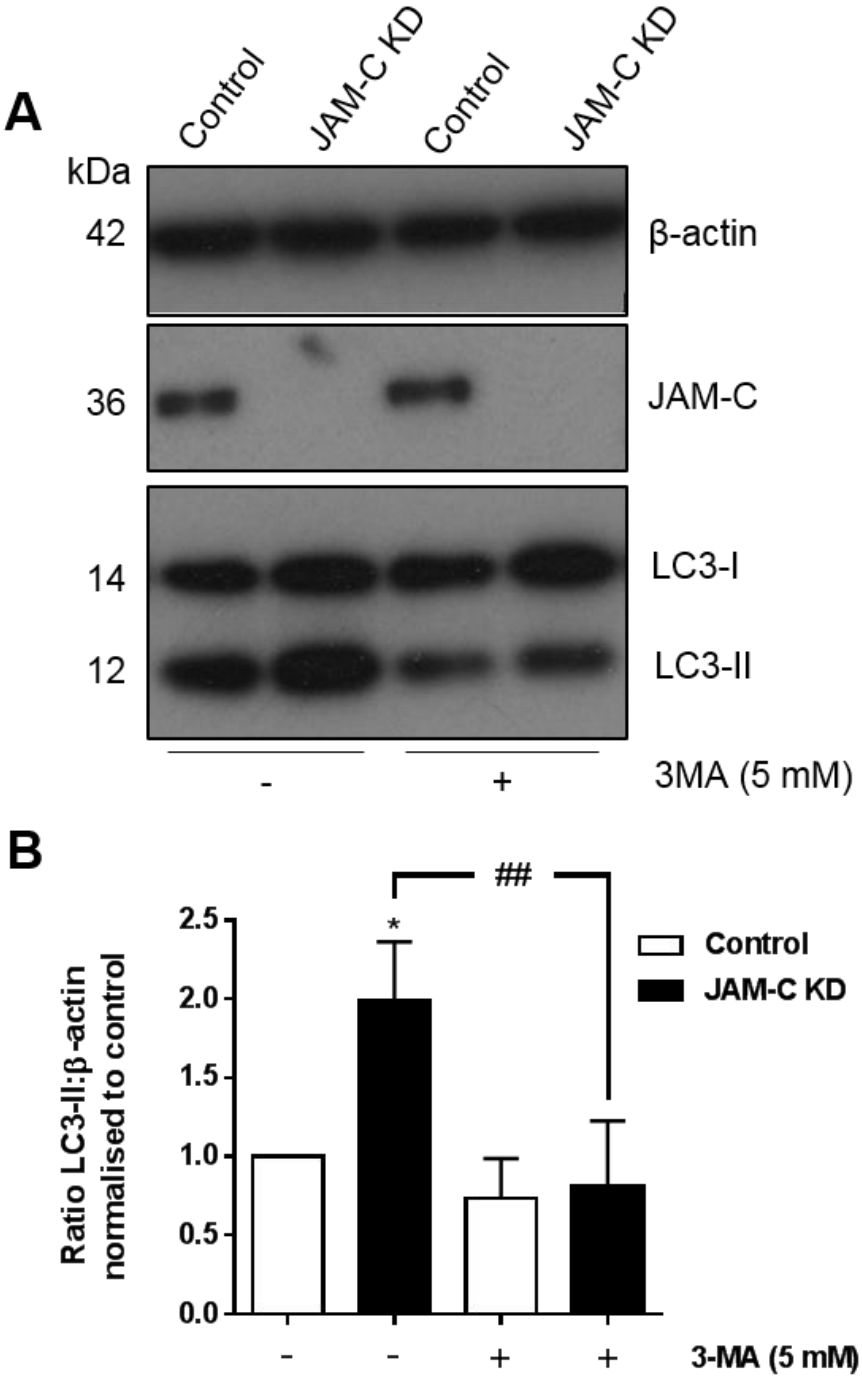

Figure 4.7. JAM-C mediated autophagy in HUVECs is dependent on PI3K activity.
(A) HUVECs were transfected with control or JAM-C siRNA, then left for 72 h for maximum efficiency of KD. Cells were then subjected to treatment with 5 mM 3-MA or vehicle control for 4 h (in the presence of 100 nM Bafilomycin A1) prior to lysis and then immunoblotted for LC3-II and β-actin.
(B) LC3-II protein levels were quantified and normalised to β-actin using ImageJ and using GraphPad Prism software. Error bars represent SEM from n=6 experiments. * = $p<0.05$, ## = $p<0.01$, student's t-test. This work was conducted in collaboration with Dr Natalia Reglero.

4.3.4 JAM-C KD induced autophagy in HUVECs is inhibited by 3-MA

Next, we addressed whether increased autophagy in JAM-C KD HUVECs was dependent on PI3K activity. For this purpose, control and JAM-C KD HUVECs were treated with 5 mM 3-MA or vehicle control for 4 h, then analysed for LC3-II protein levels. Concordant with previous data, JAM-C KD significantly increased LC3-II protein levels ($p<0.05$) under basal conditions (Figure 4.7, lanes 1 & 2). Addition of 3-MA for 4 h significantly reduced LC3-II protein in JAM-C KD HUVECs ($p<0.01$) to similar levels of those observed in control HUVECs under basal conditions (Figure 4.7).

4.3.5 IL-1β-mediated increase in LC3-II is not inhibited by 3-MA.

Next, we tested the effect of IL-1β stimulation on the autophagy in cultured HUVECs to observe whether a similar response was observed as for that with starvation. Indeed, pro-inflammatory cytokines such as TNFα have been shown to induce autophagy in a range of different cell types, although the effects of IL-1β stimulation on autophagy in endothelial cells is less clear (Chu et al., 2017).

Therefore, HUVECs were stimulated with IL-1β (1 ng/ml) for 4 hours and then analysed for LC3-II protein levels. A two-fold increase in LC3-II levels was seen in IL-1β stimulated HUVECs as compared to unstimulated, although this was not quite significant at this stage (Figure 4.8 $p=0.068$, $n=4$). Interestingly, treatment with the autophagy inhibitor 3-MA had no diminishing effect on the levels of LC3-II protein in IL-1β stimulated HUVECs, unlike that observed for starvation induced autophagy. This indicates that IL-1β induced increases in LC3-II protein are not induced through PI3K signalling and as such, are likely formed through a non-canonical autophagic pathway. This response is currently being tested in JAM-C KD HUVECs to analyse any potential differences in the response.

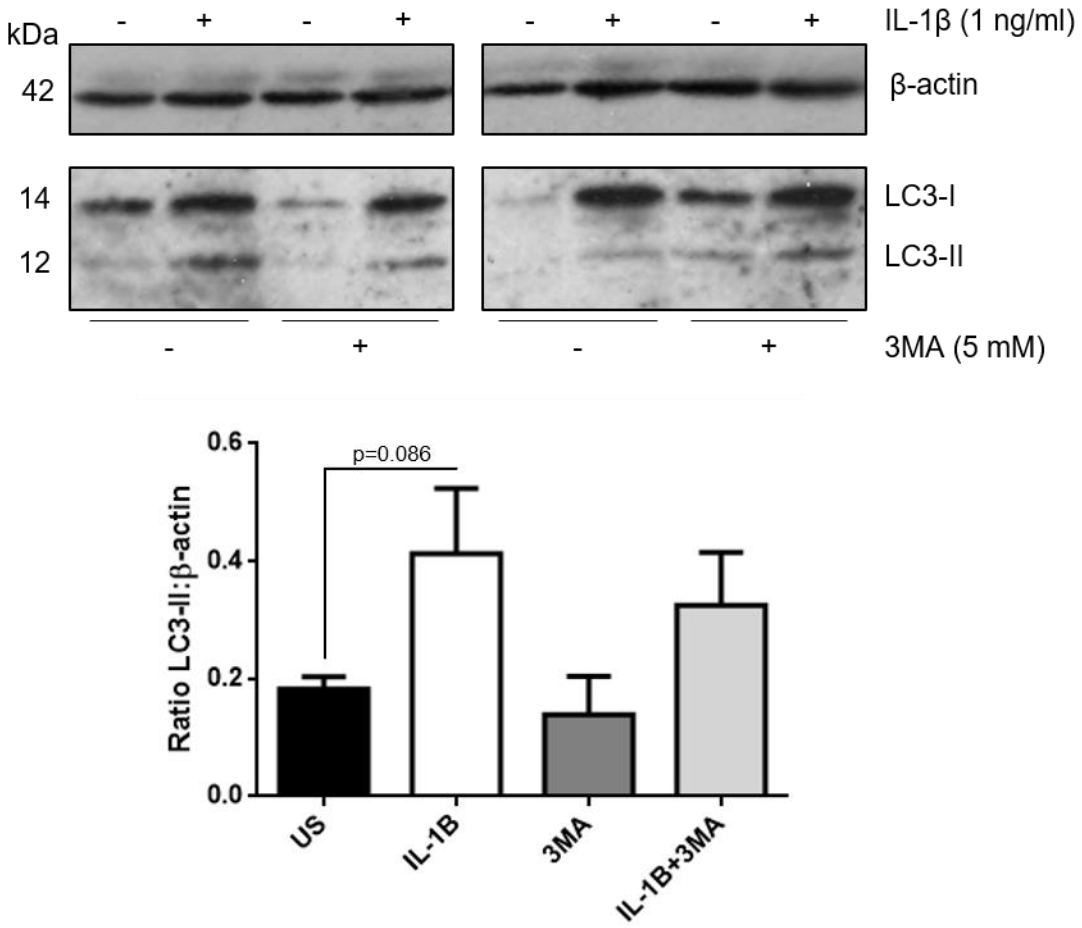

Figure 4.8. IL-1β stimulation of HUVECs increases LC3-II protein levels in HUVECs. (A) HUVECs were stimulated with IL-1β (1 ng/ml) for 4 hours in the presence of either 5 mM 3MA inhibitor or vehicle control. Cells were then lysed and immunoblotted for LC3-II and β-actin.
(B) LC3-II protein levels were quantified relative to β-actin loading control using ImageJ and GraphPad Prism software. Error bars represent SEM from n=4 experiments. Statistics conducted using student's t-test.

4.4 Discussion

This chapter sought to investigate EC autophagy, and more specifically whether disrupted expression of JAM-C impacted upon this cellular process. First, it was essential to establish a reliable method for detection of autophagy in cultured ECs. To achieve this, HUVECs were subjected to starvation, which is the classical inducer of autophagy in many different cell types (Mizushima, 2007). In agreement with this dogma and the well-established literature (Liu et al., 2015, Xiong et al., 2014), starvation did indeed induce autophagy in HUVECs in the present model, as measured by both increased LC3-II protein levels and increased LC3 puncta formation. Nutrient

starvation (specifically amino acid deprivation) induces autophagy through the canonical mechanism, which involves the inhibition of mTOR and subsequent downstream activation of class III PI3Ks (Jaber and Zong, 2013, Pyo et al., 2012). Inhibition of class III PI3Ks using 3-MA in the starvation model in the present study abrogated this induction of autophagy, confirming that HUVEC autophagy induced by starvation is dependent on PI3K activity and therefore follows the canonical pathway. These results demonstrated a reliable method for analysis of autophagy in cultured HUVECs in our laboratory and enabled further novel studies to be conducted.

This model was extended to analyse the effects of IL-1β on autophagy in cultured endothelial cells. Stimulation with IL-1β induced LC3-II protein increases, which are consistent with recent work detailing that pro-inflammatory stimuli TNFα and IL-1β also induce autophagy in cultured HUVECs (Chu et al., 2017). The work in this project also determines that the IL-1β induced increases in LC3-II protein are not inhibited by 3-MA, suggesting a non-canonical autophagic pathway by which this is achieved. Interestingly, it has been reported that a non-canonical autophagy based pathway is important for secretion of IL-1β (Dupont et al., 2011) and as such, our findings that IL-1β may induce a non-canonical autophagic pathway could suggest that exogenous IL-1β might feed into this pathway.

The results in the second part of this chapter focused on the hypothesis that loss of JAM-C might impact EC autophagy. This work built upon the findings in the previous chapter that loss of EC JAM-C did not result in increased apoptosis nor increased cell cytotoxicity due to necrotic cell death. Autophagy and cell death, in particular apoptotic cell death, can be thought of as two sides of a balancing scale. Broadly speaking, autophagy functions to maintain cell survival and blocks the induction of apoptosis by selectively reducing the amount of pro-apoptotic proteins. Apoptosis functions to limit the impact of cell stress and damage on the collateral tissue and as such, induction of caspase activity during the initial stages of apoptotic cell death acts to switch off autophagy (Marino et al., 2014). With this in mind and considering that JAM-C KD HUVECs do not exhibit increased apoptosis (Chapter 3), we hypothesised that they might instead upregulate autophagy to counterbalance the effects of JAM-C deficiency. Thus, the established model of siRNA mediated JAM-C KD in HUVECs was used to investigate the loss of EC JAM-C on autophagy.

The findings from this part of the work demonstrated that loss of JAM-C from ECs induces autophagy under basal conditions, a completely novel finding. Even more striking is that this induction of autophagy occurs in the absence of any other stimulus. Autophagy in JAM-C KD HUVECs was completely abrogated by inhibiting class III PI3Ks with 3-MA, suggesting that JAM-C KD induced autophagy in ECs requires the activity of PI3Ks, in a similar manner to that of starvation induced autophagy. These findings are supported by previous work in the lab (conducted by Catherine Pickworth) which demonstrated that mutant mice conditionally null for EC JAM-C exhibit increased autophagy *in vivo* under basal conditions (unpublished data).

Little is known about the relationship between tight junction molecules and autophagy. In one of the few studies investigating this link, autophagy was shown to regulate tight junction dynamics by targeting epithelial cell claudin-2 for degradation, thereby decreasing epithelial permeability and enhancing cell barrier functions, and as such providing a protective effect (Nighot et al., 2015). Recently a component of epithelial cell gap junctions, Connexin 43 (Cx43), has been shown to downregulate autophagy through direct interactions with proteins involved in autophagosome biosynthesis (Bejarano et al., 2014). The authors demonstrated here that Cx43 sequestered molecules such as ATG16L and Beclin-1 at the gap junctions and thereby preventing their involvement in the initiation of autophagy. This is the first and only evidence of a cell junctional molecule of any sort regulating autophagy. However, ECs do not contain gap junctions, highlighting the novel findings presented in this chapter in relation to a role for a tight junction protein in regulating EC autophagy.

Taking a broader view of these findings leads us to speculate on how loss of EC JAM-C might induce autophagy and more specifically whether this might be direct or indirect effect of the expression level of JAM-C. The relatively scarce literature on the impact of junctional molecule expression on autophagy makes it hard to draw any comparisons. However, using the Connexin 43 study as an example (Bejarano et al., 2014), it could be conceivable that JAM-C might directly sequester molecules critical for the initiation of autophagy at the tight junctions of ECs. The cytoplasmic tail of JAM-C contains a type-II PDZ binding motif that enables binding of the partner molecules ZO-1 and PAR-3 (Mandicourt et al., 2007). As such, this motif or other portion of the C-terminus might represent a docking site for a number of proteins necessary for autophagosome

biosynthesis, although such an interaction has yet to be identified. Alternatively, and perhaps more likely, JAM-C may provide the basis for a protein scaffold structure that could facilitate the binding of key autophagy proteins through distant protein interactors within the scaffold. Thus, disrupted expression of JAM-C would remove this protein scaffold and therefore any potential pro-autophagic proteins that are necessary for the initiation of autophagy.

It is indeed intriguing that loss of an endothelial junctional molecule results in upregulation of autophagy, which is essentially a process designed to supply the cell with more energy. This begs the question why do ECs need more energy following junctional disruption? In this context, it is important to take into account the functional roles for JAM-C that have been described, such as during leukocyte transmigration (Bradfield et al., 2007, Scheiermann et al., 2009). During migration of leukocytes through the endothelial barrier, adherens and tight junctions, as well as the cytoskeleton, undergo extensive remodelling that involves the cleavage of molecules such as JAM-C (Colom et al., 2015). This process by which functional JAM-C is lost could represent a trigger that results in the upregulation of autophagy to cope with the increased energy demand subsequently placed upon the ECs.

An alternative view as to why ECs upregulate autophagy following loss of JAM-C lies within the fact that cells are always trying to maintain homeostasis. Autophagy can be stimulated by numerous physical, chemical and environmental stressors that impact upon the cell and ultimately it serves to help maintain that state of homeostasis. Loss of or dysfunctional JAM-C may serve as one such physical stressor that in turn results in the upregulation of autophagy in these cells. This would then help protect the cell from adverse effects of loss of JAM-C and maintain homeostasis and cell survival, as has been described for multiple other inducers of cell stress (Kroemer et al., 2010, Murrow and Debnath, 2013). This theory is supported by the results from this chapter and those from our groups *in vivo* works showing that JAM-C deficient ECs exhibit increased autophagy under resting conditions, where little or no leukocytes are present. As such, it is more likely that autophagy is upregulated as a mechanism to maintain homeostasis in these cells, and perhaps also to provide energy to the cell to deal with any potential subtle changes in tight junction morphology and the subsequent impact on the cell that might occur during the loss of JAM-C. Moreover,

the results described in Chapter 3 that loss of EC JAM-C does not result in increased EC apoptosis are further supportive of this reasoning. Increased autophagy induced by loss of JAM-C would serve to protect the cells from apoptotic or other forms of cell death and maintain the homeostatic state.

Current ongoing projects in the lab are aimed at identifying the specificity of this phenomena to JAM-C by looking at the impact of loss of other related junctional molecules, such as the close family member JAM-A, on EC autophagy, as well as the impact of inflammatory stimuli on autophagy in JAM-C deficient ECs.

Summary of key findings

- Starvation induces autophagy in cultured ECs.
- EC autophagy induced by starvation is dependent on PI3K activity.
- Loss of EC JAM-C induces autophagy more than 2-fold under basal growth conditions. This increase is dependent on PI3K activity.

5 Investigating the effects of JAM-C KD on EC gene expression

5.1 Introduction

5.1.1 Control of EC gene expression

ECs tightly control gene expression in order to maintain quiescence and ultimately homeostasis. This is particularly important *in vivo* in the mature vasculature, where maintenance of endothelial homeostasis is crucial to avoid unwanted inflammation, stress and subsequent tissue damage (Shah et al., 2016). Key to the regulation of endothelial functions is the transcription factor ETS related gene, or Erg. This transcription factor has been described as the "master regulator" of EC functions, acting to maintain endothelial homeostasis (Shah et al., 2016). Amongst other functions, Erg has been shown to negatively regulate the activity of the NFκB subunit p65 by preventing it from binding to target promoters of pro-inflammatory genes, thus controlling and protecting against inappropriate EC inflammation and maintaining EC homeostasis (Dryden et al., 2012).

Whilst maintenance of EC quiescence is undoubtedly important, ECs must also respond rapidly to the ever-changing tissue environment, including to environmental stressors (hypoxia and shear stress), inflammatory insults (pathogens, cytokines) and growth factors (FGF, VEGF), all of which influence EC gene expression. In particular, type II activation of ECs by pro-inflammatory mediators such as IL-1β and TNFα results in the rapid upregulation of the expression of many inflammatory genes, such as *ICAM1*, *IL-6* and *IL-8* (Minami and Aird, 2005). Much of these effects are mediated through the well-studied NFκB and mitogen activated protein kinase (MAPK) signalling pathways (Baud and Karin, 2001, Grethe et al., 2004, Mako et al., 2010).

5.1.2 Junctional molecules and gene expression

Integrity of EC junctions and the molecules that compose them is crucial for both homeostasis and EC functions. As such, some progress has been made in understanding how junctional molecules might regulate EC gene expression in order to ultimately control EC functionality. Perhaps the most well studied of the junctional molecules in this regard is VE-Cadherin. VE-Cadherin is known to bind to β-catenin at

adherens junctions and regulate the transcriptional activity of β-catenin by sequestering it away from the nucleus (Gavard 2014, Dejana and Kuhl 2010). More recently it has also been shown that VE-Cadherin controls YAP transcriptional activity in stable adherens junctions by associating with it and preventing its nuclear translocation (Giampietro et al., 2015). VE-Cadherin has also been shown to regulate expression of tight junctional molecules, i.e. induce the expression of claudin-5 in ECs through the PI3K/Akt signalling pathway under basal conditions (Taddei et al., 2008). In addition, pharmacological disruption of adherens junctions through disruption of VE-Cadherin was shown to increase VEGF expression in ECs (Castilla et al., 1999).

Other EC junctional molecules have also been shown to regulate gene expression. The scaffolding tight junctional molecule ZO-1 is known to associate with the transcription factor ZO-1 associated nucleic acid binding protein (ZONAB), sequestering it at the membrane and thus regulating gene expression and subsequently promoting epithelial cell proliferation. This transcription factor has been shown to be important for regulating epithelial cell proliferation (Balda et al., 2003).

Despite these advances, how the JAM family of junctional molecules are involved in regulating EC gene expression is poorly understood. In fact, the only finding to date reports that JAM-A KO mice show increased claudin-10 and claudin-15 expression in the intestinal epithelium (Laukoetter et al., 2007). Whether JAM-C regulates EC gene expression and, more importantly, how disrupted expression of JAM-C may impact upon this phenomenon is completely unknown.

5.2 Aims

Due to its importance in many EC functions (angiogenesis, permeability and leukocyte trafficking), it was hypothesised that loss of EC JAM-C would impact the homeostatic state of ECs and result in an altered gene expression profile. Consequently, this chapter aimed to address this hypothesis under the following key objectives:

- To investigate the silencing of JAM-C protein expression on the gene expression profile of resting ECs.

- To determine whether EC JAM-C KD impacts EC gene expression responses to inflammatory stimuli.

5.3 Results

5.3.1 Quality control assessment of EC RNA and gene expression PCA

For the purposes of this study, it was decided to use gene expression microarray technology from Illumina to investigate the global gene expression profile of control and JAM-C deficient ECs. To be effective, gene expression analysis using this technology requires RNA of high purity and integrity. Therefore, RNA was isolated from control and JAM-C KD HUVECs and tested for purity using the Agilent 2100 Bioanalyser system. Sample RNA was run alongside purified synthetic RNA control to check for presence of degradation peaks (Figure 5.1A). The sample RNA extracted from HUVECs showed very high purity and virtually no degradation, with all samples attaining an RNA integrity score (RIN score) of at least 9. This allowed the RNA to be submitted for microarray analysis.

In addition to analysing RNA quality, the samples were also analysed for level of JAM-C KD. Using the Qiagen AllPrep system, both RNA and protein were isolated from the same sample. Protein lysates were analysed for JAM-C protein and also ICAM-1 to confirm the IL-1β induced inflammation had worked appropriately. Indeed, JAM-C was effectively reduced (Figure 5.1B, lanes 2&4) in a similar manner to that previously described (Chapter 3). In addition, ICAM-1 protein was upregulated in cells treated with IL-1β (lanes 3&4) as compared to untreated control cells.

Principle component analysis (PCA) on the gene expression microarray samples revealed interesting correlations. Overall two of the replicates clustered closely when compared to the other, perhaps indicating biological diversity in the gene expression profile of the cultured HUVECs (Figure 5.2). Post IL-1β stimulation, both control and JAM-C KD HUVECs showed the same response in the PCA, as indicated by the location of those stimulated samples at the top of the PCA plot. When comparing control and JAM-C KD samples under unstimulated conditions, all samples exhibited a shift to the right in the PCA plot. The same phenotype was evident for control and JAM-C KD HUVECs post IL-1β stimulation. This indicates that despite the overall variance between replicates, there is a clear shift in expression profile in the PCA plot between control and JAM-C KD HUVECs.

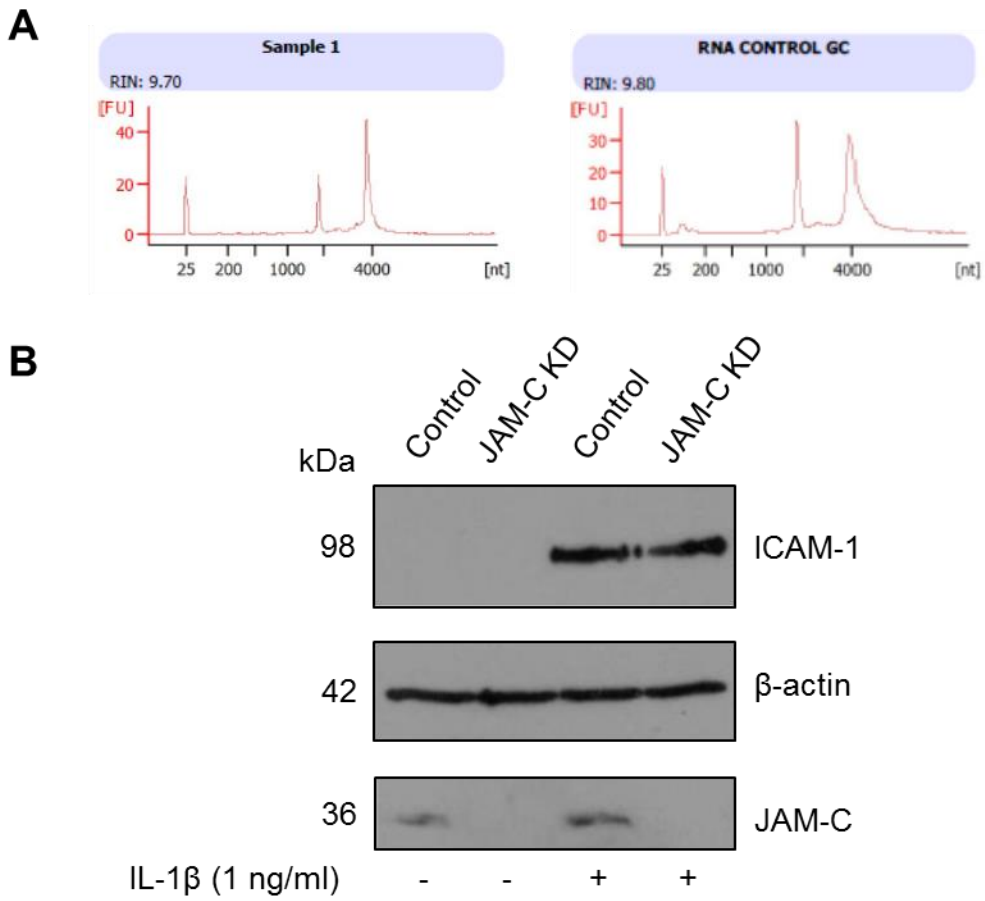

Figure 5.1. Dual purification of HUVEC protein and RNA for microarray analysis. (A) Analysis of RNA quality for gene expression microarray analysis. RNA was extracted from control and JAM-C KD HUVECs using the Qiagen RNA/Protein AllPrep system and then subjected to analysis of degradation by Bioanalyser (Agilent). Samples were run alongside synthetic purified RNA control. The data is plotted as fluorescence intensity (y-axis) versus size of the oligonucleotide (x-axis), where two main peaks for 28S and 18S ribosomal RNA can be clearly seen.
(B) Protein was purified from the same control and JAM-C KD HUVECs in (A), which were stimulated with IL-1β for 4 hours or left unstimulated. Protein lysates were analysed for ICAM-1 protein to confirm response to IL-1β and also JAM-C to confirm level of protein KD.

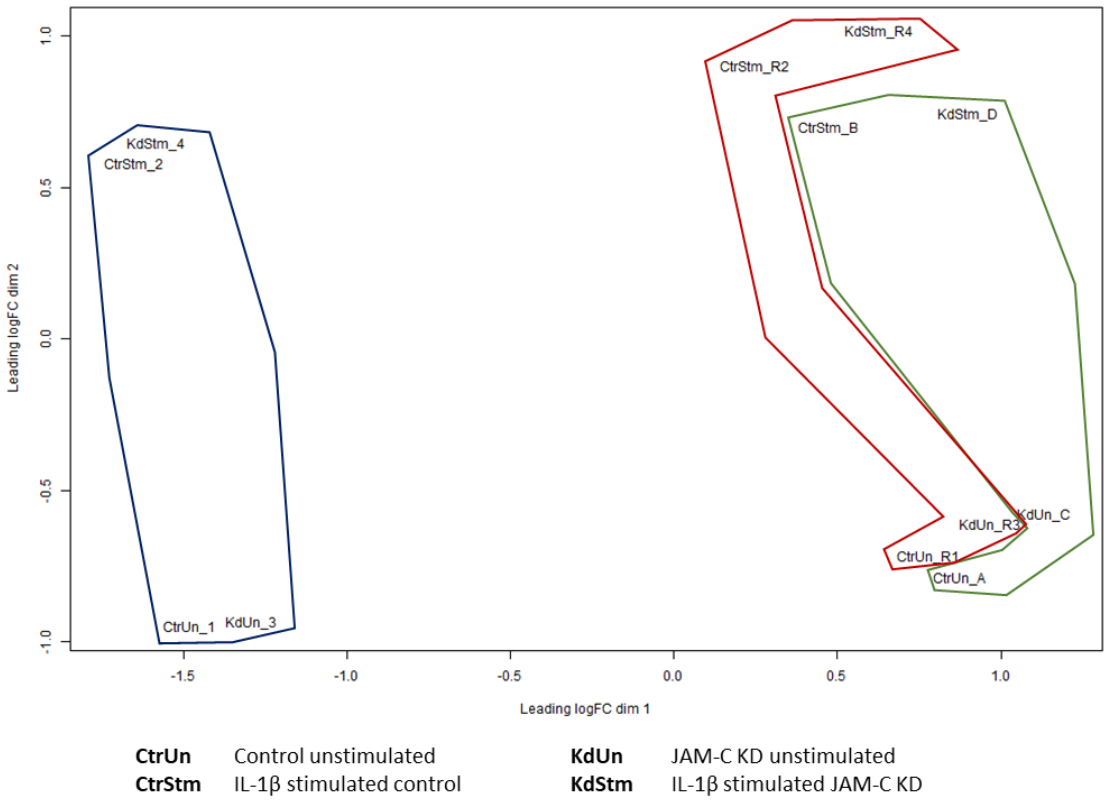

Figure 5.2. Principle component analysis of replicate samples in gene expression microarray. The three biological replicate samples from the gene expression microarray were subjected to principle component analysis (PCA) post normalisation. The three independent replicates were grouped as shown by the outlines in blue, red or green.

5.3.2 JAM-C KD in HUVECs triggers gene expression changes under basal conditions

In order to analyse differences in gene expression between control and JAM-C KD HUVECs, differential gene expression analysis under basal conditions was performed using the Limma package for R (see Chapter 2 for full details). Initial analysis using pre-determined thresholds based on a nominal P.Value of < 0.05 and a logFC of at least ± 0.5. Any genes within this category were considered significant and so used for further analysis.

Differential expression analysis of control and JAM-C KD HUVECs using those thresholds determined above revealed that 549 genes were significantly regulated by JAM-C KD under basal conditions. Of these 549 genes, the top 100 were chosen to be displayed graphically as a heatmap (Figure 5.3) and clustered based on their pattern of expression. For this representation format, all three of the replicate experiments were

plotted, despite the variance that was observed in the PCA. That variance can be quite clearly seen from the heatmap in Figure 5.3, where the first replicate has a different colour profile as compared to the other two replicates. That being said, it can be clearly observed that the 100 differentially expressed genes were clustered into two distinct groups; those that exhibit decreased expression (blue) and those that had increased expression (yellow) in JAM-C KD HUVECs as compared to their control counterparts. Overall, 65% of the genes present in the comparison were upregulated in conditions of JAM-C KD, which clustered together in the heatmap analysis. Analysis of the downregulated genes revealed a distinct cluster at the top of the heatmap where a clear reduction in expression (blue) was observed in all three samples of JAM-C HUVECs under unstimulated conditions when compared to control.

Interestingly, about 25% of the 549 genes were either uncharacterised regions of the genome or genes encoding for proteins with no reported function. Perhaps most reassuringly, the gene for JAM-C, *JAM3*, was the most significantly downregulated hit within the JAM-C KD HUVECs.

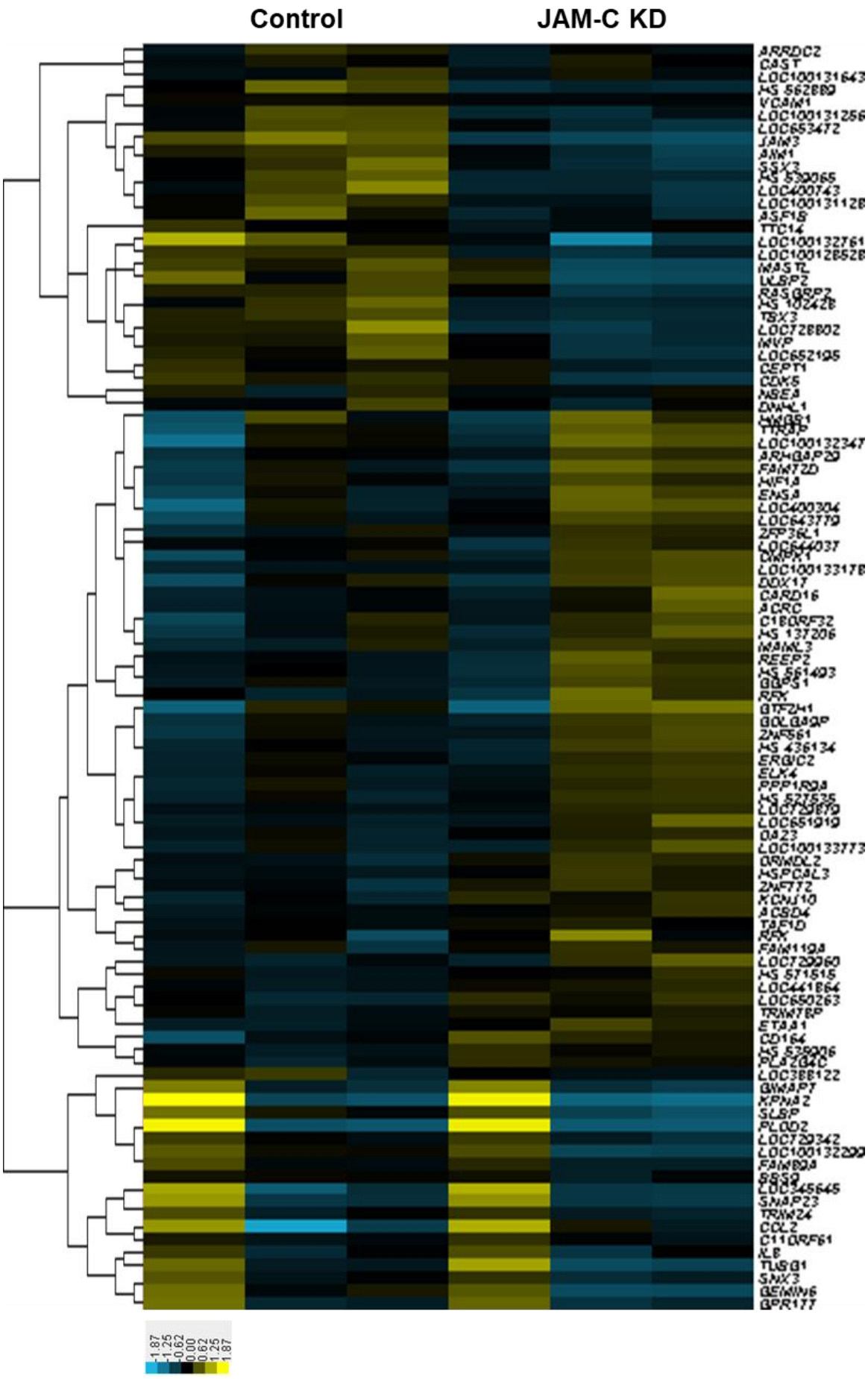
Control
JAM-C KD
ARRDC2
CAST
LOC100131643
HS.562889
VCAM1
LOC100131256
LOC653472
SAMD3
ANK1
SSX3
HS.530065
LOC400743
LOC100131128
ASF1B
TTC14
LOC100132761
LOC100128528
WASTL
LASP2
RASGRP2
HS.102428
TSKS
LOC728802
INVS
LOC652125
CEPT1
CDK5
NSE3
DNAL1
MAGI3
TYRP1
LOC100132347
ARHGAP29
FAM72D
WIF1
ENSA
LOC400204
LOC643770
ZFP36L1
LOC644037
DNPH1
LOC100133178
DDX17
CARD16
ACRC
C18ORF32
HS.137206
MAML3
REEP2
HS.561403
GBP3
RFX7
BTF3L4
GOLGA8P
ZNF561
HS.436134
ERGIC2
ELK4
PPP1R9A
HS.527535
LOC729679
LOC651919
DAZ3
LOC100133773
ORMDL2
HSPC3L3
ZNF772
KCNJ10
ACSL4
TBP1D
RFX7
FAM110A
LOC729960
HS.571515
LOC441864
LOC650263
TRNT1P
ETS1
CD164
HS.529026
PLA2G4C
LOC388122
GNAP7
KPNA2
SLBP
PLOD2
LOC729342
LOC100132299
FAM82A
SESN2
LOC345645
SNAP23
TRIM24
CCL2
C11ORF61
IL6
TUSC1
SNX3
GEMIN6
GPR177
1.87
1.25
0.62
0.00
0.62
1.25
1.87

Figure 5.3. Top 100 differentially expressed genes between control and JAM-C KD HUVECs under basal conditions.
RNA from Control and JAM-C KD HUVECs (from three independent experiments) was subjected to gene expression microarray analysis using Illumina HT-12v4.0 BeadChip technology. Data were extracted and analysed using the Limma package for Bioconductor software. Significant differentially expressed genes were selected based on a threshold of a log fold change (logFC) of greater than +/- 0.5 and $p < 0.05$. The top 100 genes in this threshold are displayed in the heatmap, where blue bars represent lower expression and yellow represents higher expression than their counterparts. These data were generated using Cluster 3.0 and Java TreeView software. This work was done in collaboration with Drs Michael Barnes and Claudia Cabrera in the Department for Bioinformatics, William Harvey Research Institute, QMUL.

5.3.3 Pathway analysis of JAM-C KD EC gene expression

In order to determine the potential biological effects of the differential gene expression pattern observed in ECs following JAM-C KD, the 549 significantly differentially expressed genes were subjected to pathway analysis using Ingenuity Pathway Analysis (Qiagen) software. Using this method, biological processes that might be up- or downregulated in conditions of JAM-C KD due to the differential gene expression pattern observed could be identified. As such, the biological processes that were upregulated in conditions of JAM-C KD are displayed in Table 5.1. A number of immune processes were predicted to be upregulated in this analysis, in particular those involved in immune cell trafficking, such as “binding of leukocytes”, “migration of neutrophils” and “emigration of leukocytes”. In addition, processes such as cellular homeostasis and cell viability were also predicted by pathway analysis to be significantly upregulated in conditions of JAM-C KD.

Following the observation that identification of a number of genes associated with immune and cellular homeostasis pathways are upregulated following JAM-C KD, it was noticed that many of these biological processes fall into one of three broad categories; 1) Immune Response, 2) Immune Cell Trafficking and 3) Cellular Homeostasis. To investigate the genes involved in each category and the overlap of common genes between these categories, a network map of all candidate genes was created. Differentially expressed genes associated with cellular processes that displayed an activation score of at least 1.5 and that could be encompassed into one of the three broad categories were used for this analysis (Figure 5.4A). The majority of the genes in this network were upregulated in response to JAM-C KD (red), many of which are pro-inflammatory genes, such as *ICAM-1* and *CXCL1*. In addition, most of the

genes in this network belonged to at least two of the categories used to create the network, indicating overlapping functions For simplicity, this data set is displayed in a Venn diagram format as shown in Figure 5.4B. This representation format shows that 14 genes are common to all three categories, and another 19 are common to at least two categories.

Diseases and Biological Functions	z Score
Angiogenesis	2.976
Vasculogenesis	2.884
Migration of myeloid cells	2.502
Binding of mononuclear leukocytes	2.381
Migration of granulocytes	2.266
Binding of leukocytes	2.218
Respiratory burst of neutrophils	2.200
Migration of neutrophils	2.040
Respiratory burst of cells	2.005
Adhesion of phagocytes	2.003
Emigration of leukocytes	2.000
Adhesion of monocytes	1.977
Extravasation of phagocytes	1.961
Cell viability	1.958
Adhesion of immune cells	1.957
Recruitment of monocytes	1.948
Cell movement of neutrophils	1.934
Cellular homeostasis	1.893

Table 5.1. List of biological processes upregulated in JAM-C KD HUVECs. The significant differentially expressed genes in JAM-C KD HUVECs under unstimulated conditions were subjected to pathway analysis using Ingenuity pathway analysis (IPA) software (Qiagen). The categories are ordered by their activation z-score, a prediction of the activation state of that process based on the predicted p value for enrichment of the pathway and the log fold change of the relevant pathway.

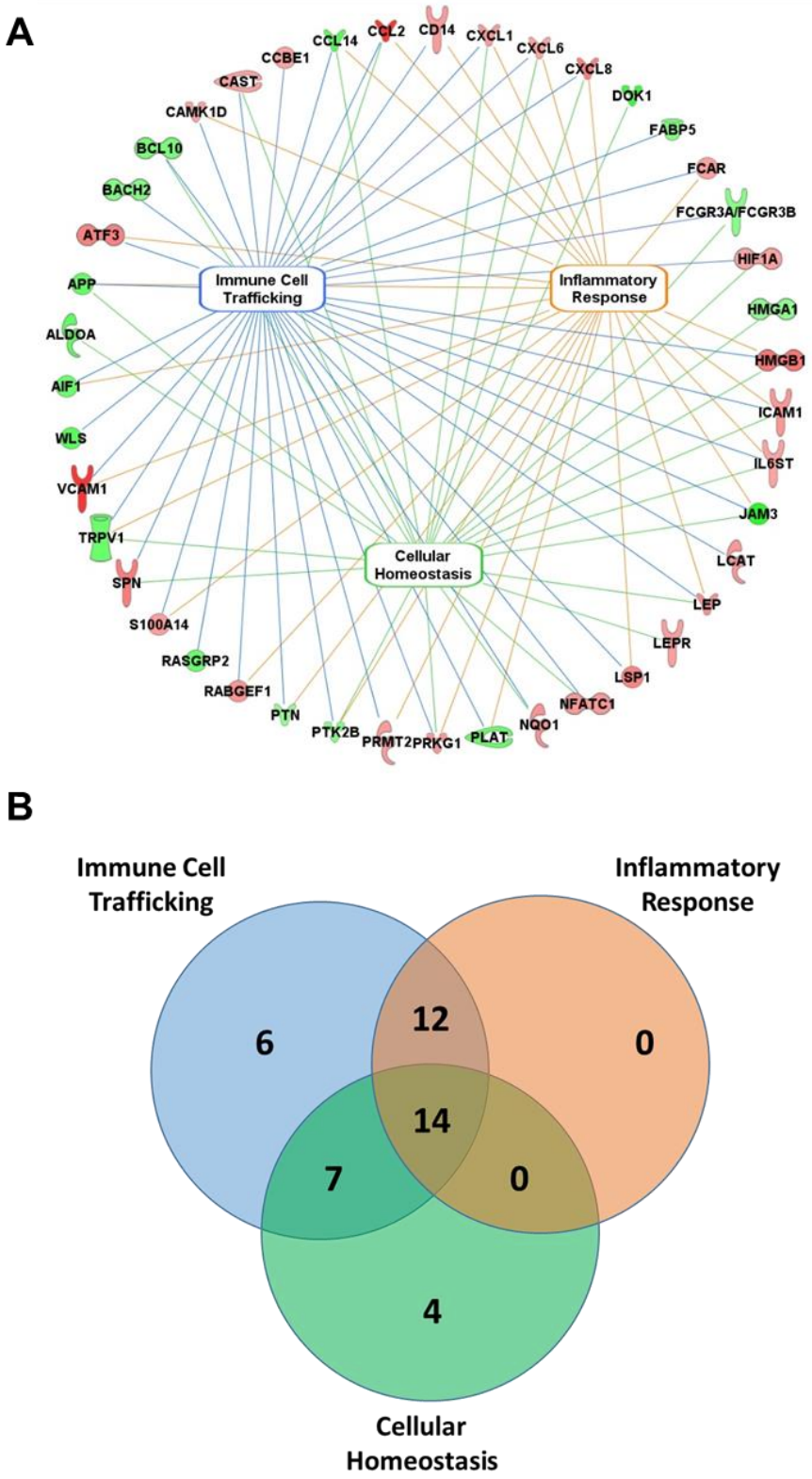

Figure 5.4. Network pathway analysis of differentially expressed genes following JAM-C KD in HUVECs.

(A) Network of genes involved in the categories "immune response", "immune cell trafficking" and "cellular homeostasis", detailing their inter-connections between each of the categories. Red and green gene symbols indicate genes upregulated and downregulated respectively under conditions of JAM-C KD.

(B) Venn diagram summarising the overlap of the indicated pathway associated genes that are differentially regulated in response to JAM-C KD.

5.3.4 Validation of differentially expressed genes by qPCR

Using this network analysis, a list of candidate genes of interest was compiled, as shown in Table 5.2. Using the normalised relative intensities from the microarray data, Figure 5.5A highlights the increase in expression shown by some of these genes under conditions of JAM-C KD, exhibiting in all cases at least 2-fold or more increased expression over control cells.

Gene ID	logFC	P.Value	Protein	Molecule function
CCL14	-0.77	1.4×10^{-3}	CXCL8	Chemokine
CCL2	1.12	2.9×10^{-4}	CCL2	Chemokine
CXCL1	0.56	3.0×10^{-3}	CXCL1	Chemokine
CXCL6	0.51	1.8×10^{-2}	CXCL6	Chemokine
IL8	0.70	6.0×10^{-5}	Interleukin-8	Chemokine
HIF1A	0.51	3.1×10^{-4}	Hypoxia inducible factor 1α	Transcription factor
HMGB1	0.76	2.4×10^{-4}	High mobility group box 1	Transcription factor
ICAM1	0.57	1.5×10^{-3}	Intercellular cell adhesion molecule 1	Adhesion receptor
IL6ST	0.50	4.7×10^{-3}	Interleukin 6 signal transducer	Inflammation signalling
JAM3	-1.31	3.3×10^{-12}	Junctional adhesion molecule 3	Adhesion receptor
PRKG1	0.58	9.2×10^{-3}	cGMP-dependent protein kinase-1	Vascular homeostasis
TRPV1	-0.65	4.8×10^{-3}	Transient receptor potential cation channel V	Cation channel
VCAM1	1.22	9.4×10^{-6}	Vascular cell adhesion molecule 1	Adhesion receptor

Table 5.2. List of selected candidate genes to be validated by qPCR that are significantly differentially expressed following JAM-C KD.

The expression of a number of these genes was subsequently validated by qPCR, including *JAM3* (JAM-C), *VCAM1*, *ICAM1*, *CXCL1*, *IL8*, *CCL2*, *HMGB1* and *HIF1A* (Figure 5.5B). Reassuringly, *JAM3* was the gene most significantly reduced in expression following JAM-C KD while *VCAM1* was upregulated about four-fold in JAM-C KD HUVECs and this was statistically significant. Another adhesion molecule gene *ICAM1* was also upregulated significantly in conditions of JAM-C KD. The chemokines *IL8*, *CXCL1* and *CCL2* all showed significantly increased expression at the mRNA level in JAM-C KD conditions, in all cases at least two-fold or more above control conditions (Figure 5.5B). The genes *HMGB1* and *HIF1A* were also significantly increased in expression in JAM-C KD HUVECs, both of which have been extensively implicated in

inflammatory reactions and hence were identified as candidate genes from the network pathway analysis (Figure 5.4) (Hellwig-Burgel et al., 2005, Palazon et al., 2014, Huebener et al., 2015), (Klune et al., 2008), Palazon et al., 2014, (Schiraldi et al., 2012).

The classical pro-inflammatory genes investigated here (*ICAM1, CXCL1, CCL2*) showed generally low expression in control HUVECs, in agreement with the dogma that Erg controls EC homeostasis by restricting pro-inflammatory gene expression. The expression of *HIF1A* and *HMGB1* by contrast showed higher expression in control HUVECs under basal conditions, so even the smaller changes in the expression of these genes observed in JAM-C KD HUVECs could have a potentially large impact on protein expression.

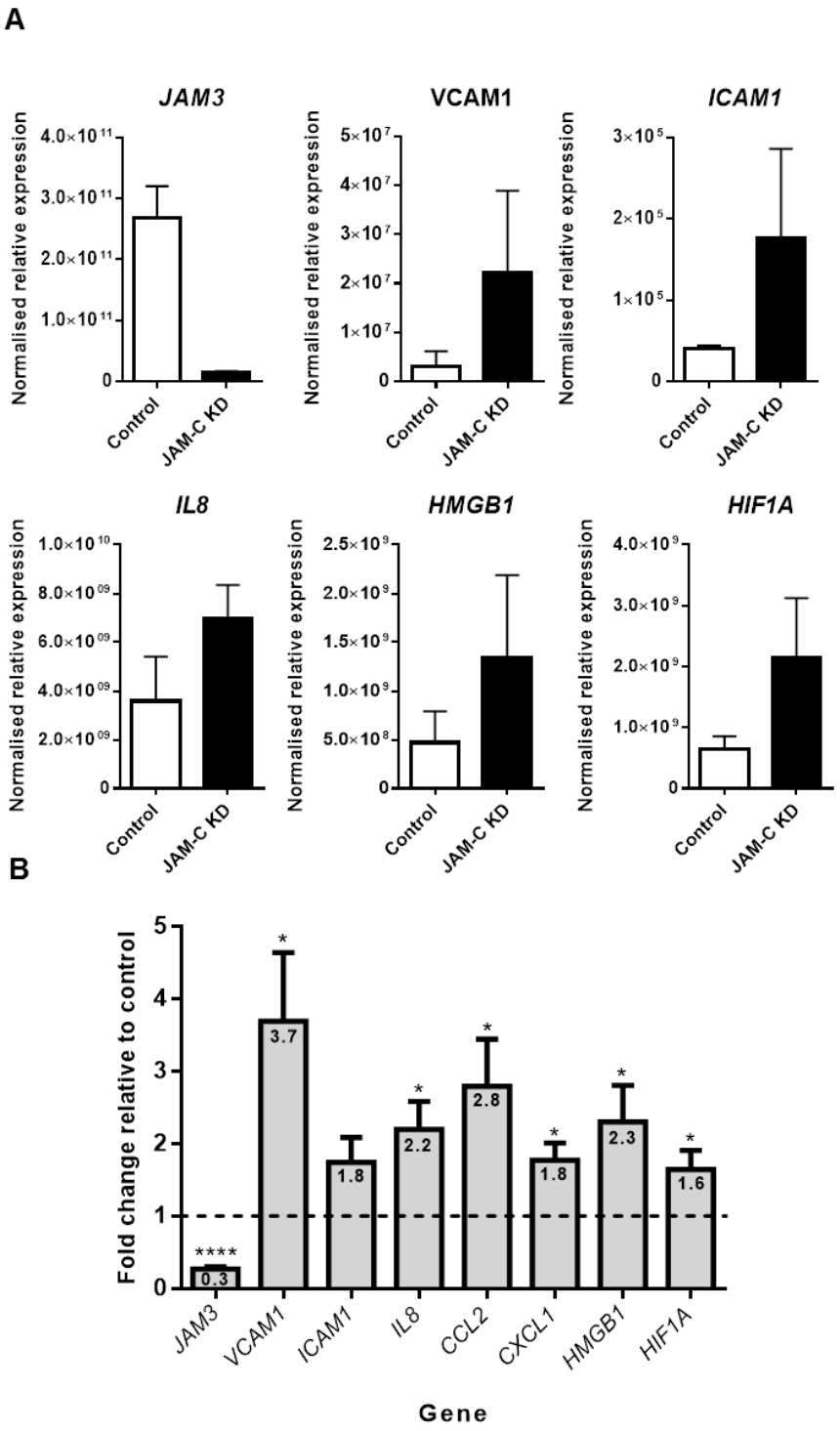

Figure 5.5. qPCR validation of candidate genes selected from the microarray and pathway analysis.

(A) Normalised intensities for individual genes were extracted from the microarray analysis and plotted in histograms to indicate the differential expression of candidate genes in JAM-C KD HUVECs compared to control HUVECs under basal conditions. (B) RNA was isolated from control and JAM-C KD HUVECs and reverse transcribed to cDNA. Primers specific for *JAM-C*, *VCAM1*, *IL8*, *CXCL1*, *CCL2*, *HMGB1*, and *HIF1A* (detailed in section 2.4.5) were used to specifically amplify those transcripts. Data was plotted as fold change over control cells using the ΔΔCt method, where primers for *ACTB* and *PPIA* were used as

housekeeping controls. Data is representative of at least four independent experiments. Error bars represent mean ± SEM. * = p<0.05, **=p<0.01 paired t-test.

5.3.5 JAM-C KD increases the basal activation of the NFκB pathway in HUVECs

Many of the genes present in the differential expression analysis of JAM-C KD HUVECs, including those validated by qPCR in Figure 5.5B, are hallmarks of increased NFκB pathway activation. NFκB is a rapid-response family of transcription factors important in regulating a number of key cellular processes, including proliferation, cell death and response to inflammation among others (Baeuerle and Henkel, 1994, Joyce et al., 2001). This family of transcription factors can homo and hetero-dimerise to direct the transcription of target genes. The most studied of these is the p65 subunit which is activated by phosphorylation on two serine residues, S276 and S536 (Christian et al., 2016). To investigate whether the NFκB pathway was activated in JAM-C KD HUVECs, the S536 phosphorylation status of p65 was investigated in this model.

Using Western Blot analysis, phosphorylated p65 levels were found to be elevated in JAM-C KD HUVECs when compared to control HUVECs (Figure 5.6A, lanes 1&2). Of importance, total levels of p65 were similar in control and JAM-C KD HUVECs under basal conditions, indicating that the increased p65 phosphorylation is not due to an increase in overall protein levels of p65 but rather a *bona fide* increase in phosphorylation status. Quantification of this revealed a significant increase in phosphorylated p65 levels (Figure 5.6B, left panel), suggesting a significant activation of the NFκB pathway in JAM-C KD HUVECs as compared to control HUVECs under basal conditions.

Cell signalling pathways are notoriously complex and each individual pathway has been shown to crosstalk with one or more other signalling pathways. This is particularly evident during inflammation, where one or more signalling pathways can be activated by the same stimulus, or even where one signalling pathway can activate others (Korus et al., 2002). As such, the activation status of two components of the MAPK signalling pathway, Extracellular signal-regulated kinases 1 and 2 (ERK1 and ERK2) were also investigated. Indeed, the MAPK pathway has been well studied in the context of regulating gene expression responses to inflammatory cues, including where ERK1/2 and p38 MAPK mediate the upregulation in gene expression of pro-inflammatory

molecules such as IL-6 and IL-8 (Yang et al., 2008). In the present study, phosphorylated levels of both ERK1 and ERK2 were low under basal conditions in control cells (Figure 5.6A, lanes 1&2), with no visible increase observed following JAM-C KD. This was reflected in the quantification shown in Figure 5.6B, lower right panel.

Subsequent immunofluorescence studies were carried out to analyse nuclear translocation and phosphorylation of NFκB p65 in JAM-C KD HUVECs (Figure 5.7). Phospho-p65 was clearly upregulated in control cells stimulated with IL-1β for 30 minutes as compared to control unstimulated cells. In addition, total-p65 was clearly translocated to the nucleus in these IL-1β stimulated cells. In unstimulated JAM-C KD HUVECs, there was a clear increase in phospho-p65 levels in the cytoplasm of the cells, correlating with the total protein data observed in Figure 5.6. However, very little nuclear translocation was observed in either control or JAM-C KD unstimulated HUVECs, where the staining was predominantly cytoplasmic.

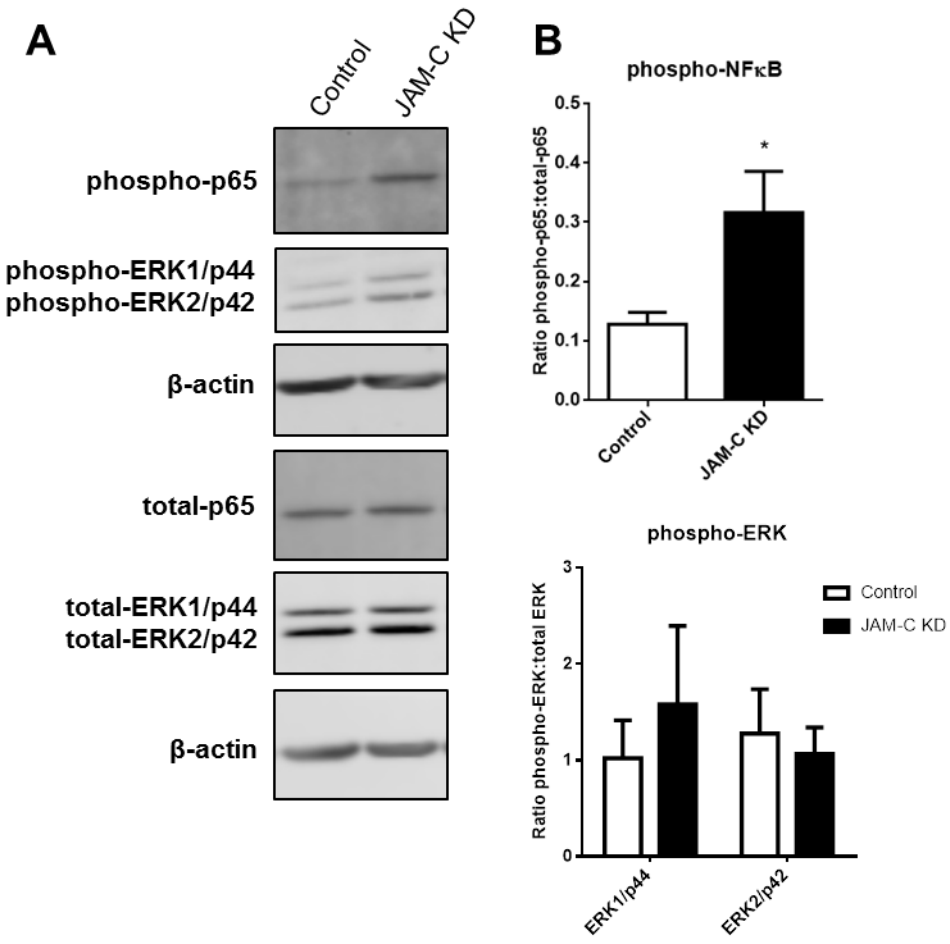

Figure 5.6. NFκB pathway is upregulated in JAM-C KD HUVECs.
(A) HUVECs were transfected with control or JAM-C siRNA and cultured for 72 h to reach confluence and then lysed for protein analysis. Lysates were analysed by Western blot for total and phosphorylated NFκB, total and phosphorylated ERK1/2 and β-actin loading control. Representative blot of four independent experiments.
(B) Quantification of Western Blots in (A). Phosphorylated NFκB was normalised to total NFκB for each sample and the same process repeated for ERK1 and ERK2. Data is representative of n=4 independent experiments, error bars represent mean ± SEM. *=$p<0.05$, unpaired t-test.

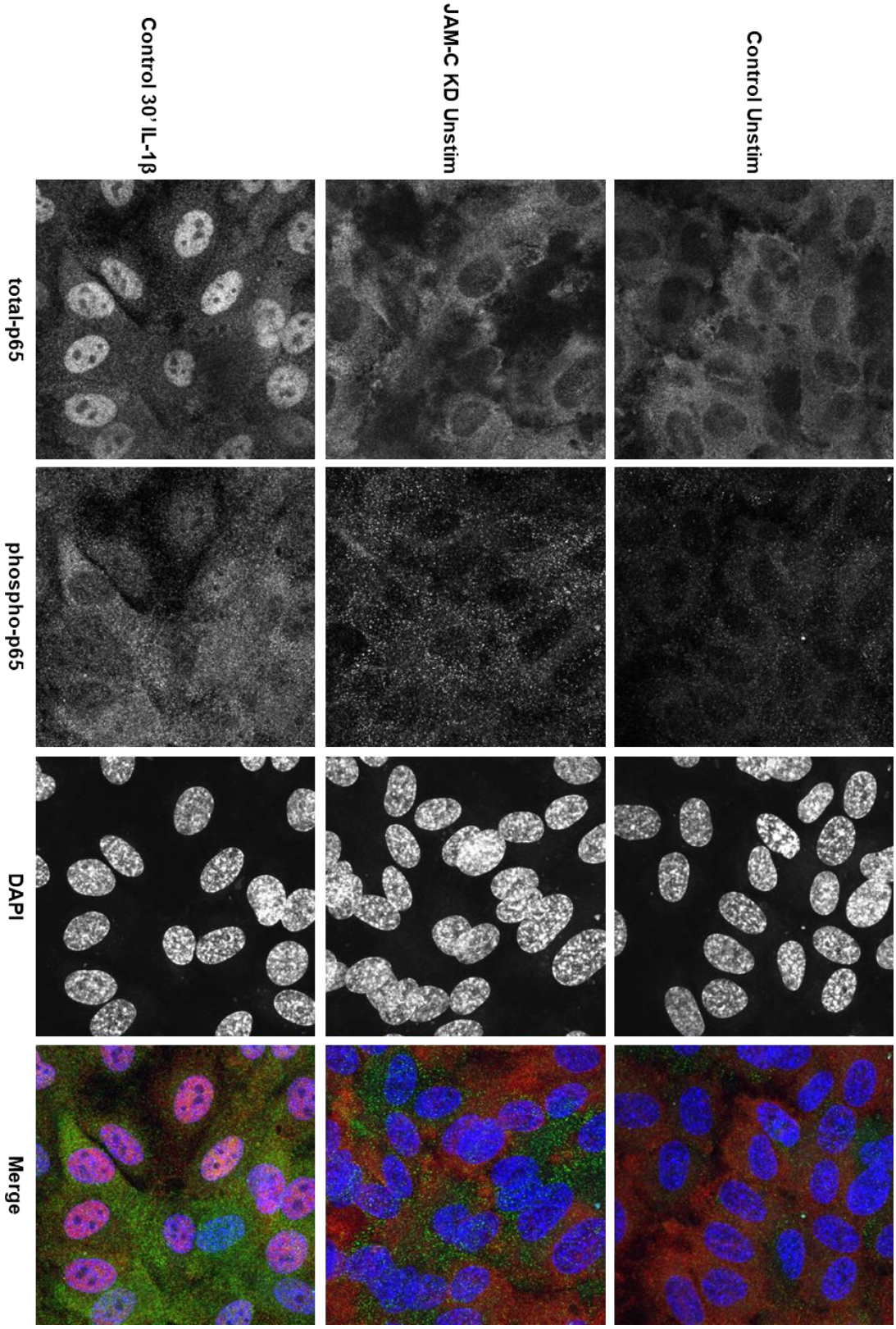

Figure 5.7. Immunofluorescence staining of total and phospho-p65 in JAM-C KD HUVECs. HUVECs were transfected with control or JAM-C siRNA, then cultured for 72 h to achieve maximum efficiency of KD. Control cells were also stimulated with IL-1β for 30 mins as a positive control for NFκB activation and nuclear translocation. Cells were then fixed in 4% PFA at room temperature 15 min. Cells were immuno-stained for total-p65 (red), phospho-p65 (green) and DAPI (blue) and imaged using a Zeiss LSM 800 confocal microscope. Data is representative of two independent experiments.

5.3.6 JAM-C KD HUVECs show increased protein expression of IL-8 and ICAM-1

Following the finding of increased inflammatory gene expression in JAM-C KD HUVECs under basal conditions, it was decided to investigate whether this increase was translated into increased protein expression. For this purpose, levels of the chemokine IL-8 and the adhesion molecule ICAM-1 were investigated by ELISA and Western Blot techniques, respectively. Under basal conditions, ICAM-1 protein was found to be elevated in JAM-C KD HUVECs when compared to control HUVECs (Figure 5.8A). This increase was above two-fold and statistically significant, corresponding with the increase in *ICAM1* gene expression observed in Figure 5.5B.

The levels of IL-8 were measured in both the cell associated (lysate) and secreted (conditioned medium) fractions of control and JAM-C KD HUVECs under basal conditions. JAM-C KD HUVECs showed an increase (1.9 fold) in IL-8 protein in cell lysates as compared to control HUVECs (Figure 5.8B, left panel), though this increase did not reach statistical significance ($p=0.13$, $n=7$). In a similar manner, secreted IL-8 was also slightly increased (1.55 fold) in JAM-C KD HUVECs but again this was not statistically significant ($p=0.10$, $n=8$).

The results described in this part of the chapter indicate that silencing of JAM-C expression in ECs results in a pro-inflammatory primed state of the ECs. This is illustrated in the form of increased pro-inflammatory gene expression, potentially due to increased NFκB pathway activation, that translates to increased protein levels in the case of ICAM-1 and the chemokine IL-8.

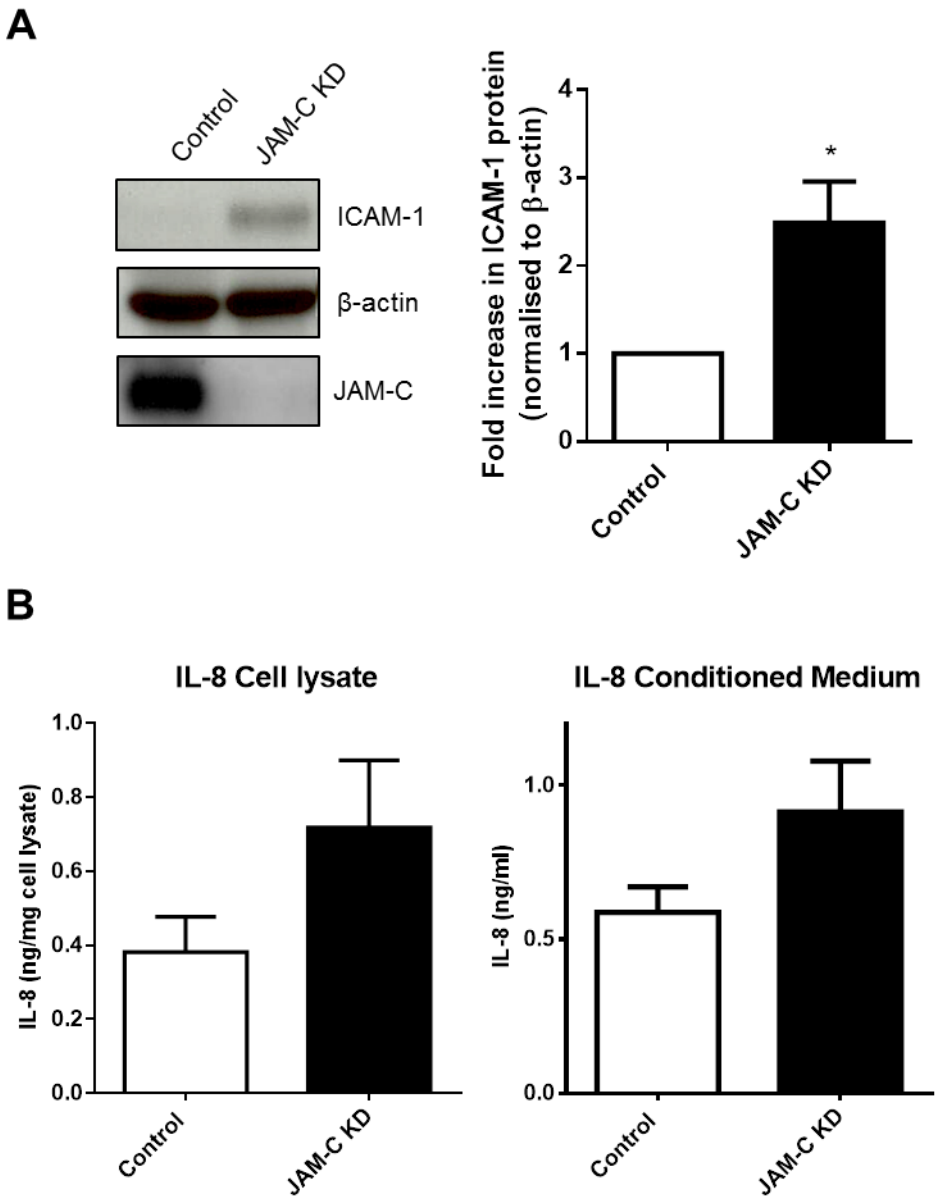

Figure 5.8. IL-8 and ICAM-1 proteins are elevated in JAM-C KD HUVECs.
(A) HUVECs were transfected with control or JAM-C siRNA and cultured for a further 72 h to reach confluence. Cells were lysed and then analysed for ICAM-1 protein levels by Western Blot. Data is represented as the ratio of ICAM-1 to β-actin and then normalised to control conditions. Error bars represent mean ± SEM from n=4 independent experiments. * = $p<0.05$, paired t-test.
(B) HUVECs were transfected with control or JAM-C siRNA and cultured for a further 72 h to reach confluence. Conditioned cell culture medium was collected and cells lysed for the collection of protein lysate. Both lysate and medium were analysed for IL-8 protein levels by ELISA. Lysate IL-8 levels were normalised to total protein content of the lysates. Error bars represent mean ± SEM from n=7 independent experiments for lysate and n=8 for conditioned medium. Data not significant at $p=0.05$ from unpaired t-test.

5.3.7 Differential gene expression analysis of IL-1β stimulated HUVECs

Using the pre-determined thresholds set out in section 0, comparison of IL-1β stimulated control HUVECs (1 ng/ml for 4 h) with unstimulated conditions revealed 1951 genes that were differentially regulated by IL-1β. In this large gene-set, the split between up- and down-regulation by IL-1β was 55% to 45% respectively. Table 5.3 and Table 5.4 display the top 25 upregulated and downregulated differentially expressed genes following IL-1β stimulation of HUVECs. Of the top upregulated genes, many correspond to classical EC inflammatory response genes, notably adhesion molecules such as E-selectin (*SELE*) and ICAM-1 and also chemokines such as CXCL2, CXCL1 and CCL2.

Analysis of the most highly downregulated genes post IL-1β stimulation highlighted some interesting findings, most notable of which is that nearly one third of the top downregulated genes appeared to be unidentified loci or open reading frames of the genome. In addition, while many of the most highly upregulated genes are similar in function (adhesion molecules or chemokines), the most highly downregulated genes show a variety of functions, such as transcription factors, receptors and ion channels.

Gene ID	logFC	P.Value	Protein
SELE	8.15	7.30E-24	E-selectin
VCAM1	7.05	3.69E-17	Vascular Cell Adhesion Molecule-1
CXCL2	6.53	1.27E-17	Chemokine CXCL2
CX3CL1	5.87	4.21E-18	Chemokine CX_3CL1
CCL20	5.71	1.32E-15	Chemokine CCL20
ICAM1	5.50	2.82E-17	Intercellular Adhesion Molecule-1
CCL2	5.46	1.05E-13	Chemokine CCL2
CXCL6	5.23	4.87E-15	Chemokine CXCL6
IL8	5.13	8.54E-15	Interleukin-8
CXCL1	5.08	4.38E-16	Chemokine CXCL1
SLC7A2	4.65	5.33E-16	Solute carrier family 7 member 2
CSF2	4.64	1.65E-13	Colony stimulating factor 2 (GM-CSF)
TNFAIP2	4.64	3.87E-17	TNF alpha induced protein 2
BIRC3	4.57	1.85E-16	Baculoviral IAP repeat-containing protein 3
LTB	4.47	2.39E-15	Lymphotoxin beta
CEBPD	4.29	5.75E-14	CCAAT/enhancer-binding protein delta
SLC25A24	3.96	2.65E-14	Calcium-binding mitochondrial carrier SCaMC-1
PDE5A	3.90	9.96E-14	Phosphodiesterase 5A
TNFAIP3	3.71	3.41E-13	TNF alpha induced protein 3
C2CD4B	3.68	1.06E-17	C2 calcium-dependent domain containing 4B
NLF2	3.65	2.03E-17	Nuclear localised factor 2
CSF3	3.57	3.47E-15	Colony stimulating factor 3 (G-CSF)
IL18R1	3.52	1.65E-13	Interleukin 18 Receptor 1
IL6	3.51	4.26E-11	Interleukin-6

Table 5.3. Top 25 significantly upregulated differentially expressed genes induced by IL-1β in HUVECs.
The top differentially expressed genes in control cells stimulated with IL-1β compared to unstimulated cells were determined by displaying a logFC > 0.5 and P.Value < 0.05.

Gene ID	logFC	P.Value	Protein
PRICKLE1	-1.65	4.62E-09	Prickle
RUNX1T1	-1.49	3.64E-07	RUNX1 translocation partner 1
ZNF395	-1.43	1.15E-07	Zinc finger protein 395
GFOD1	-1.39	1.79E-08	Glucose-fructose oxidoreductase domain containing 1
LOC100132564	-1.35	7.66E-04	Unidentified locus LOC100132564
FRMD3	-1.34	4.49E-06	FERM domain containing 3
MGC16121	-1.32	7.35E-07	Uncharacterised protein MGC16121
HS.538121	-1.31	2.98E-03	Unidentified locus HS.538121
C14ORF139	-1.27	2.17E-05	C14 open reading frame 139
PCDH7	-1.22	3.34E-06	Protocadherin 7
CYP26B1	-1.19	1.38E-08	Cytochrome P450 family 26 subfamily B member 1
NFIA	-1.19	2.33E-07	Nuclear factor I/A
FAM113B	-1.17	8.83E-07	PC-Esterase Domain Containing 1B
PPFIBP2	-1.15	1.05E-06	PPFIA binding protein 2
HS.492187	-1.14	6.10E-07	Unidentified locus HS.492187
CALCRL	-1.14	6.19E-05	Calcitonin receptor like receptor
SETBP1	-1.14	5.19E-07	SET binding protein 1
TYSND1	-1.13	3.30E-08	Trypsin domain containing 1
ST8SIA4	-1.12	5.40E-08	CMP-N-acetylneuraminate-poly-alpha-2,8-sialyltransferase
LOC791120	-1.10	6.60E-06	Unidentified locus LOC791120
FLJ32255	-1.10	1.07E-05	Unidentified locus LOC643977
SLC45A3	-1.10	2.98E-07	Solute Carrier Family 45 Member 3
SERTAD4	-1.09	3.84E-06	SERTA domain containing 4
ELMOD1	-1.09	1.16E-06	ELMO Domain Containing 1
SOBP	-1.09	7.78E-06	Sine oculis-binding protein homolog

Table 5.4. Top 25 significantly downregulated differentially expressed genes following IL-1β stimulation of HUVECs.
The top differentially expressed genes in control cells stimulated with IL-1β compared to unstimulated cells were determined by displaying a logFC < 0.5 and P.Value < 0.05.

5.3.8 Impact of IL-1β on differential gene expression in JAM-C KD HUVECs

Following the findings of increased pro-inflammatory gene expression in JAM-C KD HUVECs under basal conditions, the analysis was extended to investigate the impact of JAM-C KD on EC gene expression in stimulated ECs. Initially, control and JAM-C KD HUVECs stimulated with IL-1β for 4 hours were compared directly using the differential expression analysis model applied previously. Using this method, 987 genes were found to be differentially expressed in JAM-C KD HUVECs compared to control HUVECs following IL-1β stimulation. Out of these genes, there was an even 50% split of up- and down-regulation in expression in JAM-C KD HUVECs. Figure 5.9 shows the top 100 of those genes displayed graphically in heatmap form, indicating the clustering of upregulated (yellow) and downregulated (blue) genes in JAM-C KD HUVECs. In a similar manner to that observed under basal conditions, many of the differentially expressed genes in this comparison were found to be unidentified loci, transcripts with only putative protein reported or open reading frame regions of the genome.

While nearly 1000 genes were found using this differentially expressed model, it was interesting to observe that not one those genes there were previously identified in the unstimulated differential gene expression analysis were present in this cohort. Indeed, as shown in Table 5.5, many of these genes showed no significant difference in expression between control and JAM-C KD HUVECs post IL-1β stimulation. It was previously detailed in Table 5.3 that these prototypical inflammation induced genes are highly upregulated in control cells following IL-1β stimulation and that is also the case in IL-1β stimulated JAM-C KD HUVECs. Taken together, these findings suggest that IL-1β-induced expression of proto-typical endothelial pro-inflammatory genes such as *ICAM1, VCAM1, IL8* and *CXCL1* are unaffected by depletion of JAM-C in ECs.

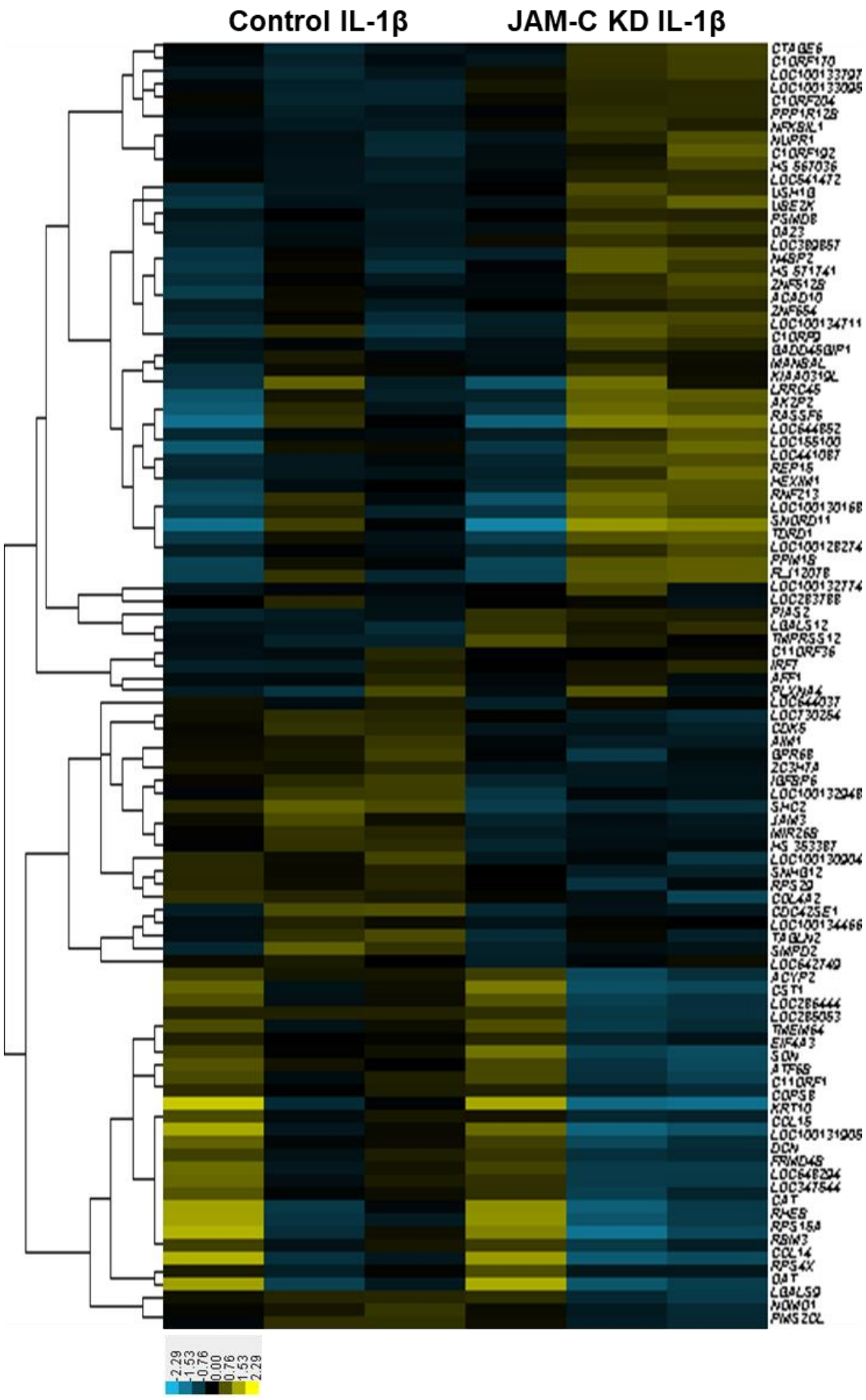
Control IL-1β
JAM-C KD IL-1β
-2.29
-1.53
-0.76
0.00
0.76
1.53
2.29

Figure 5.9. The top 100 differentially expressed genes between control and JAM-C KD HUVECs following IL-1β stimulation.
RNA from Control and JAM-C KD HUVECs stimulated with 1 ng/ml IL-1β for 4 h (from three independent experiments) was subjected to gene expression microarray analysis using Illumina HT-12v4.0 BeadChip technology. Data were extracted and analysed using the Limma package for Bioconductor software. Significant differentially expressed genes were selected based on a threshold of a log fold change (logFC) of greater than +/- 0.5 and $p < 0.05$. The top 100 genes in this threshold are displayed in the heatmap, where blue bars represent lower expression and yellow represents higher expression than their counterparts. These data were generated using Cluster 3.0 and Java TreeView software. This work was done in collaboration with Drs Michael Barnes and Claudia Cabrera in the Department for Bioinformatics, William Harvey Research Institute, QMUL.

Gene ID	logFC	P.Value
VCAM1	0.088	0.650
CCL2	-0.323	0.197
HMGB1	0.397	0.025
IL8	-0.026	0.844
ICAM1	0.282	0.072
CXCL1	-0.095	0.561
HIF1A	0.374	0.004

Table 5.5. Candidate genes from unstimulated comparison subjected to differential expression analysis following IL-1β stimulation.
The candidate genes that showed upregulation under basal conditions in JAM-C KD HUVECs in Table 5.2 were analysed for differential expression in JAM-C KD HUVECs following IL-1β stimulation as compared to control HUVECs. They are displayed here with the logFC of expression and P.value.

Building on these analyses, an additional approach was taken to analyse the effects of JAM-C KD on IL-1β-mediated gene expression in ECs. Using the differential expression analysis of the response of control cells to IL-1β (see section 0), the 1951 detected regulated genes were plotted in a normalised differential expression heatmap (Figure 5.10 A&C) to indicate the EC response to IL-1β in control cells. Differential expression analysis of these genes was then performed on IL-1β stimulated HUVECs, but this time using unstimulated control cells as the comparison. The resulting analysis was plotted on the same heatmap (Figure 5.10 A&C, right column). This analysis allowed for detection of areas which show no up-regulation (Figure 5.10A) or down-regulation

(Figure 5.10C) in gene expression in JAM-C KD HUVECs following IL-1β stimulation (green boxes). These genes were extracted and analysed for patterns of expression. Here, 147 genes failed to show upregulation (the top 20 of which are detailed in Figure 5.10B) and instead were downregulated in JAM-C KD HUVECs. Interestingly, a number of the unidentified loci of the genome are again present, even in this smaller cohort. Analysing the genes that failed to show downregulation in response to IL-1β in JAM-C KD HUVECs revealed 154 candidates. The top 20 of these are displayed in Figure 5.10D, again indicating a number of those unidentified loci.

From this analysis, the 301 candidate genes identified were subjected to gene ontology enrichment analysis (GO) to identify potential biological pathways that might be impacted by JAM-C KD in IL-1β stimulated HUVECs. The top 10 biological processes are listed in Table 5.6. Amongst these, processes such as “intracellular signal transduction” and “immune system processes” were of interest to the theme of this project and as such warrant further investigation. This analysis highlighted a number of inflammatory genes which are dysregulated in JAM-C KD HUVECs following IL-1β stimulation, genes that are detailed in Table 5.7. Collectively, the present novel studies indicate that JAM-C deficient ECs respond abberantly to inflammatory stimululation in the form of disrupted gene expression.

A

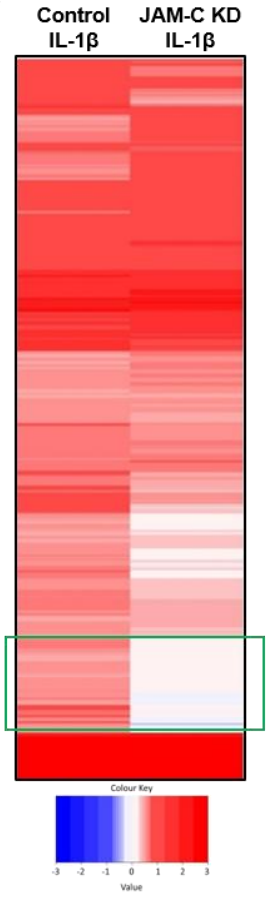

B

Gene ID	Control logFC	JAM-C KD logFC
PGAM4	0.619	-0.495
LOC648390	0.599	-0.385
RNU105C	0.778	-0.280
DCN	0.767	-0.261
SSSCA1	0.521	-0.261
HNRNPH2	0.502	-0.236
LOC644739	0.610	-0.203
LOC100129022	0.538	-0.193
LOC401561	0.638	-0.191
LOC283953	0.500	-0.188
PTPN2	0.535	-0.169
ZNF654	0.541	-0.167
LOC100134466	0.744	-0.158
HS.577935	0.529	-0.148
LOC100130775	0.537	-0.137
C6ORF155	0.512	-0.13
RAD51	0.570	-0.127
HS.545236	0.680	-0.125
ETV2	0.613	-0.119
HS.550282	0.655	-0.119

C

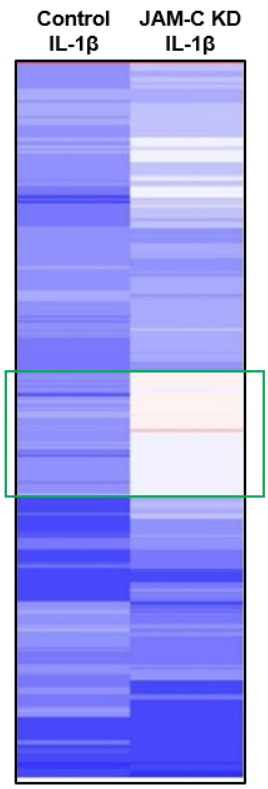

D

Gene ID	Control logFC	JAM-C KD logFC
SSTR2	-0.535	0.451
HEXIM1	-0.626	0.313
CHRNA5	-0.515	0.300
AK2P2	-0.748	0.287
UBE2K	-0.699	0.280
TMPRSS12	-0.552	0.247
PLXNA4	-0.559	0.238
LOC100128098	-0.552	0.230
ZNF93	-0.545	0.208
LOC100134711	-0.731	0.207
RBM3	-0.554	0.201
ZNF682	-0.514	0.194
CFC1B	-0.541	0.193
LOC730254	-0.586	0.189
LOC401098	-0.508	0.188
PPAP2C	-0.524	0.178
ERGIC1	-0.521	0.172
LOC389765	-0.600	0.170
PRRG4	-0.534	0.150
TDRD1	-0.861	0.148

Figure 5.10. Normalised differential expression heatmap of IL-1β stimulated HUVECs.
(A&C) IL-1β stimulated control HUVECs were subjected to differential expression analysis compared to unstimulated control HUVECs. Using the pre-determined thresholds of logFC > ± 0.5 and P.value < 0.05, significant genes were plotted in heatmap form. Those same genes

were analysed in JAM-C KD HUVECs stimulated with IL-1β again using control unstimulated HUVECs as the comparison and plotted in the same heatmap. Regions of dysregulated expression are highlighted by the green boxes.
(B) Genes that were not upregulated in JAM-C KD HUVECs were isolated from the heatmap in (A). The top 20 were displayed in table negatively ordered by logFC level in JAM-C KD HUVECs.
(D) Genes that were not downregulated in JAM-C KD HUVECs were isolated from the heatmap in (A). The top 20 were displayed in table positively ordered by logFC level in JAM-C KD HUVECs.

Gene Set Name	# Genes in overlap	p-value
Protein modification process	21	1.34E-09
Intracellular signal transduction	19	2.66E-08
Negative regulation of protein metabolism	15	8.68E-08
Immune system processes	20	9.06E-08
Cellular response to organic substance	19	1.47E-07
Regulation of hydrolase activity	16	1.94E-07
Cell death	14	2.06E-07
Hemostasis	10	2.78E-07
Intracellular signal transduction	17	3.57E-07
Regulation of phosphorous metabolic process	17	5.31E-07

Table 5.6. Gene ontology enrichment analysis (GO) of dysregulated genes in IL-1β stimulated JAM-C KD HUVECs.
The candidate genes identified from the heatmap in Figure 5.10 were subjected to gene enrichment analysis using gene ontology software (Broad Institute, Cambridge, MA, USA).

Gene ID	Control logFC	JAM-C KD logFC
ADAM15	0.508	0.158
CCL7	0.601	0.113
CTSH	0.537	0.089
CXCR4	0.841	0.127
DCN	0.768	-0.261
IRF6	0.590	-0.048
IRF7	0.774	0.052
PTPN2	0.535	-0.169
TJP2	0.542	0.172
TNFRSF10B	0.695	0.068

Table 5.7. Candidate genes isolated from GO analysis.

5.3.9 Differential expression of semaphorins by JAM-C KD HUVECs

One of the main aims of this chapter and the project as a whole was to identify molecules and novel mechanisms by which loss of EC JAM-C leads to disrupted modes of neutrophil migration. In this context, a potential avenue is the possibility that EC JAM-C deficiency promotes the generation of chemorepulsive molecules. As such, a list of chemorepulsive molecules was compiled (see Appendix 3) and the differential gene expression analysis of control and JAM-C KD HUVECs under IL-1β stimulation overlayed onto the list to isolate candidate molecules. This process indicated that a number of the semaphorin family of molecules were differentially expressed in IL-1β stimulated JAM-C KD HUVECs, particularly *SEMA3E, SEMA3G* and *SEMA4F* (Figure 5.11A&B). Upon further examination, it was also found that some of the semaphorin receptors, the plexins and neuropilins, as well as the functionally related molecule RMA, also showed differential expression in JAM-C KD HUVECs. The semaphorin molecules and their receptors were originally identified due to their role as axonal cone guidance molecules (Kruger et al., 2006, Worzfield et al., 2014). More recently, however, they have been found to have a role in a number of other biological processes, particularly in immune responses (Potiron et al., 2007, Takamatsu et al., 2010) and the regulation of leukocyte migration (Movassagh et al., 2016, Morote-Garcia et al., 2012, van Rijn et al., 2016).

To verify the differences observed, the expression of a number of these genes was validated by qPCR (Figure 5.12). The findings indicate that there is an increase in gene expression of several members of the semaphorin family in JAM-C KD HUVECs following IL-1β stimulation, particularly *SEMA4F* and *SEMA3G*. With respect to *SEMA4F*, expression is equal in control and JAM-C KD HUVECs under basal conditions and slightly reduced in IL-1β stimulated control HUVECs when compared to - unstimulated control ECs. However, IL-1β stimulated JAM-C KD HUVECs exhibited a statistically significant increase in *SEMA4F* gene expression as compared to control stimulated HUVECs. *SEMA3G* expression was also increased in JAM-C KD HUVECs compared to control HUVECs following IL-1β stimulation, though this was a smaller two-fold increase and was not statistically significant. In a similar manner, *SEMA6B* expression was increased in JAM-C KD HUVECs under both basal and IL-1β stimulated conditions, though again these changes were not statistically significant. Together, the

present results identify a novel role for EC JAM-C as a regulator of gene expression of chemorepulsive molecules, most notably members of the semaphorin family. Further work is currently being conducted to confirm the findings for *SEMA3E* and *SEMA6B* and also to validate the expression of additional genes detailed in Figure 5.11A.

A

Molecule	Gene ID	logFC	P.Value
Semaphorins	*SEMA3G*	0.518	8.03×10^{-3}
	SEMA3E	0.529	1.47×10^{-2}
	SEMA4C	-0.390	7.77×10^{-3}
	SEMA4F	0.518	5.43×10^{-4}
	SEMA6B	0.354	5.99×10^{-3}
Plexins	*PLXNA4*	0.780	8.58×10^{-5}
	PLXND1	0.378	1.29×10^{-3}
Neuropilins	*NRP1*	-0.492	6.22×10^{-4}
Repulsive-guidance molecules	*RGMA*	0.390	3.45×10^{-2}

B

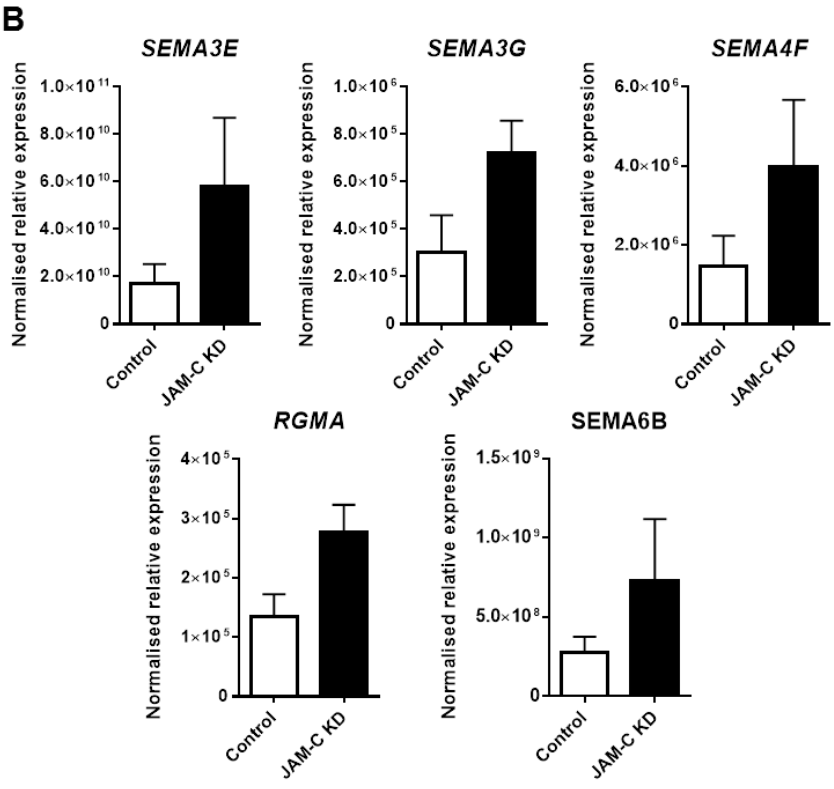

Figure 5.11. Several members of the Semaphorin family of molecules are differentially expressed in JAM-C KD HUVECs following IL-1β stimulation.
(A) Control and JAM-C KD HUVECs stimulated with IL-1β were subjected to differential expression analysis. Semaphorin and related genes are displayed in the table.

(B) Normalised intensities were extracted from the microarray data chips and plotted for *SEMA3E, SEMA3G, SEMA4F, RGMA* and *SEMA6B* genes.

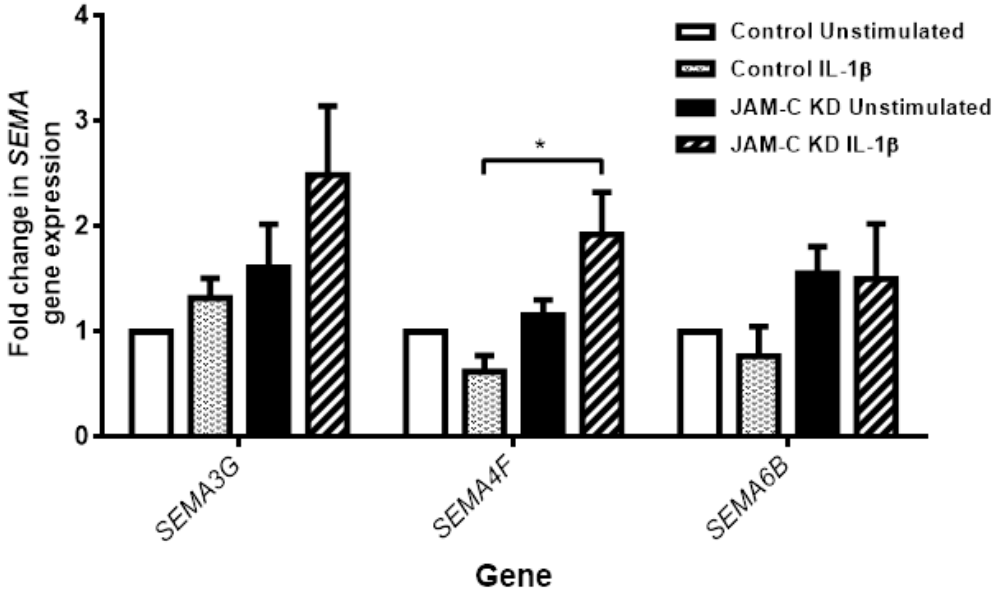

Figure 5.12. qPCR validation of Semaphorin gene expression in JAM-C KD HUVECs. RNA was isolated from control and JAM-C KD HUVECs, both unstimulated and IL-1β stimulated and reverse transcribed to cDNA. Primers specific for *SEMA3G, SEMA4F* and *SEMA6B* (detailed in section 2.4.5) were used to specifically amplify those transcripts. Data is plotted as fold change over control cells using the ΔΔCt method, where primers for *ACTB* and *PPIA* were used as housekeeping controls. Data is representative of at least four independent experiments. Error bars represent mean ± SEM. * = $p<0.05$, **=$p<0.01$ one-way ANOVA.

5.4 Discussion

The aim of this chapter was to investigate the role of JAM-C in regulation of EC gene expression. To achieve this, the model of JAM-C KD in HUVECs described in Chapter 3 was used, with purified RNA from control and JAM-C KD HUVECs under both unstimulated and IL-1β stimulated conditions being submitted to gene expression microarray analysis using the Illumina HT-12 expression chips. While next generation RNA-sequencing has become the more preferred method for analysing gene expression, at the time of this work it was considerably more cost effective to use the gene expression microarray approach for the present project. This aspect of my PhD was significantly facilitated by the Barts and the London Genome Centre.

The most commonly used approach to analyse gene expression data is the use of differential gene expression analysis. In collaboration with Dr Michael Barnes and Dr Claudia Cabrera of the Centre for Translation Bioinformatics (QMUL), differential expression analysis of control and JAM-C KD HUVECs was performed. A variety of methods can be used to identify thresholds for such analysis in order to select significant changes in this model. Indeed, while the use of False Detection Rate (FDR) corrected P.Values alone is a popular method, this can be quite restrictive depending on the biological question at hand. The use of logFC cutoffs and/or P.Values can however provide a wider range of genes to investigate (Dalman et al., 2012). As such, it was decided to using a combination of logFC and P.Value cut offs to determine significant genes in these comparisons, more specifically, logFC increase/decrease of ± 0.5 and a P.Value of ≤ 0.05. This approach enabled investigations into moderate changes in gene expression and associated pathways that might occur following loss of JAM-C in ECs.

5.4.1 JAM-C regulates EC gene expression under basal conditions

Initial investigations into the effects of JAM-C KD on EC gene expression focussed on resting ECs. Using both differential gene expression and subsequent pathway analysis models, JAM-C KD HUVECs were found to exhibit increased gene expression associated with numerous inflammatory pathways, most intriguing of which were leukocyte migration related pathways. This was characterised by increased expression of a

number of pro-inflammatory genes, including *VCAM1, ICAM1, CXCL1, CCL2* and *IL8*. These are the prototypical molecules whose expression is induced by inflammation in ECs to recruit leukocytes, particularly monocytes and neutrophils. In many cases this increased expression was observed at two or more fold over that of control HUVECs. Further characterisation suggested that these gene expression increases are also translated into increased protein levels, as indicated by increased protein levels of ICAM-1 and IL-8. This represents a novel finding for the field and demonstrates how an EC junctional molecule can control the basal inflammatory status of the cell through regulating gene expression.

From these findings, it could be suggested that loss of JAM-C from ECs results in an inflammatory priming of ECs. Intriguing though this is, one must also consider the physiological impact of such expression. While this increase in gene expression is clearly not as high as the induction detected post stimulation of ECs with IL-1β, it was nevertheless a significant response. As such, perhaps JAM-C KD HUVECs might support increased rolling and/or adhesion of leukocytes (neutrophils specifically) under basal conditions. This analysis could be extended to an *in vivo* model, using endothelial specific JAM-C KO mice to investigate whether they exhibit increased leukocyte rolling flux, adhesion and/or transmigration under basal conditions.

Initial investigations into how loss of JAM-C might induce increased pro-inflammatory gene expression under basal conditions focussed on the role of the NFκB pathway. Each of the genes discussed here have been shown to be induced through activation of the NFκB family of transcription factors and its signalling pathway (van Uden et al., 2008, Moynagh et al., 1994, Anisowicz et al., 1991). Classically, NFκB is activated in response to pro-inflammatory mediators such as IL-1β, TNFα and LPS. Stimulation by such mediators triggers signalling that ultimately results in the phosphorylation and translocation of NFκB to nucleus where it initiates the transcription of a variety of pro-inflammatory genes (Christian et al., 2016). In the model of EC JAM-C deficiency used in this project, JAM-C KD HUVECs showed significantly increased phosphorylated levels of the NFκB subunit p65 under basal conditions, although this was not correlated with increased p65 nuclear translocation. This suggests that loss of JAM-C from ECs signals through the NFκB pathway to induce expression of pro-inflammatory genes. However, activation by protein kinase mediated phosphorylation of the individual NFκB subunits

is not the only mechanism by which the pathway is regulated (Oeckinghaus et al., 2009). Inhibitor of κB (IκB) sequesters NFκB in the cytoplasm to prevent its translocation to the nucleus. Upon inflammatory cues, IKK phosphorylates and targets IκB for degradation, freeing NFκB for nuclear translocation (Yamamoto and Gaynor, 2004). As such, phosphorylation of the IκB subunits is also a method for analysing NFκB pathway activation and could be used in this model of JAM-C KD to obtain further evidence for the involvement of NFκB pathway activation post JAM-C KD.

As mentioned previously, numerous different signalling pathways can be activated by an inflammatory stimulus such as IL-1β, notably the MAPK pathway (Weber et al., 2010). Hence, it is entirely possible that multiple signalling pathways, such as the MAPK pathway, are activated following JAM-C KD, which could contribute to the noted pro-inflammatory gene expression. While the activation of two MAPKs, ERK1 and ERK2, were unaffected by JAM-C KD, these are not the only MAPKs that are associated with inflammatory signalling. Indeed, p38 MAPK and c-Jun N-terminal kinase (JNK) are two kinases that should also be investigated in this model. Indeed, p38 MAPK has been shown to activate the expression of the candidate genes identified in this model such as *ICAM1* (Yan et al., 2002) and *VCAM1* (Dong et al., 2011). Not only that, but p38 MAPK has also been shown to increase activation of NFκB (Korus et al., 2002), highlighting the complex crosstalk that can occur between intracellular signalling pathways.

In addition to increased pro-inflammatory gene expression, the pathway analysis of unstimulated JAM-C KD HUVECs under basal conditions also revealed that pathways involved in cellular homeostasis were predicted to be upregulated in JAM-C KD cells. Further examination of these pathways revealed two genes in particular, *HIF1A* and *HMGB1*, with qPCR validating that their expression was significantly upregulated in JAM-C KD HUVECs under basal conditions. Hypoxia inducible 1-alpha (HIF1α) protein, is a critical part of the cellular response to changing oxygen levels (Bartels et al., 2013, Semenza, 2014). In addition to this crucial role, HIF1α is also documented to play a role in the inflammatory response (Hellwig-Burgel et al., 2005, Palazon et al., 2014) and it has also been shown to be regulated by the NFκB pathway, suggesting that upregulation of phosphorylated p65 detected in JAM-C KD HUVECs might also be responsible for increased *HIF1A* expression. HMGB1 has a wide range of functions,

including facilitating gene transcription (Lotze and Tracey, 2005), regulating autophagy (Tang et al., 2010a) and also in inflammation where it functions as a danger associated molecular pattern (DAMP) (Klune et al., 2008). Macrophages and monocytes release HMGB1 as a pro-inflammatory cytokine acting as a potentiator of local inflammation (Schiraldi et al., 2012). In addition, it has also been shown that epithelial cell derived HMGB1 acts as a chemoattractant to induce the recruitment of leukocytes by forming a complex with CXCL12 chemokine (Huebener et al., 2015). As such, HMGB1 represents an exciting candidate molecule for investigation with regards to how JAM-C regulates EC biology, particularly given its wide range of known pro-inflammatory functions.

5.4.2 JAM-C KD ECs respond aberrantly to cytokine stimulation

Following the analysis of unstimulated HUVECs, it was hypothesised that JAM-C KD ECs may respond to an inflammatory stimulus in a different manner to control cells. To investigate this, control and JAM-C KD HUVECs were stimulated with the pro-inflammatory cytokine IL-1β for 4 hours and then analysed for differential gene expression. Rather surprisingly, no difference in expression of any typical EC pro-inflammatory molecules, such as adhesion molecules, chemokines or cytokines was found. In fact, in terms of these molecules, JAM-C KD ECs appear to respond in the same way as control cells, at the gene expression level at least.

Differential expression and cluster analysis of IL-1β stimulated control or JAM-C KD HUVECs compared to unstimulated conditions revealed two distinct clusters of gene dysregulation in IL-1β stimulated JAM-C KD HUVECs (Figure 5.10). Isolation of the genes in these clusters revealed a large percentage (30%) of uncharacterised loci and transcripts. This indicates that there is a large amount of the gene expression response of ECs to inflammatory stimuli such as IL-1β that remains to be characterised. More interestingly, loss of JAM-C seems to disrupt the normal expression pattern of these targets and as such highlights a number of potential avenues by which JAM-C might be crucial to regulating EC gene expression responses to IL-1β.

Another important finding from this analysis was that, upon subjection of these clusters to GSEA analysis, pathways such as intracellular signal transduction were

predicted as potentially being regulated by loss of JAM-C in IL-1β stimulated HUVECs. While the investigations into this are still at a very early stage, a number of interesting observations were made when examining the genes responsible for these predicted pathways. These genes, normally upregulated in HUVECs in response to IL-1β, are not induced when JAM-C is lost. Some of the genes dysregulated here include *IRF6* and *IRF7*, two members of the IRF family of transcription factors that are part of the JAK-STAT signalling pathway. Interferon regulatory factor 7 (IRF7) is considered the master regulator of type I interferon responses, coordinating signalling responses (Honda et al., 2005). It has also been shown to interact with Myeloid differentiation primary response gene 88 (MyD88), an important adaptor protein in the IL-1β receptor complex (Honda et al., 2005). Indeed, if this reduced gene expression correlates to reduced protein levels, perhaps loss of JAM-C might impact EC and tissue responses to prolonged inflammation and the subsequent resolution of inflammation. Rather intriguingly, the gene for the tight junction molecule ZO-2, *TJP2*, was also not upregulated in JAM-C KD HUVECs. These results provide the first evidence for the ability of EC JAM-C to regulate the gene expression of another junctional molecule.

Overall, JAM-C KD HUVECs seem to exhibit a partial failure to respond to IL-1β in terms of their gene expression profile. This dysregulation does not appear to occur in any of the typical IL-1β responsive pro-inflammatory genes (such as *ICAM1* or *CXCL1*). Therefore, altered gene expression may not account for the disrupted modes of neutrophil migration that are observed under conditions of JAM-C loss *in vivo*. Nevertheless, the disrupted gene expression profile is highly intriguing and while investigations into this phenotype are at a very early stage, the present finding could provide valuable insights into how JAM-C regulates EC gene expression responses to inflammatory stimuli such as IL-1β.

5.4.3 JAM-C regulates Semaphorin expression during inflammation

Expression of some members of the Semaphorin family of molecules was found to be differentially regulated in IL-1β stimulated JAM-C KD HUVECs. To date, only *SEMA4F* has been validated by qPCR as showing a significant increase in expression in JAM-C KD

HUVECs following stimulation, but others such as *SEMA3G* and *SEMA3E* also indicate a trend for increased expression.

Semaphorins and their receptors, while classically studied as axonal guidance molecules in nervous system development, have also been shown to be expressed in ECs and have been reported to regulate endothelial functions and inflammatory responses (Takamatsu et al., 2010, Sakurai et al., 2012, Aghajanian et al., 2014). For example, a number of the Semaphorins have been shown to have either pro-or anti-angiogenic properties (Acevedo et al., 2008, Sakurai et al., 2012, Segarra et al., 2012). In addition, Semaphorin 3A has been shown to increase vascular permeability by decreasing VE-Cadherin stability. As JAM-C can regulate both angiogenesis and vascular permeability (Orlova et al., 2006, Li et al., 2009, Rabquer et al., 2010), it would certainly be intriguing to investigate the relationship between JAM-C and endothelial semaphorin expression in such endothelial functions.

Of most interest to our lab are the emerging roles of Semaphorins in inflammatory responses and in particular their roles in leukocyte recruitment. Semaphorin 3A (SEMA3A) has been shown to have anti-inflammatory effects in models of autoimmune arthritis (Catalano, 2010) and conversely to potently recruit monocytes in diabetic retinopathy (Sapieha et al., 2015) and promote inflammation. Semaphorin 7A (SEMA7A) has been shown to increase neutrophil migration across EC monolayers *in vitro* (Morote-Garcia et al., 2012). Most notably, Semaphorin 3E (SEMA3E) has recently been shown to be a negative regulator of neutrophil migration, both *in vitro* and *in vivo* (Movassagh et al., 2017). Indeed, in this model it was shown that SEMA3E inhibits neutrophil migration towards the main neutrophil chemoattractant IL-8 and also reduces allergen-induced neutrophil recruitment in the lungs of mice. Differential expression analysis in this model found that SEMA3E expression was increased in JAM-C KD HUVECs following IL-1β stimulation as compared to control HUVECs. As loss of JAM-C has been shown to induce increased neutrophil reverse migration back into the circulation in response to stimuli such as IL-1β (Woodfin et al., 2011), the increase in expression of SEMA3E could potentially provide a crucial link between EC JAM-C expression and this phenomenon. Of course, the increased expression of SEMA3E does need to be validated at both the RNA and protein level in both JAM-C KD HUVECs and in a murine model of endothelial JAM-C deficiency *in vivo*.

Regarding Semaphorin 4F (SEMA4F), to date most of the research on this protein has focussed on its role in the nervous system (Parrinello et al., 2008, Armendariz et al., 2012), where it has been shown to provide an axonal contact inhibitory signal that prevents Schwann cell proliferation. To date there have been no reports on its expression in the endothelium. As such, the findings in this work indicating SEMA4F is expressed in HUVECs and further increased in expression upon loss of JAM-C provide a novel candidate for further investigation in EC biology, particularly under inflammatory conditions where JAM-C expression is disrupted. Given that Semaphorin 4F acts as an inhibitory molecule during axonal growth, it is potentially possible that it may have a similar function during EC processes such as EC migration during angiogenesis or perhaps even by influencing leukocyte migration in a similar manner to that seen for SEMA3E.

5.4.4 Mechanism of JAM-C regulated gene expression in ECs

At this point it is pertinent to speculate on how loss of the EC tight junctional molecule JAM-C may regulate EC gene expression. In basal conditions, while increased activation of the NFκB pathway was detected, it is still unknown how loss of JAM-C might promote the activation of this pathway. Perhaps JAM-C might interact with regulators of the signalling pathway, such as IKK, thus keeping the basal activation of NFκB low by preventing degradation of the NFκB inhibitor IκB. In this context, JAM-C has been linked to both the MAPK and PI3K pathways and indeed, soluble JAM-C was shown to mediate angiogenesis through activation of EC p38 MAPK and PI3K (Rabquer et al., 2010), while anti-JAM-C blocking antibodies prevented the activation of the MAPKs ERK1/2 in lymphoma B cells (Donate et al., 2016). Both MAPK and PI3K have been shown to regulate NFκB pathway activation (Bai et al., 2009, Saha et al., 2007) and as such might provide mechanistic links for how loss of JAM-C induces activation of the p65 NFκB pathway under basal conditions.

In a more global sense, the apparent profile of inflammatory priming observed under conditions of JAM-C KD could be interpreted as the EC being unable to maintain homeostasis. In basal, resting conditions, activation of NFκB and therefore expression of pro-inflammatory molecules such as ICAM-1 and IL-8 is kept low, maintaining the

homeostasis of ECs. This is achieved through the actions of the transcription factor Erg (Shah et al., 2016) which has been shown to repress the basal activity of NFκB subunit p65 by preventing it from directly binding to the promoter of genes such as *ICAM1* in HUVECs (Dryden et al., 2012). One can therefore hypothesise that increased NFκB p65 activation following JAM-C KD in basal conditions is due to dysregulation of Erg activity or localisation, a response that could promote increased expression of NFκB responsive genes. Interestingly, Erg expression was not changed in this model (log FC = -0.24, P.value = 0.08), indicating that perhaps if this is the mechanism then some change at the protein level of Erg may be occurring which would need to be investigated in future studies.

While inflammatory priming of JAM-C KD HUVECs was detected under basal conditions, no difference in expression of NFκB responsive inflammatory genes was noted between IL-1β stimulated control and JAM-C KD HUVECs. As such, other potential signalling mechanisms would need to be considered. It could be that loss of JAM-C disrupts the intracellular localisation of binding partners, such as ZO-1 (Ebnet, 2003). ZO-1 is known to inhibit the activity of an associated transcription factor, ZONAB, in epithelial cells (Balda et al., 2003). As such, loss of or disrupted expression of JAM-C could impact ZONAB localisation and/or activity, therefore providing a potential pathway through which some of the observed differential gene expression patterns are brought about in ECs.

5.4.5 Summary of key findings

The results presented in this chapter demonstrate that silencing of JAM-C expression has a significant impact on EC gene expression, both at a basal level and also following stimulation with the inflammatory stimuli IL-1β. This provides the first evidence that JAM-C regulates gene transcription in ECs. More specifically, this chapter has identified the following:

- EC JAM-C KD causes an apparent inflammatory priming of ECs, characterised by increased activation of the NFκB subunit p65 and subsequent increase in expression of pro-inflammatory genes such as *ICAM1*, *VCAM1* and *IL8*.

- JAM-C deficient ECs respond aberrantly to IL-1β stimulation. Further characterisation of the genes regulated in this comparison will provide valuable insight into the modes and mechanisms by which JAM-C regulates EC responses in inflammation.

6 Investigating the role of EC JAM-C in inflammatory mediator generation

6.1 Introduction

Activation of the endothelium during inflammatory reactions is critical in coordinating an effective immune response. Activation by PAMPs/DAMPs or by proinflammatory molecules released by the surrounding damaged tissue induces changes in the endothelium that ultimately promotes leukocyte recruitment. Of key importance to this response is the generation, secretion and/or presentation of cytokines and chemokines by ECs. These responses act to facilitate leukocyte recruitment and hence promote an efficient inflammatory response. Extensive characterisation of activated ECs has revealed that they are able to produce and secrete a wide range of cytokines (IL-1, IL-15, G-CSF) and chemokines (IL-8, CXCL1, CCL2) (Krishnaswamy et al., 1999, Speyer and Ward, 2011). Depending on the nature and duration of the stimulus, the exact make up of this EC response can vary considerably.

As mentioned in Chapter 1, the production and presentation of chemokines by ECs *in vivo* is crucial for directing infiltrating leukocytes to the damaged/infected tissue. Whilst the impact of pro-inflammatory insults on chemokine generation has been extensively studied, little is known about how EC junctional molecules regulate this process. More specifically, almost nothing is known regarding the impact of disrupting EC junctional molecules on the inflammatory response of ECs, such as generation of cytokines/chemokines.

Some chemokines are known to modulate EC junctions themselves, such as CCL2, which has been shown to disrupt both tight junctions through induction of Rho kinase activity and also to disrupt adherens junctions by stimulating β-catenin reorganisation (Roberts et al., 2012, Stamatovic et al., 2003). Some work in the intestinal epithelium has shown that disruption of tight junctions by pathogens reduces the intestinal barrier integrity and results in increased IL-8 secretion (Chen et al., 2006). In a related manner, studies in breast cancer cell lines have shown that the tight junction protein ZO-1 is important for regulating IL-8 production (Brysse et al., 2012). However, the literature is scarce on the role of EC junctional molecules and more specifically JAM-C

in regulating cytokine/chemokine secretion from ECs. A single study has previously shown that JAM-C can regulate chemokine secretion from fibroblast reticular cells. Here, it was shown that mice treated with anti-JAM-C antibodies exhibited decreased lymph node levels of the chemokines CXCL12, CCL21 and CCL19. This was subsequently translated into reduced T cell migration out of lymph nodes (Frontera et al., 2011). As such, it was hypothesised that JAM-C might have similar functionality in ECs.

6.2 Aims

Given the recent work from our laboratory in elucidating the role of JAM-C in disrupted modes of neutrophil migration (particularly rTEM), it was decided to investigate the role of EC JAM-C in inflammatory mediator generation by ECs. Specifically, the aims were as follows:

- To investigate inflammatory mediator generation by JAM-C KD HUVECs in response to IL-1β stimulation.
- To determine whether EC JAM-C KO mice exhibit altered chemokine levels in IL-1β stimulated tissues.
- To investigate whether there are altered plasma chemokine levels in EC JAM-C KO mice post local administration of IL-1β.

6.3 Results

6.3.1 Effect of JAM-C KD on IL-1β-stimulated HUVEC chemokine generation

The findings in Chapter 5 indicated that loss of EC JAM-C had no effect on IL-1β induced expression of the prototypical inflammatory EC response genes, such as *IL8* and *CXCL1*. As such, the same model of JAM-C KD HUVECs was utilised to investigate the protein levels of inflammatory mediators by ECs and thereby assess their response to a pro-inflammatory stimulus.

Protein levels of the chemokine IL-8 had already been shown to be elevated in JAM-C KD HUVECs under basal conditions (Chapter 5), and so this analysis was extended to HUVECs stimulated with IL-1β for 4 hours. Both control and JAM-C KD HUVECs showed highly significant ($p<0.0001$) upregulation of IL-8 protein in the cell associated fraction (Figure 6.1A, left panel), with no differences seen between the two cell types. Taken together with the gene expression findings, these results indicated that loss of JAM-C from ECs has no effect on IL-8 production in HUVECs.

Analysis of the cell culture medium collected post IL-1β stimulation also revealed a highly significant increase in secreted IL-8 from both control and JAM-C KD HUVECs. However in contrast to the cell lysate analysis, significantly less IL-8 was secreted from JAM-C KD HUVECs (29%) following IL-1β stimulation (Figure 6.1A, right panel).

The same analysis was extended to CXCL1, also a key neutrophil chemoattractant produced by ECs. Like IL-8, both control and JAM-C KD HUVECs showed highly significant upregulation of CXCL1 protein in the cell associated fraction (Figure 6.1B, left panel). In a similar manner to IL-8, and taken together with the findings in Chapter 5 showing no difference in IL-1β induced CXCL1 gene expression, this suggests that loss of EC JAM-C has no effect on the cellular production of CXCL1 by HUVECs. Significant increased levels of secreted CXCL1 were also found from both control and JAM-C KD HUVECs post IL-1β stimulation, however unlike IL-8, no difference in secreted CXCL1 was found between the two cell types.

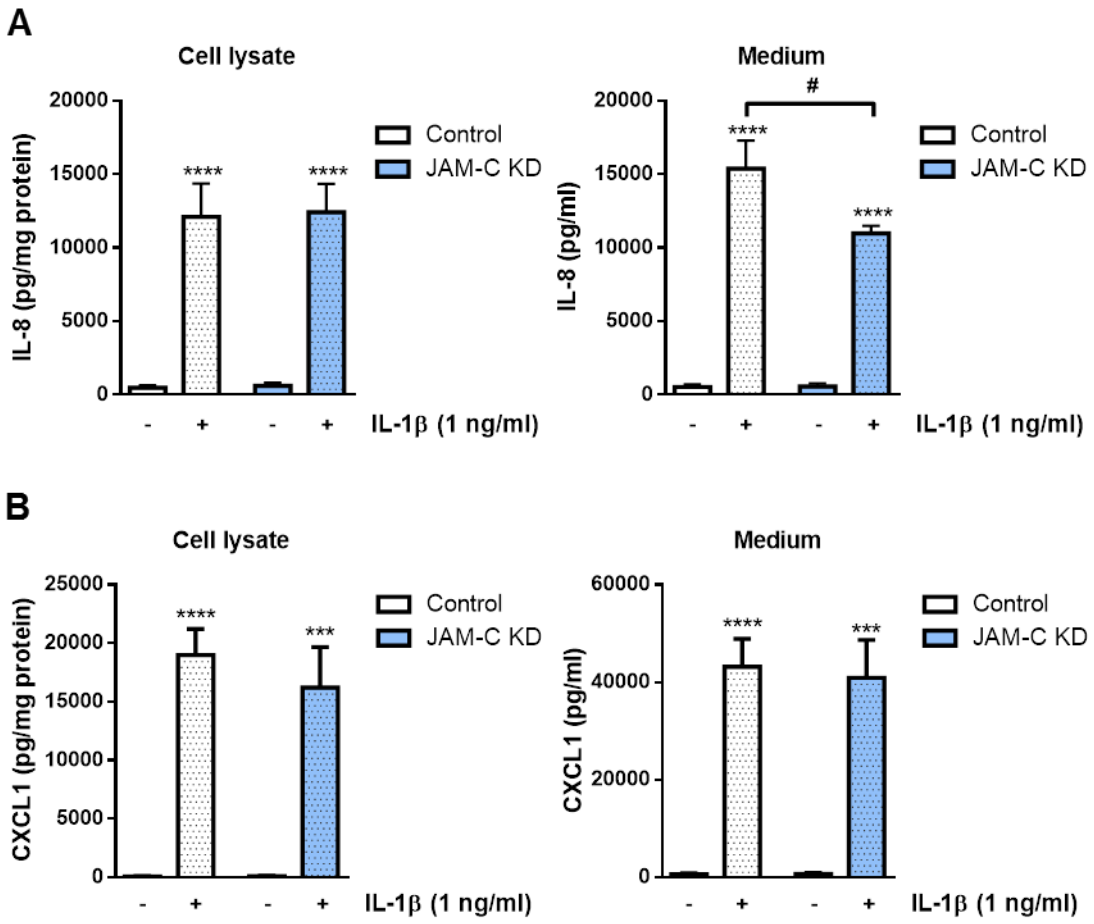

Figure 6.1. ELISA analysis of IL-1β induced chemokine generation by JAM-C KD HUVECs. HUVECs were transfected with either control or JAM-C siRNA and cultured for 72h to reach confluence. Cells were then either stimulated with IL-1β (1 ng/ml) for 4h or left unstimulated. Cell culture medium and cell lysates were collected for further ELISA analysis of either IL-8 (A) or CXCL1 (B) chemokines. Levels of secreted chemokine in cell culture medium were expressed as pg/ml. Levels of cell associated chemokine were expressed as pg/mg protein in the cell lysate. Statistical analysis performed using one-way ANOVA with Tukeys multiple comparison test. Data is represented as mean ± SEM from at least 5 independent experiments. *** = $p<0.001$, **** = $p<0.0001$, compared to control unstimulated. # = $p<0.05$ compared to control IL-1β.

Following the findings of reduced IL-8 secretion from JAM-C KD HUVECs, conditioned medium from IL-1β stimulated control and JAM-C KD HUVECs was investigated more broadly to assess the potential impact of JAM-C on a wider range of cytokines/chemokines. For this purpose, the conditioned medium was subjected to analysis by cytokine array, where 32 different mediators were analysed. Conditioned medium from three independenet experients was pooled and assayed using a Proteome Profiler^{TM} human cytokine array. Membranes were probed with IRDye-Streptavidin to enable accurate quantification of cytokine expression. Read-outs less than 1000 A.U. were considered to be below the range of accurate detection.

From the 32 proteins analysed, 12 were noted to be secreted in control cells in response to IL-1β (all with read-outs > 1000 A.U.). For ease of analysis, these repsonses were plotted according to high (Figure 6.2A), mid (Figure 6.2B) or low (Figure 6.2C) expression level. Reassuringly, IL-8 showed the same trend of reduction in IL-1β JAM-C KD HUVECs as had been previously verified in Figure 6.1. However, very few differences were seen in most other expressed cytokines such as IL-15, CCL2, and G-CSF. Interestingly CCL1 seemed to indicate a reduction in levels in IL-1β stimulated JAM-C KD HUVECs in a similar manner to that observed for IL-8. Overall though, the cytokine profile of IL-1β stimulated control and JAM-C KD HUVECs remained very similar, with only IL-8 and CCL1 showing a decrease in secretion from JAM-C KD HUVECs.

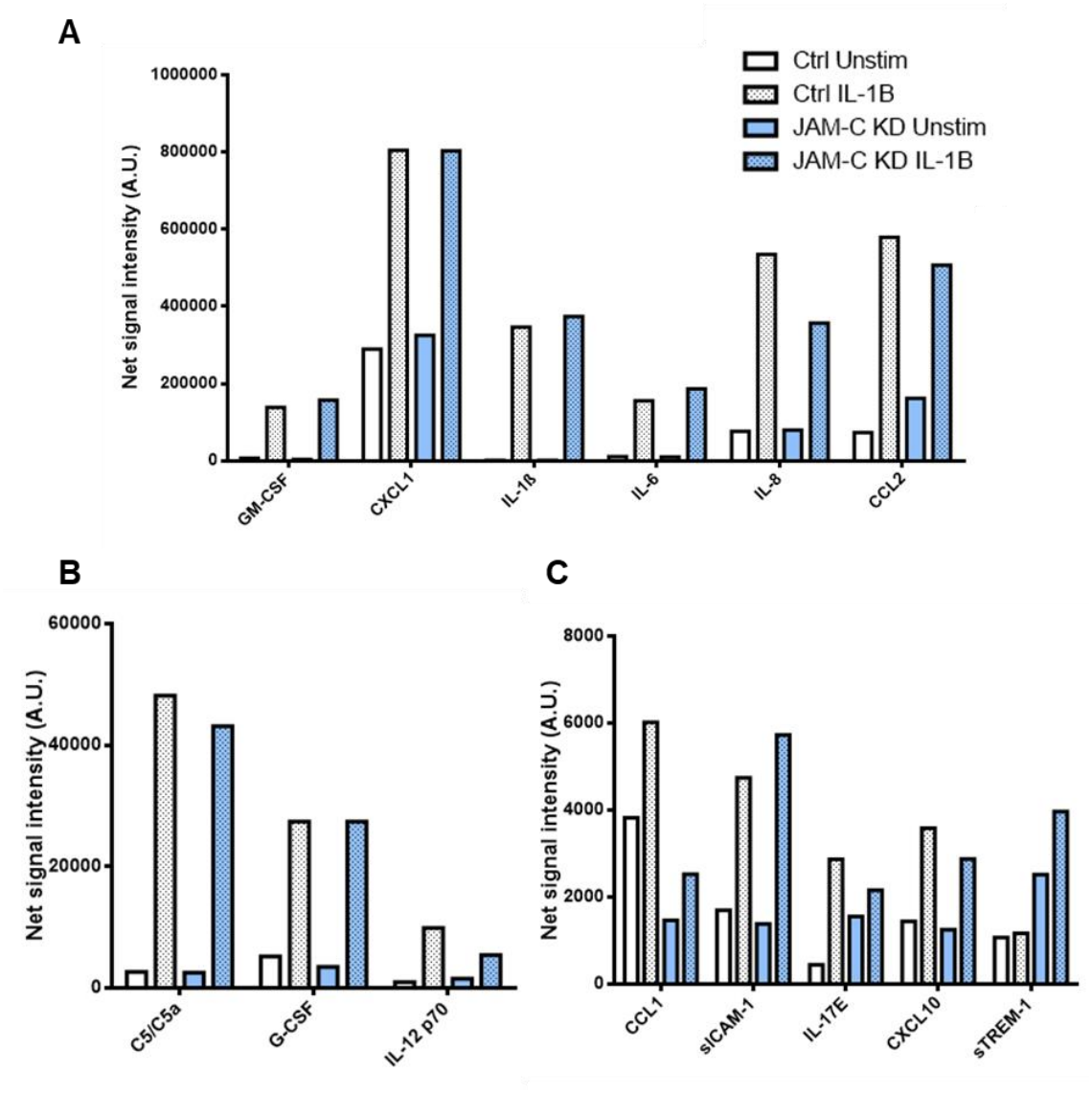

Figure 6.2. Cytokine array analysis of secreted mediators from JAM-C KD HUVECs.
HUVECs were transfected with either control or JAM-C siRNA and cultured for 72h to reach confluence. Cells were then either stimulated with IL-1β (1 ng/ml) for 4h or left unstimulated. Cell culture medium was collected from three independent experiments, pooled and then subjected to cytokine array analysis. Samples were added to Human Cytokine Array Kit (R&D systems) and analysed according to the manufacturer's instructions. Membranes were scanned using the Odyssey system (LI-COR). Levels of individual cytokines were expressed as net signal intensity and plotted according to high (A), mid (B) or low (C) expression.

6.3.2 Mouse model of EC JAM-C deficiency

To further investigate the role of EC JAM-C in EC inflammatory mediator generation, a mouse model of EC JAM-C deficiency was used. Here, mice homozygous for a floxed JAM-C allele were crossed with Tie2Cre transgenic mice in which expression of Cre recombinase is driven by the endothelial specific Tie2 promoter. As such, this results in the deletion of a portion of the JAM-C allele specifically in ECs, thereby generating an EC JAM-C KO mouse. Littermate controls (EC JAM-C WT) were Tie2Cre negative JAM-C floxed mice.

To assess the level of JAM-C expression in ECs in this model, cremaster muscles from EC JAM-C KD and littermate control (WT) mice were immunostained for JAM-C, PECAM-1 and VE-Cadherin (Figure 6.3A). Post-capillary venules from both EC JAM-C WT and KO mice showed similar levels and distribution of VE-Cadherin and PECAM-1 immunostaining, with most expression of these markers localised to the junctional compartment. Junctional JAM-C was also clearly visible in EC JAM-C WT mice, adopting a similar pattern of expression to VE-Cadherin and PECAM-1. Some non-junctional cell surface JAM-C was also observed. Contrastingly, the post-capillary venules of EC JAM-C KO mice showed markedly reduced junctional JAM-C expression, with only some immunostaining found in a few cells of venular segments. This was suggestive of a good level genetic deficiency of JAM-C (about 50-60%), a result that is in accordance with other reports of Tie2Cre recombinase efficiency (Ohashi et al., 2010, Kisanuki et al., 2001). However, it should be noted here the findings that Tie2 is also expressed in endothelial cells and so use of this model as to generate endothelial specific mouse knockouts is not strictly true (Tang et al., 2010b). Indeed, in this study it was found that nearly all lineages of hematopoietic precursors (including lymphocytes, monocytes and granulocytes) were of Tie2 origin. While expression of JAM-C has not been observed in mouse leukocyte populations, one should still be cautious when analysing this as a strictly endothelial specific JAM-C KO model.

Quantification of the level of junctional JAM-C deficiency in this model was performed by creating an artificial surface on junctional VE-Cadherin using IMARIS software (Bitplane). The mean fluorescence intensity of junctional JAM-C and PECAM-1 was then calculated for that surface and is shown in Figure 6.3B. Analysis of JAM-C expression revealed a 50% reduction in junctional JAM-C, while PECAM-1 was

unaffected. This is in agreement with previous published findings from our laboratory (Woodfin et al., 2011) that observed a 40-60% KO efficiency in this model.

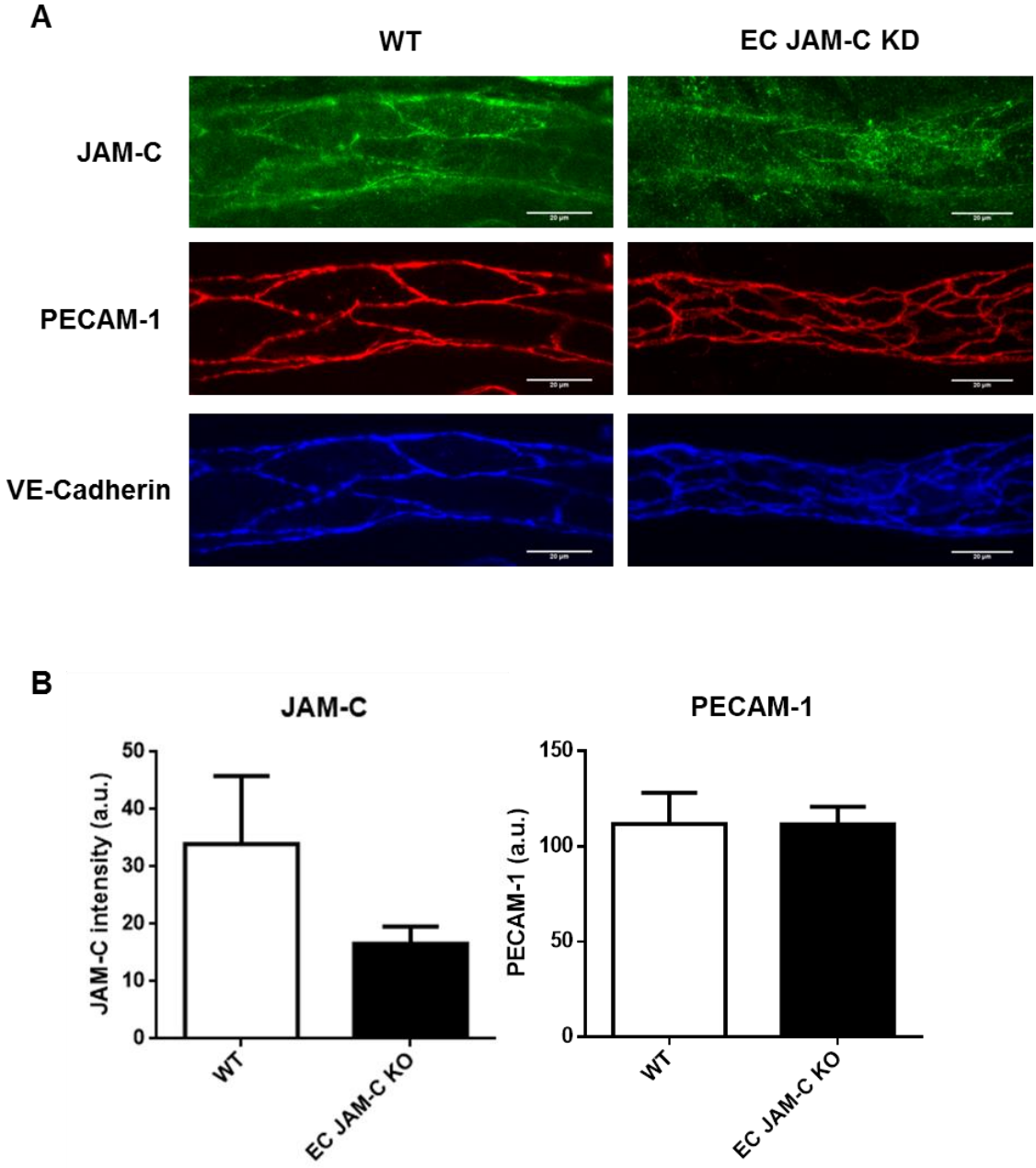

Figure 6.3. Immunofluorescence staining of EC JAM-C in cremaster muscle venules.
(A) Cremaster muscles were isolated from EC JAM-C KO and littermate control WT mice and immunostained *ex vivo* for JAM-C (green) PECAM-1 (red) and VE-Cadherin (blue). Images are representative from n=3 mice per group and 4-7 vessels per mouse.
(B) Fluorescence intensity of JAM-C and PECAM-1 at EC junctions was quantified using IMARIS Bitplane software. Data are displayed as mean ± SEM from n=3 mice per group.

6.3.3 Establishment of a mouse neutrophil depletion protocol

In an acute inflammatory reaction, neutrophils are the primary responding cells that act to counter the offending stimulus and also to release a range of cytokines, chemokines and other proinflammatory molecules that facilitate the recruitment of additional immune cells. As such, when studying the role of EC JAM-C in pro-inflammatory mediator generation *in vivo*, neutrophil-derived mediators could contribute to the overall results. Thus, to eliminate the potential role of neutrophils, and to gain a better insight into the release of mediators from ECs, control and JAM-C KO mice were depleted of their circulating neutrophils prior to investigating cytokine/chemokine responses *in vivo*.

To achieve this, the well documented method of GR1 mediated neutrophil depletion was employed. Specifically, mice were injected with low dose (25 µg) anti-GR-1 antibody for three consecutive days (Voisin et al., 2009). This antibody binds to GR1 expressed on neutrophils to target them for removal through the complement/macrophage pathway. GR1 is also expressed to some extent on monocytes and so it was hypothesised that the lower dose treatment regime would limit the impact of the protocol on circulating monocytes.

Following three days of depletion, blood samples were taken and analysed for total leukocytes ($CD45^+$), neutrophils ($Ly6G^+$) and monocytes ($CD115^+$) by FACS (Figure 6.4). As can be seen in the FACS plots in Figure 6.4A, non-depleted mice showed both a population of $Ly6G^+$ neutrophils (left panel) and $CD115^+$ monocytes (right panel). In comparison, mice treated with anti-GR1 antibody showed a complete depletion of circulating neutrophils, while the monocyte population was unaffected in these mice. Quantification of this depletion is shown in Figure 6.4B, where neutrophils and monocytes were represented as percentage of total $CD45^+$ cells. This analysis revealed that non-depleted mice had on average 9.1% neutrophils and 4.2% monocytes. By contrast, GR1 depleted mice had a greater than 98% depletion of circulating neutrophils with a small but non-significant increase in the average monocyte count (6.1%). This increase is likely due to the loss of the 9.1% of circulating neutrophils.

This method of neutrophil depletion was obtained from well-established protocols, in which a number of reports have compared anti-GR1 and IgG control antibodies to

monitor neutrophil responses. However, this model required only the depletion of neutrophils to obtain a clearer picture of EC responses *in vivo* and as such, mice treated with IgG control were not used.

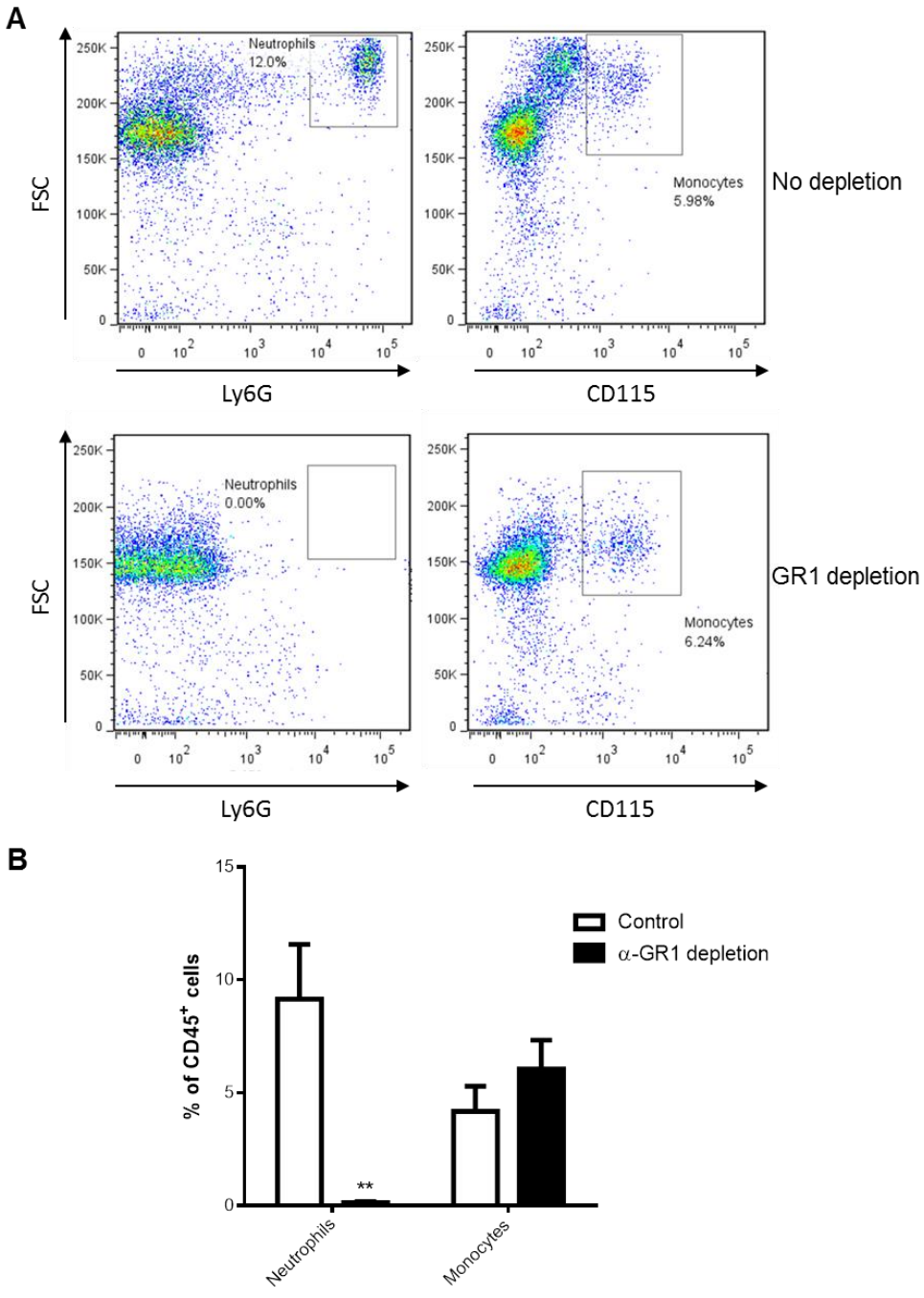

Figure 6.4. GR-1 mediated depletion of circulating mouse neutrophils
(A) Neutrophil depletion of EC JAM-C KO and littermate control (WT) mice was induced by intraperitoneal injection of anti-GR1 antibody at 25µg/day for 3 consecutive days. Blood samples were collected on the fourth day and analysed by FACS for levels of blood neutrophils ($Ly6G^+$, $CD115^{low}$) and monocytes ($Ly6G^-$, $CD115^+$).
(B) Quantification of neutrophil depletion by FACS. Levels of circulating neutrophils and monocytes in GR1 depleted and non-depleted mice were calculated as percentage of $CD45^+$ cells. Data are representative of n=5 independent experiments and 3-8 mice per group.

Statistical significance was calculated using two-way ANOVA with Sidak correction for multiple comparisons. Data represented as mean ± SEM, ** = p<0.01.

6.3.4 Impact of EC JAM-C deficiency on tissue mediator generation

To investigate the role of EC JAM-C in generating inflammatory mediators in tissue *in vivo*, neutrophil depleted EC JAM-C KO and WT mice were injected with IL-1β intrascrotally to induce cremaster muscle inflammation. After 4 hours, cremasters muscles were dissected out, homogenised and assessed for mediator generation using a mouse XL Proteome Profiler^{TM} cytokine array. Samples from three mice per group were pooled and assayed using this method. In the same manner as Figure 6.2, IRDye-streptavidin was used to enable accurate quantification of each cytokine. All signal intensities were normalised to total amount of protein added to each membrane, and signal intensities lower than 1000 A.U. were deemed as below the range for reliable detection.

Using this method enabled the analysis of over 100 different molecules, not all of which could be graphically displayed in Figure 6.5. Candidate molecules were selected in a similar manner to that for Figure 6.2, where molecules that showed notable upregulation in response to IL-1β in WT mice were analysed.

As shown in Figure 6.5, the majority of the molecules that showed a response to inflammation were chemokines, many of which showed interesting differences between WT and EC JAM-C KO mice following IL-1β stimulation. Chemokines such as CCL2 (MCP1) and CXCL1 (KC) were elevated in response to IL-1β in both groups, however there seemed to be a partial reduction in the levels of both in EC JAM-C KO mice. Other chemokines, such as CCL12 (6Ckine) and CXCL5 (LIX) showed a complete failure to respond to IL-1β in EC JAM-C deficient mice. Overall, these results indicated that reduced expression of EC JAM-C can impact tissue chemokine generation.

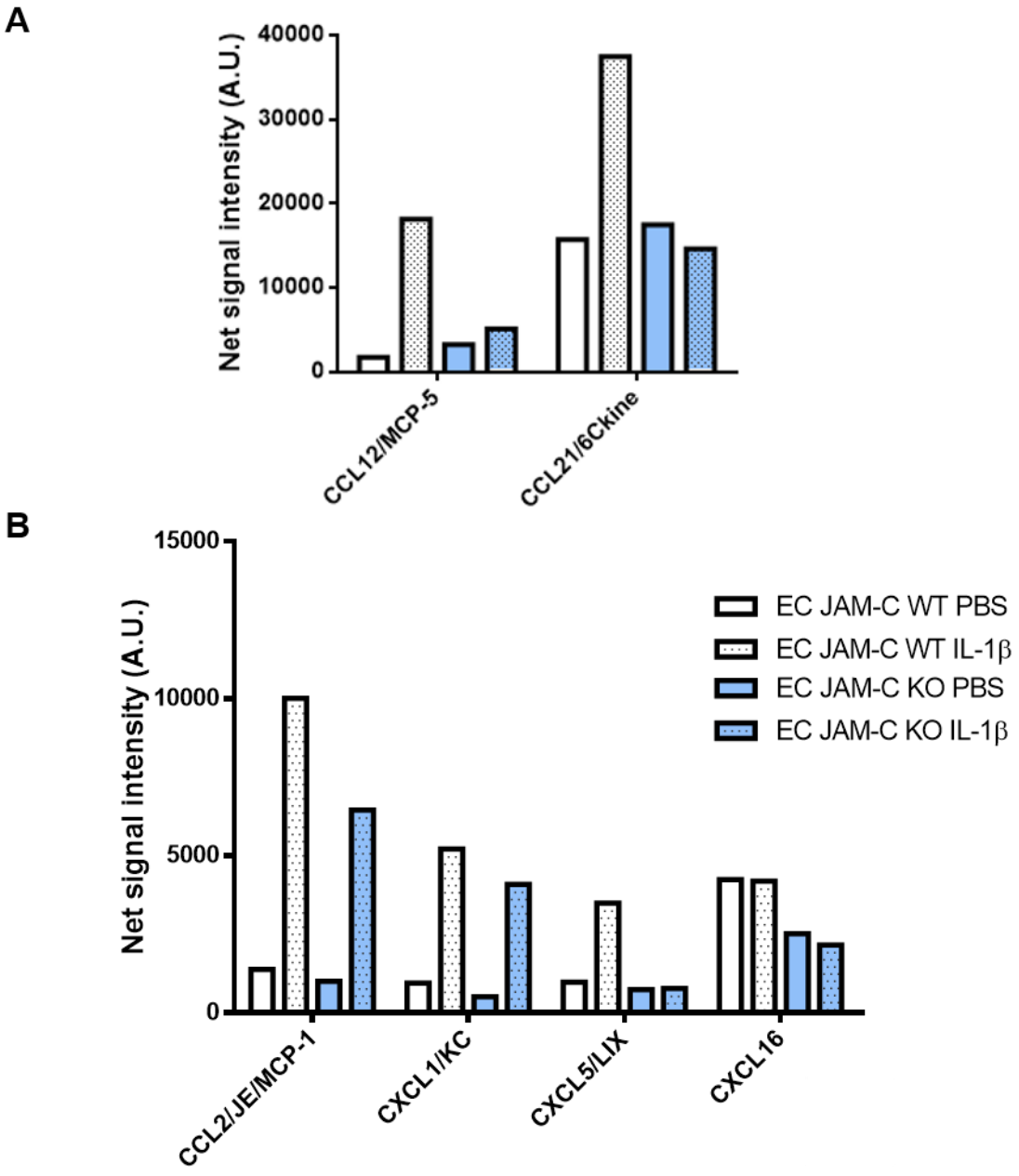

Figure 6.5. Cytokine array analysis of IL-1β-induced cremaster muscle chemokine generation.

Mouse cremaster muscles of EC JAM-C KO and littermate control (WT) mice were stimulated by intrascrotal injection of IL-1β (50 ng in 400 µl PBS) or PBS alone as control. Cremasters were exteriorised, dissected out and 162homogenised for analysis of chemokine generation. N=3 cremasters from each group were pooled and analysed using a Mouse XL Cytokine Array kit. Levels of each cytokine/chemokine were expressed as net signal intensity and plotted according to high (A) or low (B) expression.

To further investigate these findings, a number of chemokines were selected for validation by ELISA (Figure 6.6). The findings here largely mirrored that from the cytokine array. Tissue KC levels were significantly increase in both WT and EC JAM-C KO mice following IL-1β stimulation (Figure 6.6A). CXCL1 levels in EC JAM-C KO mice were slightly reduced (≈20%) compared to WT mice, but this was not statistically significant ($p=0.19$). CCL2 was also significantly increased in both WT and KO mice following IL-1β stimulation, but unlike CXCL1 no difference between the two mouse groups was noted.

CXCL5 and CCL5 were generated at much lower levels than KC and MCP1 following IL-1β stimulation. Nevertheless, CXCL5 showed a 2.5 fold increase in tissue levels following IL-1β stimulation in WT mice, though this was variable and did not reach significance in this study ($p=0.16$). EC JAM-C KD mice showed markedly less CXCL5 following IL-1β stimulation, about 50% of that observed in WT mice, but again this was not statistically significant due to varibility ($p=0.28$). CCL5 was significantly increased in WT mice following IL-1β stimulation and this increase was not observed in EC JAM-C KO mice. In fact, CCL5 levels in these mice were the same for both PBS and IL-1β stimulation. This resulted in a significant reduction in CCL5 levels in EC JAM-C KO mice as compared to WT mice post IL-1β stimulation.

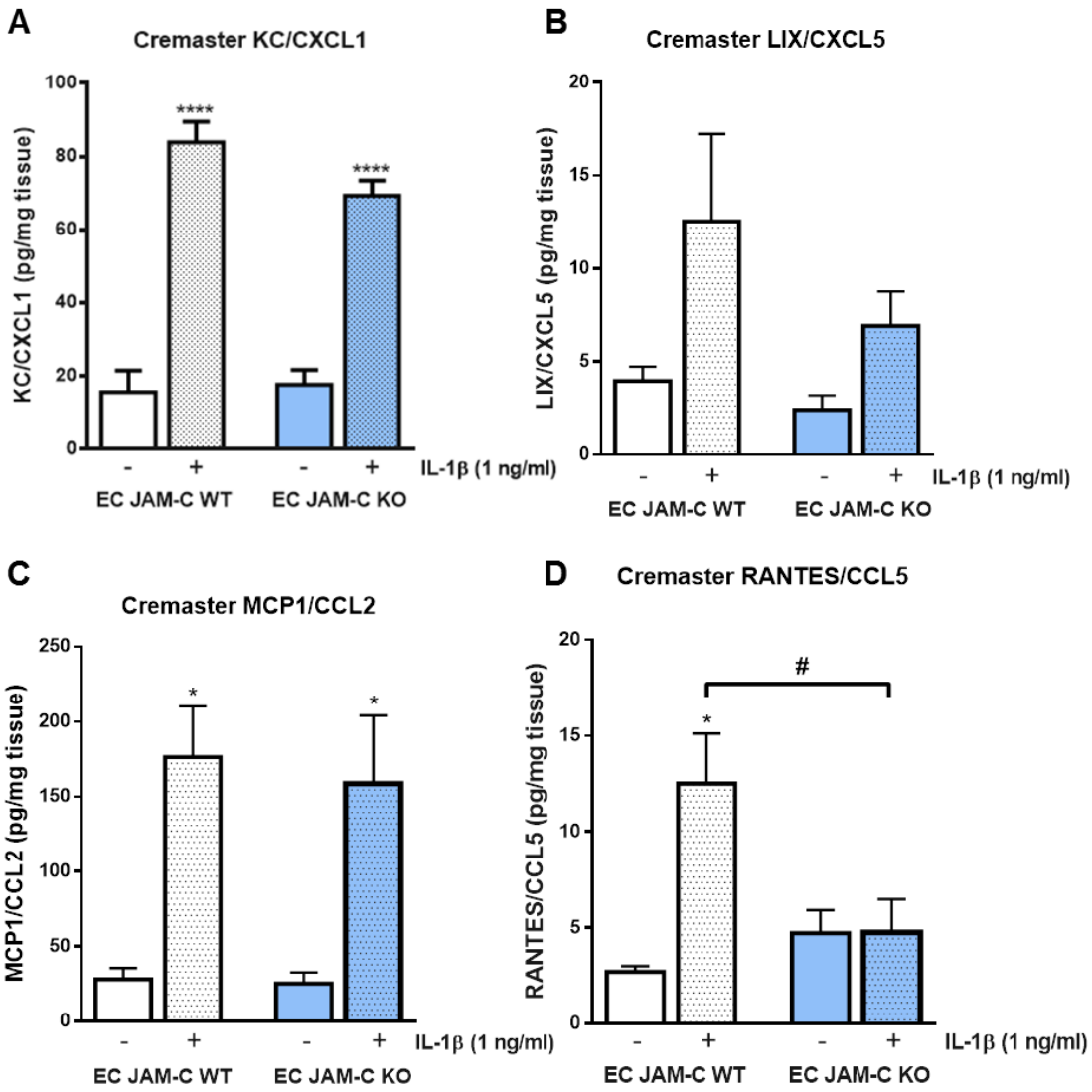

Figure 6.6. Analysis of chemokine levels in IL-1β-stimulated cremaster muscles as quantified by ELISA.

Mouse cremaster muscles of EC JAM-C KO and littermate control (WT) mice were stimulated by intrascrotal injection of IL-1β (50 ng in 400 µl PBS) or PBS alone as control. Cremaster muscles were exteriorised, dissected out and homogenised for ELISA analysis of CXCL1 (A), CXCL5 (B), CCL2 (C) and CCL5 (D) generation. Data represent mean ± SEM of 6-8 mice per group. Statistical significance determined by one-way ANOVA, * = $p<0.05$, **** = $p<0.0001$ compared to WT PBS. # = $p<0.05$ compared to WT IL-1β.

6.3.5 Local administration of IL-1β increased circulating chemokine levels

As previously stated, ECs are key generators of chemokines following inflammatory stimulation, a process crucial for the recruitment of leukocytes. Having established that disrupted JAM-C expression in ECs impacts tissue chemokine generation, the plasma chemokine profile of these mice following local IL-1β stimulation was also investigated. Cremaster inflammation was induced in the same manner as previously detailed, by intrascrotal injection of IL-1β into neutrophil depleted WT and EC JAM-C KD deficient mice for 4 hours, upon which blood was collected and harvested for plasma and analysis of chemokine content by ELISA (Figure 6.7).

The same four chemokines detailed in Figure 6.6 were analysed for plasma levels. Local IL-1β caused a significant increase in circulating plasma levels of CXCL1 (Figure 6.7A) in EC JAM-C WT mice compared to PBS controls. By contrast, EC JAM-C KO mice showed a much smaller increase in CXCL1 post IL-1β stimulation, about 50% of that seen in WT mice. This difference did not reach statistical significance at this time due to low n numbers ($p=0.11$, $n=3-4$). In a similar manner, CCL2 levels were also signigicantly increased post IL-1β stimulation in WT mice, whereas in EC JAM-C KO mice no such upregulation was observed in IL-1β treated mice ($p=0.069$ $n=3-4$).

CXCL5 plasma levels showed a trend to increase post IL-1β stimulation in WT mice, though this was variable and not significant. Nevertheless, the same trend seen for MCP1 was also observed here, with no such signal being present in the EC JAM-C KO mice. By contrast, plasma CCL5 levels were much lower in this model following IL-1β stimulation. A modest increase was seen in WT mice following IL-1β stimulation, with a slight decrease seen in EC JAM-C KD mice. The low levels of CCL5, and the noted variability in response, make it hard to draw any conclusions regarding this chemokine.

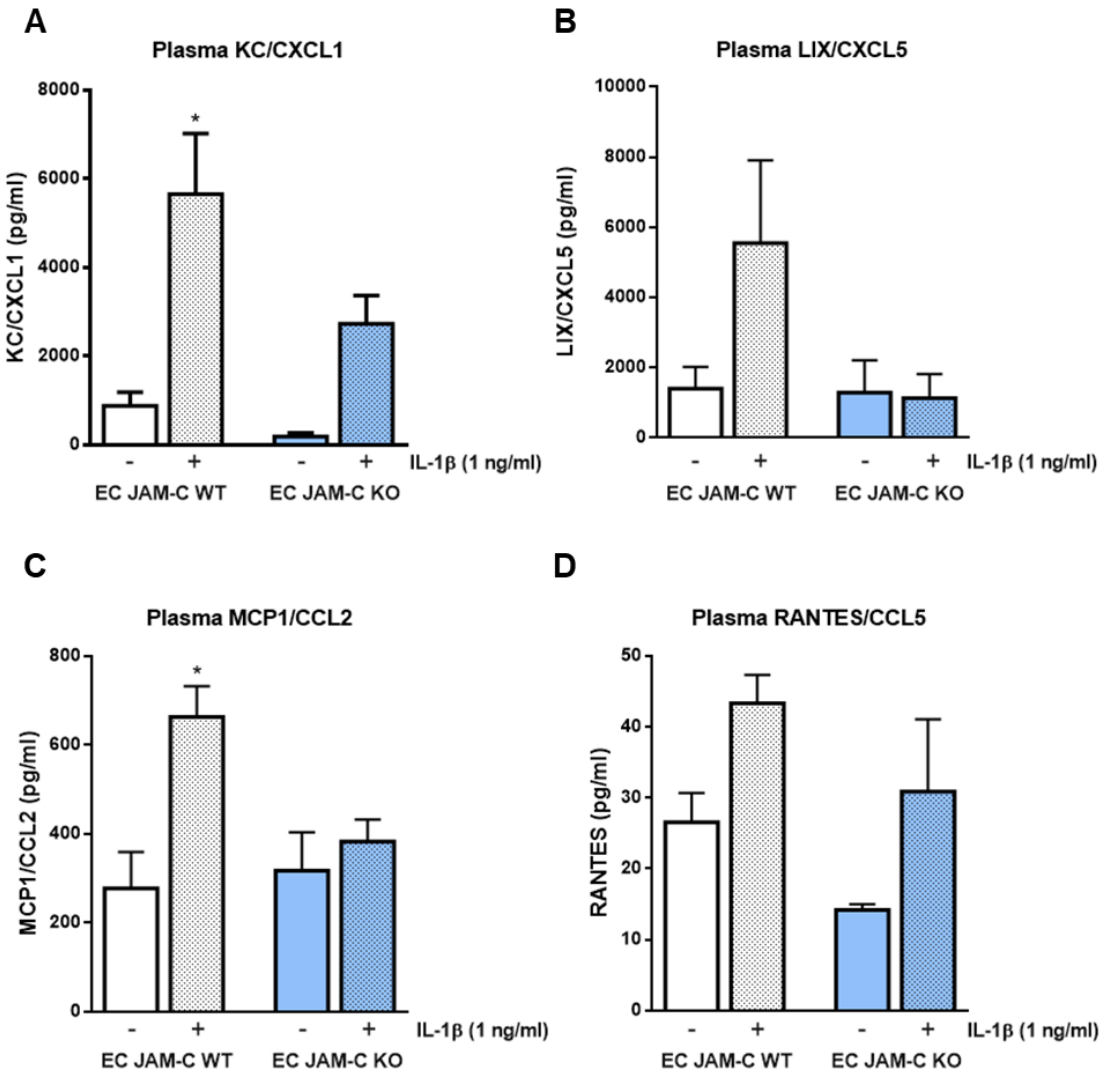

Figure 6.7. Analysis of plasma chemokine levels post-IL-1β stimulation of cremaster muscles. Mouse cremaster muscles of EC JAM-C KO and littermate control (WT) mice were stimulated by intrascrotal injection of IL-1β (50 ng in 400 µl PBS) or PBS alone as control. After 4h, blood was harvested and spun down to collect plasma for analysis of CXCL1 (A), CXCL5 (B), CCL2 (C) and CCL5 (D) generation. Data represent mean ± SEM of 2-4 mice per group. Statistical significance determined by one-way ANOVA, * = $p<0.05$ compared to EC JAM-C WT PBS.

6.4 Discussion

It has been well established by our laboratory that disrupted expression of EC JAM-C leads to increased frequency of disrupted neutrophil TEM *in vivo* following inflammatory stimulations such as that induced by local IL-1β (Woodfin et al., 2011). Generation of chemokines and the subsequent formation of chemokine gradients following this stimulation are crucial for guiding effective leukocyte recruitment. ECs are well known to produce a wide range of cytokines, chemokines and other inflammatory mediators in response to proinflammatory stimuli such as IL-1β, hence it was hypothesised that disrupted generation of mediators by JAM-C deficient ECs could provide a potential mechanism for aberrant neutrophil trafficking that is observed in EC JAM-C deficient mice.

While much is known about how ECs generate and secrete chemokines, little is known about how EC junctional molecules may regulate this process. It has previously been shown that fibroblast expressed JAM-C is important for controlling chemokine generation in lymph nodes *in vivo* (Frontera et al., 2011), further strengthening our hypothesis that EC expressed JAM-C may function in a similar manner. As such, the results in this chapter investigated the role of EC JAM-C in this response, utilising both the established *in vitro* model of JAM-C KD HUVECs and also an EC JAM-C KO mouse model.

6.4.1 Loss of JAM-C reduces IL-8 secretion from cultured ECs

Initial studies focussed on using the model of JAM-C KD HUVECs that was established in Chapter 3. As subsequently demonstrated in Chapter 5, JAM-C KD HUVECs showed no difference in gene expression of the proto-typical EC response genes to IL-1β; *ICAM1, CXCL1, IL8, CCL2* etc. This chapter extended this work to investigate the protein levels of some of those molecules in JAM-C KD HUVECs, particularly the chemokines IL-8 and CXCL1. In this context, secreted IL-8 levels were found to be significantly lower in JAM-C KD HUVECs. IL-8 is important for directing neutrophil recruitment in humans, and as such reduced secretion could impact on neutrophil transmigration (Godaly et al., 1997, Hammond et al., 1995). Follow up studies could monitor the transmigration of neutrophils over control and JAM-C KD HUVEC monolayers that have been

stimulated with IL-1β, so as to assess the functional impact of this reduced IL-8 secretion in the latter. With regards to other cytokines and chemokines, the secretion profile of IL-1β JAM-C KD HUVECs was very similar to that of control HUVECs when analysed by cytokine array, suggesting that in this model disrupted expression of JAM-C has a relatively selective impact upon IL-8 secretion. It is important here to note however that HUVECs are macrovascular ECs, and as such it is important to extend this work to a microvascular EC culture models. Ongoing work in the lab is currently aimed at analysing primary ECs isolated from the lungs of EC JAM-C KO mice with respect to cytokine/chemokine responses to IL-1β.

6.4.2 EC JAM-C regulates tissue chemokine production and secretion *in vivo*

As a means to investigate the role of EC JAM-C in chemokine production *in vivo*, neutrophil depleted mice were subjected to local IL-1β stimulation of the cremaster muscle. In this way, removal of circulating neutrophils enabled a clearer picture of EC chemokine signatures to be obtained in EC JAM-C KD mice. Cytokine array and ELISA analysis revealed that a number of tissue chemokines were present at reduced levels in inflamed tissues of EC JAM-C KD mice. The neutrophil chemoattractants and functional mouse homologs of human IL-8, CXCL1 and CXCL5 (Hol et al., 2010, Smith et al., 2008), were both partially reduced. Functionally, this could have an impact on total neutrophil recruitment and transmigration in response to IL-1β. Indeed, it has been shown that mice treated with a JAM-C blocking antibody exhibited a 33% reduction in transmigrated neutrophils in response to IL-1β, using the same cremaster inflammation model (Woodfin et al., 2011). As such, it is conceivable therefore that reduced tissue production of these neutrophil chemoattractants in conditions of disrupted or reduced expression of EC JAM-C could cause the reduction in total neutrophil extravasation that was observed in this model.

In addition, chemokines such as CCL21 and CCL5 were shown not to be upregulated in EC JAM-C KD mice in response to IL-1β stimulation, significantly in the case of CCL5. The reduction in CCL21 production is similar to those findings reported in fibroblast reticular cells (Frontera et al., 2011), suggesting JAM-C may be regulating CCL21 production through a similar mechanism in fibroblasts and ECs. Given that CCL5 and

CCL21 are both important T cell chemoattractants (Christopherson et al., 2003, Schall et al., 1990), it would be important to investigate T cell recruitment in this model.

The chemokine levels analysed are representative of the whole tissue environment. As such, many different cell types can and will respond to the IL-1β stimulation and contribute to the chemokine microenvironment that is created. It is intriguing therefore that loss of JAM-C from ECs specifically causes this striking phenotype across the tissue as a whole. While ECs might be directly responsible for the reduced levels of some of these chemokines (e.g. CXCL1, CXCL5), the loss of JAM-C from ECs could conceivably have a paracrine effect on the surrounding tissue cells, thus resulting in reduced production of a number of chemokines and inflammatory mediators.

As well as generation of chemokines in the tissue, secretion of chemokines into the lumen of blood vessels can impact directional migration of leukocytes (Speyer and Ward, 2011). As such, the plasma chemokine levels following local cremaster IL-1β were also investigated in this model using both WT and EC JAM-C deficient mice. Collectively, the results demonstrated that chemokine secretion from ECs was considerably reduced under conditions of EC JAM-C deficiency. In particular, CXCL1 plasma levels were reduced by ≈50% in EC JAM-C KD mice, suggesting a defect in secretion of CXCL1 from ECs with reduced JAM-C expression. This could disrupt the CXCL1 chemokine gradient that is important for neutrophil TEM and as such could have two impacts. Firstly, it could contribute to the reduced number of infiltrating neutrophils that has already been reported using the same model (Woodfin et al., 2011). Secondly, it could lead to disrupted chemokine gradients such that disrupted modes of neutrophil TEM, particularly rTEM, are induced.

In this context, it is also important to note the findings of reduced IL-8 secretion from JAM-C KD HUVECs earlier in this chapter, given that this is the functional human equivalent of mouse CXCL1. Given the importance of these chemokines in neutrophil recruitment, it is possible that there exists a common mechanism through which JAM-C regulates the secretion of key chemokines from ECs both *in vitro* and *in vivo*.

Interestingly, CCL2 levels were also not elevated by IL-1β stimulation in EC JAM-C KD mice. CCL2 is a key chemoattractant for monocytes and as such this suggests loss of EC JAM-C could also impact monocyte recruitment in response to IL-1β. Indeed, it is well

established that EC JAM-C is important for directing monocyte TEM. Studies have shown that blockade of JAM-C reduces monocyte infiltration and also increases monocyte rTEM *in vitro* and *in vivo* (Bradfield et al., 2016, Bradfield et al., 2007).

It is easy to assume here that increased levels of plasma chemokine observed post-IL-1β stimulation is contributed to mostly by ECs, especially considering they produce large quantities of both CXCL1 and CCL2 in response to IL-1β (Vernier et al., 1996). At this stage though, one cannot rule out the possibility that chemokines derived from other cell types, such as tissue resident macrophages, also contribute to plasma levels of these chemokines, which are then transported across the endothelium by ECs themselves. Indeed, it is well established that ECs are able to transport chemokines from basolateral to apical surfaces (Mordelet et al., 2007, Pruenster et al., 2009) and as such, disrupted expression of JAM-C could also impact this chemokine transport.

The results of this chapter highlight the importance of EC JAM-C in regulating chemokine production and secretion, particularly in an *in vivo* setting. These are novel findings, providing the first evidence that an EC junctional molecule can regulate responses to inflammation by controlling chemokine generation and secretion from ECs. In addition, it adds a new role for JAM-C in regulating EC biology beyond those already reported for angiogenesis and leukocyte trafficking. At this point it is pertinent to speculate on the specificity of this phenomenon to JAM-C, or whether this regulation of chemokine secretion is due to a global instability of EC junctions following loss of JAM-C. To address this important point, future works should investigate the potential role of additional junctional molecules, such as JAM-A and VE-Cadherin, in regulation of chemokine generation and secretion.

6.4.3 Key findings

- JAM-C KD HUVECs secrete significantly less IL-8 than control HUVECs following IL-1β stimulation.
- No other major changes in cytokine or chemokine responses were observed in IL-1β-stimulated JAM-C KD HUVECs.
- EC JAM-C KO mice have reduced tissue levels of a number of chemokines post IL-1β stimulation, notably CCL5, CXCL1 and CXCL5.

- Local IL-1β stimulation of EC JAM-C KO mice results in markedly lower plasma levels of chemokines CXCL1, CCL2 and CXCL5 as compared to responses noted in littermate WT controls.

7 General Discussion

7.1 Project overview

The tight junction adhesion molecule JAM-C, expressed in a range of cell types and tissues, has been shown to be important in regulating endothelial and vascular processes such as angiogenesis, permeability and leukocyte transmigration (Lamagna et al., 2005a, Orlova et al., 2006, Rabquer et al., 2010, Scheiermann et al., 2009, Woodfin et al., 2011). However, the cellular roles of JAM-C within ECs remain poorly understood. In particular, the mechanism behind the phenomenon of neutrophil rTEM that occurs under conditions of disrupted EC JAM-C expression (Colom et al., 2015, Woodfin et al., 2011) is not known. As such, this project sought to identify novel cellular functions of JAM-C in ECs and more importantly how this might give insight into the JAM-C directed endothelial processes. The findings of this work have demonstrated a number of novel findings that contribute to our understanding of the role of JAM-C in EC functions:

- JAM-C deficient ECs exhibit increased autophagy under basal conditions.
- JAM-C deficient ECs show increased pro-inflammatory gene expression under basal conditions.
- EC JAM-C expression regulates semaphorin gene expression following IL-1β stimulation *in vitro*.
- EC JAM-C expression is necessary for maintaining plasma chemokine levels *in vivo*.

7.2 *In vitro* KD of JAM-C enabled the functional study of JAM-C in EC biology

The inherent complexity in using *in vivo* models to study cellular functions of a specific molecule dictated the need for a simplified model of JAM-C deficiency in ECs. As such, transfection of cultured HUVECs with JAM-C specific siRNA was utilised to transiently KD JAM-C *in vitro*. Western Blot and immunofluorescence analysis of these HUVECs confirmed a significant KD of JAM-C total protein which was also detected at the junctional compartment of confluent HUVECs. Furthermore, this KD was specific to JAM-C, with expression of other EC junctional molecules such as JAM-A and VE-

Cadherin unaffected by transfection with JAM-C siRNA. Of course, the expression of other junctional markers should also be investigated under these conditions, especially ZO-1 which is a known binding partner of JAM-C (Ebnet, 2003). Investigations are currently being undertaken in the lab into further analysing the junctional molecule expression in both macrovascular (HUVEC) and microvascular (HDMEC and MLEC) ECs deficient in JAM-C expression.

Having established a reliable and robust level of JAM-C KD in HUVECs, these were assessed for basic cellular properties such as proliferation and cell death. Use of siRNA for gene silencing can have some off-target activity that could lead to such unwanted toxicities on the cells. We purposefully used a pool of two siRNA sequences to target JAM-C taken from published research (Li et al., 2009) that target two distinct coding regions of the JAM-C transcript. Initially, the two siRNAs were tested individually, but were then used in combination and in this way, it enabled them to be used in lower individual concentrations. This approach was necessary to help avoid unwanted off-target and non-specific effects of the siRNAs. JAM-C KD HUVECs showed no difference in proliferative capacity when compared to control HUVECs, nor did they exhibit increased cell death by apoptosis or necrosis. This enabled us to use this model for further investigations into the cellular function of JAM-C in ECs.

7.3 JAM-C KD ECs exhibit increased autophagy *in vitro*

Using the aforementioned system, initial investigations into the impact of JAM-C loss on EC cellular functions focussed on the basal characteristics of these cells. Interestingly, JAM-C deficient ECs were found to exhibit significantly higher levels of LC3-II than their control counterparts under basal growth conditions. Furthermore, this increase in LC3-II was abrogated by treatment with the pan-PI3K inhibitor 3-MA, indicating that the canonical pathway that leads to the induction of autophagy is increased in JAM-KD HUVECs. This is the first demonstration that an endothelial tight junction molecule can modulate such a cellular process. Importantly, these findings are consistent with previous unpublished works from our laboratory (Catherine Pickworth) which have shown that EC JAM-C deficient mice also exhibit increased EC LC3 positive vesicles under basal conditions.

Classically, autophagy is a process used by cells to turnover defunct proteins and organelles to provide the cell with recycled nutrients in times of cellular stress (e.g. starvation, hypoxia). It has also been shown to be increased by numerous other cellular stressors (e.g. inflammation, shear stress). As such, our data suggests that loss of JAM-C could represent a destabilisation of EC junctions that might in turn induce a stress response in ECs, resulting in the upregulation of autophagy.

This study has not explored the mechanism by which loss of JAM-C results in increased EC autophagy. However, some recent findings on the golgi stacking protein GRASP55 enable us to speculate on a potential mechanism. GRASP55 has been shown to interact with JAM-C in germ cells (Cartier-Michaud et al., 2017) and has also been shown to be necessary for secretion of IL-1β through an unconventional secretory autophagy pathway (Dupont et al., 2011). While an interaction between JAM-C and GRASP55 has not yet been identified in ECs, it is plausible to speculate that binding of JAM-C to GRASP55 sequesters GRASP55 at EC junctions. Under conditions of JAM-C deficiency, GRASP55 could be released enabling it to regulate the autophagy pathway.

7.4 JAM-C controls pro-inflammatory gene expression under basal conditions

To continue characterising JAM-C KD ECs, we performed genome wide expression analysis of these cells. Under basal conditions, the expression of a number of pro-inflammatory genes (e.g. *ICAM1, CXCL1, IL8 & VCAM1*) were increased in JAM-C KD HUVECs, suggestive of a primed or pro-inflammatory state of these cells. Indeed, the NFκB pathway was significantly upregulated in JAM-C KD HUVECs under basal conditions, a response that could potentially be responsible for the noted increase in expression of pro-inflammatory genes.

To date, there are no reports of JAM family members regulating EC gene expression. In fact, the literature is rather scarce on the role of any junctional molecules in regulating cellular gene expression responses. The TJ molecule ZO-1 is known to interact with the transcription factor ZONAB which is important for regulating gene expression in epithelial cells (Lima et al., 2010, Nie et al., 2009). Given the relative lack of knowledge of this area, the findings from this thesis are novel additions to the field. Ongoing

works are aimed at unravelling how JAM-C regulates pro-inflammatory gene expression in ECs and the functional consequences of this.

At this point it is pertinent to discuss these findings in relation to the observations of increased autophagy in JAM-C deficient ECs. Generally speaking, autophagy is an anti-inflammatory process, functioning to dampen aberrant inflammation and maintain cellular homeostasis under basal conditions. In particular, it has been shown that autophagy acts to negatively regulate the NFκB signalling pathway by increasing IKK protein degradation and hence prevent pro-inflammatory gene expression (Qing et al., 2006). It is intriguing therefore that JAM-C deficient ECs exhibit both increased autophagy and increased NFκB mediated pro-inflammatory gene expression. Why this is the case remains unclear, although it is possible that loss of EC JAM-C activates the NFκB pathway independently of IKK proteins.

While the gene expression analysis has identified a number of interesting avenues and pathways, there is potential for further interpretations to be made from this data set. Indeed, over 500 genes from the unstimulated comparison and nearly 1000 from the IL-1β stimulated comparison were defined as differentially regulated by JAM-C in ECs. As such, further network and pathway analysis could provide further insight into the role of JAM-C in EC functions beyond those already described in the literature.

7.5 JAM-C regulates semaphorin gene expression in ECs

Expansion of the gene expression analysis to JAM-C KD ECs stimulated with IL-1βs highlighted a number of interesting findings. Perhaps one of the most interesting was the differential expression of a number of genes in the semaphorin family. In particular, *SEMA4F* and *SEMA3G* expression was upregulated in JAM-C KD HUVECs following IL-1β stimulation. The semaphorin family of molecules were originally identified as axonal guidance molecules that regulate the development of the central nervous system. More recently however, there is growing evidence for roles for these molecules in functions of ECs, where they have been shown to regulate processes such as angiogenesis, vascular permeability and also leukocyte TEM (Sakurai et al., 2012, Hou et al., 2015, Morote-Garcia et al., 2012, Takamatsu et al., 2010). These findings

are the first to indicate that an EC junctional molecule can regulate the expression of semaphorin molecules.

How this increase in expression of semaphorins might relate to JAM-C-dependent is unknown. *SEMA3E*, has been shown to negatively regulate neutrophil migration (Movassagh et al., 2017) and was shown to be increased in expression in JAM-C KD HUVECs. As such, increased expression of this chemorepellent semaphorin could provide a link between loss of JAM-C and the increased frequency of neutrophil reverse migration in response to IL-1β stimulation that has been demonstrated by our lab (Woodfin et al., 2011). In addition, increased expression of these markers could provide insight into the mechanisms by which JAM-C regulates other endothelial processes, such as angiogenesis and permeability. A number of semaphorins are known to be either pro- or anti-angiogenic, or to modulate vascular permeability. For example, Semaphorin 3E is potently anti-angiogenic (Sakurai et al., 2010) and its expression is increased in this model, while it has previously been shown that blockade of JAM-C reduces angiogenesis *in vivo* (Lamagna et al., 2005a). As such, it is possible that these two findings are intrinsically linked, where increased semaphorin expression contributes to the mechanism through which JAM-C blockade inhibits angiogenesis (Lamagna et al., 2005a).

While the investigations into the relationship between JAM-C and semaphorin expression are at an early stage, they provide a number of exciting avenues for further work. The results detailed in this thesis only describe an increase in gene expression of these molecules and future works need to confirm protein levels of these markers, as well as investigating the functional impacts of this increased expression on leukocyte migration and angiogenesis using *in vivo* models.

7.6 JAM-C regulates chemokine secretion *in vivo*

One of the key aims of this project was to identify potential mechanisms by which loss of EC JAM-C results in an increased frequency of neutrophil rTEM, especially post IL-1β stimulation. As such, it was hypothesised that disrupted production of chemokines from ECs deficient in JAM-C might result in a disrupted chemokine gradient that could subsequently account for this phenomenon.

This part of the project was investigated mostly in an *in vivo* setting, taking advantage of EC specific JAM-C KO mice to investigate tissue and plasma chemokine levels following a local inflammatory stimulation. Neutrophil depleted mice were given an intrascrotal injection of IL-1β, following which cremaster muscles and plasma were analysed for IL-1β-induced chemokine production. On the whole, tissue chemokine levels remained largely unaffected by loss of EC JAM-C, with the exception of CCL5, which was not upregulated in EC JAM-C KO mice. As this chemokine is classically associated with the chemotaxis of T-cells (Kawai et al., 1999, Schall et al., 1990), this could highlight a potential defect in recruitment of T cells JAM-C is shed from ECs. Furthermore, this chemokine has also been shown to be chemotactic and activating for a number of other leukocyte sub-types, including neutrophils (Di Stefano et al., 2009), and as such could therefore also impact on their migration in this model also. Analysis of plasma chemokine levels revealed a distinctive change in EC JAM-C KO mice following a local IL-1β stimulation. In particular, chemokines such as CXCL1, CCL2 and CXCL5 were all reduced in the plasma of EC JAM-C KO mice. In concordance, JAM-C KD HUVECs showed significantly reduced secretion of IL-8 chemokine, the functional human homolog of mouse CXCL1. While this chemokine secretion defect has only been described here in response to IL-1β, additional works can investigate whether other inflammatory stimuli such as LPS and I/R injury have the same effect in in EC JAM-C KO mice and JAM-C KD ECs.

The results in Chapter 5 detailed that there was no difference in gene expression of many pro-inflammatory markers, including chemokines, in cultured JAM-C KD ECs. As such, this suggests that this reduction in chemokine levels exists purely at the protein level, and more specifically points towards a defect in secretory pathways. The mechanism behind this reduced secretion was not investigated in this project due to time constraints, but it could be hypothesised that increased EC autophagy, exhibited both *in vitro* and *in vivo* by JAM-C deficient ECs, could be pivotal to this process. Taking these findings together, it can be hypothesised that in JAM-C deficient ECs stimulated with IL-1β, chemokines are expressed by the cell, but may be abnormally trafficked to autophagosomes, where they might be degraded rather than secreted. Conversely, the increase in canonical autophagy might sequester autophagy proteins away from the pathway of unconventional secretory autophagy, therefore leading to the decreased

secretion phenotype that is observed. While unconventional secretory autophagy has so far only been described for the secretion of IL-1β and HMGB1 (Dupont et al., 2011), it is not inconceivable that chemokine secretion from ECs could also involve this pathway. Alternatively, this defective chemokine secretion could be in part due to disrupted polarisation of JAM-C deficient ECs. JAM-C is known to bind to the polarity protein partitioning defective 3 homolog (PAR3) and regulate cell polarity (Ebnet, 2003) and as such, disrupted polarity of JAM-C KD ECs could result in dysregulated polarity of protein secretion.

7.7 Future perspectives

7.7.1 Targeted KD of additional EC junctional molecules and comparison with EC JAM-C KD phenotype

Whilst this project has identified the role of JAM-C in regulating a number of cellular functions of ECs, a number of important works need to be done to confirm these findings. Of most importance is the comparison of the observed phenotypes in JAM-C KD ECs with ECs deficient in other EC junctional molecules, such as JAM-A, VE-Cadherin and PECAM-1. Such experiments would be aimed at confirming the specificity of the observed phenotypes to JAM-C, and more importantly to confirm that they are not due to global junctional instability. As such, evaluation of the key findings in JAM-A and/or VE-Cadherin KD ECs in terms of autophagy, gene expression and chemokine secretion are required.

In addition, the majority of the *in vitro* works in this project were undertaken in macrovascular ECs using HUVECs. Additional experiments on JAM-C KD microvascular ECs would further increase the understanding of the role of JAM-C in regulating EC functions in different vascular cell types. Such works could be undertaken using microvascular cells isolated from lungs of EC JAM-C KO mice, that could also help to reinforce ongoing associated *in vivo* works.

7.7.2 Investigation into the impact of increased pro-inflammatory gene expression under basal conditions

The results presented here showed an increase in expression of a number of pro-inflammatory molecules in JAM-C KD ECs, both at the mRNA and protein level, including molecules such as ICAM-1 and IL-8. This begs the question as to whether JAM-C deficient ECs might support increased rolling, adhesion, or even transmigration of leukocytes under basal conditions, thus providing a functional readout to these findings. This could be investigated in both an *in vitro* and *in vivo* setting. Human neutrophils and monocytes could be perfused over control and JAM-C KD HUVECs cultured in transwell plates, an assay that would enable the monitoring of rolling, adhesion and transmigration. In addition, brightfield IVM experiments could be used to monitor the rolling and adhesion of leukocytes in EC JAM-C KO mice, whilst confocal microscopy of whole mount tissues could be used to monitor leukocyte transmigration in unstimulated EC JAM-C KO mice.

In addition, it would be interesting to analyse the naïve circulating leukocyte numbers of EC JAM-C KO mice under unstimulated conditions. The increased expression of chemokines that was observed in JAM-C KD HUVECs could be translated to an effect on the level of circulating neutrophils and/or monocytes in EC JAM-C KO mice. Indeed, increased basal tissue expression of such chemokines such as CXCL1 and CCL2 might induce increased leukocyte mobilisation into the circulation. Analysis of this could be achieved through FACS analysis of whole blood from EC JAM-C KO mice and littermate controls to identify leukocyte subsets.

7.7.3 Physiological impact of increased EC autophagy in JAM-C deficient ECs

The data in this project has shown that JAM-C KD ECs have increased autophagy under basal conditions. The consequence of this increased autophagy on endothelial functions is yet to be identified and as such represents an important next step for this project. Work is currently ongoing to investigate the level of autophagy in JAM-C KD ECs following inflammatory stimulation, such as with IL-1β and LPS. This will be performed both *in vitro*, using the established JAM-C KD HUVEC model, and also *in vivo*, using EC JAM-C KO mice. In addition, it would also be useful to perform rescue-of-function experiments and investigate whether the overexpression of an siRNA

resistant or mouse JAM-C construct in JAM-C KD HUVECs restores the basal level of autophagy.

Following this, additional studies could be conducted using EC ATG5 KO mice, a model of autophagy deficiency in ECs. Such a mouse colony could be used to identify the role of autophagy in leukocyte migration, which could be conducted by brightfield and confocal IVM using the cremaster model of inflammation. As blockade of JAM-C with functional blocking antibodies achieves a similar increase in autophagy to that seen in EC JAM-C KO mice, this method could also be used to investigate whether abrogating autophagy when JAM-C is disrupted affects neutrophil rTEM phenotype in response to IL-1β stimulation.

7.7.4 Mechanism of reduced chemokine secretion and impact on neutrophil TEM

As discussed in section 7.6, the mechanism by which the reduced chemokine secretion from JAM-C deficient ECs occurs is not known. As such, future experiments could use the EC ATG5 KD mice to investigate chemokine secretion into the plasma following inflammatory stimulation. This could be confirmed by using ATG5 KD HUVECs and evaluating levels of secreted chemokines such as IL-8, which is known to be reduced from JAM-C KD HUVECs. Following this, a double KD of both JAM-C and ATG5 *in vitro* could be used to see if abrogating autophagy in JAM-C KD ECs restores the normal secretory phenotype. While this is difficult to replicate in an *in vivo* setting, one approach could be to use JAM-C blocking antibodies in EC ATG5 KO mice, thus enabling the investigation *in vivo* into whether reduced autophagy in ECs with disrupted JAM-C expression rescues the plasma levels of chemokines.

The effect of JAM-C KD on the polarised secretion phenotype of ECs could be investigated in an *in vitro* setting. Using a transwell system, JAM-C KD HUVECs and MLECs isolated from EC JAM-C KO mice could be assessed for apical and basolateral secretion of chemokines, to investigate whether depolarised secretion is responsible for decreased plasma chemokine levels in EC JAM-C KO mice.

On the other hand, the physiological impact of this reduced chemokine secretion *in vivo* needs to be addressed. In particular, investigations should be undertaken to identify whether the reduced plasma chemokine levels in EC JAM-C KO mice are

connected to the phenomenon of increased neutrophil rTEM that is observed in these mice. As such, experiments could be designed by which WT mice are given intrascrotal injection of IL-1β to induce inflammation and then analysed for neutrophil and/or monocyte transmigration events by confocal IVM. It would also be interesting to try to mimic the reduced plasma chemokine levels from EC JAM-C KO mice in WT mice. One approach could be to use blocking antibodies to KC and LIX that could be injected in low doses intravenously following IL-1β stimulation, in order to achieve a partial reduction in the circulating levels of these chemokines. Confocal IVM could then be used to assess leukocyte migration dynamics in this model.

7.8 Wider implications of this work

The aim of this project was to deepen our understanding of the role of JAM-C in EC biology, so that this can be translated to human conditions where JAM-C is known to be important. The mouse model of ischemia reperfusion, which results in disrupted and reduced EC JAM-C expression (Woodfin et al., 2011), can be clinically linked to many forms of major human trauma. Here the hypoxic environments created by the trauma affect tissues and organs is key in the pathogenesis of disease, such as stroke, myocardial infarction, or major traumatic events. It has been shown by our group that in such inflammatory reactions, cleavage of JAM-C by neutrophil elastase (NE) leads to reduced endothelial JAM-C expression (Colom et al., 2012) as well as increased soluble JAM-C in the plasma of mice, and subsequently an increase in reverse migrated neutrophils. In a similar manner, major trauma patients also exhibit increased serum levels of JAM-C. Increased frequency of neutrophil rTEM is associated with increased second organ injury, a phenomenon which occurs with high frequency in major trauma patients, where susceptibility to developing conditions such as acute respiratory distress syndrome (ARDS) not related to the original trauma are high (Bakowitz et al., 2012, De'Ath et al., 2012). As such, the findings presented in this thesis are crucial in unravelling the mechanisms by which such phenomenon occur and provide the groundwork for investigating the link between neutrophil rTEM and secondary organ injury. This work also opens up potential for new biomarkers in the pathogenesis of JAM-C related diseases, such as trauma, as described earlier. For example, JAM-C itself, or rather soluble levels of JAM-C, could also be a potential predictive biomarker

for disease severity in these patients. Cleavage of JAM-C by neutrophil elastase during neutrophil TEM increases circulating levels of sJAM-C in mice and correlates with distant organ injury. This concept which is currently being investigated in the lab, where serum samples of trauma patients with varying disease severities and distant organ injury are being analysed for sJAM-C.

JAM-C is also known to be important for the pathogenesis of other human conditions, such as Rheumatoid Arthritis, where JAM-C expressed on both the endothelium and synovial fibroblasts acts to recruit and retain leukocytes in the synovium, so progressing the state of this disease (Rabquer et al., 2008). As such, it has been postulated that targeting JAM-C in this model would be beneficial in preventing leukocyte retention. However, our findings here dictate that more considerations need to be taken before applying such methods as treatment. For example, the data in this thesis suggests that while targeting EC JAM-C expression could impact plasma chemokine levels, this may also be the mechanism by which increased neutrophil rTEM is brought about. As such, targeting of JAM-C in this model, while potentially limiting local leukocyte infiltration, might also have the unwanted adverse effect of increasing second organ injury as a result of increased reverse migrated neutrophils.

Atherosclerosis models have proposed a role for JAM-C in retention of monocytes in atherosclerotic plaques and that blockade of JAM-C reduces the number of atherogenic monocytes by increasing their rTEM out of the plaques (Bradfield et al., 2016). As such, JAM-C again provides an attractive target for treatment in this disease but considering our findings this should also be approached with caution. While targeting JAM-C in this model might achieve the desired effect of monocyte rTEM out of atherogenic plaques and so halting disease progression, such treatment might also potentially have adverse effects. Indeed, atherosclerotic patients are also likely to be at higher risk of events such as stroke and myocardial infarction, episodes in which a JAM-C targeted therapy could exacerbate the disease and increase likelihood of secondary organ inflammations such as ARDS.

7.9 Conclusions

In conclusion, this study undertook rigorous investigations into the cellular role of EC JAM-C, with the aim to identify potential mechanisms behind the functional consequences of its disrupted expression that can occur during various inflammatory situations. We have identified a novel role for JAM-C in regulating both EC autophagy and EC pro-inflammatory gene expression under basal conditions. Furthermore, we have also identified a new relationship between the level of JAM-C expression and expression of semaphorins in ECs, an exciting and novel concept. And finally, this project has also begun to unravel the role of JAM-C in inflammatory responses, in particular how it is important in regulating EC chemokine secretion, an avenue that needs further investigation within the context of leukocyte migration. Taken together, the results presented in this thesis highlight the importance of JAM-C in EC biology at multiple novel angles.

Appendices

Appendix 1. Isotype control antibody staining for JAM-C. Untransfected HUVECs were cultured for 48-72 h to reach confluence and then fixed for 15 mins in 4% PFA at room temperature. Cells were then immuno-stained for VE-Cadherin and DRAQ5 (lower panel) and with either Rabbit anti-JAM-C (top-left panel) or Rabbit IgG control antibodies (top-right panel). Images were taken using a Zeiss LSM800 confocal microscope.

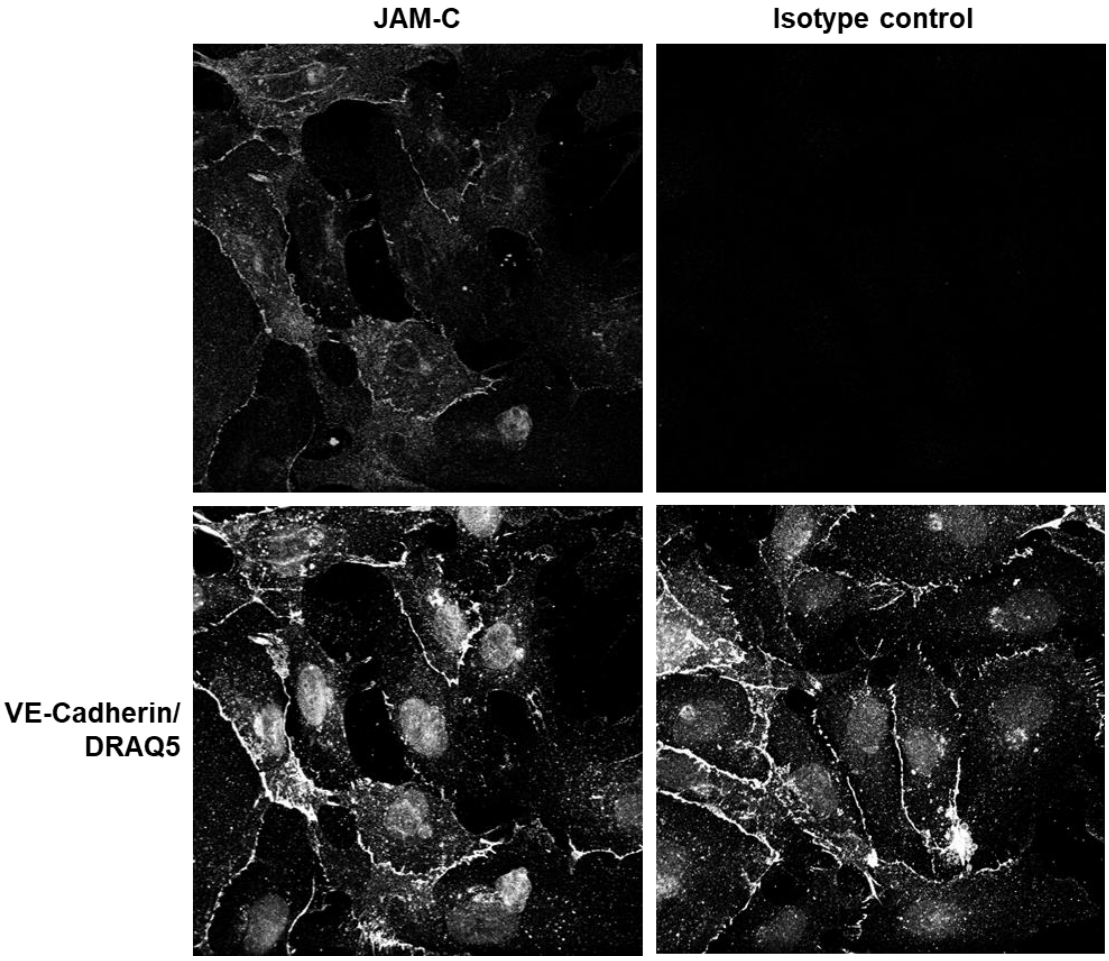

Appendix 2. Isotype control antibody staining for LC3. Untransfected HUVECs were cultured for 48-72 h to reach confluence, then subjected to 2 hours of starvation treatment with addition of Bafilomycin A1 (100 nM) to induce LC3 puncta formation, then fixed for 3-5 mins in 100% methanol at -20^{o}C. Cells were then immuno-stained for VE-Cadherin and DRAQ5 (lower panel) and with either Rabbit anti-LC3 (top-left panel) or Rabbit IgG control antibodies (top-right panel). Images were taken using a Zeiss LSM800 confocal microscope.

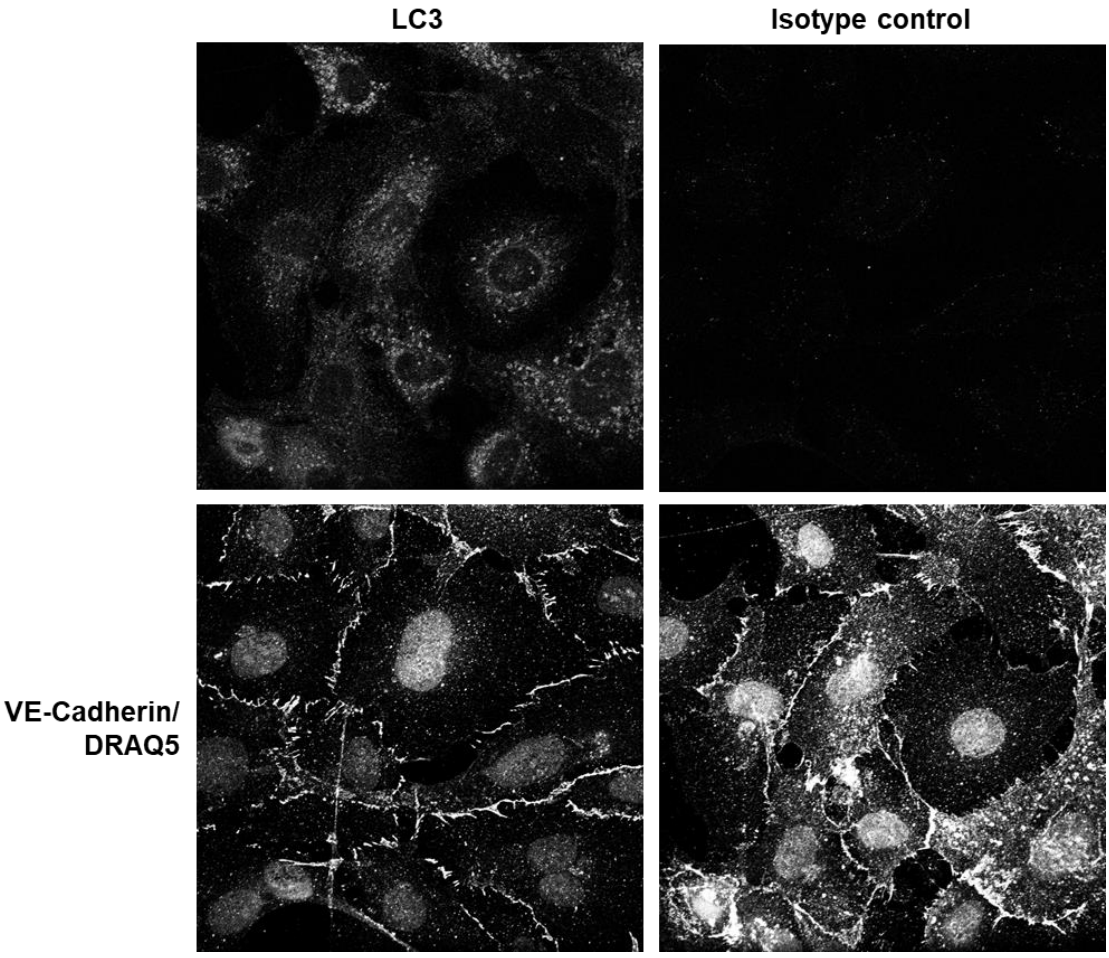

Appendix 3. List of chemorepulsive genes from pathway analysis.

Gene	Molecule name
BDNF	Brain-derived neurotrophic factor
BMP7	Bone morphogenic protein 7
CXCL12	Chemokine CXCL12
CXCR4	Chemokine Receptor CXCR40
cAMP	Cyclic AMP
FLT1	VEGFR1
FYN	Fyn kinase
GDF7	Growth differentiation factor 7
GDNF	Glial cell derived neurotrophic factor
NRCAM	Neuronal cell adhesion molecule
NRP1	Neuropilin 1
NRP2	Neuropilin 2
NTN1	Netrin-1
PKA	Protein kinase A
PLXND1	Plexin D1
PTPRZ1	Receptor-type tyrosine-protein phosphatase ζ
RHOD	RhoD
ROBO1	Roundabout guidance receptor 1
ROBO2	Roundabout guidance receptor 2
SCN1B	Sodium channel subunit β1
SCN2B	Sodium channel subunit β2
SEMA3A	Semaphorin 3A
SEMA3B	Semaphorin 3B
SEMA3D	Semaphorin 3D
SEMA3E	Semaphorin 3E
SEMA3F	Semaphorin 3F
SLIT2	Slit homolog 2 protein
TNR	Tenascin-R
UNC5A	Netrin receptor 5A

References

ABDEL-MALAK, N. A., SRIKANT, C. B., KRISTOF, A. S., MAGDER, S. A., DI BATTISTA, J. A. & HUSSAIN, S. N. 2008. Angiopoietin-1 promotes endothelial cell proliferation and migration through AP-1-dependent autocrine production of interleukin-8. *Blood,* 111**,** 4145-54.

ACEVEDO, L. M., BARILLAS, S., WEIS, S. M., GOTHERT, J. R. & CHERESH, D. A. 2008. Semaphorin 3A suppresses VEGF-mediated angiogenesis yet acts as a vascular permeability factor. *Blood,* 111**,** 2674-80.

ADAIR, T. H. & MONTANI, J. P. 2010. *Angiogenesis.* San Rafael (CA).

ADAMSON, R. H. 1993. Microvascular endothelial cell shape and size in situ. *Microvasc Res,* 46**,** 77-88.

ALLINGHAM, M. J., VAN BUUL, J. D. & BURRIDGE, K. 2007. ICAM-1-mediated, Src- and Pyk2-dependent vascular endothelial cadherin tyrosine phosphorylation is required for leukocyte transendothelial migration. *J Immunol,* 179**,** 4053-64.

ALLPORT, J. R., MULLER, W. A. & LUSCINSKAS, F. W. 2000. Monocytes induce reversible focal changes in vascular endothelial cadherin complex during transendothelial migration under flow. *J Cell Biol,* 148**,** 203-16.

ARCANGELI, M. L., FRONTERA, V., BARDIN, F., OBRADOS, E., ADAMS, S., CHABANNON, C., SCHIFF, C., MANCINI, S. J., ADAMS, R. H. & AURRAND-LIONS, M. 2011. JAM-B regulates maintenance of hematopoietic stem cells in the bone marrow. *Blood,* 118**,** 4609-19.

ARRATE, M. P., RODRIGUEZ, J. M., TRAN, T. M., BROCK, T. A. & CUNNINGHAM, S. A. 2001. Cloning of human junctional adhesion molecule 3 (JAM3) and its identification as the JAM2 counter-receptor. *J Biol Chem,* 276**,** 45826-32.

AURRAND-LIONS, M., DUNCAN, L., BALLESTREM, C. & IMHOF, B. A. 2001a. JAM-2, a novel immunoglobulin superfamily molecule, expressed by endothelial and lymphatic cells. *J Biol Chem,* 276**,** 2733-41.

AURRAND-LIONS, M., JOHNSON-LEGER, C., WONG, C., DU PASQUIER, L. & IMHOF, B. A. 2001b. Heterogeneity of endothelial junctions is reflected by differential expression and specific subcellular localization of the three JAM family members. *Blood,* 98**,** 3699-707.

AURRAND-LIONS, M., LAMAGNA, C., DANGERFIELD, J. P., WANG, S., HERRERA, P., NOURSHARGH, S. & IMHOF, B. A. 2005. Junctional Adhesion Molecule-C Regulates the

Early Influx of Leukocytes into Tissues during Inflammation. *The Journal of Immunology,* 174**,** 6406-6415.

AURRAND-LIONS, M. D., L; DU PASQUIER, L; IMHOF, BA 2000. Cloning of JAM-2 and JAM-3: an emerging junctional adhesion molecular family. *Curr Top Microbiol Immunol***,** 91-98.

AWAN, M. U. & DENG, Y. 2014. Role of autophagy and its significance in cellular homeostasis. *Appl Microbiol Biotechnol,* 98**,** 5319-28.

BAEUERLE, P. A. & HENKEL, T. 1994. Function Amd Activation of Nf-Kappa-B in the Immune-System. *Annual Review of Immunology,* 12**,** 141-179.

BAKOWITZ, M., BRUNS, B. & MCCUNN, M. 2012. Acute lung injury and the acute respiratory distress syndrome in the injured patient. *Scand J Trauma Resusc Emerg Med,* 20**,** 54.

BALDA, M. S., GARRETT, M. D. & MATTER, K. 2003. The ZO-1-associated Y-box factor ZONAB regulates epithelial cell proliferation and cell density. *J Cell Biol,* 160**,** 423-32.

BARGATZE, R. F. & BUTCHER, E. C. 1993. Rapid G protein-regulated activation event involved in lymphocyte binding to high endothelial venules. *J Exp Med,* 178**,** 367-72.

BARTELS, K., GRENZ, A. & ELTZSCHIG, H. K. 2013. Hypoxia and inflammation are two sides of the same coin. *Proc Natl Acad Sci U S A,* 110**,** 18351-2.

BAUD, V. & KARIN, M. 2001. Signal transduction by tumor necrosis factor and its relatives. *Trends Cell Biol,* 11**,** 372-7.

BAZZONI, G., MARTINEZ-ESTRADA, O. M., ORSENIGO, F., CORDENONSI, M., CITI, S. & DEJANA, E. 2000. Interaction of junctional adhesion molecule with the tight junction components ZO-1, cingulin, and occludin. *J Biol Chem,* 275**,** 20520-6.

BAZZONI, G. D., E 2004. Endothelial cell-to-cell junctions: molecular organisation and role in vascular homeostasis. *Physiol Rev,* 84**,** 869-901.

BEJARANO, E., YUSTE, A., PATEL, B., STOUT, R. F., JR., SPRAY, D. C. & CUERVO, A. M. 2014. Connexins modulate autophagosome biogenesis. *Nat Cell Biol,* 16**,** 401-14.

BERLIN, C., BERG, E. L., BRISKIN, M. J., ANDREW, D. P., KILSHAW, P. J., HOLZMANN, B., WEISSMAN, I. L., HAMANN, A. & BUTCHER, E. C. 1993. Alpha 4 beta 7 integrin mediates lymphocyte binding to the mucosal vascular addressin MAdCAM-1. *Cell,* 74**,** 185-95.

BIRDSEY, G. M., DRYDEN, N. H., AMSELLEM, V., GEBHARDT, F., SAHNAN, K., HASKARD, D. O., DEJANA, E., MASON, J. C. & RANDI, A. M. 2008. Transcription factor Erg regulates angiogenesis and endothelial apoptosis through VE-cadherin. *Blood,* 111**,** 3498-506.

BODOLAY, E., KOCH, A. E., KIM, J., SZEGEDI, G. & SZEKANECZ, Z. 2002. Angiogenesis and chemokines in rheumatoid arthritis and other systemic inflammatory rheumatic diseases. *J Cell Mol Med,* 6**,** 357-76.

BOSSY-WETZEL, E. & GREEN, D. R. 2000. Detection of apoptosis by annexin V labeling. *Methods Enzymol,* 322**,** 15-8.

BOUIS, D., HOSPERS, G. A., MEIJER, C., MOLEMA, G. & MULDER, N. H. 2001. Endothelium in vitro: a review of human vascular endothelial cell lines for blood vessel-related research. *Angiogenesis,* 4**,** 91-102.

BRADFIELD, P. F., MENON, A., MILJKOVIC-LICINA, M., LEE, B. P., FISCHER, N., FISH, R. J., KWAK, B., FISHER, E. A. & IMHOF, B. A. 2016. Divergent JAM-C Expression Accelerates Monocyte-Derived Cell Exit from Atherosclerotic Plaques. *PLoS One,* 11**,** e0159679.

BRADFIELD, P. F., SCHEIERMANN, C., NOURSHARGH, S., ODY, C., LUSCINSKAS, F. W., RAINGER, G. E., NASH, G. B., MILJKOVIC-LICINA, M., AURRAND-LIONS, M. & IMHOF, B. A. 2007. JAM-C regulates unidirectional monocyte transendothelial migration in inflammation. *Blood,* 110**,** 2545-55.

BREIER, G., BREVIARIO, F., CAVEDA, L., BERTHIER, R., SCHNURCH, H., GOTSCH, U., VESTWEBER, D., RISAU, W. & DEJANA, E. 1996. Molecular cloning and expression of murine vascular endothelial-cadherin in early stage development of cardiovascular system. *Blood,* 87**,** 630-41.

BROWN, Z., GERRITSEN, M. E., CARLEY, W. W., STRIETER, R. M., KUNKEL, S. L. & WESTWICK, J. 1994. Chemokine gene expression and secretion by cytokine-activated human microvascular endothelial cells. Differential regulation of monocyte chemoattractant protein-1 and interleukin-8 in response to interferon-gamma. *Am J Pathol,* 145**,** 913-21.

BRYSSE, A., MESTDAGT, M., POLETTE, M., LUCZKA, E., HUNZIKER, W., NOEL, A., BIREMBAUT, P., FOIDART, J. M. & GILLES, C. 2012. Regulation of CXCL8/IL-8 expression by zonula occludens-1 in human breast cancer cells. *Mol Cancer Res,* 10**,** 121-32.

CARMAN, C. V. & SPRINGER, T. A. 2004. A transmigratory cup in leukocyte diapedesis both through individual vascular endothelial cells and between them. *J Cell Biol,* 167**,** 377-88.

CARMELIET, P., LAMPUGNANI, M. G., MOONS, L., BREVIARIO, F., COMPERNOLLE, V., BONO, F., BALCONI, G., SPAGNUOLO, R., OOSTHUYSE, B., DEWERCHIN, M., ZANETTI, A., ANGELLILO, A., MATTOT, V., NUYENS, D., LUTGENS, E., CLOTMAN, F., DE RUITER, M. C., GITTENBERGER-DE GROOT, A., POELMANN, R., LUPU, F., HERBERT, J. M., COLLEN, D. & DEJANA, E. 1999. Targeted deficiency or cytosolic truncation of the VE-cadherin gene in mice impairs VEGF-mediated endothelial survival and angiogenesis. *Cell,* 98**,** 147-57.

CARTIER-MICHAUD, A., BAILLY, A. L., BETZI, S., SHI, X., LISSITZKY, J. C., ZARUBICA, A., SERGE, A., ROCHE, P., LUGARI, A., HAMON, V., BARDIN, F., DERVIAUX, C., LEMBO, F., AUDEBERT, S., MARCHETTO, S., DURAND, B., BORG, J. P., SHI, N., MORELLI, X. & AURRAND-LIONS, M. 2017. Genetic, structural, and chemical insights into the dual function of GRASP55 in germ cell Golgi remodeling and JAM-C polarized localization during spermatogenesis. *PLoS Genet,* 13**,** e1006803.

CASTILLA, M. A., ARROYO, M. V., ACEITUNO, E., ARAGONCILLO, P., GONZALEZ-PACHECO, F. R., TEXEIRO, E., BRAGADO, R. & CARAMELO, C. 1999. Disruption of cadherin-related junctions triggers autocrine expression of vascular endothelial growth factor in bovine aortic endothelial cells : effects on cell proliferation and death resistance. *Circ Res,* 85**,** 1132-8.

CATALANO, A. 2010. The neuroimmune semaphorin-3A reduces inflammation and progression of experimental autoimmune arthritis. *J Immunol,* 185**,** 6373-83.

CERA, M. R., DEL PRETE, A., VECCHI, A., CORADA, M., MARTIN-PADURA, I., MOTOIKE, T., TONETTI, P., BAZZONI, G., VERMI, W., GENTILI, F., BERNASCONI, S., SATO, T. N., MANTOVANI, A. & DEJANA, E. 2004. Increased DC trafficking to lymph nodes and contact hypersensitivity in junctional adhesion molecule-A-deficient mice. *J Clin Invest,* 114**,** 729-38.

CHATTERJEE, S., WANG, Y., DUNCAN, M. K. & NAIK, U. P. 2013. Junctional adhesion molecule-A regulates vascular endothelial growth factor receptor-2 signaling-dependent mouse corneal wound healing. *PLoS One,* 8**,** e63674.

CHAVAKIS, T., KEIPER, T., MATZ-WESTPHAL, R., HERSEMEYER, K., SACHS, U. J., NAWROTH, P. P., PREISSNER, K. T. & SANTOSO, S. 2004. The junctional adhesion molecule-C promotes neutrophil transendothelial migration in vitro and in vivo. *J Biol Chem,* 279**,** 55602-8.

CHEN, K., WANG, J. M., YUAN, R., YI, X., LI, L., GONG, W., YANG, T., LI, L. & SU, S. 2016. Tissue-resident dendritic cells and diseases involving dendritic cell malfunction. *Int Immunopharmacol,* 34**,** 1-15.

CHEN, M. L., GE, Z., FOX, J. G. & SCHAUER, D. B. 2006. Disruption of tight junctions and induction of proinflammatory cytokine responses in colonic epithelial cells by Campylobacter jejuni. *Infect Immun,* 74**,** 6581-9.

CHOI, K., KENNEDY, M., KAZAROV, A., PAPADIMITRIOU, J. C. & KELLER, G. 1998. A common precursor for hematopoietic and endothelial cells. *Development,* 125**,** 725-32.

CHRISTEN, S., COPPIETERS, K., ROSE, K., HOLDENER, M., BAYER, M., PFEILSCHIFTER, J. M., HINTERMANN, E., VON HERRATH, M. G., AURRAND-LIONS, M., IMHOF, B. A. & CHRISTEN, U. 2013. Blockade but not overexpression of the junctional adhesion molecule C influences virus-induced type 1 diabetes in mice. *PLoS One,* 8**,** e54675.

CHRISTIAN, F., SMITH, E. L. & CARMODY, R. J. 2016. The Regulation of NF-kappaB Subunits by Phosphorylation. *Cells,* 5.

CHRISTOPHERSON, K. W., 2ND, HOOD, A. F., TRAVERS, J. B., RAMSEY, H. & HROMAS, R. A. 2003. Endothelial induction of the T-cell chemokine CCL21 in T-cell autoimmune diseases. *Blood,* 101**,** 801-6.

CHU, L. Y., HSUEH, Y. C., CHENG, H. L. & WU, K. K. 2017. Cytokine-induced autophagy promotes long-term VCAM-1 but not ICAM-1 expression by degrading late-phase IkappaBalpha. *Sci Rep,* 7**,** 12472.

CINES, D. B., POLLAK, E. S., BUCK, C. A., LOSCALZO, J., ZIMMERMAN, G. A., MCEVER, R. P., POBER, J. S., WICK, T. M., KONKLE, B. A., SCHWARTZ, B. S., BARNATHAN, E. S., MCCRAE, K. R., HUG, B. A., SCHMIDT, A. M. & STERN, D. M. 1998. Endothelial cells in physiology and in the pathophysiology of vascular disorders. *Blood,* 91**,** 3527-61.

COLOM, B., BODKIN, J. V., BEYRAU, M., WOODFIN, A., ODY, C., ROURKE, C., CHAVAKIS, T., BROHI, K., IMHOF, B. A. & NOURSHARGH, S. 2015. Leukotriene B4-Neutrophil Elastase Axis Drives Neutrophil Reverse Transendothelial Cell Migration In Vivo. *Immunity,* 42**,** 1075-86.

COLOM, B., POITELON, Y., HUANG, W., WOODFIN, A., AVERILL, S., DEL CARRO, U., ZAMBRONI, D., BRAIN, S. D., PERRETTI, M., AHLUWALIA, A., PRIESTLEY, J. V., CHAVAKIS, T., IMHOF, B. A., FELTRI, M. L. & NOURSHARGH, S. 2012. Schwann cell-specific JAM-C-deficient mice reveal novel expression and functions for JAM-C in peripheral nerves. *FASEB J,* 26**,** 1064-76.

CONTRERAS, R. G., SHOSHANI, L., FLORES-MALDONADO, C., LAZARO, A., MONROY, A. O., ROLDAN, M. L., FIORENTINO, R. & CEREIJIDO, M. 2002. E-Cadherin and tight junctions between epithelial cells of different animal species. *Pflugers Arch,* 444**,** 467-75.

COOKE, V. G., NAIK, M. U. & NAIK, U. P. 2006. Fibroblast growth factor-2 failed to induce angiogenesis in junctional adhesion molecule-A-deficient mice. *Arterioscler Thromb Vasc Biol,* 26**,** 2005-11.

CROTZER, V. L. & BLUM, J. S. 2009. Autophagy and its role in MHC-mediated antigen presentation. *J Immunol,* 182**,** 3335-41.

DALMAN, M. R., DEETER, A., NIMISHAKAVI, G. & DUAN, Z. H. 2012. Fold change and p-value cutoffs significantly alter microarray interpretations. *BMC Bioinformatics,* 13 Suppl 2**,** S11.

DALY, C., WONG, V., BUROVA, E., WEI, Y., ZABSKI, S., GRIFFITHS, J., LAI, K. M., LIN, H. C., IOFFE, E., YANCOPOULOS, G. D. & RUDGE, J. S. 2004. Angiopoietin-1 modulates endothelial cell function and gene expression via the transcription factor FKHR (FOXO1). *Genes Dev,* 18**,** 1060-71.

DAVIES, L. C., JENKINS, S. J., ALLEN, J. E. & TAYLOR, P. R. 2013. Tissue-resident macrophages. *Nat Immunol,* 14**,** 986-95.

DE'ATH, H. D., ROURKE, C., DAVENPORT, R., MANSON, J., RENFREW, I., UPPAL, R., DAVIES, L. C. & BROHI, K. 2012. Clinical and biomarker profile of trauma-induced secondary cardiac injury. *Br J Surg,* 99**,** 789-97.

DEANFIELD, J. E., HALCOX, J. P. & RABELINK, T. J. 2007. Endothelial function and dysfunction: testing and clinical relevance. *Circulation,* 115**,** 1285-95.

DEJANA, E. 2004. Endothelial cell-cell junctions: happy together. *Nat Rev Mol Cell Biol,* 5**,** 261-70.

DENIS, C. V., ANDRE, P., SAFFARIPOUR, S. & WAGNER, D. D. 2001. Defect in regulated secretion of P-selectin affects leukocyte recruitment in von Willebrand factor-deficient mice. *Proc Natl Acad Sci U S A,* 98**,** 4072-7.

DERETIC, V., SAITOH, T. & AKIRA, S. 2013. Autophagy in infection, inflammation and immunity. *Nat Rev Immunol,* 13**,** 722-37.

DETMERS, P. A., LO, S. K., OLSEN-EGBERT, E., WALZ, A., BAGGIOLINI, M. & COHN, Z. A. 1990. Neutrophil-activating protein 1/interleukin 8 stimulates the binding activity of the leukocyte adhesion receptor CD11b/CD18 on human neutrophils. *J Exp Med,* 171**,** 1155-62.

DI STEFANO, A., CARAMORI, G., GNEMMI, I., CONTOLI, M., BRISTOT, L., CAPELLI, A., RICCIARDOLO, F. L., MAGNO, F., D'ANNA, S. E., ZANINI, A., CARBONE, M., SABATINI, F., USAI, C., BRUN, P., CHUNG, K. F., BARNES, P. J., PAPI, A., ADCOCK, I. M. & BALBI, B. 2009. Association of increased CCL5 and CXCL7 chemokine expression with neutrophil activation in severe stable COPD. *Thorax,* 64**,** 968-75.

DONG, A., SHEN, J., ZENG, M. & CAMPOCHIARO, P. A. 2011. Vascular cell-adhesion molecule-1 plays a central role in the proangiogenic effects of oxidative stress. *Proc Natl Acad Sci U S A,* 108**,** 14614-9.

DRECHSLER, M., MEGENS, R. T., VAN ZANDVOORT, M., WEBER, C. & SOEHNLEIN, O. 2010. Hyperlipidemia-triggered neutrophilia promotes early atherosclerosis. *Circulation,* 122**,** 1837-45.

DREES, F., POKUTTA, S., YAMADA, S., NELSON, W. J. & WEIS, W. I. 2005. Alpha-catenin is a molecular switch that binds E-cadherin-beta-catenin and regulates actin-filament assembly. *Cell,* 123**,** 903-15.

DRYDEN, N. H., SPERONE, A., MARTIN-ALMEDINA, S., HANNAH, R. L., BIRDSEY, G. M., KHAN, S. T., LAYHADI, J. A., MASON, J. C., HASKARD, D. O., GOTTGENS, B. & RANDI, A.

M. 2012. The transcription factor Erg controls endothelial cell quiescence by repressing activity of nuclear factor (NF)-kappaB p65. *J Biol Chem,* 287**,** 12331-42.

DU, J., TENG, R. J., GUAN, T., EIS, A., KAUL, S., KONDURI, G. G. & SHI, Y. 2012. Role of autophagy in angiogenesis in aortic endothelial cells. *Am J Physiol Cell Physiol,* 302**,** C383-91.

DUPONT, N., JIANG, S., PILLI, M., ORNATOWSKI, W., BHATTACHARYA, D. & DERETIC, V. 2011. Autophagy-based unconventional secretory pathway for extracellular delivery of IL-1beta. *EMBO J,* 30**,** 4701-11.

DURAN, J. M., ANJARD, C., STEFAN, C., LOOMIS, W. F. & MALHOTRA, V. 2010. Unconventional secretion of Acb1 is mediated by autophagosomes. *J Cell Biol,* 188**,** 527-36.

EBNET, K., KUMMER, D., STEINBACHER, T., SINGH, A., NAKAYAMA, M. & MATIS, M. 2017. Regulation of cell polarity by cell adhesion receptors. *Semin Cell Dev Biol*.

EBNET, K., SUZUKI, A., OHNO, S. & VESTWEBER, D. 2004. Junctional adhesion molecules (JAMs): more molecules with dual functions? *J Cell Sci,* 117**,** 19-29.

EBNET, K. A.-L., M; KUHN, A; KIEFER, F; BUTZ, S; ZANDER, K; MEYER ZU BRICKWEDDE, MK; SUZUKI, A; IMHOF, BA; VESTWEBER, D 2003. The junctional adhesion molecule (JAM) family members JAM-2 and JAM-3 associate with the cell polarity protein PAR-3: a possible role for JAMs in endothelial cell polarity. *J Cell Sci,* 1**,** 3879-91.

ECONOMOPOULOU, M., HAMMER, J., WANG, F., FARISS, R., MAMINISHKIS, A. & MILLER, S. S. 2009. Expression, localization, and function of junctional adhesion molecule-C (JAM-C) in human retinal pigment epithelium. *Invest Ophthalmol Vis Sci,* 50**,** 1454-63.

FRAEMOHS, L., KOENEN, R. R., OSTERMANN, G., HEINEMANN, B. & WEBER, C. 2004. The functional interaction of the beta 2 integrin lymphocyte function-associated antigen-1 with junctional adhesion molecule-A is mediated by the I domain. *J Immunol,* 173**,** 6259-64.

FRONTERA, V., ARCANGELI, M. L., ZIMMERLI, C., BARDIN, F., OBRADOS, E., AUDEBERT, S., BAJENOFF, M., BORG, J. P. & AURRAND-LIONS, M. 2011. Cutting edge: JAM-C controls homeostatic chemokine secretion in lymph node fibroblastic reticular cells expressing thrombomodulin. *J Immunol,* 187**,** 603-7.

FUSE, C., ISHIDA, Y., HIKITA, T., ASAI, T. & OKU, N. 2007. Junctional adhesion molecule-C promotes metastatic potential of HT1080 human fibrosarcoma. *J Biol Chem,* 282**,** 8276-83.

GAVARD, J. & GUTKIND, J. S. 2008. VE-cadherin and claudin-5: it takes two to tango. *Nat Cell Biol,* 10**,** 883-5.

GHO, Y. S., KIM, P. N., LI, H. C., ELKIN, M. & KLEINMAN, H. K. 2001. Stimulation of tumor growth by human soluble intercellular adhesion molecule-1. *Cancer Res,* 61**,** 4253-7.

GHO, Y. S., KLEINMAN, H. K. & SOSNE, G. 1999. Angiogenic activity of human soluble intercellular adhesion molecule-1. *Cancer Res,* 59**,** 5128-32.

GLICK, D., BARTH, S. & MACLEOD, K. F. 2010. Autophagy: cellular and molecular mechanisms. *J Pathol,* 221**,** 3-12.

GLIKI, G., EBNET, K., AURRAND-LIONS, M., IMHOF, B. A. & ADAMS, R. H. 2004. Spermatid differentiation requires the assembly of a cell polarity complex downstream of junctional adhesion molecule-C. *Nature,* 431**,** 320-4.

GODALY, G., PROUDFOOT, A. E., OFFORD, R. E., SVANBORG, C. & AGACE, W. W. 1997. Role of epithelial interleukin-8 (IL-8) and neutrophil IL-8 receptor A in Escherichia coli-induced transuroepithelial neutrophil migration. *Infect Immun,* 65**,** 3451-6.

GOTSCH, U., BORGES, E., BOSSE, R., BOGGEMEYER, E., SIMON, M., MOSSMANN, H. & VESTWEBER, D. 1997. VE-cadherin antibody accelerates neutrophil recruitment in vivo. *J Cell Sci,* 110 (Pt 5)**,** 583-8.

GRANGER, D. N. & SENCHENKOVA, E. 2010. *Inflammation and the Microcirculation.* San Rafael (CA).

GRETHE, S., ARES, M. P., ANDERSSON, T. & PORN-ARES, M. I. 2004. p38 MAPK mediates TNF-induced apoptosis in endothelial cells via phosphorylation and downregulation of Bcl-x(L). *Exp Cell Res,* 298**,** 632-42.

GUO, F., LI, X., PENG, J., TANG, Y., YANG, Q., LIU, L., WANG, Z., JIANG, Z., XIAO, M., NI, C., CHEN, R., WEI, D. & WANG, G. X. 2014. Autophagy regulates vascular endothelial cell eNOS and ET-1 expression induced by laminar shear stress in an ex vivo perfused system. *Ann Biomed Eng,* 42**,** 1978-88.

GUPTA, S. K., PILLARISETTI, K. & OHLSTEIN, E. H. 2000. Platelet agonist F11 receptor is a member of the immunoglobulin superfamily and identical with junctional adhesion molecule (JAM): regulation of expression in human endothelial cells and macrophages. *IUBMB Life,* 50**,** 51-6.

HAMMOND, M. E., LAPOINTE, G. R., FEUCHT, P. H., HILT, S., GALLEGOS, C. A., GORDON, C. A., GIEDLIN, M. A., MULLENBACH, G. & TEKAMP-OLSON, P. 1995. IL-8 induces neutrophil chemotaxis predominantly via type I IL-8 receptors. *J Immunol,* 155**,** 1428-33.

HARRIS, D. M., COHN, H. I., PESANT, S. & ECKHART, A. D. 2008. GPCR signalling in hypertension: role of GRKs. *Clin Sci (Lond),* 115**,** 79-89.

HE, C. & KLIONSKY, D. J. 2009. Regulation mechanisms and signaling pathways of autophagy. *Annu Rev Genet,* 43**,** 67-93.

HELLWIG-BURGEL, T., STIEHL, D. P., WAGNER, A. E., METZEN, E. & JELKMANN, W. 2005. Review: hypoxia-inducible factor-1 (HIF-1): a novel transcription factor in immune reactions. *J Interferon Cytokine Res,* 25**,** 297-310.

HIRASE, T., STADDON, J. M., SAITOU, M., ANDO-AKATSUKA, Y., ITOH, M., FURUSE, M., FUJIMOTO, K., TSUKITA, S. & RUBIN, L. L. 1997. Occludin as a possible determinant of tight junction permeability in endothelial cells. *J Cell Sci,* 110 (Pt 14)**,** 1603-13.

HOELZLE, M. K. & SVITKINA, T. 2012. The cytoskeletal mechanisms of cell-cell junction formation in endothelial cells. *Mol Biol Cell,* 23**,** 310-23.

HOL, J., WILHELMSEN, L. & HARALDSEN, G. 2010. The murine IL-8 homologues KC, MIP-2, and LIX are found in endothelial cytoplasmic granules but not in Weibel-Palade bodies. *J Leukoc Biol,* 87**,** 501-8.

HONDA, K., YANAI, H., NEGISHI, H., ASAGIRI, M., SATO, M., MIZUTANI, T., SHIMADA, N., OHBA, Y., TAKAOKA, A., YOSHIDA, N. & TANIGUCHI, T. 2005. IRF-7 is the master regulator of type-I interferon-dependent immune responses. *Nature,* 434**,** 772-7.

HOU, S. T., NILCHI, L., LI, X., GANGARAJU, S., JIANG, S. X., AYLSWORTH, A., MONETTE, R. & SLINN, J. 2015. Semaphorin3A elevates vascular permeability and contributes to cerebral ischemia-induced brain damage. *Sci Rep,* 5**,** 7890.

HUEBENER, P., PRADERE, J. P., HERNANDEZ, C., GWAK, G. Y., CAVIGLIA, J. M., MU, X., LOIKE, J. D., JENKINS, R. E., ANTOINE, D. J. & SCHWABE, R. F. 2015. The HMGB1/RAGE axis triggers neutrophil-mediated injury amplification following necrosis. *J Clin Invest,* 125**,** 539-50.

IMHOF, B. A., ZIMMERLI, C., GLIKI, G., DUCREST-GAY, D., JUILLARD, P., HAMMEL, P., ADAMS, R. & AURRAND-LIONS, M. 2007. Pulmonary dysfunction and impaired granulocyte homeostasis result in poor survival of Jam-C-deficient mice. *J Pathol,* 212**,** 198-208.

IMMENSCHUH, S., NAIDU, S., CHAVAKIS, T., BESCHMANN, H., LUDWIG, R. J. & SANTOSO, S. 2009. Transcriptional induction of junctional adhesion molecule-C gene expression in activated T cells. *J Leukoc Biol,* 85**,** 796-803.

ISLAS, S., VEGA, J., PONCE, L. & GONZALEZ-MARISCAL, L. 2002. Nuclear localization of the tight junction protein ZO-2 in epithelial cells. *Exp Cell Res,* 274**,** 138-48.

IVANOV, D., PHILIPPOVA, M., ANTROPOVA, J., GUBAEVA, F., ILJINSKAYA, O., TARARAK, E., BOCHKOV, V., ERNE, P., RESINK, T. & TKACHUK, V. 2001. Expression of cell adhesion molecule T-cadherin in the human vasculature. *Histochem Cell Biol,* 115**,** 231-42.

JABER, N. & ZONG, W. X. 2013. Class III PI3K Vps34: essential roles in autophagy, endocytosis, and heart and liver function. *Ann N Y Acad Sci,* 1280**,** 48-51.

JACKSON, A. L. & LINSLEY, P. S. 2010. Recognizing and avoiding siRNA off-target effects for target identification and therapeutic application. *Nat Rev Drug Discov,* 9**,** 57-67.

JIANG, F. 2016. Autophagy in vascular endothelial cells. *Clin Exp Pharmacol Physiol,* 43**,** 1021-1028.

JOYCE, D., ALBANESE, C., STEER, J., FU, M., BOUZAHZAH, B. & PESTELL, R. G. 2001. NF-kappaB and cell-cycle regulation: the cyclin connection. *Cytokine Growth Factor Rev,* 12**,** 73-90.

KATSUNO, T., UMEDA, K., MATSUI, T., HATA, M., TAMURA, A., ITOH, M., TAKEUCHI, K., FUJIMORI, T., NABESHIMA, Y., NODA, T., TSUKITA, S. & TSUKITA, S. 2008. Deficiency of zonula occludens-1 causes embryonic lethal phenotype associated with defected yolk sac angiogenesis and apoptosis of embryonic cells. *Mol Biol Cell,* 19**,** 2465-75.

KAUR, J. & DEBNATH, J. 2015. Autophagy at the crossroads of catabolism and anabolism. *Nat Rev Mol Cell Biol,* 16**,** 461-72.

KAWAI, T., SEKI, M., HIROMATSU, K., EASTCOTT, J. W., WATTS, G. F., SUGAI, M., SMITH, D. J., PORCELLI, S. A. & TAUBMAN, M. A. 1999. Selective diapedesis of Th1 cells induced by endothelial cell RANTES. *J Immunol,* 163**,** 3269-78.

KEIPER, T., AL-FAKHRI, N., CHAVAKIS, E., ATHANASOPOULOS, A. N., ISERMANN, B., HERZOG, S., SAFFRICH, R., HERSEMEYER, K., BOHLE, R. M., HAENDELER, J., PREISSNER, K. T., SANTOSO, S. & CHAVAKIS, T. 2005. The role of junctional adhesion molecule-C (JAM-C) in oxidized LDL-mediated leukocyte recruitment. *FASEB J,* 19**,** 2078-80.

KISANUKI, Y. Y., HAMMER, R. E., MIYAZAKI, J., WILLIAMS, S. C., RICHARDSON, J. A. & YANAGISAWA, M. 2001. Tie2-Cre transgenic mice: a new model for endothelial cell-lineage analysis in vivo. *Dev Biol,* 230**,** 230-42.

KLUGER, M. S., CLARK, P. R., TELLIDES, G., GERKE, V. & POBER, J. S. 2013. Claudin-5 controls intercellular barriers of human dermal microvascular but not human umbilical vein endothelial cells. *Arterioscler Thromb Vasc Biol,* 33**,** 489-500.

KLUNE, J. R., DHUPAR, R., CARDINAL, J., BILLIAR, T. R. & TSUNG, A. 2008. HMGB1: endogenous danger signaling. *Mol Med,* 14**,** 476-84.

KORUS, M., MAHON, G. M., CHENG, L. & WHITEHEAD, I. P. 2002. p38 MAPK-mediated activation of NF-kappaB by the RhoGEF domain of Bcr. *Oncogene,* 21**,** 4601-12.

KRALING, B. M., RAZON, M. J., BOON, L. M., ZURAKOWSKI, D., SEACHORD, C., DARVEAU, R. P., MULLIKEN, J. B., CORLESS, C. L. & BISCHOFF, J. 1996. E-selectin is present in proliferating endothelial cells in human hemangiomas. *Am J Pathol,* 148**,** 1181-91.

KRISHNASWAMY, G., KELLEY, J., YERRA, L., SMITH, J. K. & CHI, D. S. 1999. Human endothelium as a source of multifunctional cytokines: Molecular regulation and possible role in human disease. *Journal of Interferon and Cytokine Research,* 19**,** 91-104.

KROEMER, G., MARINO, G. & LEVINE, B. 2010. Autophagy and the integrated stress response. *Mol Cell,* 40**,** 280-93.

LAMAGNA, C., HODIVALA-DILKE, K. M., IMHOF, B. A. & AURRAND-LIONS, M. 2005a. Antibody against junctional adhesion molecule-C inhibits angiogenesis and tumor growth. *Cancer Res,* 65**,** 5703-10.

LAMAGNA, C., MEDA, P., MANDICOURT, G., BROWN, J., GILBERT, R. J., JONES, E. Y., KIEFER, F., RUGA, P., IMHOF, B. A. & AURRAND-LIONS, M. 2005b. Dual interaction of JAM-C with JAM-B and alpha(M)beta2 integrin: function in junctional complexes and leukocyte adhesion. *Mol Biol Cell,* 16**,** 4992-5003.

LANDMESSER, U., HORNIG, B. & DREXLER, H. 2004. Endothelial function: a critical determinant in atherosclerosis? *Circulation,* 109**,** II27-33.

LANGER, H. F., DAUB, K., BRAUN, G., SCHONBERGER, T., MAY, A. E., SCHALLER, M., STEIN, G. M., STELLOS, K., BUELTMANN, A., SIEGEL-AXEL, D., WENDEL, H. P., AEBERT, H., ROECKEN, M., SEIZER, P., SANTOSO, S., WESSELBORG, S., BROSSART, P. & GAWAZ, M. 2007. Platelets recruit human dendritic cells via Mac-1/JAM-C interaction and modulate dendritic cell function in vitro. *Arterioscler Thromb Vasc Biol,* 27**,** 1463-70.

LANGER, H. F., ORLOVA, V. V., XIE, C., KAUL, S., SCHNEIDER, D., LONSDORF, A. S., FAHRLEITNER, M., CHOI, E. Y., DUTOIT, V., PELLEGRINI, M., GROSSKLAUS, S., NAWROTH, P. P., BARETTON, G., SANTOSO, S., HWANG, S. T., ARNOLD, B. & CHAVAKIS, T. 2011. A novel function of junctional adhesion molecule-C in mediating melanoma cell metastasis. *Cancer Res,* 71**,** 4096-105.

LAUKOETTER, M. G., NAVA, P., LEE, W. Y., SEVERSON, E. A., CAPALDO, C. T., BABBIN, B. A., WILLIAMS, I. R., KOVAL, M., PEATMAN, E., CAMPBELL, J. A., DERMODY, T. S., NUSRAT, A. & PARKOS, C. A. 2007. JAM-A regulates permeability and inflammation in the intestine in vivo. *J Exp Med,* 204**,** 3067-76.

LEINSTER, D. A., COLOM, B., WHITEFORD, J. R., ENNIS, D. P., LOCKLEY, M., MCNEISH, I. A., AURRAND-LIONS, M., CHAVAKIS, T., IMHOF, B. A., BALKWILL, F. R. & NOURSHARGH,

S. 2013. Endothelial cell junctional adhesion molecule C plays a key role in the development of tumors in a murine model of ovarian cancer. *FASEB J,* 27**,** 4244-53.

LEVINE, B., MIZUSHIMA, N. & VIRGIN, H. W. 2011. Autophagy in immunity and inflammation. *Nature,* 469**,** 323-35.

LEY, K., LAUDANNA, C., CYBULSKY, M. I. & NOURSHARGH, S. 2007. Getting to the site of inflammation: the leukocyte adhesion cascade updated. *Nat Rev Immunol,* 7**,** 678-89.

LEY, K. & REUTERSHAN, J. 2006. Leucocyte-endothelial interactions in health and disease. *Handb Exp Pharmacol***,** 97-133.

LI, X., STANKOVIC, M., LEE, B. P., AURRAND-LIONS, M., HAHN, C. N., LU, Y., IMHOF, B. A., VADAS, M. A. & GAMBLE, J. R. 2009. JAM-C induces endothelial cell permeability through its association and regulation of {beta}3 integrins. *Arterioscler Thromb Vasc Biol,* 29**,** 1200-6.

LIAO, H., HE, H., CHEN, Y., ZENG, F., HUANG, J., WU, L. & CHEN, Y. 2014. Effects of long-term serial cell passaging on cell spreading, migration, and cell-surface ultrastructures of cultured vascular endothelial cells. *Cytotechnology,* 66**,** 229-38.

LIMA, W. R., PARREIRA, K. S., DEVUYST, O., CAPLANUSI, A., N'KULI, F., MARIEN, B., VAN DER SMISSEN, P., ALVES, P. M., VERROUST, P., CHRISTENSEN, E. I., TERZI, F., MATTER, K., BALDA, M. S., PIERREUX, C. E. & COURTOY, P. J. 2010. ZONAB promotes proliferation and represses differentiation of proximal tubule epithelial cells. *J Am Soc Nephrol,* 21**,** 478-88.

LIU, J., BI, X., CHEN, T., ZHANG, Q., WANG, S. X., CHIU, J. J., LIU, G. S., ZHANG, Y., BU, P. & JIANG, F. 2015. Shear stress regulates endothelial cell autophagy via redox regulation and Sirt1 expression. *Cell Death Dis,* 6**,** e1827.

LIU, J. J., STOCKTON, R. A., GINGRAS, A. R., ABLOOGLU, A. J., HAN, J., BOBKOV, A. A. & GINSBERG, M. H. 2011. A mechanism of Rap1-induced stabilization of endothelial cell--cell junctions. *Mol Biol Cell,* 22**,** 2509-19.

LIU, Y., NUSRAT, A., SCHNELL, F. J., REAVES, T. A., WALSH, S., POCHET, M. & PARKOS, C. A. 2000. Human junction adhesion molecule regulates tight junction resealing in epithelia. *J Cell Sci,* 113 (Pt 13)**,** 2363-74.

LIVAK, K. J. & SCHMITTGEN, T. D. 2001. Analysis of relative gene expression data using real-time quantitative PCR and the 2(-Delta Delta C(T)) Method. *Methods,* 25**,** 402-8.

LOTZE, M. T. & TRACEY, K. J. 2005. High-mobility group box 1 protein (HMGB1): nuclear weapon in the immune arsenal. *Nat Rev Immunol,* 5**,** 331-42.

LUDWIG, R. J., HARDT, K., HATTING, M., BISTRIAN, R., DIEHL, S., RADEKE, H. H., PODDA, M., SCHON, M. P., KAUFMANN, R., HENSCHLER, R., PFEILSCHIFTER, J. M., SANTOSO, S. & BOEHNCKE, W. H. 2009. Junctional adhesion molecule (JAM)-B supports lymphocyte rolling and adhesion through interaction with alpha4beta1 integrin. *Immunology,* 128**,** 196-205.

LUDWIG, R. J., ZOLLNER, T. M., SANTOSO, S., HARDT, K., GILLE, J., BAATZ, H., JOHANN, P. S., PFEFFER, J., RADEKE, H. H., SCHON, M. P., KAUFMANN, R., BOEHNCKE, W. H. & PODDA, M. 2005. Junctional adhesion molecules (JAM)-B and -C contribute to leukocyte extravasation to the skin and mediate cutaneous inflammation. *J Invest Dermatol,* 125**,** 969-76.

LUISSINT, A. C., LUTZ, P. G., CALDERWOOD, D. A., COURAUD, P. O. & BOURDOULOUS, S. 2008. JAM-L-mediated leukocyte adhesion to endothelial cells is regulated in cis by alpha4beta1 integrin activation. *J Cell Biol,* 183**,** 1159-73.

LUPU, C., GOODWIN, C. A., WESTMUCKETT, A. D., EMEIS, J. J., SCULLY, M. F., KAKKAR, V. V. & LUPU, F. 1997. Tissue factor pathway inhibitor in endothelial cells colocalizes with glycolipid microdomains/caveolae. Regulatory mechanism(s) of the anticoagulant properties of the endothelium. *Arterioscler Thromb Vasc Biol,* 17**,** 2964-74.

MAKO, V., CZUCZ, J., WEISZHAR, Z., HERCZENIK, E., MATKO, J., PROHASZKA, Z. & CERVENAK, L. 2010. Proinflammatory activation pattern of human umbilical vein endothelial cells induced by IL-1beta, TNF-alpha, and LPS. *Cytometry A,* 77**,** 962-70.

MALERGUE, F., GALLAND, F., MARTIN, F., MANSUELLE, P., AURRAND-LIONS, M. & NAQUET, P. 1998. A novel immunoglobulin superfamily junctional molecule expressed by antigen presenting cells, endothelial cells and platelets. *Mol Immunol,* 35**,** 1111-9.

MANDICOURT, G., IDEN, S., EBNET, K., AURRAND-LIONS, M. & IMHOF, B. A. 2007. JAM-C regulates tight junctions and integrin-mediated cell adhesion and migration. *J Biol Chem,* 282**,** 1830-7.

MARINO, G., NISO-SANTANO, M., BAEHRECKE, E. H. & KROEMER, G. 2014. Self-consumption: the interplay of autophagy and apoptosis. *Nat Rev Mol Cell Biol,* 15**,** 81-94.

MARTIN-PADURA, I., LOSTAGLIO, S., SCHNEEMANN, M., WILLIAMS, L., ROMANO, M., FRUSCELLA, P., PANZERI, C., STOPPACCIARO, A., RUCO, L., VILLA, A., SIMMONS, D. & DEJANA, E. 1998. Junctional adhesion molecule, a novel member of the immunoglobulin superfamily that distributes at intercellular junctions and modulates monocyte transmigration. *J Cell Biol,* 142**,** 117-27.

MARTIN, S. E. & CAPLEN, N. J. 2007. Applications of RNA interference in mammalian systems. *Annu Rev Genomics Hum Genet,* 8**,** 81-108.

MASKREY, B. H., MEGSON, I. L., WHITFIELD, P. D. & ROSSI, A. G. 2011. Mechanisms of resolution of inflammation: a focus on cardiovascular disease. *Arterioscler Thromb Vasc Biol,* 31**,** 1001-6.

MEDZHITOV, R. 2008. Origin and physiological roles of inflammation. *Nature,* 454**,** 428-35.

MEGUENANI, M., MILJKOVIC-LICINA, M., FAGIANI, E., ROPRAZ, P., HAMMEL, P., AURRAND-LIONS, M., ADAMS, R. H., CHRISTOFORI, G., IMHOF, B. A. & GARRIDO-URBANI, S. 2015. Junctional adhesion molecule B interferes with angiogenic VEGF/VEGFR2 signaling. *FASEB J,* 29**,** 3411-25.

MERTENS, G., CASSIMAN, J. J., VAN DEN BERGHE, H., VERMYLEN, J. & DAVID, G. 1992. Cell surface heparan sulfate proteoglycans from human vascular endothelial cells. Core protein characterization and antithrombin III binding properties. *J Biol Chem,* 267**,** 20435-43.

METCALF, D. J., NIGHTINGALE, T. D., ZENNER, H. L., LUI-ROBERTS, W. W. & CUTLER, D. F. 2008. Formation and function of Weibel-Palade bodies. *J Cell Sci,* 121**,** 19-27.

MILLAN, J., CAIN, R. J., REGLERO-REAL, N., BIGARELLA, C., MARCOS-RAMIRO, B., FERNANDEZ-MARTIN, L., CORREAS, I. & RIDLEY, A. J. 2010. Adherens junctions connect stress fibres between adjacent endothelial cells. *BMC Biol,* 8**,** 11.

MILLER, S., TAVSHANJIAN, B., OLEKSY, A., PERISIC, O., HOUSEMAN, B. T., SHOKAT, K. M. & WILLIAMS, R. L. 2010. Shaping development of autophagy inhibitors with the structure of the lipid kinase Vps34. *Science,* 327**,** 1638-42.

MINAMI, T. & AIRD, W. C. 2005. Endothelial cell gene regulation. *Trends Cardiovasc Med,* 15**,** 174-84.

MIRZA, M., HREINSSON, J., STRAND, M. L., HOVATTA, O., SODER, O., PHILIPSON, L., PETTERSSON, R. F. & SOLLERBRANT, K. 2006. Coxsackievirus and adenovirus receptor (CAR) is expressed in male germ cells and forms a complex with the differentiation factor JAM-C in mouse testis. *Exp Cell Res,* 312**,** 817-30.

MIZUSHIMA, N. 2007. Autophagy: process and function. *Genes Dev,* 21**,** 2861-73.

MONCADA, S., GRYGLEWSKI, R., BUNTING, S. & VANE, J. R. 1976. An enzyme isolated from arteries transforms prostaglandin endoperoxides to an unstable substance that inhibits platelet aggregation. *Nature,* 263**,** 663-5.

MOORE, C. B., GUTHRIE, E. H., HUANG, M. T. & TAXMAN, D. J. 2010. Short hairpin RNA (shRNA): design, delivery, and assessment of gene knockdown. *Methods Mol Biol,* 629**,** 141-58.

MORDELET, E., DAVIES, H. A., HILLYER, P., ROMERO, I. A. & MALE, D. 2007. Chemokine transport across human vascular endothelial cells. *Endothelium,* 14**,** 7-15.

MOROTE-GARCIA, J. C., NAPIWOTZKY, D., KOHLER, D. & ROSENBERGER, P. 2012. Endothelial Semaphorin 7A promotes neutrophil migration during hypoxia. *Proc Natl Acad Sci U S A,* 109**,** 14146-51.

MOVASSAGH, H., SAATI, A., NANDAGOPAL, S., MOHAMMED, A., TATARI, N., SHAN, L., DUKE-COHAN, J. S., FOWKE, K. R., LIN, F. & GOUNNI, A. S. 2017. Chemorepellent Semaphorin 3E Negatively Regulates Neutrophil Migration In Vitro and In Vivo. *J Immunol,* 198**,** 1023-1033.

MULLER, W. 2013. Getting Leukocytes to the Site of Inflammation. *Vet Pathol,* 50**,** 7-22.

MULLER, W. A. 1995. The role of PECAM-1 (CD31) in leukocyte emigration: studies in vitro and in vivo. *J Leukoc Biol,* 57**,** 523-8.

MULLER, W. A. 2011. Mechanisms of leukocyte transendothelial migration. *Annu Rev Pathol,* 6**,** 323-44.

MULLER, W. A. 2014. How endothelial cells regulate transmigration of leukocytes in the inflammatory response. *Am J Pathol,* 184**,** 886-96.

MULLER, W. A., WEIGL, S. A., DENG, X. & PHILLIPS, D. M. 1993. PECAM-1 is required for transendothelial migration of leukocytes. *J Exp Med,* 178**,** 449-60.

MURAKAMI, M. & HIRANO, T. 2012. The molecular mechanisms of chronic inflammation development. *Front Immunol,* 3**,** 323.

MURROW, L. & DEBNATH, J. 2013. Autophagy as a stress-response and quality-control mechanism: implications for cell injury and human disease. *Annu Rev Pathol,* 8**,** 105-37.

NAGAMATSU, G., OHMURA, M., MIZUKAMI, T., HAMAGUCHI, I., HIRABAYASHI, S., YOSHIDA, S., HATA, Y., SUDA, T. & OHBO, K. 2006. A CTX family cell adhesion molecule, JAM4, is expressed in stem cell and progenitor cell populations of both male germ cell and hematopoietic cell lineages. *Mol Cell Biol,* 26**,** 8498-506.

NAIK, M. U., MOUSA, S. A., PARKOS, C. A. & NAIK, U. P. 2003. Signaling through JAM-1 and alphavbeta3 is required for the angiogenic action of bFGF: dissociation of the JAM-1 and alphavbeta3 complex. *Blood,* 102**,** 2108-14.

NAIK, M. U. & NAIK, U. P. 2006. Junctional adhesion molecule-A-induced endothelial cell migration on vitronectin is integrin alpha v beta 3 specific. *J Cell Sci,* 119**,** 490-9.

NAVARRO, P., RUCO, L. & DEJANA, E. 1998. Differential localization of VE- and N-cadherins in human endothelial cells: VE-cadherin competes with N-cadherin for junctional localization. *J Cell Biol,* 140**,** 1475-84.

NIE, M., AIJAZ, S., LEEFA CHONG SAN, I. V., BALDA, M. S. & MATTER, K. 2009. The Y-box factor ZONAB/DbpA associates with GEF-H1/Lfc and mediates Rho-stimulated transcription. *EMBO Rep,* 10**,** 1125-31.

NIGHOT, P. K., HU, C. A. & MA, T. Y. 2015. Autophagy enhances intestinal epithelial tight junction barrier function by targeting claudin-2 protein degradation. *J Biol Chem,* 290**,** 7234-46.

NOTTEBAUM, A. F., CAGNA, G., WINDERLICH, M., GAMP, A. C., LINNEPE, R., POLASCHEGG, C., FILIPPOVA, K., LYCK, R., ENGELHARDT, B., KAMENYEVA, O., BIXEL, M. G., BUTZ, S. & VESTWEBER, D. 2008. VE-PTP maintains the endothelial barrier via plakoglobin and becomes dissociated from VE-cadherin by leukocytes and by VEGF. *J Exp Med,* 205**,** 2929-45.

NOURSHARGH, S. & ALON, R. 2014. Leukocyte migration into inflamed tissues. *Immunity,* 41**,** 694-707.

ODENWALD, M. A., CHOI, W., BUCKLEY, A., SHASHIKANTH, N., JOSEPH, N. E., WANG, Y., WARREN, M. H., BUSCHMANN, M. M., PAVLYUK, R., HILDEBRAND, J., MARGOLIS, B., FANNING, A. S. & TURNER, J. R. 2017. ZO-1 interactions with F-actin and occludin direct epithelial polarization and single lumen specification in 3D culture. *J Cell Sci,* 130**,** 243-259.

ODY, C., JUNGBLUT-RUAULT, S., COSSALI, D., BARNET, M., AURRAND-LIONS, M., IMHOF, B. A. & MATTHES, T. 2007. Junctional adhesion molecule C (JAM-C) distinguishes CD27+ germinal center B lymphocytes from non-germinal center cells and constitutes a new diagnostic tool for B-cell malignancies. *Leukemia,* 21**,** 1285-93.

OH, J. E. & LEE, H. K. 2014. Pattern recognition receptors and autophagy. *Front Immunol,* 5**,** 300.

OHASHI, K., OUCHI, N., HIGUCHI, A., SHAW, R. J. & WALSH, K. 2010. LKB1 deficiency in Tie2-Cre-expressing cells impairs ischemia-induced angiogenesis. *J Biol Chem,* 285**,** 22291-8.

ORLOVA, V. V., ECONOMOPOULOU, M., LUPU, F., SANTOSO, S. & CHAVAKIS, T. 2006. Junctional adhesion molecule-C regulates vascular endothelial permeability by modulating VE-cadherin-mediated cell-cell contacts. *J Exp Med,* 203**,** 2703-14.

OSTERMANN, G., WEBER, K. S., ZERNECKE, A., SCHRODER, A. & WEBER, C. 2002. JAM-1 is a ligand of the beta(2) integrin LFA-1 involved in transendothelial migration of leukocytes. *Nat Immunol,* 3**,** 151-8.

OYNEBRATEN, I., BAKKE, O., BRANDTZAEG, P., JOHANSEN, F. E. & HARALDSEN, G. 2004. Rapid chemokine secretion from endothelial cells originates from 2 distinct compartments. *Blood,* 104**,** 314-20.

PALAZON, A., GOLDRATH, A. W., NIZET, V. & JOHNSON, R. S. 2014. HIF transcription factors, inflammation, and immunity. *Immunity,* 41**,** 518-28.

PALMER, G., BUSSO, N., AURRAND-LIONS, M., TALABOT-AYER, D., CHOBAZ-PECLAT, V., ZIMMERLI, C., HAMMEL, P., IMHOF, B. A. & GABAY, C. 2007. Expression and function of junctional adhesion molecule-C in human and experimental arthritis. *Arthritis Res Ther,* 9**,** R65.

PALMERI, D., VAN ZANTE, A., HUANG, C. C., HEMMERICH, S. & ROSEN, S. D. 2000. Vascular endothelial junction-associated molecule, a novel member of the immunoglobulin superfamily, is localized to intercellular boundaries of endothelial cells. *J Biol Chem,* 275**,** 19139-45.

PAMUKCU, B., LIP, G. Y., DEVITT, A., GRIFFITHS, H. & SHANTSILA, E. 2010. The role of monocytes in atherosclerotic coronary artery disease. *Ann Med,* 42**,** 394-403.

PANZER, U. & UGUCCIONI, M. 2004. Prostaglandin E2 modulates the functional responsiveness of human monocytes to chemokines. *Eur J Immunol,* 34**,** 3682-9.

PELLEGRINI, M., CLAPS, G., ORLOVA, V. V., BARRIOS, F., DOLCI, S., GEREMIA, R., ROSSI, P., ROSSI, G., ARNOLD, B., CHAVAKIS, T., FEIGENBAUM, L., SHARAN, S. K. & NUSSENZWEIG, A. 2011. Targeted JAM-C deletion in germ cells by Spo11-controlled Cre recombinase. *J Cell Sci,* 124**,** 91-9.

PHILLIPSON, M., HEIT, B., COLARUSSO, P., LIU, L., BALLANTYNE, C. M. & KUBES, P. 2006. Intraluminal crawling of neutrophils to emigration sites: a molecularly distinct process from adhesion in the recruitment cascade. *J Exp Med,* 203**,** 2569-75.

POBER, J. S. & SESSA, W. C. 2007. Evolving functions of endothelial cells in inflammation. *Nat Rev Immunol,* 7**,** 803-15.

POTENTE, M., GHAENI, L., BALDESSARI, D., MOSTOSLAVSKY, R., ROSSIG, L., DEQUIEDT, F., HAENDELER, J., MIONE, M., DEJANA, E., ALT, F. W., ZEIHER, A. M. & DIMMELER, S. 2007. SIRT1 controls endothelial angiogenic functions during vascular growth. *Genes Dev,* 21**,** 2644-58.

PRAME KUMAR, K., NICHOLLS, A. J. & WONG, C. H. Y. 2018. Partners in crime: neutrophils and monocytes/macrophages in inflammation and disease. *Cell Tissue Res,* 371**,** 551-565.

PRASAD CHENNAZHY, K. & KRISHNAN, L. K. 2005. Effect of passage number and matrix characteristics on differentiation of endothelial cells cultured for tissue engineering. *Biomaterials,* 26**,** 5658-67.

PRIVRATSKY, J. R. & NEWMAN, P. J. 2014. PECAM-1: regulator of endothelial junctional integrity. *Cell Tissue Res,* 355**,** 607-19.

PRUENSTER, M., MUDDE, L., BOMBOSI, P., DIMITROVA, S., ZSAK, M., MIDDLETON, J., RICHMOND, A., GRAHAM, G. J., SEGERER, S., NIBBS, R. J. & ROT, A. 2009. The Duffy antigen receptor for chemokines transports chemokines and supports their promigratory activity. *Nat Immunol,* 10**,** 101-8.

PYO, J. O., NAH, J. & JUNG, Y. K. 2012. Molecules and their functions in autophagy. *Exp Mol Med,* 44**,** 73-80.

QING, G., YAN, P. & XIAO, G. 2006. Hsp90 inhibition results in autophagy-mediated proteasome-independent degradation of IkappaB kinase (IKK). *Cell Res,* 16**,** 895-901.

RABQUER, B. J., AMIN, M. A., TEEGALA, N., SHAHEEN, M. K., TSOU, P. S., RUTH, J. H., LESCH, C. A., IMHOF, B. A. & KOCH, A. E. 2010. Junctional adhesion molecule-C is a soluble mediator of angiogenesis. *J Immunol,* 185**,** 1777-85.

RABQUER, B. J., PAKOZDI, A., MICHEL, J. E., GUJAR, B. S., HAINES, G. K., 3RD, IMHOF, B. A. & KOCH, A. E. 2008. Junctional adhesion molecule C mediates leukocyte adhesion to rheumatoid arthritis synovium. *Arthritis Rheum,* 58**,** 3020-9.

RAO, D. D., VORHIES, J. S., SENZER, N. & NEMUNAITIS, J. 2009. siRNA vs. shRNA: similarities and differences. *Adv Drug Deliv Rev,* 61**,** 746-59.

RICCIOTTI, E. & FITZGERALD, G. A. 2011. Prostaglandins and inflammation. *Arterioscler Thromb Vasc Biol,* 31**,** 986-1000.

ROBERTS, T. K., EUGENIN, E. A., LOPEZ, L., ROMERO, I. A., WEKSLER, B. B., COURAUD, P. O. & BERMAN, J. W. 2012. CCL2 disrupts the adherens junction: implications for neuroinflammation. *Lab Invest,* 92**,** 1213-33.

ROTZIUS, P., SOEHNLEIN, O., KENNE, E., LINDBOM, L., NYSTROM, K., THAMS, S. & ERIKSSON, E. E. 2009. ApoE(-/-)/lysozyme M(EGFP/EGFP) mice as a versatile model to study monocyte and neutrophil trafficking in atherosclerosis. *Atherosclerosis,* 202**,** 111-8.

RYTER, S. W., CLOONAN, S. M. & CHOI, A. M. 2013. Autophagy: a critical regulator of cellular metabolism and homeostasis. *Mol Cells,* 36**,** 7-16.

SAITOH, T., FUJITA, N., JANG, M. H., UEMATSU, S., YANG, B. G., SATOH, T., OMORI, H., NODA, T., YAMAMOTO, N., KOMATSU, M., TANAKA, K., KAWAI, T., TSUJIMURA, T.,

TAKEUCHI, O., YOSHIMORI, T. & AKIRA, S. 2008. Loss of the autophagy protein Atg16L1 enhances endotoxin-induced IL-1beta production. *Nature,* 456**,** 264-8.

SAKURAI, A., DOCI, C. L. & GUTKIND, J. S. 2012. Semaphorin signaling in angiogenesis, lymphangiogenesis and cancer. *Cell Res,* 22**,** 23-32.

SAKURAI, A., GAVARD, J., ANNAS-LINHARES, Y., BASILE, J. R., AMORNPHIMOLTHAM, P., PALMBY, T. R., YAGI, H., ZHANG, F., RANDAZZO, P. A., LI, X., WEIGERT, R. & GUTKIND, J. S. 2010. Semaphorin 3E initiates antiangiogenic signaling through plexin D1 by regulating Arf6 and R-Ras. *Mol Cell Biol,* 30**,** 3086-98.

SANTOSO, S., ORLOVA, V. V., SONG, K., SACHS, U. J., ANDREI-SELMER, C. L. & CHAVAKIS, T. 2005. The homophilic binding of junctional adhesion molecule-C mediates tumor cell-endothelial cell interactions. *J Biol Chem,* 280**,** 36326-33.

SANTOSO, S., SACHS, U. J. H., KROLL, H., LINDER, M., RUF, A., PREISSNER, K. T. & CHAVAKIS, T. 2002. The Junctional Adhesion Molecule 3 (JAM-3) on Human Platelets is a Counterreceptor for the Leukocyte Integrin Mac-1. *Journal of Experimental Medicine,* 196**,** 679-691.

SAPIEHA, P., MAWAMBO, G. & AGNIESZKA, D. 2015. Semaphorin 3A and VEGF promote inflammation retinopathy. *Faseb Journal,* 29.

SARKAR, S., RAVIKUMAR, B., FLOTO, R. A. & RUBINSZTEIN, D. C. 2009. Rapamycin and mTOR-independent autophagy inducers ameliorate toxicity of polyglutamine-expanded huntingtin and related proteinopathies. *Cell Death Differ,* 16**,** 46-56.

SCHALL, T. J., BACON, K., TOY, K. J. & GOEDDEL, D. V. 1990. Selective attraction of monocytes and T lymphocytes of the memory phenotype by cytokine RANTES. *Nature,* 347**,** 669-71.

SCHEIERMANN, C., COLOM, B., MEDA, P., PATEL, N. S., VOISIN, M. B., MARRELLI, A., WOODFIN, A., PITZALIS, C., THIEMERMANN, C., AURRAND-LIONS, M., IMHOF, B. A. & NOURSHARGH, S. 2009. Junctional adhesion molecule-C mediates leukocyte infiltration in response to ischemia reperfusion injury. *Arterioscler Thromb Vasc Biol,* 29**,** 1509-15.

SCHEIERMANN, C. M., P; AURRAND-LIONS, M; MADANI, R; YIANGOU, Y; COFFEY, P; SALT, TE; DUCREST-GAY, D; CAILLE, D; HOWELL, O; REYNOLDS, R; LOBRINUS, A; ADAMS, RH; YU, AS; ANAND, P; IMHOF, BA; NOURSHARGH S 2007. Expression and function of junctional adhesion molecule-C in myelinated peripheral nerves. *Science,* 30**,** 1472-1475.

SCHENKEL, A. R., CHEW, T. W. & MULLER, W. A. 2004a. Platelet endothelial cell adhesion molecule deficiency or blockade significantly reduces leukocyte emigration in a majority of mouse strains. *J Immunol,* 173**,** 6403-8.

SCHENKEL, A. R., MAMDOUH, Z. & MULLER, W. A. 2004b. Locomotion of monocytes on endothelium is a critical step during extravasation. *Nat Immunol,* 5**,** 393-400.

SCHIRALDI, M., RAUCCI, A., MUNOZ, L. M., LIVOTI, E., CELONA, B., VENEREAU, E., APUZZO, T., DE MARCHIS, F., PEDOTTI, M., BACHI, A., THELEN, M., VARANI, L., MELLADO, M., PROUDFOOT, A., BIANCHI, M. E. & UGUCCIONI, M. 2012. HMGB1 promotes recruitment of inflammatory cells to damaged tissues by forming a complex with CXCL12 and signaling via CXCR4. *J Exp Med,* 209**,** 551-63.

SEGARRA, M., OHNUKI, H., MARIC, D., SALVUCCI, O., HOU, X., KUMAR, A., LI, X. & TOSATO, G. 2012. Semaphorin 6A regulates angiogenesis by modulating VEGF signaling. *Blood,* 120**,** 4104-15.

SEMENZA, G. L. 2014. Oxygen sensing, hypoxia-inducible factors, and disease pathophysiology. *Annu Rev Pathol,* 9**,** 47-71.

SHAH, A. V., BIRDSEY, G. M., PEGHAIRE, C., PITULESCU, M. E., DUFTON, N. P., YANG, Y., WEINBERG, I., OSUNA ALMAGRO, L., PAYNE, L., MASON, J. C., GERHARDT, H., ADAMS, R. H. & RANDI, A. M. 2017. The endothelial transcription factor ERG mediates Angiopoietin-1-dependent control of Notch signalling and vascular stability. *Nat Commun,* 8**,** 16002.

SHAH, A. V., BIRDSEY, G. M. & RANDI, A. M. 2016. Regulation of endothelial homeostasis, vascular development and angiogenesis by the transcription factor ERG. *Vascul Pharmacol,* 86**,** 3-13.

SHANG, L., CHEN, S., DU, F., LI, S., ZHAO, L. & WANG, X. 2011. Nutrient starvation elicits an acute autophagic response mediated by Ulk1 dephosphorylation and its subsequent dissociation from AMPK. *Proc Natl Acad Sci U S A,* 108**,** 4788-93.

SHAW, S. K., PERKINS, B. N., LIM, Y. C., LIU, Y., NUSRAT, A., SCHNELL, F. J., PARKOS, C. A. & LUSCINSKAS, F. W. 2001. Reduced expression of junctional adhesion molecule and platelet/endothelial cell adhesion molecule-1 (CD31) at human vascular endothelial junctions by cytokines tumor necrosis factor-alpha plus interferon-gamma Does not reduce leukocyte transmigration under flow. *Am J Pathol,* 159**,** 2281-91.

SHIBUYA, E., MASUDA, K. & IZAWA, Y. 1976. Effects of prostaglandins on leukocyte migration. *Prostaglandins,* 12**,** 165-74.

SIRCAR, M., BRADFIELD, P. F., AURRAND-LIONS, M., FISH, R. J., ALCAIDE, P., YANG, L., NEWTON, G., LAMONT, D., SEHRAWAT, S., MAYADAS, T., LIANG, T. W., PARKOS, C. A., IMHOF, B. A. & LUSCINSKAS, F. W. 2007. Neutrophil Transmigration under Shear Flow Conditions In Vitro Is Junctional Adhesion Molecule-C Independent. *The Journal of Immunology,* 178**,** 5879-5887.

SMITH, D. F., DEEM, T. L., BRUCE, A. C., REUTERSHAN, J., WU, D. & LEY, K. 2006. Leukocyte phosphoinositide-3 kinase {gamma} is required for chemokine-induced, sustained adhesion under flow in vivo. *J Leukoc Biol,* 80**,** 1491-9.

SMITH, E., MCGETTRICK, H. M., STONE, M. A., SHAW, J. S., MIDDLETON, J., NASH, G. B., BUCKLEY, C. D. & ED RAINGER, G. 2008. Duffy antigen receptor for chemokines and CXCL5 are essential for the recruitment of neutrophils in a multicellular model of rheumatoid arthritis synovium. *Arthritis Rheum,* 58**,** 1968-73.

SPERONE, A., DRYDEN, N. H., BIRDSEY, G. M., MADDEN, L., JOHNS, M., EVANS, P. C., MASON, J. C., HASKARD, D. O., BOYLE, J. J., PALEOLOG, E. M. & RANDI, A. M. 2011. The transcription factor Erg inhibits vascular inflammation by repressing NF-kappaB activation and proinflammatory gene expression in endothelial cells. *Arterioscler Thromb Vasc Biol,* 31**,** 142-50.

SPEYER, C. L. & WARD, P. A. 2011. Role of endothelial chemokines and their receptors during inflammation. *J Invest Surg,* 24**,** 18-27.

STAMATOVIC, S. M., KEEP, R. F., KUNKEL, S. L. & ANDJELKOVIC, A. V. 2003. Potential role of MCP-1 in endothelial cell tight junction 'opening': signaling via Rho and Rho kinase. *J Cell Sci,* 116**,** 4615-28.

STAMATOVIC, S. M., SLADOJEVIC, N., KEEP, R. F. & ANDJELKOVIC, A. V. 2012. Relocalization of junctional adhesion molecule A during inflammatory stimulation of brain endothelial cells. *Mol Cell Biol,* 32**,** 3414-27.

STELLOS, K., PANAGIOTA, V., GNERLICH, S., BORST, O., BIGALKE, B. & GAWAZ, M. 2012. Expression of junctional adhesion molecule-C on the surface of platelets supports adhesion, but not differentiation, of human CD34 cells in vitro. *Cell Physiol Biochem,* 29**,** 153-62.

SUBRAMANIAN, B. C., MAJUMDAR, R. & PARENT, C. A. 2017. The role of the LTB4-BLT1 axis in chemotactic gradient sensing and directed leukocyte migration. *Semin Immunol,* 33**,** 16-29.

SULLIVAN, D. P. & MULLER, W. A. 2014. Neutrophil and monocyte recruitment by PECAM, CD99, and other molecules via the LBRC. *Semin Immunopathol,* 36**,** 193-209.

TADDEI, A., GIAMPIETRO, C., CONTI, A., ORSENIGO, F., BREVIARIO, F., PIRAZZOLI, V., POTENTE, M., DALY, C., DIMMELER, S. & DEJANA, E. 2008. Endothelial adherens junctions control tight junctions by VE-cadherin-mediated upregulation of claudin-5. *Nat Cell Biol,* 10**,** 923-34.

TAKAMATSU, H., TAKEGAHARA, N., NAKAGAWA, Y., TOMURA, M., TANIGUCHI, M., FRIEDEL, R. H., RAYBURN, H., TESSIER-LAVIGNE, M., YOSHIDA, Y., OKUNO, T., MIZUI, M., KANG, S., NOJIMA, S., TSUJIMURA, T., NAKATSUJI, Y., KATAYAMA, I., TOYOFUKU, T.,

KIKUTANI, H. & KUMANOGOH, A. 2010. Semaphorins guide the entry of dendritic cells into the lymphatics by activating myosin II. *Nat Immunol,* 11**,** 594-600.

TAKAMI, M., TERRY, V. & PETRUZZELLI, L. 2002. Signaling pathways involved in IL-8-dependent activation of adhesion through Mac-1. *J Immunol,* 168**,** 4559-66.

TANG, D., KANG, R., LIVESEY, K. M., CHEH, C. W., FARKAS, A., LOUGHRAN, P., HOPPE, G., BIANCHI, M. E., TRACEY, K. J., ZEH, H. J., 3RD & LOTZE, M. T. 2010a. Endogenous HMGB1 regulates autophagy. *J Cell Biol,* 190**,** 881-92.

TANG, Y., HARRINGTON, A., YANG, X., FRIESEL, R. E. & LIAW, L. 2010b. The contribution of the Tie2+ lineage to primitive and definitive hematopoietic cells. *Genesis,* 48**,** 563-7.

TANIDA, I., UENO, T. & KOMINAMI, E. 2008. LC3 and Autophagy. *Methods Mol Biol,* 445**,** 77-88.

THIYAGARAJAN, M., CHENG, T. & ZLOKOVIC, B. V. 2007. Endothelial cell protein C receptor: role beyond endothelium? *Circ Res,* 100**,** 155-7.

TILGHMAN, R. W. & HOOVER, R. L. 2002. E-selectin and ICAM-1 are incorporated into detergent-insoluble membrane domains following clustering in endothelial cells. *FEBS Lett,* 525**,** 83-7.

TOJKANDER, S., GATEVA, G. & LAPPALAINEN, P. 2012. Actin stress fibers--assembly, dynamics and biological roles. *J Cell Sci,* 125**,** 1855-64.

TORISU, T., TORISU, K., LEE, I. H., LIU, J., MALIDE, D., COMBS, C. A., WU, X. S., ROVIRA, II, FERGUSSON, M. M., WEIGERT, R., CONNELLY, P. S., DANIELS, M. P., KOMATSU, M., CAO, L. & FINKEL, T. 2013. Autophagy regulates endothelial cell processing, maturation and secretion of von Willebrand factor. *Nat Med,* 19**,** 1281-7.

TORNAVACA, O., CHIA, M., DUFTON, N., ALMAGRO, L. O., CONWAY, D. E., RANDI, A. M., SCHWARTZ, M. A., MATTER, K. & BALDA, M. S. 2015. ZO-1 controls endothelial adherens junctions, cell-cell tension, angiogenesis, and barrier formation. *J Cell Biol,* 208**,** 821-38.

TRAWEGER, A., FUCHS, R., KRIZBAI, I. A., WEIGER, T. M., BAUER, H. C. & BAUER, H. 2003. The tight junction protein ZO-2 localizes to the nucleus and interacts with the heterogeneous nuclear ribonucleoprotein scaffold attachment factor-B. *J Biol Chem,* 278**,** 2692-700.

TROCOLI, A. & DJAVAHERI-MERGNY, M. 2011. The complex interplay between autophagy and NF-kappaB signaling pathways in cancer cells. *Am J Cancer Res,* 1**,** 629-49.

TURNER, M. D., NEDJAI, B., HURST, T. & PENNINGTON, D. J. 2014. Cytokines and chemokines: At the crossroads of cell signalling and inflammatory disease. *Biochim Biophys Acta,* 1843**,** 2563-2582.

UTGAARD, J. O., JAHNSEN, F. L., BAKKA, A., BRANDTZAEG, P. & HARALDSEN, G. 1998. Rapid secretion of prestored interleukin 8 from Weibel-Palade bodies of microvascular endothelial cells. *J Exp Med,* 188**,** 1751-6.

VAN BUUL, J. D., VAN RIJSSEL, J., VAN ALPHEN, F. P., VAN STALBORCH, A. M., MUL, E. P. & HORDIJK, P. L. 2010. ICAM-1 clustering on endothelial cells recruits VCAM-1. *J Biomed Biotechnol,* 2010**,** 120328.

VAN LEEUWEN, M., GIJBELS, M. J., DUIJVESTIJN, A., SMOOK, M., VAN DE GAAR, M. J., HEERINGA, P., DE WINTHER, M. P. & TERVAERT, J. W. 2008. Accumulation of myeloperoxidase-positive neutrophils in atherosclerotic lesions in LDLR-/- mice. *Arterioscler Thromb Vasc Biol,* 28**,** 84-9.

VERNIER, A., DIAB, M., SOELL, M., HAAN-ARCHIPOFF, G., BERETZ, A., WACHSMANN, D. & KLEIN, J. P. 1996. Cytokine production by human epithelial and endothelial cells following exposure to oral viridans streptococci involves lectin interactions between bacteria and cell surface receptors. *Infect Immun,* 64**,** 3016-22.

VOISIN, M. B., WOODFIN, A. & NOURSHARGH, S. 2009. Monocytes and neutrophils exhibit both distinct and common mechanisms in penetrating the vascular basement membrane in vivo. *Arterioscler Thromb Vasc Biol,* 29**,** 1193-9.

WASSERMAN, S. M., MEHRABAN, F., KOMUVES, L. G., YANG, R. B., TOMLINSON, J. E., ZHANG, Y., SPRIGGS, F. & TOPPER, J. N. 2002. Gene expression profile of human endothelial cells exposed to sustained fluid shear stress. *Physiol Genomics,* 12**,** 13-23.

WEGMANN, F., PETRI, B., KHANDOGA, A. G., MOSER, C., KHANDOGA, A., VOLKERY, S., LI, H., NASDALA, I., BRANDAU, O., FASSLER, R., BUTZ, S., KROMBACH, F. & VESTWEBER, D. 2006. ESAM supports neutrophil extravasation, activation of Rho, and VEGF-induced vascular permeability. *J Exp Med,* 203**,** 1671-7.

WILLIAMS, L. A., MARTIN-PADURA, I., DEJANA, E., HOGG, N. & SIMMONS, D. L. 1999. Identification and characterisation of human Junctional Adhesion Molecule (JAM). *Mol Immunol,* 36**,** 1175-88.

WILSON, R. C. & DOUDNA, J. A. 2013. Molecular mechanisms of RNA interference. *Annu Rev Biophys,* 42**,** 217-39.

WOJCIAK-STOTHARD, B., WILLIAMS, L. & RIDLEY, A. J. 1999. Monocyte adhesion and spreading on human endothelial cells is dependent on Rho-regulated receptor clustering. *J Cell Biol,* 145**,** 1293-307.

WOODFIN, A., VOISIN, M. B., BEYRAU, M., COLOM, B., CAILLE, D., DIAPOULI, F. M., NASH, G. B., CHAVAKIS, T., ALBELDA, S. M., RAINGER, G. E., MEDA, P., IMHOF, B. A. & NOURSHARGH, S. 2011. The junctional adhesion molecule JAM-C regulates polarized transendothelial migration of neutrophils in vivo. *Nat Immunol,* 12**,** 761-9.

WOODFIN, A., VOISIN, M. B., IMHOF, B. A., DEJANA, E., ENGELHARDT, B. & NOURSHARGH, S. 2009. Endothelial cell activation leads to neutrophil transmigration as supported by the sequential roles of ICAM-2, JAM-A, and PECAM-1. *Blood,* 113**,** 6246-57.

WOODFIN, A., VOISIN, M. B. & NOURSHARGH, S. 2007. PECAM-1: a multi-functional molecule in inflammation and vascular biology. *Arterioscler Thromb Vasc Biol,* 27**,** 2514-23.

WOOLLARD, K. J. & GEISSMANN, F. 2010. Monocytes in atherosclerosis: subsets and functions. *Nat Rev Cardiol,* 7**,** 77-86.

WU, L., FENG, Z., CUI, S., HOU, K., TANG, L., ZHOU, J., CAI, G., XIE, Y., HONG, Q., FU, B. & CHEN, X. 2013. Rapamycin upregulates autophagy by inhibiting the mTOR-ULK1 pathway, resulting in reduced podocyte injury. *PLoS One,* 8**,** e63799.

WYSS, L., SCHAFER, J., LIEBNER, S., MITTELBRONN, M., DEUTSCH, U., ENZMANN, G., ADAMS, R. H., AURRAND-LIONS, M., PLATE, K. H., IMHOF, B. A. & ENGELHARDT, B. 2012. Junctional adhesion molecule (JAM)-C deficient C57BL/6 mice develop a severe hydrocephalus. *PLoS One,* 7**,** e45619.

XIONG, Y., YEPURI, G., FORBITEH, M., YU, Y., MONTANI, J. P., YANG, Z. & MING, X. F. 2014. ARG2 impairs endothelial autophagy through regulation of MTOR and PRKAA/AMPK signaling in advanced atherosclerosis. *Autophagy,* 10**,** 2223-38.

YAMADA, S., POKUTTA, S., DREES, F., WEIS, W. I. & NELSON, W. J. 2005. Deconstructing the cadherin-catenin-actin complex. *Cell,* 123**,** 889-901.

YAMAMOTO, Y. & GAYNOR, R. B. 2004. IkappaB kinases: key regulators of the NF-kappaB pathway. *Trends Biochem Sci,* 29**,** 72-9.

YAN, W., ZHAO, K., JIANG, Y., HUANG, Q., WANG, J., KAN, W. & WANG, S. 2002. Role of p38 MAPK in ICAM-1 expression of vascular endothelial cells induced by lipopolysaccharide. *Shock,* 17**,** 433-8.

YANG, Y. P., HU, L. F., ZHENG, H. F., MAO, C. J., HU, W. D., XIONG, K. P., WANG, F. & LIU, C. F. 2013. Application and interpretation of current autophagy inhibitors and activators. *Acta Pharmacol Sin,* 34**,** 625-35.

YANG, Z. J., CHEE, C. E., HUANG, S. & SINICROPE, F. A. 2011. The role of autophagy in cancer: therapeutic implications. *Mol Cancer Ther,* 10**,** 1533-41.

YUAN, L., LE BRAS, A., SACHARIDOU, A., ITAGAKI, K., ZHAN, Y., KONDO, M., CARMAN, C. V., DAVIS, G. E., AIRD, W. C. & OETTGEN, P. 2012. ETS-related gene (ERG) controls endothelial cell permeability via transcriptional regulation of the claudin 5 (CLDN5) gene. *J Biol Chem,* 287**,** 6582-91.

YUKAMI, T., HASEGAWA, M., MATSUSHITA, Y., FUJITA, T., MATSUSHITA, T., HORIKAWA, M., KOMURA, K., YANABA, K., HAMAGUCHI, Y., NAGAOKA, T., OGAWA, F., FUJIMOTO, M., STEEBER, D. A., TEDDER, T. F., TAKEHARA, K. & SATO, S. 2007. Endothelial selectins regulate skin wound healing in cooperation with L-selectin and ICAM-1. *J Leukoc Biol,* 82**,** 519-31.

ZEN, K., BABBIN, B. A., LIU, Y., WHELAN, J. B., NUSRAT, A. & PARKOS, C. A. 2004. JAM-C is a component of desmosomes and a ligand for CD11b/CD18-mediated neutrophil transepithelial migration. *Mol Biol Cell,* 15**,** 3926-37.

ZEN, K., LIU, Y., MCCALL, I. C., WU, T., LEE, W., BABBIN, B. A., NUSRAT, A. & PARKOS, C. A. 2005. Neutrophil migration across tight junctions is mediated by adhesive interactions between epithelial coxsackie and adenovirus receptor and a junctional adhesion molecule-like protein on neutrophils. *Mol Biol Cell,* 16**,** 2694-703.

ZHAO, Z., FUX, B., GOODWIN, M., DUNAY, I. R., STRONG, D., MILLER, B. C., CADWELL, K., DELGADO, M. A., PONPUAK, M., GREEN, K. G., SCHMIDT, R. E., MIZUSHIMA, N., DERETIC, V., SIBLEY, L. D. & VIRGIN, H. W. 2008. Autophagosome-independent essential function for the autophagy protein Atg5 in cellular immunity to intracellular pathogens. *Cell Host Microbe,* 4**,** 458-69.